Universidad de Huelva

Departamento de Ingeniería Química, Química Física y Ciencias de los Materiales

Development of polyurethane formulations based on cellulose acetate and castor oil

Memoria para optar al grado de doctor
presentada por:

Adrián Tenorio Alfonso

Fecha de lectura: 28 de marzo de 2019

Bajo la dirección de los doctores:

José María Franco Gómez

María del Carmen Sánchez Carrillo

Huelva, 2019

UNIVERSITY OF HUELVA

Department of Chemical Engineering, Physical Chemistry and Materials Science

DEVELOPMENT OF POLYURETHANE FORMULATIONS BASED ON CELLULOSE ACETATE AND CASTOR OIL

Ph.D. Thesis

Doctoral Programme in Industrial and Environmental Science and Technology

ADRIÁN TENORIO ALFONSO

2019

Supervisors

Prof. Dr. José María Franco Gómez

Dr. María del Carmen Sánchez Carrillo

UNIVERSIDAD DE HUELVA

Departamento de Ingeniería Química, Química Física y Ciencia de los Materiales

DESARROLLO DE FORMULACIONES TIPO POLIURETANO BASADAS EN ACETATO DE CELULOSA Y ACEITE DE RICINO

Tesis Doctoral

Programa de Doctorado en Ciencia y Tecnología Industrial y Ambiental

ADRIÁN TENORIO ALFONSO

2019

Directores:

Cat. Dr. José María Franco Gómez

Dra. María del Carmen Sánchez Carrillo

DESARROLLO DE FORMULACIONES TIPO POLIURETANO BASADAS EN ACETATO DE CELULOSA Y ACEITE DE RICINO

Memoría presentada por Adrián Tenorio Alfonso para aspirar al Grado de Doctor con Mención Internacional por la Universidad de Huelva

Adrián Tenorio Alfonso

La presente tesis ha sido realizada en el Departamento de Ingeniería Química, Química Física y Ciencia de los Materiales de la Universidad de Huelva bajo la dirección del Dr. José María Franco Gómez y Dra. María del Carmen Sánchez Carrillo, los cuales autorizan su presentación:

Dr. José María Franco Gómez Dra. María del Carmen Sánchez Carrillo

Huelva, febrero de 2019

AUTORIZACIÓN PARA LA DEFENSA DE LA TESIS DOCTORAL EMITIDA POR EL DIRECTOR Y EL TUTOR Y POR LA COMISIÓN ACADÉMICA DEL PROGRAMA DE DOCTORADO

DATOS DEL DOCTORANDO:

Apellidos, nombre: Tenorio Alfonso, Adrián	NIF: 49062942D	Nacionalidad: Española
Dirección a efectos de notificaciones: C/ Alfonso XIII, Nº 18, 3º A, CP: 21002, Huelva		
Teléfono: 677818634	email: adrian.tenorio@diq.uhu.es	

DATOS DE LA TESIS DOCTORAL:

Título: Desarrollo de formulaciones tipo poliuretano basadas en acetato de celulosa y aceite de ricino
Programa Oficial de Doctorado al que se adscribe y órgano responsable: Ciencia y Tecnología Industrial y Ambiental; Departamento de Ingeniería Química, Química Física y Ciencia de los Materiales
Línea de investigación a la que se adscribe y órgano responsable: Ingeniería de Procesos y Productos Químicos; Departamento de Ingeniería Química, Química Física y Ciencia de los Materiales

A CUMPLIMENTAR POR EL DIRECTOR Y POR EL TUTOR DE LA TESIS DOCTORAL: (en caso de que el Director y Tutor sean la misma persona, no es necesario cumplimentar los campos relativos al Tutor ni se precisa la firma de éste).

Director/es:	Tutor/es:
Dr./Dra.: José María Franco Gómez Dr./Dra.: María del Carmen Sánchez Carrillo	Dr./Dra.: José María Franco Gómez
como Director/Tutor de la Tesis Doctoral antes indicada AUTORIZA LA DEFENSA DE LA MISMA.	

En Huelva a, _____ de _____ de 2019

Firma del/los Director/es de la Tesis Doctoral

Fdo.: José María Franco Gómez Fdo.: María del Carmen Sánchez Carrillo

A CUMPLIMENTAR POR LA COMISIÓN ACADÉMICA DEL PROGRAMA DE DOCTORADO:

Cumplidos los criterios de calidad aprobados para este Programa de Doctorado por el Comité de Dirección de la Escuela de Doctorado de la Universidad de Huelva y una vez valorada la Tesis Doctoral presentada por el Doctorando y haber incorporado éste las modificaciones y/o cambios que esta Comisión Académica le pudiera haber indicado, **se AUTORIZA** en reunión de fecha _____ **LA DEFENSA** de la misma.

En Huelva a, _____ de _____ de 2019

Firma y sello del Presidente de la Comisión Académica

Fdo. .....

Acknowledgments

At this point, I have so much to be thankful for, that I hope to forget no one of those, who, somehow, enabled the execution and completion of this project I am so proud of.

In the first place, I would like to thank my supervisors, Dr. José María Franco Gómez and Dr. Mª Carmen Sánchez Carrillo, for their incommensurable support, demonstrating a commendable patience, tenacity and ability, capable of leading and teaching me all I know, and helping me in my first steps in the arduous research pathway. Thank you very much for giving me the chance to learn from you both.

On the other hand, I would like to thank the *Research Centre in Chemical Products and Processes Technology* (Pro^{2}TecS) and the *Complex Fluids Engiineering Group* (TEP-185) for giving me the opportunity to start my research career, becoming part of such a great family. In particular, I wish to thank to Dr. Concepción Valencia Barragán, for being that "*guardian angel*" that has helped all PhD studens of this group so much. Many thanks.

To Professor Erik Kuhn and the rest of the members of the *Laboratory of Machine Elements and Tribology* (MuT) from the *University of Applied Sciences of Hamburg* (HAW Hamburg), Thomas Rieling, Niels Eiben y Nazli Acar, for their great help and warm welcome during those marvelous three months, allowing me both to grow professionally and to enjoy once again such captivating culture and city.

Thank to the *Ministerio de Educación, Cultura y Deporte* for the concession of the scholarship *Formación del Profesorado Universitario* (FPU13/01114) that allowed my incorporation into the *Department of Chemical Engineering, Physical Chemistry and Materials Science* from the *University of Huelva*.

Also, many thanks to those with who I started my academic career, sharing memorable experiences, my colleagues and friends, Clara, Fran and Almudena, not forgetting many others, Julio, José Carlos, Fran J., Sergio, etc. Thousand thanks to all of them.

I cannot forget those who, during my research stage, have become part of my life and really good friends, Ortega, Rocío, Antonio, Avido, Isa, Elena, as well as many others who have already left or just arrived. Thank you all.

Thank to my life-long friends, who have always been with me, Jorge, Álvaro and Lourdes, who will be always hold a very special place in my heart. Thank you for all the unforgettable moments lived, that taught me so much, and those yet to be lived.

Finally, and for that reason more importantly, to my family. To Espe, my half, my life. Thank you so much for making me to understand that just one person can be capable of strikingly changing and improving somebody else. Thank you for giving me the opportunity to be part of your life and to be so unbelievably happy. To my best friend, my brother Juan, who has been my brother, my friend, my father… whatever I needed and who has given me so much to become the man I am. Never leave me. Thank you very much brother. And to my mother, the best woman and person I have ever known, a great fighter whose inexhaustible effort, sacrifice and love make me feel proud of being her son. I will never have time enough to show you how much I owe you.

Thank you very much.

Agradecimientos

Llegado este momento, tengo tanto de lo que estar agradecido que espero no olvidar a ninguno de todos aquellos que, de una u otra forma, hicieron posible la realización y finalización de este proyecto del que me siento tan orgulloso.

En primer lugar, quisiera dar las gracias a mis directores de tesis, Dr. José María Franco Gómez y Dra. Mª Carmen Sánchez Carrillo por su inconmensurable apoyo, demostrando una paciencia, tenacidad y habilidad admirables, capaces de guiarme y enseñarme todo lo que sé y ayudándome a dar mis primeros pasos en el arduo camino de la investigación. Muchas gracias por concederme la oportunidad de aprender de vosotros.

Por otro lado, me gustaría agradecer al *Centro de Investigación en Tecnología de Productos y Procesos Químicos* (Pro^{2}TecS) y al *Grupo de Ingeniería de Fluidos Complejos* (TEP-185) por darme la oportunidad de formarme como investigador, pasando a formar parte de esta gran familia. En especial, me gustaría dar las gracias a la Dra. Concepción Valencia Barragán, por seguir siendo ese "*ángel de la guarda*" que tanto nos ha ayudado a todos los doctorandos de este grupo de investigación. Muchas gracias.

Gracias al Profesor Erik Kuhn y al resto de los miembros del *Laboratorio de Elementos de Maquina y Tribología* (MuT) de la *Universidad de Ciencias Aplicadas de Hamburgo* (HAW Hamburg), Thomas Rieling, Niels Eiben y Nazli Acar, por su gran ayuda y tan acogedora bienvenida durante esos maravillosos tres meses de estancia, concediéndome la oportunidad de crecer profesionalmente, así como de disfrutar una vez más de tan cautivadoras cultura y ciudad.

Debo agradecer al *Ministerio de Educación, Cultura y Deporte* la concesión de la *Beca de Formación del Profesorado Universitario* (FPU13/01114) que posibilitaron mi incorporación al *Departamento de Ingeniería Química, Química Física y Ciencia de los Materiales* de la *Universidad de Huelva*.

Por otro lado, a aquellos con quiénes comencé mi carrera académica, viviendo momentos inolvidables, mis compañeros y amigos de promoción, Clara, Fran y Almudena, sin olvidar a otros tantos, Julio, José Carlos, Fran J., Sergio, … y muchos más. Mil gracias a todos ellos.

No me puedo olvidar de todos aquellos que durante mi etapa investigadora han pasado a formar parte de mi vida, llegando a ser buenos amigos, Ortega, Rocío, Antonio, Avido, Isa, Elena, así como otros muchos que ya se marcharon y otros que han llegado. Muchas gracias.

Como no agradecer a mis grandes amigos, los que siempre me han acompañado, Jorge, Álvaro y Lourdes, quienes siempre ocuparán un lugar especial en mi corazón. Gracias por todos los momentos vividos, que tanto me han enseñado y por lo que aún nos quedan.

Por último, y por ello más importante, a mi familia. A Espe, mi mitad, mi vida. Muchísimas gracias por hacerme ver que una sola persona pueda cambiar y mejorar la vida de otra de forma tan rotunda. Gracias por darme la oportunidad de formar parte de tu vida y hacerme tan increíblemente feliz. A mi mejor amigo, mi hermano Juan, quién ha sido hermano, amigo, padre… todo lo que he necesitado y que tanto me ha dado para llegar a ser el hombre que soy. No me faltes nunca. Muchas gracias hermano. Y a mi madre, la mejor mujer y persona que he conocido, una gran luchadora cuyo inagotable esfuerzo, sacrificio y amor hacen sentirme orgulloso de ser su hijo. Nunca tendré tiempo suficiente de demostraros cuanto os lo agradezco.

Muchas gracias.

Contents

Chapter 1
Introduction

1. Summary

Given the emerging environmental concern prevailing in the industrial production and awareness of the use of non-renewable raw materials, this PhD Thesis has been devoted to the development of sustainable alternatives to the traditional petroleum-based polyurethane adhesives, which are also generally associated with the release of toxic solvents during curing. Therefore, the development of bio-sourced polyurethane adhesives with a remarkable renewable content was proposed in this work by using natural polyols, viz. cellulose acetate and castor oil, which were subjected to the reaction with reactive aromatic or aliphatic diisocyanates ―4,4'-methylenediphenyl (MDI) and 1,6-hexamethylene (HMDI) diisocyanates, respectively― through a two-step polycondensation reaction. More specifically, cellulose acetate was first functionalized to a certain degree with the diisocyanates at room temperature and under inert atmosphere, using a reaction solvent (toluene) and a catalyst (triethylamine). Subsequently, the resulting NCO-modified biopolymer was blended with castor oil in specific weight proportions, yielding bio-based polyurethanes which were left for curing under room conditions upon application.

Furthermore, the chemical structure and properties of the thus prepared polyurethane adhesives were assessed by means of diverse experimental techniques. First, Fourier transform infrared (FTIR) spectroscopic analysis was conducted to characterize the polyurethanes' chemical structure as well as to monitor their curing process. Thermogravimetric analysis (TGA), along with standard and temperature modulated differential scanning calorimetric tests (DSC and MDSC) were carried ouy to analyse their thermal transitions and stability. Finally, the rheological behaviour and adhesion performance of the fully cured bio-sourced adhesives were studied by carrying out dynamic oscillatory torsional measurements and standardized mechanical tests to determine shear, peeling and flexural strengths and further compared with those found in commercial benchmarks. By dint of these methods, the influence of the diisocyanate ―whether comprising aromatic or aliphatic backbones― and the reagent proportions were studied. In addition, the impact of the modification of the previously

described two-step protocol by a simpler and more sustainable solvent-free straight-through synthetic pathway on the ultimate polyurethane properties was evaluated.

The conventional two-step procedure was successfully applied to synthesize bio-inspired polyurethane adhesives from mixtures of NCO-functionalized cellulose acetate and castor oil. In all cases, thermal and spectroscopic characterization confirmed the typical microphase segregated chemical structure, exhibiting glass transition temperatures attributed to both soft and hard segment domains. Moreover, a rise in the NCO:OH molar ratio was proven to favour the thermodynamic phase compatibility, leading to higher values of both soft domain glass transition temperatures and viscoelastic functions. Optimum adhesion properties on wood were achieved when using a 1:1 castor oil/HMDI-functionalized cellulose acetate weight ratio, associated to a NCO:OH molar ratio of 1.87, slightly higher than the 1.45 corresponding to their more reactive aromatic diisocyanate-based counterparts. Synthesized bio-based polyurethane developed adhesion strengths comparable or even superior to the studied benchmarks on wood and steel substrates, while failing in bonding non-polar polymeric surfaces, such as polyethylene, or at high temperatures (100 ºC). A thermo-rheological simplicity of the cellulose acetate-based polyurethanes was found throughout the temperature range analysed (-10 up to 200 ºC), even achieving the glass region when using MDI. On the contrary, the t-T superposition principle was restricted to temperatures below 80-100 ºC, limited to the rubbery region, for the HMDI-based systems. The implementation of the proposed single-step procedure highlighted not only its feasibility for a more sustainable preparation of these polyurethane adhesives, but also the resulting improvement in their adhesion performance. The reinforcing effect of the cellulose derivative was also confirmed using this straightforward protocol. Finally, the utilization of cellulose acetate revealed an increase of the polyurethane thermal stability, while reducing the time scale of the moisture-induced curing process.

2. Resumen

Ante la creciente conciencia medioambiental que actualmente prevalece en el sector industrial y la sensibilización sobre el uso de recursos no renovables, esta Tesis Doctoral se ha centrado fundamentalmente en el desarrollo de alternativas sostenibles a los

adhesivos de poliuretanos tradicionales basados en derivados petroquímicos, los cuales implican, además, por lo general, la liberación de disolventes tóxicos al medioambiente durante el curado. Por consiguiente, en este trabajo se propone desarrollar adhesivos de poliuretanos con un contenido renovable importante mediante el uso de polioles de origen natural, más concretamente, acetato de celulosa y aceite de ricino. Estos polioles se someten a un proceso de reacción con diisocianatos alifáticos o aromáticos reactivos ―diisocianatos de 4,4'-difenil metano (MDI) y 1,6-hexametileno (HMDI), respectivamente― mediante una reacción de condensación convencional en dos etapas. De este modo, en una primera etapa se llevó a cabo la funcionalización total o parcial del acetato de celulosa con diisocianatos a temperatura ambiente y en atmósfera inerte, empleando tanto disolvente para la reacción (tolueno) como catalizador (trietilamina). Posteriormente, el biopolímero modificado se mezcló con aceite de ricino en determinadas proporciones, produciendo así poliuretanos bio-basados que se dejaron curar en condiciones ambientales tras su aplicación.

Por otro lado, los adhesivos sintetizados fueron caracterizados mediante diversas técnicas experimentales. En primer lugar, los análisis de espectroscopía de infrarrojos permitieron evaluar la estructura química de los poliuretanos, así como monitorizar la evolución del proceso de curado. Además, se llevaron a cabo ensayos térmicos, incluyendo análisis termo-gravimétricos (TGA) y ensayos de calorimetría diferencial de barrido estándar y modulado (DSC y MDSC), con el fin de evaluar las transiciones y estabilidad térmicas. Finalmente, se estudió el comportamiento reológico y la capacidad adhesiva de los poliuretanos sintetizados a partir de recursos naturales, mediante medidas de torsión oscilatorias y ensayos mecánicos estandarizados para la determinación de las fuerzas de tracción, pelado y flexión, respectivamente, comparándolas con las obtenidas con marcas comerciales de referencia. Mediante esta metodología experimental se evaluó la influencia de la naturaleza del isocianato empleado―ya sea aromático o alifático― y de las proporciones de los reactivos empleados. Además, se estudió el impacto que sobre las propiedades finales produce una modificación del procedimiento de síntesis en dos pasos previamente descrito, usando una ruta sintética simplificada y más sostenible al constar de una sola etapa reactiva en ausencia de disolvente y catalizador.

El protocolo de síntesis tradicional en dos etapas resultó ser adecuado para la producción de adhesivos de poliuretanos a partir de diversas combinaciones de acetato de celulosa funcionalizado con isocianatos difuncionales (HMDI o MDI) y aceite de ricino. En todos los casos, los resultados obtenidos de las medidas térmicas y espectroscópicas confirmaron la naturaleza segmentada característica de los poliuretanos, presentando temperaturas de transición vítreas correspondientes a cada uno de los dominios, duros y blandos. El incremento de la relación molar NCO:OH demostró favorecer la compatibilidad termodinámica entre fases, ocasionando un aumento tanto en las funciones viscoelásticas como en la temperatura de transición vítrea asociada a los segmentos blandos. Se obtuvieron propiedades de adhesión óptimas en madera con una relación en peso 1:1 de aceite de ricino y acetato de celulosa funcionalizado con HMDI, equivalente a una relación NCO:OH de 1.87, ligeramente superior al 1.45 correspondiente a su homólogo aromático de mayor reactividad.

Por otro lado, los adhesivos naturales sintetizados produjeron fuerzas de adhesión en madera y acero inoxidable equiparables o incluso superiores a las correspondientes obtenidas con los adhesivos comerciales de referencia, a pesar de presentar una drástica reducción en sus rendimientos a altas temperaturas (100 ºC) o sobre sustratos poliméricos apolares, como es el caso del polietileno. Los poliuretanos obtenidos con MDI exhibieron un comportamiento termo-reológicamente simple en todo el rango de temperaturas analizado (desde -10 a 200 ºC), alcanzando la región vítrea del espectro mecánico. Por el contrario, la aplicación del principio de superposición t-T se restringe a temperaturas inferiores a 80-100 ºC, en la región plateau del espectro mecánico, para los sistemas sintetizados a partir del isocianato alifático (HMDI).

La implantación de un proceso reactivo directo, en una sola etapa, demostró no sólo su viabilidad para la preparación de adhesivos de poliuretanos conforme, en mayor medida, a los principios de la *Química Verde*, sino también una mejora de la respuesta adhesiva de los mismos, junto al efecto de fortalecimiento suscitado por el empleo del derivado celulósico. Finalmente, la adición de acetato de celulosa causó un incremento en la estabilidad térmica de los adhesivos preparados, al mismo tiempo que redujo la duración del proceso de curado inducido por la humedad, en condiciones ambientales.

3. Justification

On account of the irreversible environmental damage caused by the utilization of non-renewable raw materials in the industrial production, since the end of 20th century, the interest in replacing the traditionally applied petroleum-based starting compounds in the adhesive field by more sustainable feedstocks has grown enormously. This ever-increasing environmental consciousness in pursuit of the development of both greener products and methodologies, thereby meeting to a larger extent the principles of *Green Chemistry*, has been fostered by the implementation of a set of national and international initiatives and stricter regulations.

Therefore, during the last decades some adhesives derived from natural resources, like sugars, starch and proteins, have been proposed to satisfy such expectations. Unfortunately, however, their application has been limited, owing to their reduced lifespan and low resistance to solvents and chemicals. The well-known remarkable properties of polyurethanes, mainly synthesized through a selective polycondensation reaction between active isocyanate and hydroxyl groups, has enabled to surpass the limitations of their aforementioned natural-based forerunners in the adhesive area.

Additionally, the feasibility of manufacturing polyurethanes from various natural platforms has been amply demonstrated. Indeed, among others, lignocellulosic biomass, primarily composed of hemicellulose, cellulose and lignin, has been proven effective in increasing the renewability of polyurethanes, due to their significant hydroxyl content, thereupon implemented as elastomers, coatings, lubricants, etc. On the other hand, vegetable oils have emerged as promising polyol precursors. For that purpose, given their scant reactivity, most investigations have encompassed a series of chemical modifications in order to confer hydroxyl functionality upon these plant oils. Even though some natural oils already exhibit a certain hydroxyl character (lesquerella or castor oils), which allows them to be implemented without further functionalization, some investigations revealed that their application as replacement for traditional petro-based polyols is constrained, yielding a significant loss in the ultimate performance of resulting polyurethanes.

Nevertheless, the research group in which this PhD thesis has been developed has succeeded in completely replacing non-renewable polyols by a hydroxylated vegetable oil, more specifically castor oil, improving the physical and mechanical stability of the resulting polyurethanes, through the chemical modification of lignocellulosic substances, devised for their application as effective lubricating greases. Following this approach, albeit previous studies have assessed the application of castor oil, whether modified or in its original form, for adhesion purposes, this dissertation attempts to delve into the potential production of efficient and competitive bio-based polyurethane adhesives from a hitherto unexplored combination of environmentally compatible natural resources, namely cellulose acetate and unmodified castor oil, together with reactive diisocyanates, viz. 1,6-hexamethylene diisocyanate and diphenylmethane-4,4'-diisocyanate.

4. Objectives

As spelled out in the previous section, this PhD thesis aims at devising novel bio-sourced polyurethane adhesives, raising their renewable nature through a complete replacement of the traditional petroleum-derived polyols by hydroxyl-bearing natural substances, more specifically cellulose acetate and castor oil, deemed as polyurethane platforms.

Pursuant to such target, first cellulose acetate functionalization with reactive isocyanates, conceived to improve its subsequent chemical interaction with castor oil, was intended to be optimized. Therefore, this study aims to elucidate the role of the associated reaction conditions and parameters, including the isocyanate chemical structure (whether aliphatic or aromatic) and the degree of cellulose acetate modification (evaluated in terms of the NCO:OH molar ratio), along with the further NCO-terminated cellulose acetate to castor oil weight proportion, as the main parameters enabling to tailor the ultimate polyurethane performance. This issue was addressed by means of different experimental techniques towards a comprehensive products' characterization with the additional objective of comparing their ultimate adhesion performance with that found in commercial benchmarks.

Finally, the impact assessment of implementing a greener solvent-free straight-through synthetic pathway, thereby preventing the application of more complex procedures and avoiding the use of associated potentially dangerous chemicals has been one of the specific objectives of this work.

5. Structure of the manuscript

The present manuscript, stemming from a doctoral research framed within the actions intended to reduce the environmental impact of polyurethane adhesives, is structured into five main sections, which are briefly detailed below.

The present introductory *Chapter 1* allows to gain an insight into the background that inspired the development of this investigation. In addition, the objectives to be implemented, along with a summary of the investigation progress, are also established in this chapter.

Chapter 2 State of the art includes the basics of polyurethane chemistry and properties, beside a review of the approaches hitherto pursued towards a polyurethane preparation meeting the *Green Chemistry* tenets. Moreover, this section highlights the fundamental notions of adhesives and adhesion processes, stating their common rheological and adhesion responses, and finally focusing on the research advancement on the synthesis of bio-based polyurethane adhesives.

Chapter 3 Materials and methods. This part of the manuscript, besides outlining the synthetic pathways and the deployed materials for the preparation of bio-sourced polyurethanes, highlights the characterization techniques applied to gain a comprehensive understanding of the synthesized adhesives.

Chapter 4 Results and discussion, representing the keystone of this PhD Thesis, is divided into four main blocks, comprising the studies conducted during this research which are organised following the model of scientific journal manuscripts. Block 1, which embraces the already published articles (see Annexe 1), refers to the synthesis and characterization of natural polyurethanes based on an aliphatic diisocyanate (HMDI), as well as the comparison of the optimal formulation with commercial benchmarks. Block

2 examines the influence of using different input NCO:OH molar ratios, ranging from 2 up to 4.53, when considering an aromatic isocyanate in lieu of its aliphatic counterpart, while Block 3 evaluates the impact of replacing the traditional two-step preparation protocol by a greener synthetic pathway, consisting of a single-step procedure devoid of any reaction solvent and catalyst for the production of polyurethane wood-adhesives. The articles associated to Blocks 2 and 3 comprise the manuscripts pendant of acceptance in renowned scientific peer-reviewed journals.

Chapter 5 Conclusions comprises the most significant findings inferred from the results obtained in this experimental work.

Chapter 2
State of the art

1. Basics of polyurethanes: historical impact, properties and synthesis

Under the stimulus of high molecular weight polyamides auspiciously synthesized by E.I. DuPont, Otto Bayer and collaborators, through the genuine discovery of the polycondensation reaction between alcohols and isocyanate by Wûrtz, succeed in developing polyurethane fibres in 1937 (Bayer, *1947*) aimed to compete with commercialized nylon-based counterparts. However, they were unaware of the rapid expansion such materials would experience, representing a milestone in the polymer chemistry. Nonetheless, it was not till the recognition of their exceptional elasticity by DuPont and ICI in 1940 when their industrial manufacturing commenced. This was the beginning of the history of a sort of polymer whose dynamism would make them expand towards unimaginable limits (Szycher, *2013*).

Indeed, worldwide average annual polyurethane consumption rose from 12.9 until 16.1 Mt from 2011 to 2016, and according to the worldwide statistical study conducted by The Statistics Portal (*2018*), a growth of 20% is envisaged till 2021.

Polyurethanes excel by their unrivalled features, including exceptional flexibility, tear and adhesion strengths and outstanding resistance to solvents, chemicals and abrasion, what allows them for being applied in a plethora of areas, such as footwear (Che et al., *2017*) or wood (Sahoo et al., *2017*) adhesives, foams (Akintayo et al., *2013*), coatings (Liu, G. et al., *2016*), among others.

1.1. Polyurethane synthesis

Although the fabrication of polyurethanes can be performed through an array of synthetic pathways, polycondensation reaction between organic polyfunctional isocyanate (-NCO) and alcohols (-OH) leading to the carbamate linkage (Figure 2.1) is the most widely applied industrial procedure (Ali et al., *2014*; Yeganeh and Mehdizadeh, *2004*).

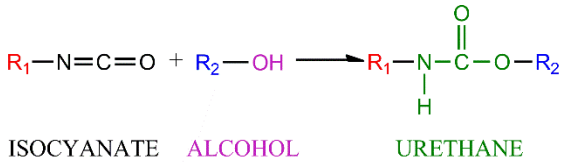

Figure 2.1 Main reaction for urethane production

Moreover, polyaddition reaction can be conducted via following any of these two methods: the *prepolymer method* in which an isocyanate-terminated prepolymer is developed, subsequently undergoing a crosslinking or chain extension by adding low molecular weight chain extenders (CE) or crosslinking agents (CA), respectively (Krol, *2007*; Manjula et al., *2010*); while in the *one-shot process* the polymerization is carried out by blending all reagents in a single step (Szycher, *2013*) (Figure 2.2).

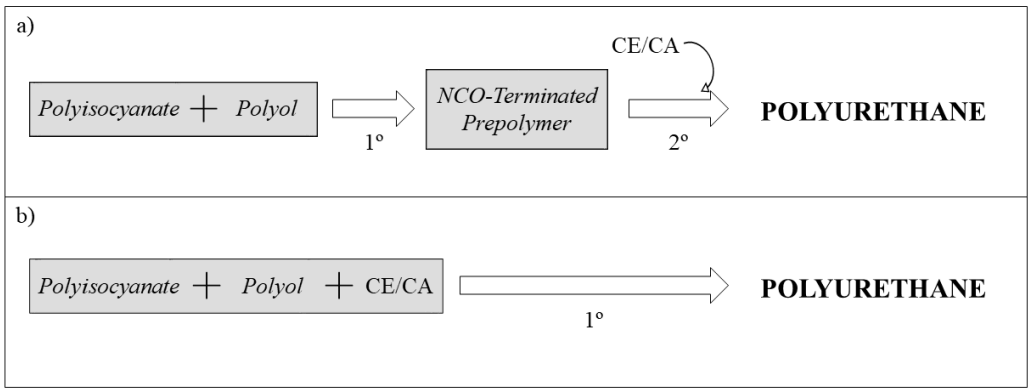

Figure 2.2 Schematic polyurethane synthesis via a) prepolymer process and b) one-shot procedure

Nevertheless, polymeric urethanes seldom contain solely urethane repeating units, since manifold side or other secondary desired reactions are expected, as it is the case of those environmental moisture-curing polyurethanes prepared by Daniel da Silva et al.(*2006*; *2008*), Narute and Palanisamy (*2016*) or Campanella et al. (*2009*) for adhesive and foam purposes. Therefore, when polyurethanes still containing free reactive NCO functional groups come into contact with atmospheric humidity, free isocyanates are hydrolysed producing carbamic acid (Figure 2.3), whose instability provokes its dissociation into carbon dioxide and amine, which may further react with an additional NCO group leading to urea bonds.

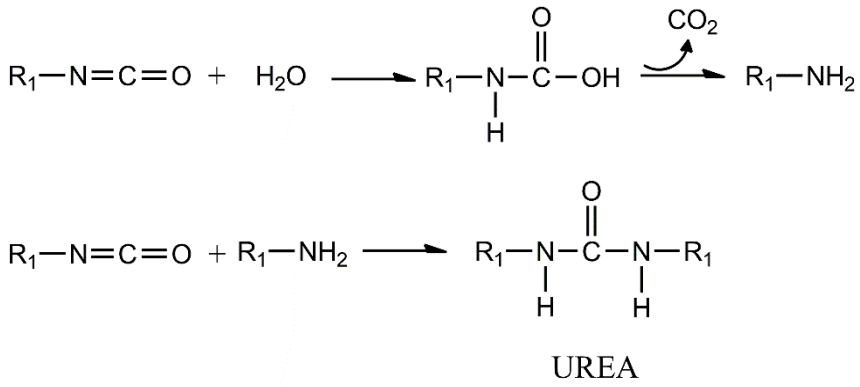

Figure 2.3 Reactions taking place in environmental conditions

Owing to their beneficial properties, polyurethane-urea materials have increasingly been developed thus appearing a wide range of investigations assessing the kinetics study of moisture-curable polyurethanes (Allauddin et al., *2013*; Malucelli et al., *2005*).

Although, moisture-curing has been recently proved to be the fastest side reaction, under conducive circumstances, urea and/or amine are not the only likely by-products, given the variety of products arising from interactions of isocyanate with the starting materials leading among others to biuret, allophanate, isocyanurate or uretidione, whose appearance is especially favoured at high temperatures (Ling et al., *2018*; Saunders, *1959*).

1.2. Raw materials

Polyurethane building blocks, containing two or more functional groups, can be divided into: polyisocyanates, polyols and chain extender/crosslinking agents. Concerning polyols, they typically consist of polyesters, polyethers or polycarbonates, whereas isocyanates can be eventually classified into aromatic and linear- or cyclic-aliphatic. Notwithstanding the most popular utilization of aromatic isocyanates, due to their higher reactivity and more affordable price (Gabriel et al., *2016*), they have been claimed to exhibit lower light and ultraviolet resistance, leading to toxic and carcinogenic products through photodegradation (Rezayan et al., *2017*).

Table 2.1 Typical isocyanate structures

a) $H_{12}MDI$

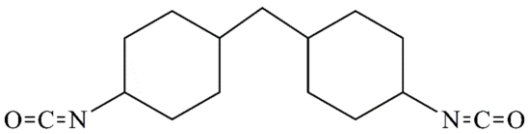

b) HMDI

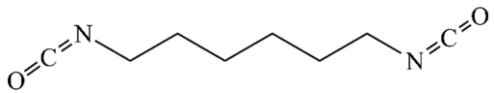

d) LDI

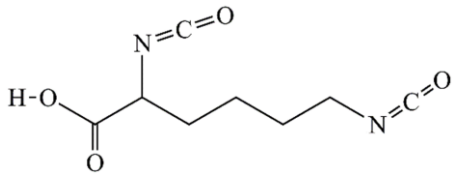

c) IPDI

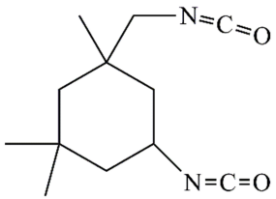

e) MDI

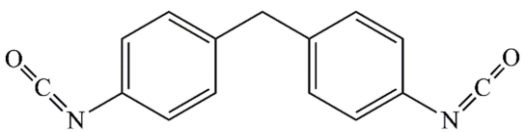

g) 2,6-TDI

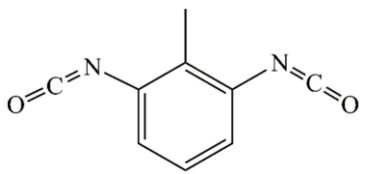

h) XDI

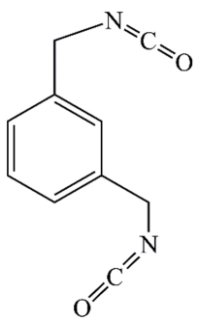

f) 2,4-TDI

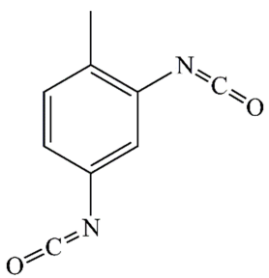

i) PPDI

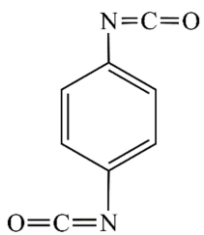

Table 2.1 collects the most common isocyanates, including among others 4,4'-diphenyl methane diisocyanate (MDI), 2,4-toluene diisocyanate (2,4-TDI), 2,6-toluene diisocyanate (2,6-TDI), 4,4'-dicyclohexylmethane diisocyanate (H_{12}MDI), xylene diisocyanate (XDI), naphthalene 1,5-diisocyanate (NDI), lysine-diisocyanate (LDI), p-phenylene diisocyanate (PPDI), 1,6-hexamethylene diisocyanate (HMDI), isophorone diisocyanate (IPDI) (Chattopadhyay and Raju, *2007*; Pawar et al., *2015*).

The functionality of both isocyanate and alcohol strongly influence the nature of the ensuing polyurethane, so that linear thermoplastic polyurethanes are obtained when their raw materials exhibit a functionality of 2, while a more crosslinked thermosetting polymer network can be achieved by increasing the functional groups per molecule (Lligadas, et al., *2010*).

Finally, not only low-molecular weight difunctional alcohols or amines can act as chain extenders in the polyurethane preparation, but also dicarboxylic acids can be considered, as revealed the studies of Manjula and co-workers (Manjula, *2007*; Manjula et al., *2010*) who reported the use of di- or tri-carboxylic acids, including glutaric, maleic or citric acids, in the chain extension step. As happened with isocyanates and alcohols, in order to prepare highly crosslinked polyurethanes, a greater functionality is sometimes required.

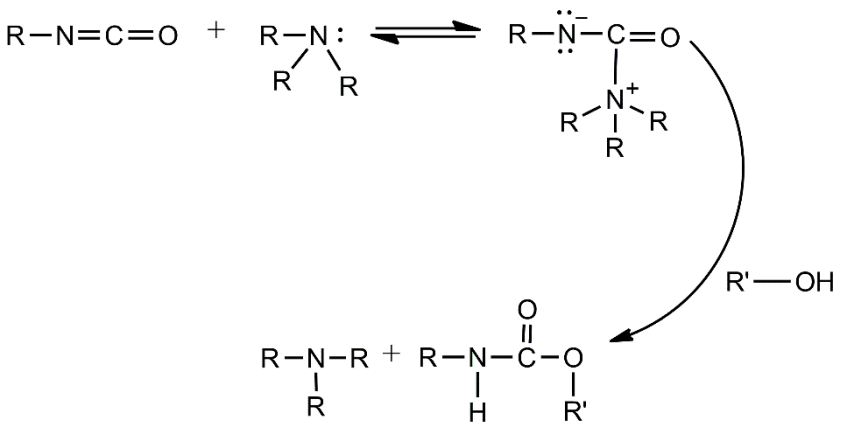

Figure 2.4 Example of catalytic mechanism for tertiary amine catalysts

Moreover, aimed at facilitating the polycondensation reaction at milder conditions and at high rates, tertiary amines and organometallic compounds effectively catalyse the polyurethane synthesis according to the catalytic mechanism shown in Figure 2.4.

1.3. Microphase separation and hydrogen bonding

Polyurethanes typically consist of an elastomeric segregated structure, comprising a flexible non-polar segment domain so-called *soft segments* (*SS*), and a stiff polar segment domain also known as *hard segments* (*HS*). While the former segments usually proceed from the hydroxyl bearing polymers representing the amorphous low-glass transition elastomeric blocks in the polyurethane network, the latter involve chain extender and isocyanate backbones and render the high-glass transition and partially ordered macromolecular frame (Abdolhosseini and Givi, *2016*; Xiao et al., *2017*).

Therefore, as a consequence of the difference in polarity of these microdomains, hydrogen bond type interactions between hard segments are expected, causing a thermodynamic incompatibility between both phases, what in turn leads to their well-known phase separation limited to the microscale (Corcuera et al., *2010*). Furthermore, hard segments are randomly distributed along the soft segment matrix forming discrete aggregates, thus acting as reinforcing crosslinking points in the flexible domain.

Phase separation has become such a fundamental issue in polyurethane chemistry that innumerable scientific researches, with the aid of different techniques such as electro-spin resonance (ESR), differential scanning calorimetry (DSC) or wide-angle X-ray diffraction (WAXD) (Culin et al., *2004*; Wang, G. et al., *1994*), have dealt with the influence of different parameters on the microphase segregation. Among them, Velankar and Cooper (*1998*) and Güney and Hasirci (*2014*) analysed the chemical structure and content of soft domains when using poly-ε-caprolactone as polyols with intended biocompatible features, corroborating the improved flexibility and strength with longer chain-polyols. Despite the simple determination of different phases through DSC analysis by identifying independent glass transition temperatures (T_gs) corresponding to each domain, recently Xiao et al. (*2017*) noveltyly applied energy dispersive spectrometry (EDS), together with more conventional methods, to analyse the degree of

phase segregation in waterborne polyurethane systems. Besides, other studies also addressed the influence of not only the isocyanate-bearing adducts content (Somani et al., *2003*) and nature (Corcuera et al., *2011*), but also the chemical composition of the chain extenders (Corcuera et al., *2010*) on the phase mixing properties developed by elastomeric polyurethanes.

Therefore, the degree of phase miscibility is the key to allow tuning their outstanding properties and can be controlled by judiciously modifying the chemical nature and functionality of their building blocks, molecular weight, isocyanate to alcohol ratio, processing conditions, etc. Consequently, polyurethanes' properties can be easily tailored to meet the requirement for a certain application, emerging a class of polymers characterised by a well-recognised tunability allowing for the production of materials whose ultimate properties range from viscous to elastic, from soft to hard and even from fibrous to porous (Deka and Karak, *2009*; Güney and Hasirci, *2014*).

Given the primary responsibility of hydrogen bonding between polar fractions for the occurrence of a segmented three-dimensional polyurethane networks and its significant role in the resistance to hydrolysis (Yilgör et al., *2000*), the appropriate understanding of this interaction is particularly important. Even though hydrogen bridges are a type of secondary bonds in which a partially positively charged hydrogen atom is weakly linked to a partially negatively charged atom (typically nitrogen or oxygen), hydrogen bonding is not a simple issue in polyurethane systems. Thus, H-bonds can be established between hard segments, so that the N-H groups may act as proton donors, while carbonyl (C=O) and alkoxy (C-O-C) functional groups serving as proton acceptors, provoking the self-association of HSs. However, soft domains, arising from polyols, contribute with electronegatively charged functional groups, including carbonyl unit (C=O) and the ether or ester oxygen atoms (C-O-C) (Queiroz et al., *2003*; Zimmer et al., *2017*), leading to what Mattia and Painter (*2007*) called inter-association between both microdomains. Consequently, the existence of proton donor not only in urethane, but also in urea linkages, in conjunction with the wide arrange of proton acceptors, whose bond strengths noticeably differ from one another, results in a complex competition between self- and inter-association via hydrogen bonding (Figure 2.5) (Queiroz et al., *2003*; Su et al., *2016*).

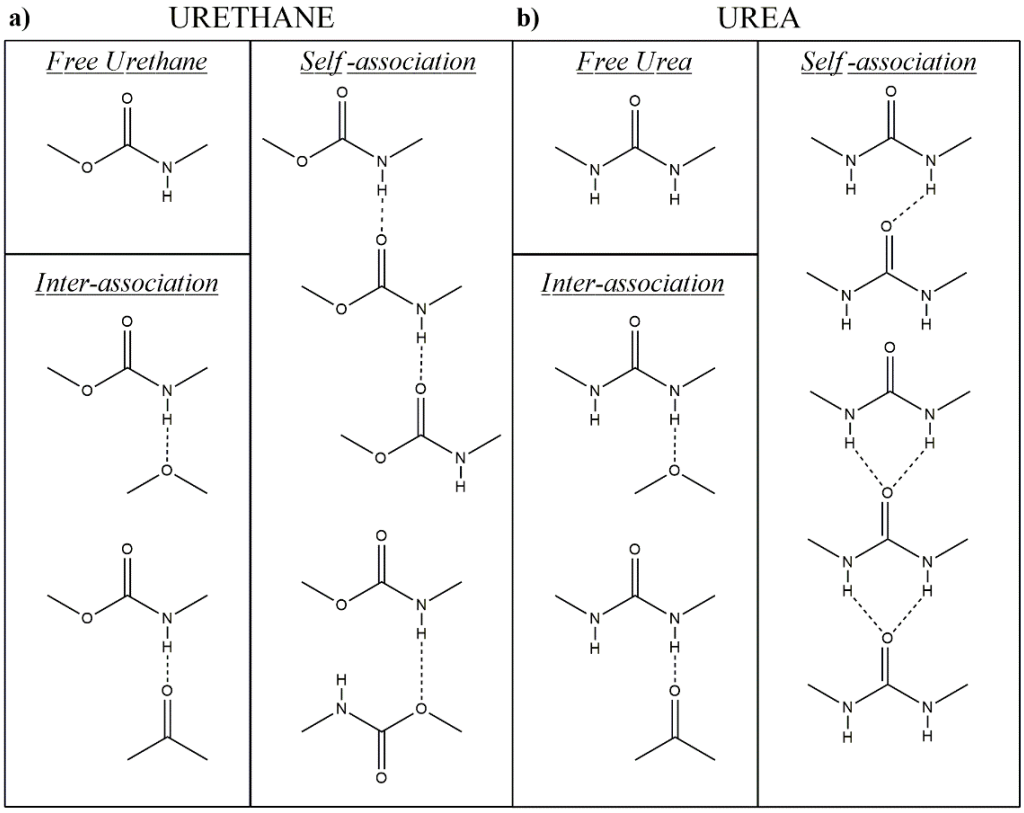

Figure 2.5 Factible hydrogen bonds in poly(urethane-urea) systems considering self- and inter-association with a) urethane and b) urea linkages

Bearing in mind its significant influence on the polyurethane properties at both micro and macro scales, the assessment of the microphase separation resulting from the formation of the hydrogen bonds between hard and soft segments has become the main focus of a large number of investigations (Ayres et al., *2007*; Bistričić et al., *2010*; Lee, H. S. et al., *1987*; Ruanpan and Manuspiya, *2018*). Among other analytical techniques, Fourier-transform Infrared Spectroscopy (FTIR) excels by its applicability for the determination of the phase-separated structure of polyurethanes through hydrogen bonds identification, since the characteristic intensity and frequency attributed to vibrational absorption peaks reveal a certain sensitivity to the occurrence of H-bonds, so that the stronger hydrogen bridges the greater shift to lower wavenumbers experience the stretching absorption bands in the amine (N-H) and carbonyl (C=O) regions (Gurunathan et al., *2015*). In fact, at the end of the 20th century such susceptibility was confirmed by the investigations of Coleman et al. (*1986*; *1988*), Lee et al. (*1987*) and Ning et al. (*1996*;

1997) finding out within hydrogen-bonded carbonyl functional groups different degrees of ordered, thus appearing the so-known concepts of "*ordered*" and "*disordered*" carbonyl groups, and, no long after, the complementary character of the DSC analysis in the evaluation of hydrogen bonding was released (Fernández d'Arlas et al., *2008*; Yilgör et al., *2000*).

Nevertheless, infrared spectroscopy not always allows for a quantitative analysis owing to the usual overlapping between different contributions, resulting from negligible differences in terms of hydrogen bond's strengths. For that purpose, it is necessary to make use of additional mathematical procedures aimed to decompose or deconvolute the obtained results into the different individual contributions, as it has been conducted in previous studies (Gurunathan et al., *2015*; Ruanpan and Manuspiya, *2018*; Rueda-Larraz et al., *2009*) (Figure 2.6).

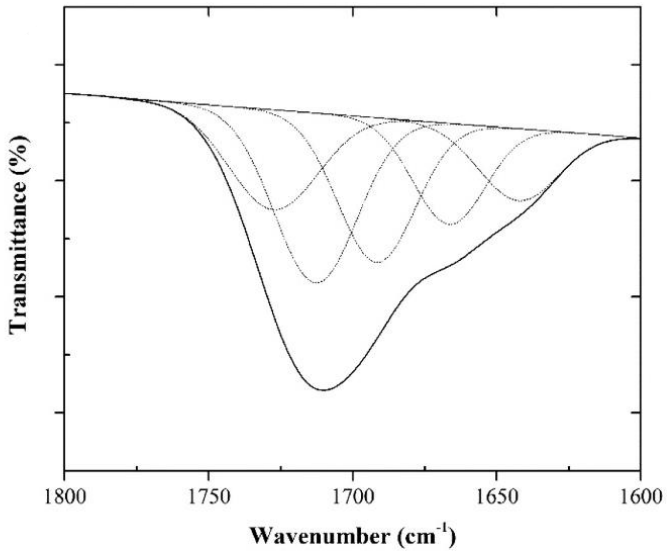

Figure 2.6 Deconvolution of the C=O region into individual Gaussian-curves (Rueda-Larraz et al., 2009)

1.4. Polyurethane modifications

Despite their appealing and beneficial features, polyurethanes conventionally exhibit a relatively low resistance towards high temperatures and mechanical stress, beside their lacking electrical conductivity or deficient flame retardance (Javni et al., *2000*). Due to

these inherent constraints, the research activity has been forced to devise novel strategies and/or mechanisms to meet these emerging requirements.

For that purpose, the most widely recognized procedure focuses on the production of nanocomposites by either *in situ* or *ex situ* pathways, so that additional nanoparticles may interact with the polyurethane network via strong primary forces or by mere secondary interactions, respectively (Guo, Z. et al., *2008*). The addition of inorganic nanoparticles (ZnO, $CaCO_3$, Al_2O_3, SiO_2 or TiO_2) to polyurethanes not just based on polyester polyols (Petrović et al., *2000*), but also on polyether (Bistričić et al., *2010*) and polycarbonates (Pavličević et al., *2014*), in order to modify their properties via hydrogen bonds rearrangement has been reported. Notwithstanding the potential applications of other feasible choices, like the production of PU-hydroxyapatite composites with auspicious features for their application in living organisms (Gabriel et al., *2016*), or the addition of silane-modified talc fillers (Bajsić et al., *2017*), the utilization of silica particles at the nanoscale is greatly spread, which according to Petrovic's study (Petrović et al., *2000*) can lead to more suitable enhancements compared to silica microparticles. Therefore, SiO_2 fillers have been added in the raw state, as reported by Bistričić et al. (*2010*) or Lee et al. (*2005*) whose optimum concentrations range from 1-3%, or even after different thermal modifications in order to reduce the silanol content at the surface (Vega-Baudrit et al., *2007*) whose density proved to strongly influence the reinforcing effect of silica nanoparticles thanks to the improved hydrogen bonding ability.

Furthermore, silicon has also been applied in the form of the soft phyllosilicate montmorillonite, most commonly known as clay, to achieve the expected thermal and mechanical responses of polyurethanes. In this sense, the utilization of naturally occurring nanoclays (Cervantes-Uc et al., *2009*) has been proposed, although their compatibility with the polyurethane network might be enhanced with the aid of organic modifications (Berta et al., *2006*; Strankowski et al., *2012*), demonstrating the flame retardant and mechanical reinforcing effects of these montmorillonite nanoparticles, reaching an increase of 600% in the mechanical strength, as Xiong et al. (*2004*) revealed in their study when preparing organic-montmorillonite with methylene-bis-*ortho*-chloroanilline (MOCA).

Moreover, as a consequence of their apparent advantages, such as low price, sustainability and biodegradability, high strength, etc., natural fibres, either of animal (inter alia silk (Manjula et al., *2010*) and flax (Tayfun et al., *2015*) fibres) or vegetable (i.e. lignocellulosic materials) origin, embody another type of conventional fillers. Consequently, in the last decade the use of cellulose microcrystals (Głowińska and Datta, *2015*; Głowińska and Datta, *2016*) and microfibrils or their derivatives, cellulose nanowhiskers (Park et al., *2013*) and nanofibrillated cellulose (Benhamou et al., *2015*), have been considered for the *in situ* copolymerization to produce polyurethane composites, achieving a proper reinforcement effect at low particles' concentrations (0.5-3%) due to the improved cellulose-polyurethane interactions through physical and chemical bonds.

On the other hand, whether the electrical conductivity is intended to be improved besides mechanical and thermal degradation behaviour, the synthesis of nanohybrids of polyurethanes in conjunction with the allotropes of carbon, graphene, graphite and carbon nanotubes (Figure 2.7) appears as the most effective alternative (Ciecierska et al., *2016*; Otieno and Kim, *2008*; Wu et al., *2016*). Moreover, when graphene is considered, it is typically used after undergoing a reduction pretreatment to produce graphene oxide (Thakur and Karak, *2014*), what may allow for their simultaneous use as reinforcements and reactive chain extenders. Similarly, the aggregation of carbon nanotubes can be avoided by means of covalent bonds establishment, between NCO-terminated prepolymer and reactive carbon nanotubes upon surface modification (Zhang et al., *2015*).

Hitherto, all the reported modifications have been focused on the *in situ* or *ex situ* copolymerization technology by the incorporation of supplementary substances, albeit their shortcomings could be surpassed via modifying their building blocks. Thereby Sung et al. (*2016*) modified methylene diphenyl diisocyanate by inserting uretonimine linkages, while, for their part, Liu and Ye (*2010*) synthesized difunctional fluorinated polyether alcohol, both of them intended to ameliorate the ultimate polyurethane weaknesses. Finally, since chain extension is regarded as a critical issue in the polyurethane production, the incorporation of unconventional chain extenders has also been the focus of some investigations, like those conducted by Yarmohammadi and

Shahidzadeh (*2018*) or Kultys and coworkers (Kultys and Pikus, *2001*; Rogulska et al., *2017*), which used sulfur-containing chain extenders allowing the authors to appropriately tune their properties, even producing colourless polyurethane systems. It is also noteworthy the improvements obtained by the inclusion of fluorine groups in the polyurethane structure reported by Su et al. (*2016*) owing to the hydrogen bonding taking place between fluorine (-CF_3) and amine (N-H) functional groups.

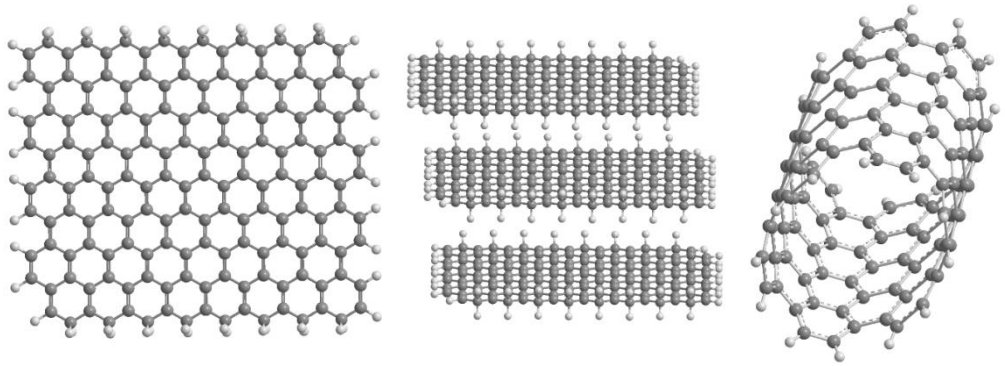

a) b) c)

Figure 2.7 Carbon allotropes commonly used in PU modification: a) Graphene; b) Graphite and c) Carbon nanotubes

2. New strategies in the polyurethane production towards Green Chemistry

In the previous section all the properties and benefits associated to urethane polymers have been highlighted. Nevertheless, the conventional industrial production of these systems deeply relies on petroleum stocks. As a consequence of the exhaustion of crude reserves, its subsequent floating price, along with the stringent regulations and environmental awareness, the present paradigm in the polyurethane research has shifted towards the exploration of new synthetic routes characterised by the utilization of sustainable raw materials and leading to renewable bio-based products (More et al., *2013*).

In addition, the term "*bio-based product*" means any product derived from natural and renewable resources of any kind, but it entails neither biodegradability nor biocompatibility (Desroches et al., *2012*). Indeed, biodegradable polyurethanes,

typically intended to temporary biomedical applications, are required to contain linkages ready to degrade under biological circumstances, also showing biocompatible properties, i.e. easy metabolisation and lacking of toxicity, able to play their role without causing hazardous effects in the living organism (Cherng et al., *2013*).

In this sense, considering the polyol building block, enzymatic hydrolysis of the ester bond in polyester-polyols makes them more appealing for the production of biodegradable polyurethanes (Abdollahi et al., *2015*). Thus, polyester polyols like polycaprolactone (Kupka et al., *2016*), polylactic acid (Rezayan et al., *2017*), and polyacrylic or polyglycolic acids (Su et al., *2016*; Wu et al., *2016*) have demonstrated not to produce toxic decomposition products. However, not only polyester but also polycarbonate polyols can be proposed as biocompatible polyurethane precursors, as it has been shown by Zhu et al. (*2016*) when assessing the biostability of poly(1,6-hexanediol) carbonate diol-based polyurethanes. Furthermore, as shown in the investigations of Calvo-Correas et al. (*2015*; *2016*), Li et al. (*2014*) and Basterretxea et al. (*2016*), *L*-lysine and dimeryl diisocyanates exhibited suitable biocompatible and biodegradable behaviour.

Moreover, the renewability and biocompatibility in the polyurethane network can be raised by means of chain extenders, as can be found in the investigation of Abdollahi et al. (*2015*), who conducted the prepolymer chain extension with different combinations of 1,4-butanediol and curcumin aiming to preserve the polyurethane biocompatibility, while Kavanaugh et al. (*2016*), in pursuit of medical regeneration, combined the use of biodegradable polyols (poly-ε-caprolactone) with a series of osteogenically active molecules, among which β-glycerol phosphate demonstrated its capacity to act as chain extender in the production of cytocompatible segmented polyurethanes, showing a potential consideration in subsequent *in vivo* analysis. Moreover, Oprea et al. (*2016*) succeeded in improving the biodegradation of polyurethane composites owing to the fungal susceptibility of ester group located in the vegetable oil (viz. castor oil) chain extender and the cellulose filler, strongly bonded to the urethane network through covalent bonds.

To summarise, the main focus of the current investigation is the partial or complete replacement of non-renewable raw materials by new eco-friendly alternatives, conforming to the concept of "*sustainability*", which in agreement with Dubé and Salehpour (*2014*) means "*the ability to meet the current needs without jeopardizing the ability of future generations to meet their own needs*". Nevertheless, due to the greater difficulties in replacing non-sustainable isocyanates, most of researchers have devoted their investigations to the development of polyurethanes with improved renewable content considering the use of lignocellulosic biomass, polysaccharides and natural oils as polyol sources, as detailed below.

2.1. New alternative feedstocks: polyols and polyisocyanates

2.1.1. Lignocellulosic materials and derived compounds as polyol precursors

Lignocellulose represents the most copious natural occurring biomaterial, which together with its nonedible nature and significant hydroxyl functionality confer its particular appeal as renewable platform for the polyurethane production (Octave and Thomas, *2009*).

Lignocellulosic materials comprehend cellulose, hemicellulose and lignin, as the main compounds among other minor constituents (tannins, proteins, ash, etc.), whose composition is not evenly distributed, but strongly depends on the biomass' nature (Table 2.2). Cellulose consists of cellobiose disaccharide repeating units (*Figure 2.8*), forming mostly independent fibrils of a linear homopolymer, establishing weak hydrogen bond interconnections. Hemicellulose represents the second major component of lignocellulose and comprises different heteropolymers whose building blocks are monosaccharides, including pentoses like xylose and arabinose, and hexoses like mannose, glucose and galactose, apart from uronic acids. Moreover, lignin is essentially an aromatic amorphous polymer comprising three main phenylpropanoid units: *p*-hydroxyphenyl, guaiacyl and syringil monomers (*Figure 2.8*), acting as crosslinker between cellulose and hemicellulose (Isikgor and Becer, *2015*; Octave and Thomas, *2009*).

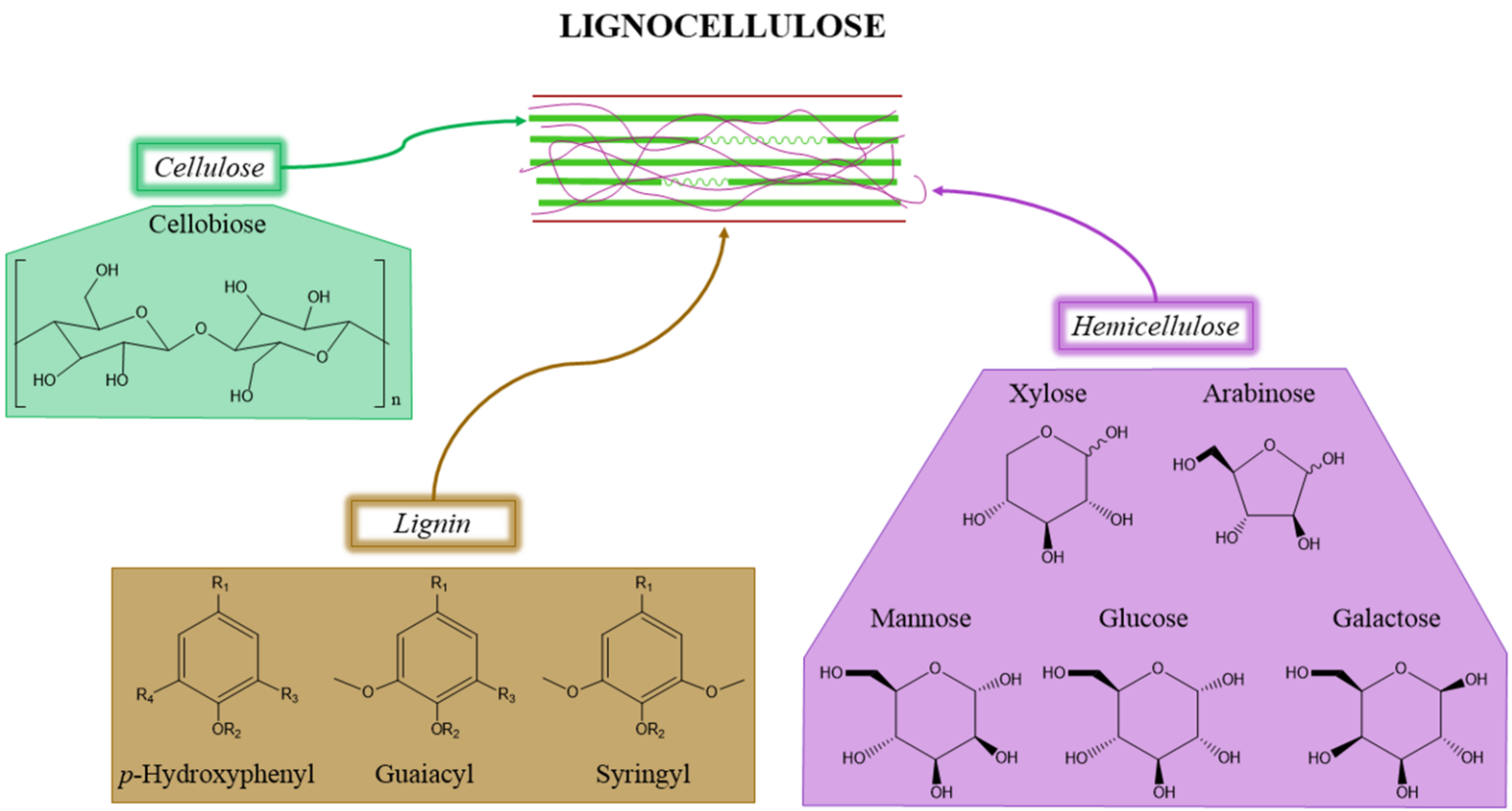

Figure 2.8 Structure of lignocellulosic biomass

Table 2.2 Composition of common lignocellulosic materials (Isikgor and Becer, 2015)

Lignocellulosic Biomass		*Cellulose [%]*	*Hemicellulose [%]*	*Lignin [%]*
Hardwood	Eucalyptus	54	18	22
Softwood	Spruce	46	23	28
Agricultural waste	Corn Cobs	34-41	32-36	6-16
	Corn Stalks	35-40	17-35	7-18
	Wheat Straw	35-39	23-30	12-16
	Rice Straw	29-35	23-26	17-19
	Sugarcane Bagasse	25-45	28-32	15-25

Due to the fact that lignin is primarily obtained as a byproduct in the paper industry, the still reduced market niche and its reactive and hydroxyl-groups bearing character, lignin appears as a potential precursor for the production of polyurethanes (Jeong et al., *2013*). As a consequence of the steric hindrance, lignocellulosic biomass may be submitted to different modifications to improve the accessibility of the hydroxyl groups, for instance to further react with isocyanate moieties (Griffini et al., *2015*). The predominant chemical modifications to do that can be classified into *liquefaction* and *oxypropylation*, which will be described in the next sections. Nevertheless, aimed to avoid the adverse impact on the competitiveness of the bio-based polyols emerging from the energy loss and the inherent economic cost associated to the implementation of such additional steps (Griffini et al., *2015*), some researchers have addressed the development of renewable polyurethanes from unmodified polysaccharides. With this aim, Araujo and Pasa (*2003*) dedicated their study to the direct utilization of a residual guaiacyl-syringyl-based lignin containing residual polysaccharide resulting from the *Eycalyptus* tar distillation, so-called biopitch, in combination with different proportions of hydroxyl-terminated polybutadiene for the preparation of elastomeric polyurethanes. Additionally, Griffini et

al. (*2015*) demonstrated the effectiveness of polyurethane film preparation from fractionated softwood Kraft lignin, revealing the improved degree of sustainability of such coatings through a simplified synthetic route. Furthermore, Gallego et al. (*2016*; *2015a*) extended the application of lignocellulosic biomass in their natural form to the achievement of bio-inspired lubricating greases, preparing NCO-terminated thickening agents through a controlled condensation reaction of HDI not only with Kraft cellulose pulp, but also with some derivatives such as methylcellulose (Gallego, *2013a*; *2013b*) or (methyl) 2-hydroxyethyl cellulose (Gallego et al., *2015b*). More recently, Borrero-López et al. (*2017*) functionalized alkali Kraft lignin with a wide selection of aliphatic and aromatic isocyanates to evaluate the curing kinetics while analysing the evolution of the viscoelastic response of the ensuing castor oil-based polyurethanes.

2.1.1.1. Liquefaction

This treatment is based on the solvolysis of lignocellulosic biomass at temperatures in the range of 150-250 ºC, leading to smaller hydroxyl-bearing molecules by dint of the utilization of polyol solvents (ethylene or polyethylene glycol), and usually an acid catalyst (Li et al., *2015*). Besides that, in order to prepare polyurethanes from long-chain polyfunctional alcohols, the resulting liquified units are typically submitted to a further transesterification producing natural polyester polyols, as reported by Sinha and coworkers (Desai, Emanuel et al., *2003*; Mishra and Sinha, *2010*) and Patel et al. (*2016*), in which the glycosides resulting from an acid liquefaction (α-D-glycoside and β-D-glycoside) with sulfuric and/or *p*-toluene sulfonic acids, were esterified with oils or fatty acids at low pressure and high temperatures (220-250 ºC), using lithium hydroxide as catalyst (Figure 2.9).

This solvolytic reaction is an effective process to increase both the functionality and sustainable nature of the starting polyols, though the optimization of the reaction conditions (temperature, time, catalyst and biomass to solvent weight ratio) to mitigate the occurrence of secondary reactions and to reduce to the minimum possible the remaining solid content (Li et al., *2015*). Thus, some studies (Soares et al., *2015*) intended to optimize, in terms of biomass conversion, the experimental conditions

(temperature, time and catalyst concentration) to obtain liquified polyols from coffee grounds, accomplishing a 70% of yield at 160 ºC, 80 min and sulfuric acid at 4% (w/w).

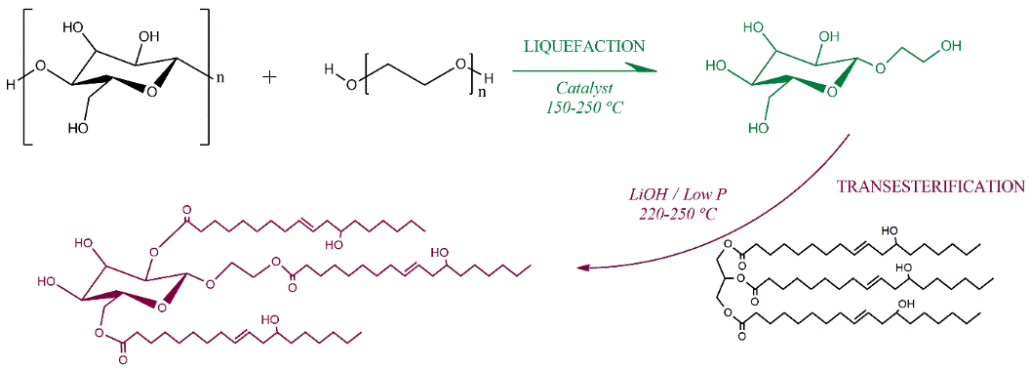

Figure 2.9 Liquefaction of cellulose with a subsequent tranesterification

Despite liquefaction modification can be conducted through the use of a series of solvents, as Liang et al. (*2007*) showcased when evaluated the kinetics of the liquefaction procedure on different feedstocks, the most challenging issue is to decrease or even eliminate its dependency on petroleum derivatives (Li et al., *2015*). On the other hand, as a consequence of the rapid expansion of the biodiesel industry, in which crude glycerol is produced as a byproduct, several studies suggest the incorporation of crude glycerol as solvent for the liquefaction of, inter alia, the solid residues of the saccharification of sunflower stalk (Kim et al., *2016*) and empty fruit bunches (Lee et al., *2016*), achieving a yield of 59% and 47.9%, respectively, in the production of bio-based polyols.

2.1.1.2. Oxypropylation

Unlike liquefaction, when optimized, oxypropylation is a chemical reaction capable of incorporating more readily available hydroxyl groups without using any solvent, simultaneously maintaining the biomass functionality (Gandini, *2008*). This modification consists of a base catalysed grafting of propylene oxide onto lignocellulosic materials under high pressure and temperature (650-1820 kPa and 100-200 ºC) (Li et al., *2015*). As a result of the incorporation of short propylene oxide chains to lignocellulosic biomass, the starting solid material can be converted into a viscous polyol (Raquez et al., *2010*).

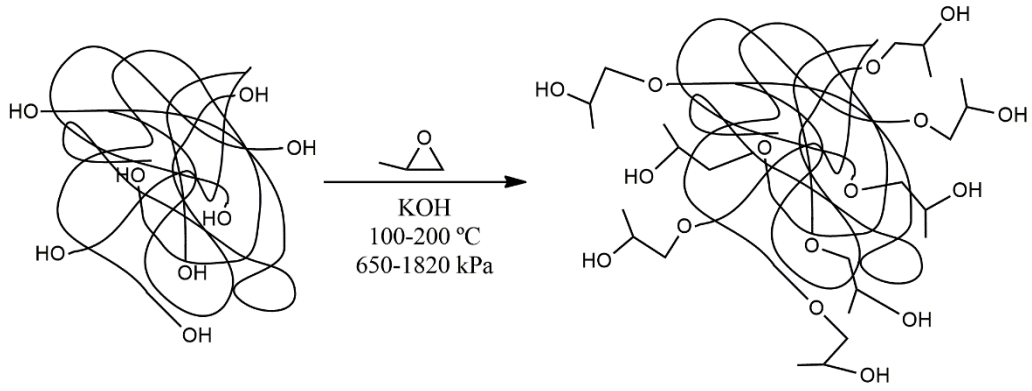

Figure 2.10 Oxypropylation of lignocellulosic biomass

As related to any chemical transformation, some side reactions can be found yielding not only to partially oxypropylated biomass, but also polypropylene oxide homopolymers, which, however, may take part in the chain extension of the polyurethane prepolymer (Li et al., *2015*; Raquez et al., *2010*). Bearing this fact in mind, and due to the high-pressure requirements, the application of oxypropylation to produce bio-sourced polyurethane may be to some extent hindered. Even so, some researchers have devoted their investigations to the production of polyurethane foams prepared from oxypropylated cork powder (Evtiouguina et al., *2002*).

2.1.2. Vegetable Oils

In search of the compliance of the sustainable development standards, vegetable oils have drawn the attention in the last decades as feasible alternatives for the partial or total replacement of unsustainable raw materials to produce cost-effective and renewable urethane polymers (Hojabri et al., *2010*). The excellent properties of such natural oils, including their abundantly availability, non-toxicity, sustainability, easy handling and structural versatility, are the driving force of their consideration as polyol sources (Lligadas et al., *2010*).

Table 2.3 Vegetable oils composition (%) (Ogunniyi, 2006; Sharma and Kundu, 2006; Shirke et al., 2015)

Fatty Acid	Palm	Canola	Soybean	Sunflower	Linseed	Castor	Cotton S.	Tung
Ricinoleic 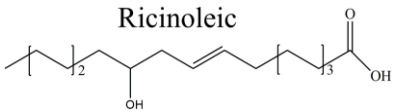						89		
Linoleic 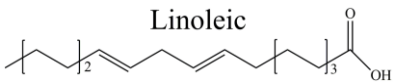	11	21.0	53.3	60	15.3	4.2	54.4	4
Oleic 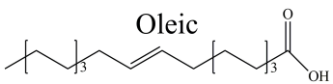	39	60.9	23.4	20	19.1	3.0	18.6	8
Stearic 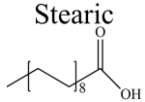	4	1.8	4.0	5	3.5	1	2.6	4
Palmitic 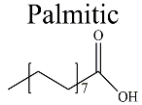	44	4.1	11.0	6	5.5	1	21.6	

Fatty acid	Palm	Canola	Soybean	Sunflower	Linseed	Castor	Cotton S.	Tung
Dihydroxystearic 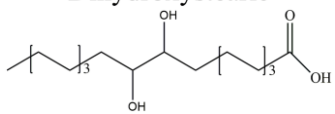						0.7		
Linolenic 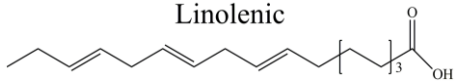	1	8.8	7.8	1	56.6	0.3	0.7	
α–Elaeostearic 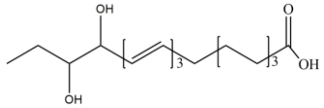								84
Eicosanoic 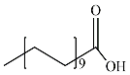						0.3		

Vegetable oils are mainly composed of triacylglycerides holding three aliphatic fatty acid chains composed of 12-22 carbon atoms and a double-bond functionality ranging from 0 to 3 per chain typically located at the 9th, 12th or 15th C-atom (Figure 2.11) (Lligadas et al., *2010*; Sharma and Kundu, *2006*). Each vegetable oil exhibits a characteristic fatty acid profile, which might even vary within the same type of oil, depending on the plant variety and provenance (Zlatanić et al., *2004*). The composition of the most common oils in terms of saturated (eicosanoic, dihydroxystearic, palmitic, stearic) and unsaturated (linolenic, linoleic, oleic, ricinoleic, α-elaeostearic) fatty acids are collected in Table 2.3.

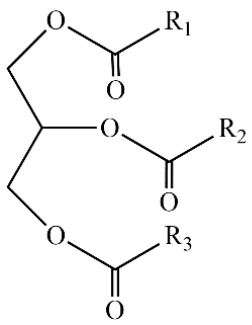

R_1, R_2, R_3: Fatty acid chains

Figure 2.11 Generic structure of vegetable oils

The improved hydrolytic and thermal resistance due to the hydrophobic character of vegetable oils are remarkable qualifications. Nevertheless, what really makes natural oils such a reasonable chemical platform for bio-polyurethane development, is the possibility to be subjected to a wide range of structural and functional variations, providing them an exceptional chemical versatility. Thus, the presence of amenable unsaturations and ester groups opens a myriad of possibilities to increase the hydroxyl functionality of vegetable oils, overcoming their relatively unreactive nature (Campanella et al., *2009*).

Even though the production of appropriately functional polyols from vegetable oils has been reported through a series of chemical modifications, as will be further discussed, some studies propose the production of "*green*" polyurethane macromolecules by direct utilization of a limited group of natural oils containing hydroxylated fatty acids, essentially castor and lesquerella oils. In this way, Ferreira et al. (*2007a*) produced bioadhesives for tissue engineering by direct modification of castor oil with IPDI via

prepolymer method, in contrast with the straight through process applied by Raghunanan et al. (*2018*) when preparing elastomeric adhesives from castor oil and HMDI. Moreover, Hablot et al. (*2008*) and Abdolhosseini and Givi (*2016*) applied the one-shot formulation procedure to synthesize elastomeric polyurethanes. Moreover, Sharma et al. (*2014*) reported the systematic substitution of polypropylene glycol by castor oil for the production of polyurethane foams, proving the still need for only a partial replacement of petro-based polyols, given the property loss when considering castor oil as the only hydroxyl group source. This fact has also been corroborated by Septevani et al. (*2015*) who gradually substituted polyether polyol by a commercial polyester polyol derived from palm kernel oil, obtaining an appropriate foam behaviour of the ensuing polyurethane until a critical degree of substitution of 30%, above which the properties of the foam became poorer.

In the following sections the major synthetic modifications affecting the functional active sites of not only vegetable oils, but also fatty acids (C-C double bonds and ester groups) will be described.

2.1.2.1. Epoxidation

The formation of oxirane groups appears as one of the most widely employed double bond modifications for the production of polyols from vegetable oils. Epoxidation may be performed by using either prepared or *in situ* generated peracids (arising from the reaction between acids and hydrogen peroxide) and sulfuric acid as catalyst, followed by an additional ring opening (Figure 2.12.a). This hydroxylation step essentially consisting of a nucleophilic attack is the controversial and most engaging point in the polyol production, since an appropriate selection of nucleophile allows for the optimization of important factors such as hydroxyl functionality, appearance of dangling chains and reactivity in terms of availability of the hydroxyl groups (Desroches et al., *2012*; Li et al., *2015*; Nohra et al., *2013*).

In this respect, the *in situ* oxirane ring opening may be performed under acid conditions with water as the reagent, obtaining two secondary hydroxyl groups per double bond. Thus, Narute and Palanisamy (*2016*) applied the epoxidation and *in situ* ring opening

with water on cottonseed oil aimed to synthesize bio-sourced polyurethane coatings with an optimum NCO:OH molar ratio of 1.8. However, the nucleophilic attack in this process can be conducted not only by water, as shown by the study of Pechar et al. (*2007*) in which the initial acetic acid giving rise the *in situ* epoxidation of soybean oil was also the responsible for the subsequent hydroxylation through a previously patented protocol (Casper and Newbold, *2006*), so that the polyol functionality halves. More recently, Mekewi et al. (*2017*) simulated the *in situ* procedure with water by blending the epoxidized vegetable oil with deionized water and *p*-toluene sulfonic acid, achieving afterwards a partial replacement of the petrochemical polyols (50%) to produce ink plasticizer polyurethanes.

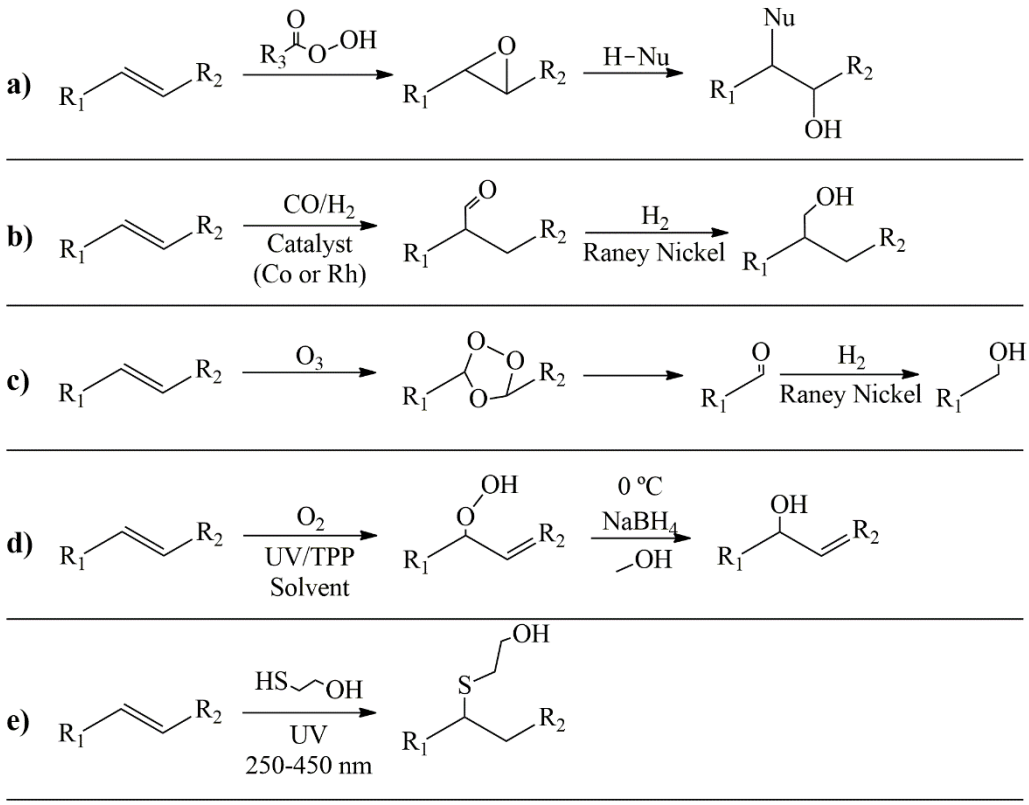

Figure 2.12 Double bonds modifications: a) epoxidation-hydroxylation; b) hydroformylation; c) ozonolysis; d) air oxidation; e) thiol-ene coupling

As a consequence of the intrinsic constraints associated to batch production, such as the unavoidable long reaction times, side reactions and the inherent start-up and shutdown stages, Ji et al. developed a novel continuous microreaction method with improved

surface to volume ratio, thus improving the mass and energy transfer during epoxidation and subsequent nucleophilic attack with water in order to produce polyurethane rigid foams (Figure 2.13) (He et al., *2013*; Ji et al., *2015*). In summary, these authors optimized the polyol production in two steps, first analysing the epoxidation conditions (75 ºC, 3% H_2SO_4, H_2O_2/formic acid/C=C of 8:8:1) leading to an optimum epoxy number of 7.3 in only 6.7 minutes of residence time (He et al., *2013*), and afterwards the hydroxylation step (75 ºC, 10% H_2SO_4, 13 min) producing soy-polyols with more uniform molecular weights characterised by a greater hydroxyl value (Ji et al., *2015*), evincing the remarkable advantages of the microflow technology over the polyol production in batch.

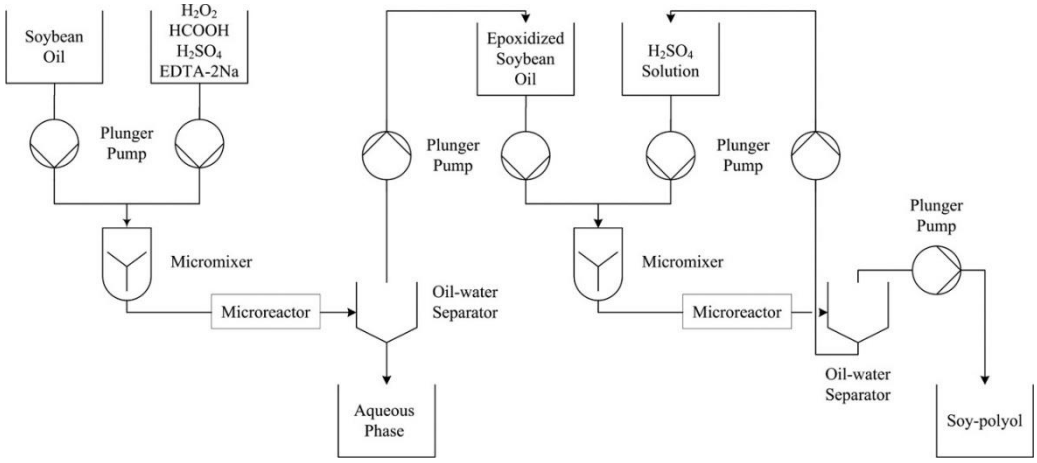

Figure 2.13 Continuous microreaction process for soy-polyols synthesis (Ji et al., 2015)

On the other hand, when considering acids as the hydroxylation agents, the polyol functionality might be improved, like for instance in the lipase-catalysed hydroxylation of epoxidized soybean oil with lactic acid performed by Miao et al. (*2010*) or in the application of castor oil fatty acids avoiding the utilization of either solvent or catalyst at the expense of increasing the temperature (130-190 ºC) (Zhang et al., *2013*; Zhang et al., *2015*). However, in some instances such as in adhesive formulations that require gelification, in some extent to ensure a suitable and safe adhesive application, a lower hydroxyl value with secondary functional groups may be required (Ang et al., *2014*). Moreover, inorganic acids such as hydrochloric o hydrobromic acids can also be used, albeit the utilization of a polar organic solvent is essential to overcome their incompatibility with vegetable oils (Guo et al., *2000*).

Furthermore, alcoholysis of the oxirane ring with monofunctional alcohols in the presence of an acid catalyst provides natural polyols with secondary OH groups (Desroches et al., *2012*). In addition, given that the unsaturation density and location in the fatty acid chains are the significant variables in natural oils, Zlatanić et al. (*2004*) analysed the influence of hydroxyl functionality (from 3 up to 5.2) and dangling chain lengths of polyols manufactured from different oils on the resulting polyurethane, reporting the strong proportional relation between glass transition temperature and density of crosslinking with polyol functionality, while the impact of the dangling chains was negligible.

On the other hand, conversion with polyfunctional polyols makes possible the simultaneous incorporation of secondary and primary hydroxyl groups into the C=C linkage. In this way, investigations dealing with diethylene glycol and 1,2- and 1,3-propanediol as hydroxylation agents can be found (Rojek and Prociak, *2012*; Zieleniewska et al., *2014*). Datta and Głowińska (*2014b*; *2014a*; Głowińska and Datta, *2015*) employed propanediols derived from glycerol resulting from the biodiesel production and corn sugar fermentation processes, while Kong et al. (*2012*) proposed an inexpensive combination of hydroxylation and transesterification with 1,2- and 1,3-propanediol in order to increase the polyol functionality and to reduce the molecular weight and viscosity of the resulting polyurethanes, increasing their resistance to hydrolysis and alkali attack. The polyol obtained from the combination of those modifications succeeded in such a way that it was quickly marketed by the name of Liprol™ (Meadow Polymers, Consolidated Biofuels Ltd., Canada), which would be further used in conjunction with cellulose nanocrystals to prepared polyurethane nanocomposites (Kong et al., *2016*). Another pioneering study is the conducted by Norhisham et al. (*2017*) which addresses the production of biodiesel fuel-based polyols (fatty acid methyl ester) combined with palm olein polyol to synthesize elastomeric polyurethanes with greater natural content and an appropriate pressure sensitive adhesive response, using boron trifluoride diethyl ether complex (BF_3) as the alcoholysis catalyst.

Catalytic hydrogenation is reckoned as another oxirane ring opening reaction leading to secondary alcohols due to the inclusion of both hydrogen atoms to the double bond with the aid of a Raney nickel catalyst (Al-Ni) at high pressures (Desroches et al., *2012*).

According to Petrović et al. (*2007*), this method shows a certain flexibility, since the ultimate hydroxyl value of the hydrogenated polyol can be tuned by carefully controlling the reaction times, what inevitably influences the properties of the resulting soybean oil-derived polyurethane, being possible to obtain from glass to rubber systems. Conversely, Monteavaro et al. (*2005*) modified the polyol functionality through different *in situ* hydrogenation times on epoxidized soybean oil as well, though the OH functionality range (1.9-3.2) did not exceed the resulting from the Petrovic et al. study (2.7-4.4). Furthermore, in former investigations, Petrovic and co-workers (Guo et al., *2000*) assessed the influence of the hydrogenation type procedure on the hydroxyl functionality, so that epoxidized soybean oil was hydrogenated by using hydrochloric and hydrobromid acids, methanolysis and catalytic hydrogenation, demonstrating the improved functionality of halogen bearing polyols (up to 4.1), whereas the only liquid polyol was the methoxylated one at room conditions.

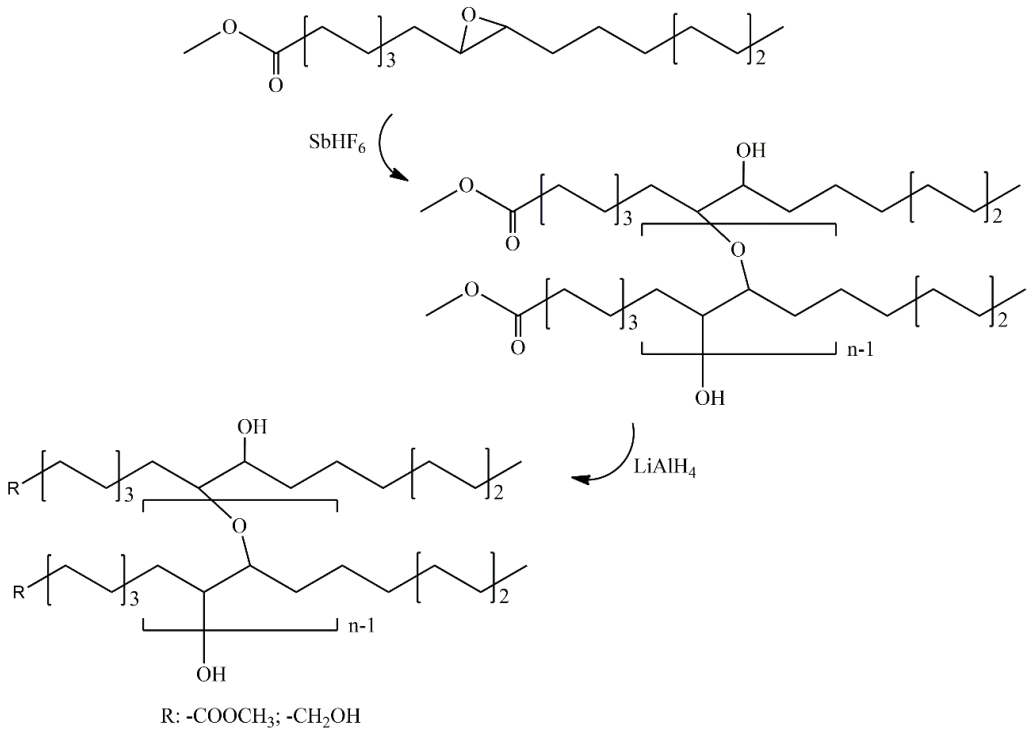

Figure 2.14 Oligomerization of fatty acids followed by carboxylate groups reduction (Lligadas et al., 2006)

Finally, an alternative to the hydroxylation through a nucleophilic attack comprises ring opening oligomerization and subsequent reduction of ester groups. Thus, Lligadas et al. (*2006*) reported the epoxidation of methyl oleate and further oligomerization catalysed by fluoroantimonic acid ($SbHF_6$), followed by a partial reduction of the carboxylate functional groups with lithium aluminium hydride ($LiAlH_4$) at room temperature, aimed to incorporate primary hydroxyl groups into the polyether polyol chemical structure (Figure 2.14). A similar reduction process was conducted by Zhang et al. (*2014*; *2015*) on epoxidized (soybean and linseed) and raw (castor) oils, but at low temperatures (0 ºC), thus obtaining hydroxyl values at least threefold higher than those reported by Lligadas et al.

2.1.2.2. Hydroformylation

Hydroformylation falls into the category of modifications providing primary alcohols from natural oils or fatty acids, without increasing their functionality, as only one OH group can be incorporated per double bond. Therefore, first an intermediate aldehyde is typically produced using an inlet flow of synthesis gas (CO/H_2) and a cobalt or rhodium catalyst, then conducting the followed reduction with H_2 and a Raney nickel catalyst (Figure 2.12.b). The choice of the catalyst is particularly important as it will directly affect the reaction yield (Co-67% vs Rh-95%). At the expense of a reduction in the yield of the reaction, the utilization of cobalt-based catalysts entails some benefits, essentially their lower prices and the possibility to act as hydrogenation catalyst as well, though under more severe conditions (Desroches et al., *2012*; Li et al., *2015*). Furthermore, the type of catalyst considered in the production of the natural polyol may also influence the response of the resulting polyurethane, as Guo et al. reported when producing hydroformylated soybean oil (Guo et al., *2002*), obtaining bio-based polyurethanes whose behaviour ranged from rigid plastic to hard rubber polyurethanes when using rhodium and cobalt catalysts, respectively.

2.1.2.3. Ozonolysis and hydrogenation

This oxidation protocol emerges as an alternative to previous modifications, where the synthesized polyols exhibit dangling chains with their respective plasticizing effect

(Nohra et al., *2013*), since ozonolysis allows for the synthesis of polyols with primary terminal hydroxyl groups, provided that vegetable oils solely comprise unsaturated fatty acids. This greater OH availability may be translated into faster condensation reactions with isocyanates thanks to the lower stearic hindrance, despite its functionality limitation of a maximum of 3 hydroxyl groups per vegetable oil molecule owing to the reaction mechanism, and the production of alcohols of low molecular weights (Petrović, *2008*) typically removed due to their deleterious effect on the final polyurethane, diminishing its microphase separation and the associated beneficial properties (Alagi and Hong, *2015*).

Ozonolysis comprises the formation of ozonide when treating double bond with ozone (O_3), which subsequently decomposes into aldehyde and carboxylic functional groups, giving raise to the C=C cleavage. Afterwards, the already known hydrogenation step with Raney nickel catalyst is performed to reduce aldehyde groups into primary alcohols (Figure 2.12.c) (Desroches et al., *2012*; Li et al., *2015*).

Nevertheless, some of the drawbacks of the ozonolysis-hydrogenation of double bonds are the extreme pressures and temperatures, and the requirement for toxic solvents in the final reduction (Raquez et al., *2010*), inasmuch as initial ozonolysis was reported to be conducted in deionized water at 0ºC and the subsequent hydroxylation in tetrahydrofuran (THF) under 130 ºC and 350 psi of hydrogen pressure (Narine et al., *2007*). Thereupon, Kong et al. (*2007*) devoted one study to the enhancement of the previous protocol via the replacement of the traditional hazardous THF by a more environmentally friendly ethyl acetate during the whole process, using zinc as a reagent for the reduction of the ozonide groups to aldehydes at room temperature. With all these improvements, along with the reduction of temperature and pressure during hydrogenation (70 ºC and 100 psi), an increase of thee hydroxyl number from 152.4 up to 235.2mg KOH/g was obtained, much closer to the theorical 251 mg OH/g. On the other hand, the efficiency of canola oil ozonolysis was even higher when performing the ozonolysis at lower temperatures (from -30 to -40 ºC) in a blend of methylene chloride/methanol, followed by a reduction with sodium borohydride ($NaBH_4$) at 10-15 ºC (Petrovic et al., *2005*). Moreover, another variant worthwhile to mention is the one-step ozonolysis in the

presence of NaOH, $CaCO_3$ or H_2SO_4 catalysts and polyols that will interact with the ozonide functional groups to produce polyester polyols (Figure 2.15) (Tran et al., *2005*).

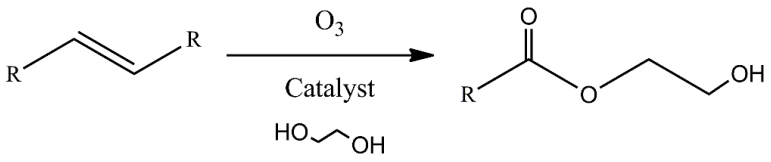

Figure 2.15 One-step ozonolysis

2.1.2.4. Oxidation with air

Similarly, oxidation with oxygen (O_2) can provide plant oil-derived polyols first producing a hydroperoxide (-OOH) through a UV-radiation process with thiamine pyrophosphate in dichloromethane, followed by the reduction with $NaBH_4$ in methanol at 0 ºC and catalytic hydrogenation in ethyl acetate (Figure 2.12.d). However, the requirement for reaction times in the order of days and the poorer oxidation control compared with other modifications, such as epoxidation, have restricted the application of air-oxidation to synthesize bio-sourced polyurethanes (Desroches et al., *2012*; Petrović, *2008*).

2.1.2.5. Thiol-ene coupling

The last modification regarding fatty acid chain unsaturations is the so-known thiol-ene coupling. This process, regarded as click chemistry and based on the addition of thiol linkages (HO-R-SH, mainly 2-mercaptoethanol) onto C=C double bonds, leads to polyols with primary hydroxyl groups through an eco-friendly and highly efficient radical mechanism (Figure 2.12.e). This procedure may be initiated by either UV-radiation (Desroches et al., *2011*) or thermal induction (Caillol et al., *2013*).

The appeal of this reaction comes from the possibility to produce bio-based polyols with a wide range of functionality through a simple, lacking of any solvent, efficient and cost-competitive procedure under air conditions (Alagi and Hong, *2015*), despite presenting some disadvantages such as the presence of dangling chains and also the production of some by-products (Nohra et al., *2013*). However, as most of the products resulting from

the side reaction have been proved to be hydroxyl-bearing compounds, they could still participate in the polycondensation reaction with reactive isocyanates. Desroches et al. (*2011*) addressed in their study the optimization of the thiol-ene coupling conditions (intensity of radiation, solvent and double bond contents) for the photoaddition of 2-mercaptoethanol onto oleic acid, to be further applied on rapeseed oil, thus reducing the reaction time, but still obtaining byproducts.

Furthermore, it is possible to obtain polyols with terminal primary hydroxyl groups if the photochemical grafting of thiols is combined with allyl esterification, as Lligadas et al. reported when preparing diols via thiol-ene coupling after esterification of oleic and 10-undecenoic acids with allyl alcohol (Paz, *2010*), and even controlling the chain length through a step-growth photopolymerization using a dithiol followed by a phototermination with 2-mercaptoethanol producing polyester polyols with a tailorable molecular weight (Lluch et al., *2010*). The versatility of thiol-ene click reaction was also highlighted by the investigations of Alagi et al., who succeeded in both controlling the soybean-based polyol functionality (Alagi et al., *2016a*) and accomplishing the quantitative conversion to hydroxyl of soybean and castor oils unsaturations (Alagi et al., *2016b*) by sensibly adjusting the reaction time and temperature, along with reagents' concentrations. Moreover, the preparation of multifunctional polyols via thiol-ene coupling incorporating silane, fluorine and ethylene oxide (Alagi et al., *2018*) or acrylate (Chen, G. et al., *2016*) functional groups has been recently reported, aimed to improve either the coating properties or the UV-curing speed, respectively.

2.1.2.6. Transamidification and (trans)esterification

Although the modification of fatty acid chains has been focused on the carbon to carbon double bonds, the production of bio-based polyols via ester functional group transformation is also attainable, by means of transamidation and (trans)esterification processes.

Amidification consists of the reaction of vegetable oils with amines and a catalyst at high temperatures (100-120 ºC) leading to amides and alcohols, although as diethanolamine is typically regarded as amidification agent of plant oils, alcoholamides are commonly

obtained together with glycerol (Figure 2.16.b) (Desroches et al., *2012*). Moreover, if triethanolamine was considered as reagent, a transesterification process would occur, leading to poly (ester urethane) instead of the previous poly (urethane amide) (Yakushin et al., *2013*). In addition, a wide array of catalysts has been reported, ranging from metal oxides (Pawar et al., *2015*) to different salts, like stannous octoate (Fridrihsone et al., *2013*) or zinc acetate (Stirna et al., *2013*).

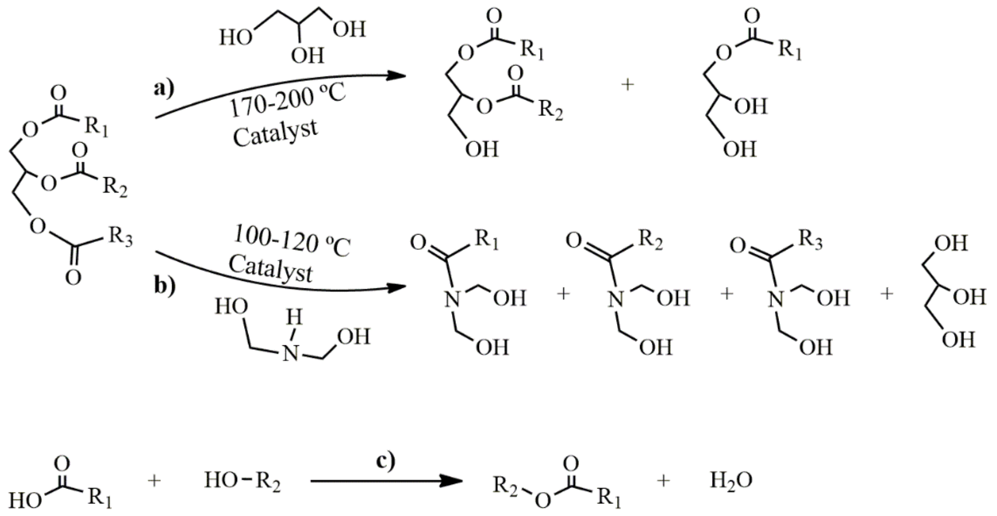

Figure 2.16 Ester group modifications: a) transesterification; b) transamidification; c) direct esterification

Especially noteworthy is the progress achieved by Patil et al. (*2017*), succeeding in the rise of polyurethane coatings natural content up to 65% with fairly competitive behaviour against the petro-based counterparts, by means of a further esterification of the cotton seed oil-based diethanolamide with bio-sourced difunctional carboxylic acids, inter alia succinic, sebacic, tartaric, maleic and azelaic acids, thus producing polyesteramide polyols as the polyurethane precursors.

Conversely, transesterification of vegetable oils comprises the reaction with multifunctional polyols, mainly glycerol, and catalysed by enzymes and organic and inorganic catalysts at high temperatures (170-200 ºC) (Figure 2.16.a) (Malik and Kaur, *2016*; Nohra et al., *2013*). Nevertheless, when considering heterogeneous catalysts, like lead oxide (PbO), greater temperatures are required, achieving values of up to 240 ºC, according to the resinification of Nahar seed oil described by Karak and coworkers (Das

et al., *2013*; Dutta et al., *2004*; Dutta and Karak, *2006*) for the development of monoglycerides to synthesize polyurethane resins. Unlike amidification, transesterification is a thermodynamically balanced reaction capable of modifying plant oil in a single step, what places it among the most appealing modifications (Alagi and Hong, *2015*). However, this reaction provides a mixture of the residual glycerol with mono-, di- and tri-glycerides, so that the maximum functionality is also limited, restricting the OH-source for polyurethane synthesis to mono- and diglyceride, along with the remaining transesterification agent (Li et al., *2015*). Moreover, the presence of dangling chains could only be advisable when flexible polyurethanes are intended to be obtained.

Due to the low apparent thermal resistance of glycerol, some studies deal with the utilization of other transesterification agents, such as pentaerythritol (Valero and Gonzalez, *2012*) or triethanolamine (Stirna et al., *2013*), as above indicated. Furthermore, a more specific reaction can be conducted when dealing with non-hydroxyl-bearing plant oils, viz. oils interesterification, as reported by Saravari and Praditvatanakit (*2013*) for the production of urethane alkyd from interesterified jatropha/castor oils.

Direct carboxylic acids esterification arises as alternative to transesterification, whether long molecular chain polyols are the primary target, obtaining water as a byproduct instead (Figure 2.16.c) (Desroches et al., *2012*). Therefore, the so-called fusion of lauric (Badri et al., *2006*) and ricinoleic (Somani et al., *2003*) acids with ethylene glycol, as well as the production of polyester polyols from direct esterification of dicarboxylic acids with castor oil (Moghadam et al., *2016*) have been reported to produce polyester polyurethane with adhesion properties.

However, these three individual chemical routes cannot be necessarily applied independently, as demonstrated not only by the transesterification with methanol and subsequent amidification of the resulting methyl ester (Dutta and Karak, *2005*; Mahapatra and Karak, *2004*), but also several-step modification of vegetable oils via transesterification-direct esterification (Xu et al., *2008*) or transamidification-direct

esterification (Patil et al., *2017*) in order to produce polyester or poly(ester amide) diols, respectively.

2.1.2.7. Other modifications

Although the modifications above detailed are the most widely applied on vegetable oils and fatty acids, to produce polyols precursors of PUs some other transformations have been spread to a lesser extent, including dimerization and subsequent reduction of carboxylic groups to polyols (Liu, X. et al., *2011*), self-metathesis coupling producing a diol to be used as an unsaturated chain extender in the polyurethane production (Fonseca et al., *2016*) or even cross-metathesis prior to other carbon-to-carbon double bonds modifications aimed to produced terminal hydroxyl groups (Zlatanic et al., *2002*).

2.1.3. Waste products as polyurethane feedstocks

The ever-increasing worldwide population, which has increased in the last 60 years in 136.9 million of people (Worldometers, *2018*), implies a huge consumption of a great variety of end-use products and its corresponding agricultural and household disposal. As a consequence, recycling and reutilization of waste materials has drawn the attention in the research field in pursuit of "*greener*" processes and products.

In this sense, some agricultural wastes, such as cardanol, a phenolic oil obtained as a byproduct of the cashew industry (Figure 2.17), enable the polyurethane production from a different perspective, despite using the above described synthetic routes, like epoxidation of double bonds and further oxirane ring opening, as reported by Suresh (*2012*) who applied afterwards an additional saponification step to increase the hydroxyl value of the oxidized cardanol. By contrast Balgude et al. (*2016*), apart from directly using a commercial grade epoxidized cardanol, considered only the epoxy ring opening with multifunctional natural acids (tartaric, citric and adipic) to produce hydrophillically modified cardanol as starting polyol for waterborne polyurethane coatings.

Figure 2.17 Chemical structure of Cardanol (Suresh, 2012)

In addition, the massive production and consumption of poly(ethylene terephthalate) (PET) has encourage the development of new recycling ways to mitigate its environmental impact. Among other mechanisms, the depolymerization of PET-soft drink bottles via liquefaction with propylene (Cakić et al., *2012*), polyethylene (Cakić et al., *2016*) or triethylene (Cakić et al., *2018*) glycols have been reported for the preparation of polyurethane dispersions. Additional to the depolymerization step, a transesterification with castor oil has been conducted, also incorporating silica nanofillers (Cakić et al., *2017*; Cakić et al., *2018*). Moreover, (Zhou et al. (*2017*) recently verified the novel incorporation of recycled PET into both, soft and hard segment domains in waterborne polyurethanes, owing to the utilization of glycolyzed oligoesters as polyols and chain extenders in the PU synthesis.

Crude glycerol also appears as a feasible choice given its vast production as a secondary product in the biodiesel industry (Nohra et al., *2013*), so that it has been successfully converted into natural polyols by means of direct esterification with fatty acids to prepare polyurethane adhesives for bonding wood (Cui et al., *2017a*; *2017b*), similarly to the transesterification with diethanolamine of tall oil obtained from Kraft pulping (Yakushin et al., *2013*).

Finally, carbon dioxide, an inexpensive and abundant greenhouse gas, can offer a new synthetic route in the manufacturing of polyurethanes (Orgilés-Calpena et al., *2016a*), which can contribute with the alleviation of environmental pollution (Liu and Wang, *2017*). The synthesis of the CO_2-based polyols consists of the fixation of CO_2 with the aid of oxirane groups-bearing materials, using a metal catalyst, leading to polycarbonate

polyols (Figure 2.18), which have served to prepared footwear polyurethane adhesives (Orgilés-Calpena et al., *2016b*).

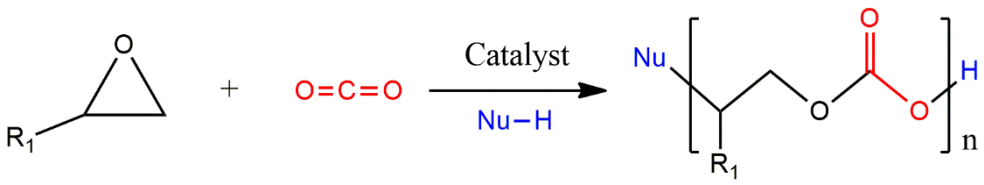

Figure 2.18 Oxirane ring carbonatation

2.1.4. Synthesis of more sustainable isocyanates

All the renewable alternatives so far reviewed are founded on the development of natural polyols that will act as a polyurethane building block. So that, most of the research production tends to deal with the synthesis of "*more*" renewable polyurethane by generating bio-based polyols, without paying attention to the other PU-major component isocyanates, which comes from petroleum resources (Raquez et al., *2010*).

Among other synthesis mechanisms, the conventional Curtius and Hoffman rearrangements, which consist of the rearrangements of acyl azide or amide groups, respectively, are typically employed to produce isocyanates at laboratory scale. Moreover, the amine phosgenation (Hetschel) is the main isocyanate production commercially applied, in spite of the fact that it requires highly toxic phosgene (Figure 2.19) (Krol, *2007*; More et al., *2013*).

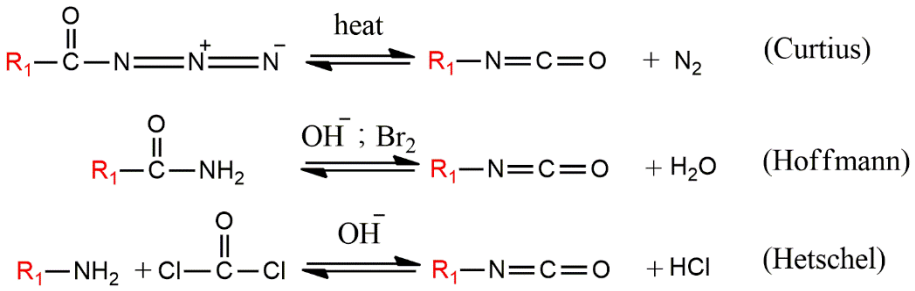

Figure 2.19 Synthesis of isocyanates

However, the application of hazardous phosgene, and the associated environmental awareness, have given rise to the seek for more eco-friendly alternatives, such as

substitution of phosgene by other equivalents, like as triphosgene to produce isocyanates at large scales (Eckert and Forster, *1987*), or dehydration of carbamate resulting from the carbonylation of amines with CO_2 (Waldman and McGhee, *1994*), although none of them has been yet industrially established (Hojabri et al., *2009*).

Even more interestingly, the increase of the renewability of polyurethanes have been achieved by synthesizing isocyanates from natural feedstocks, such as vegetable oils and fatty acids. Thus, Çaylı and Küsefoğlu (*2008*) conducted the allylic bromination of soybean oil, followed by its reaction with AgNCO at room temperature in THF, leading to NCO-terminated soybean oil, whereas Hojabri et al. (*2009*) in an effort to reduce the stearic hindrance of the present dangling chains, proposed a Curtius rearrangement of diacids with sodium azide obtaining a linear aliphatic diisocyanate (Figure 2.20.a). This process was later improved obtaining even longer unsaturated diacids when using a 2nd generation Grubbs catalyst, avoiding the occurence of explosive intermediate azelaic acid, to further synthesize the bio-based diisocyanate (Figure 2.20.b) (Hojabri et al., *2010*). In addition, More et al. (*2013*) efficiently synthesized highly pure oil-based isocyanates through a several-step protocol based on simple organic reactions in which diacyl hydrazide appears as an intermediate product.

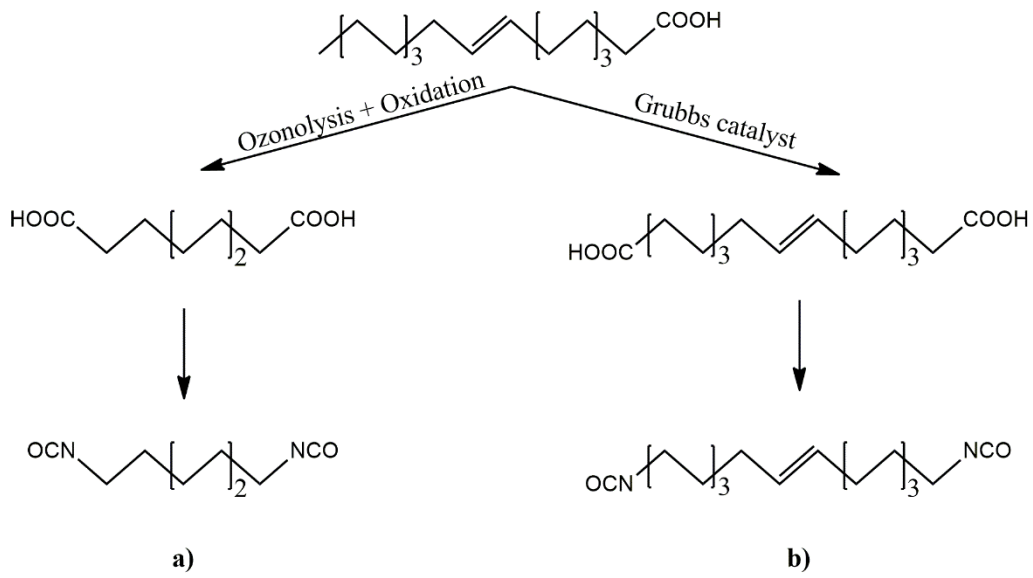

Figure 2.20 Soybean oil-based diisocyanates synthesis reported by Hojabri et al. a) (2009) and b) (2010)

In the last decade, bio-sourced diisocyanates, mainly coming from aminoacids (*L*-lysine diisocyanate) and fatty acids (dimeryldiisocyanate), have been the focus of several investigations, yielding renewable polyurethanes whose response appears to lack of toxicity, according to the *in vivo* cytotoxicity analysis results reported by Calvo-Correas et al. (*2015*).

2.2. Development of new synthetic pathways

Given that, in accordance with the *Green Chemistry* tenets, the design of PUs synthesis protocols involving "*safer solvents and reaction conditions*" (Dubé and Salehpour, *2014*) is a further step to a sustainable production, the production of *waterborne, radiation curable* and *non-isocyanate polyurethanes* have emerged in response to the ever-increasing environmental awareness. The following sections briefly describe these novel synthetic routes.

2.2.1. Waterborne polyurethanes (WPU)

Water-based polyurethane dispersions, also known as *waterborne polyurethanes* (WPU), allow for the replacement of the traditional solvent-borne polyurethanes, thus conforming with the increasingly stringent regulations, given the beneficial advantages provided by WPUs, inter alia versatile structure-properties relationship and good processability and elasticity (Gurunathan and Chung, *2016*; Saetung et al., *2016*), along with the environmental impact's reduction as revealed by the comprehensive approach of the life cycle assessment conducted by Maciel et al. (*2017*).

Waterborne polyurethanes constitute the group polyurethane systems composed of a dispersion of binary colloidal particles in an aqueous matrix, so that, as a consequence of their characteristic hydrophobicity, there is the need to insert water-compatible stabilizing groups (*emulsifiers*) into the polyurethane matrix. These emulsifiers consist of hydrophilic and amphiphilic compounds which can be classified into internal and external emulsifiers (Gurunathan and Chung, *2016*; Honarkar, *2017*). Although a wide range of internal emulsifiers, either ionic (cationic, anionic or even zwitterionic) or non-ionic, could be considered, including bis(hydroxymethyl)propionic acid (Gogoi and

Karak, *2014*) or 2,2-dimethylbutanoic acid (Liu, K. et al., *2016a*) among others, dimethylol propionic acid (DMPA) has been the most extensively used (Ayres et al., *2007*; Lei et al., *2015*; Ma, G. et al., *2017*), even finding in the literature simultaneous application of several emulsifiers in order to synthesize finer WPU dispersions (Du et al., *2008*).

Furthermore, these polyurethane dispersions may be prepared by different procedures, being the *prepolymer* (Santamaria-Echart et al., *2016*) and *acetone* (Mohamed et al., *2017*) techniques the most extensively reported. Briefly, in the prepolymer method the hydrophilic NCO-terminated prepolymer is synthesized in a first step from the emulsifier and the conventional polyurethane precursors (polyol, diisocyanate and diol chain extender). Then the carboxylic groups of the ionic emulsifier are neutralized with amines (typically triethylamine), followed by the prepolymer dispersion in water. The last chain extension with diamines terminates the preparation of waterborne polyurethanes, as shown in Figure 2.21. Conversely, the acetone process follows the same steps but performing the neutralization and further chain extension in acetone, or other water-miscible organic solvents, to ensure homogeneous conditions. This low boiling point solvent is removed through vacuum distillation after dispersion in water (Figure 2.21).

Moreover, the significant influence of the synthetic procedure on the waterborne polyurethane properties has been corroborated by Pérez-Limiñana et al. (*2006*), who demonstrated the narrower particle size distribution provided by the acetone process over the prepolymer method, due to the promotion of the prepolymer dispersion in water resulting from the lower prepolymer viscosity in the presence of an organic solvent. However, the properties of the final WPU, such as phase separation, thermal and mechanical resistance or the particle size, have been proved to be deeply dependent on other reaction factors, such as the ionic content (Cakić et al., *2013*) or chain extender chemical structure (Orgilés-Calpena et al., *2012*).

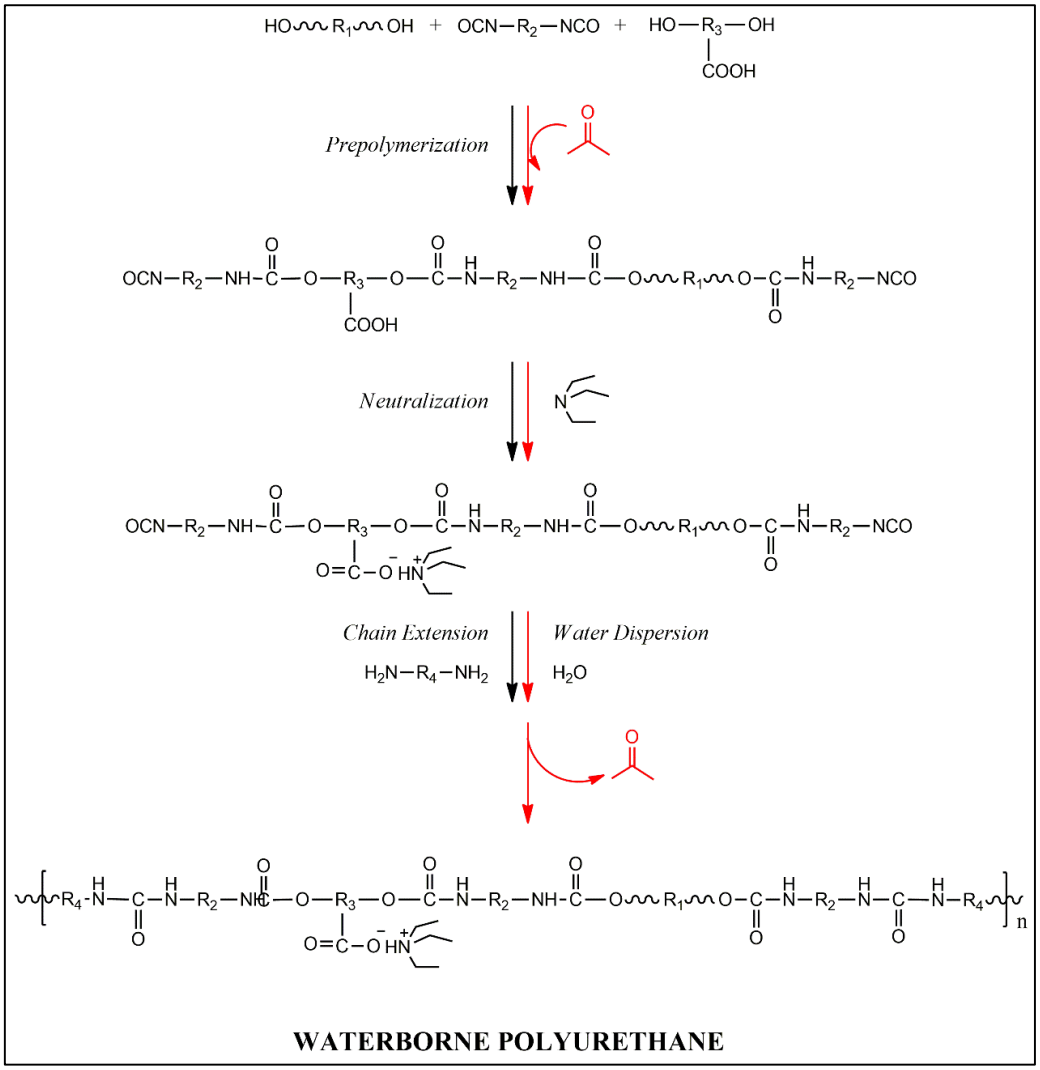

*Figure 2.21 Waterborne polyurethane synthesis via prepolymer (**black**) and acetone (**red**) processes*

The significant impact of the design of such sustainable synthetic route becomes noticeable in studies as the conducted by Li et al. (Li, Y. et al., *2014*), revealing the preparation of polyurethane systems with around a 90% of renewable content, owing to the combination of WPU synthesis procedure with the utilization of renewable resources, namely isosorbide polyol and fatty acid-based isocyanate. Additionally, Zhou et al. (*2017*) and Cakić et al. (*2017*), for their part, properly incorporated recycled PET bottles in the polyurethane structure via glycolysis, whereas Saetung et al. (*2016*) used polyols

based on natural rubber and rubber seed oil acting as the starting materials for renewable WPU for application in the footwear industry.

Waterborne polyurethanes have been mainly intended for eco-friendly adhesive production, even though other purposes such as gravure printing ink (Lei et al., *2015*; Lei et al., *2016*), thermally responsive elastomers (Chien et al., *2017*) or biomedical coatings (Liu, K. et al., *2016b*) have been reported. Notwithstanding, regardless of the application field to which these systems can be meant, there are still some shortcomings to be remedied, associated to the film stability in terms of mechanical, thermal and chemical resistance, or the lack of biocompatibility and antibacterial activity. To that end, *in situ* hybridization with silica (Cakić et al., *2018*) and sulfonic (Yong et al., *2015*) amine chain extenders, or diols more sensitive to hydrolysis linkages (Ayres et al., *2007*) like, for instance, those holding silver nanoparticles (Fu et al., *2016*) or long aliphatic branches (Lei et al., *2015*; *2016*), enable the customization of the resulting WPUs. However, as pointed out above (see section 1.4), a simpler *ex situ* incorporation of modifiers including silica nanoparticles (Heck et al., *2015*), cellulose nanocrystals (Santamaria-Echart et al., *2016*), ferric ions (Li, X. et al., *2018*) and thickeners (Orgiles-Calpena et al., *2009*) can be successfully carried out.

More interestingly, the copolymerization with acrylic monomers can provide the desired properties for waterborne polyurethanes, while simultaneously producing a controlled crosslinking process and replacing the organic solvent required to adjust the viscosity of the medium. Even though some investigations have dealt with the addition of acrylic polymer chains by radical polymerization of acrylate monomers without chemical interaction between urethane and acrylate molecules (Che et al., *2017*), grafting of hydroxyl bearing acrylate monomers (hydroxyethyl acrylate, hydroxyethyl methacrylate, bisphenol-A-glycidyl dimethyl acrylate etc.) as anchoring sites covalently embed into the PU backbone leads to stable WPU/acrylic hybrids, whose polymerization step is typically accomplished with UV-radiation and a photosensitive compound (Mehravar et al., *2017*) or in the presence of potassium persulfate (KPS) as radical initiator (Lopez et al., *2011*). Besides, Alvarez et al. (*2018*) has recently proposed a new radical polymerization methodology based on a redox initiating blend of ascorbic acid and hydrogen peroxide, allowing for conducting the polymerization at 30 ºC.

2.2.2. Radiation curable polyurethanes

Polymerization of polyurethanes with the aid of ultraviolet (UV) radiation has recently drawn the attention due to its remarkable advantages, namely process simplicity, mild reaction conditions, fast and efficient drying process, along with the absence of volatile organic solvent in an easily controlled curing process. The synthesis of photo-crosslinkable polyurethanes requires the usage of UV-sensitive monomers, mainly acrylates, and a photo-initiator, together with the traditional polyurethane building blocks, leading to the production of polyurethane acrylate systems. Therefore, some hydroxyl containing monomers, such as 2-hydroxyethyl acrylate (HEA), 2-hydroxyethyl methacrylate (HEMA) or 2-hydroxypropyl acrylate (HPA) (Figure 2.22), are typically considered to facilitate their grafting via polycondensation between their hydroxyl groups with reactive diisocyanates, so that the double bonds confer their UV-light activity. The addition of these reactive diluents is also of great important, since they confer these systems a suitable viscosity, apart from facilitating the control of the polymerization process and improving the ultimate film properties (Yildiz and Onen, *2017*).

This technique is particularly useful in biocompatible adhesives and tissue engineering, where a quick curing step is required, despite the need for oxygen inhibition in order to avoid likely side reactions, quite achievable by modifying the radiation intensity and initiator concentration (Chattopadhyay and Raju, *2007*). Thus, Liu, K. et al. (*2016b*) intended to avoid attachment of microorganisms to WPU coatings by embedding lysozyme into the polyurethane backbone via photopolymerization, while Abdalla et al. (*2016*) effectively prepared homogeneous biocompatible adhesives based on polycaprolactone and 2-isocyantoethylmethacrylate in just 60 seconds. Such UV-light susceptible isocyanates have also been applied in other studies (Li, C. et al., *2014*; Wang et al., *2013*) pointing out that UV-induced radically polymerizable functional groups can be found not only in additional monomers but also in the isocyanate source.

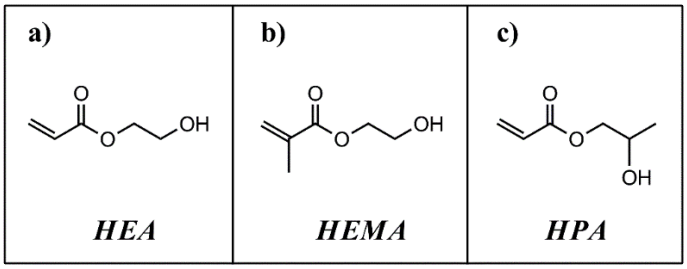

Figure 2.22 Chemical structure of the most common UV sensitive acrylate monomers: a) HEA; b) HEMA; c) HPA

As with the production of polyurethane dispersions in water, UV polymerization technique may be combined with other strategies towards a sustainable production, so that it can be supplemented with the synthesis of natural polyols via fatty acid esterification (Jiao et al., *2016*), thiol-ene coupling of vegetable oils (Chen et al., *2016*) or liquefaction of bagasse (Patel et al., *2009*). More remarkable is the dual curing polymerization proposed by Hu et al. (*2018*) when preparing bio-based coatings from castor oil-based polyurethane/acrylate and epoxidized cardanol glycidyl ether, so as to reduce the shrinkage previously observed during radical polymerization. Furthermore, the additional utilization of bio-based polyols have been reported as well, such as dextran (Wang et al., *2012*) or rosin (Liu, B. et al., *2016*).

2.2.3. Non-isocyanate polyurethanes

As stated above, the vast majority of the research production have dealt with the sustainable polyurethane synthesis by using natural occurring polyols or their derivatives. Moreover, although some studies propose the application of more eco-friendly isocyanates, one sector of the research field has opted for taking a further step removing the hazardous isocyanate from the polyurethane production, thus meeting the current environmental regulations aimed to reduce the exposure to isocyanates (EU Publications, *2010*), in such a way that polyurethanes thereby produced are known as *non-isocyanate polyurethanes* (*NIPU*).

Despite the fact that different synthetic protocols can lead to NIPUs, as reviewed recently by Cornille et al. (*2017*), exclusively the polyaddition between bicyclic carbonates and diamines, as shown in Figure 2.23, has proved to prevent the utilization of toxic

substances (phosgene, aziridines, azides, carboxamides, etc.) and the production of byproducts. Since the first patent on NIPU preparation published by Groszos and Drechsel (*1957*), this synthesis protocol has turned into the most relevant and used synthetic pathway for the production of bio-based polyurethanes.

The appearance of pendant hydroxyl groups through this aminolysis reaction, whose primary or secondary character heavily depends on the synthetic path followed (Figure 2.23), is the reason why this group of polyurethanes are also known as *polyhydroxyurethanes* (*PHU*). The improved hydrophilicity entails stronger cohesive forces, apart from enhanced thermal and chemical resistance owing to the establishment of inter- and intra-hydrogen bonds, what, in turn, gives them the chance to act as reactive polyols in further chemical modifications.

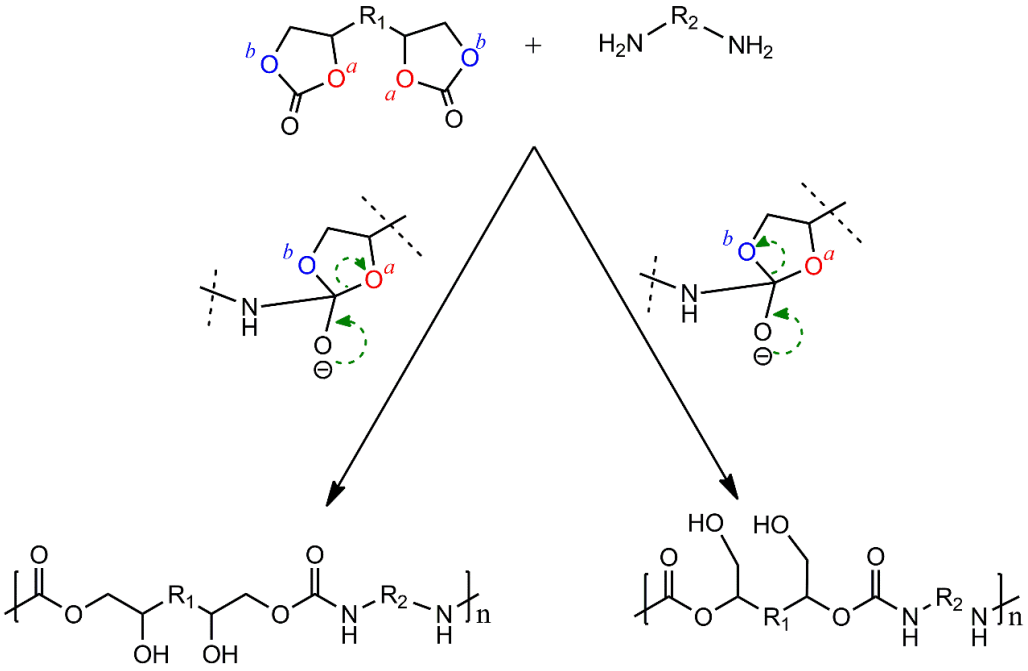

Figure 2.23 Non-isocyanate polyurethane synthesis

The reaction mechanism of this process has been analysed from different standpoints, so that, according to Tomita et al. (*2001*), this reaction is controlled by differences in electron densities giving rise to the appearance or breaking of chemical linkages, while

to Zabalov et al. (*2012*), it is based on a single- or several-step procedure in which a second amine molecule acts as catalyst. Anyhow, it was disclosed the second-order character of this reaction (Tomita et al., *2001*), beside the fact that primary amines and polar solvents seem to promote the addition reaction (Webster and Crain, *2000*).

The main disadvantage of this synthetic route is related to its low reaction rate at room conditions, given that a thermal activation may prompt side reactions (Cornille et al., *2017*). Therefore, the solution that best addresses this issue is the employment of catalysts, since, while an increase in the number of members of cyclic carbonates has frequently proved to provoke a reactivity rise (Lamarzelle et al., *2016*; Tryznowski et al., *2015*), their synthesis requires to be conducted under well-defined conditions, along with the application of harmful materials, especially regarding the manufacture of bicyclic carbonates (Nohra et al., *2013*).

Moreover, although cyclic carbonates may be obtained through transesterification and transcarbonation with diols (Carothers and Hill, *1933*), the catalytic production of the most extensively utilized 5-membered cyclic carbonate via CO_2 fixation into oxirane groups seems to be a much more appealing method to pursue an improved renewable content, while mitigating the environmental impact of this greenhouse gas. Hence, the synthesis of bicyclic carbonate from carbonation of bisphenol S-based diglycidyl ether, as described by Kim et al. (*2001*), offers a yield of 74%, similar to the 76% reported by Cornille et al. , whose polyfunctional cyclic carbonates conferred quantitative conversion with diamines in the presence of a thiourea catalyst, leading to non-isocyanate polyurethane with appropriate foam (Cornille et al., *2016b*) and adhesion (Cornille et al., *2016c*) performances.

An even more sustainable production of NIPUs deals with obtaining bio-based cyclocarbonates by means of a lipase B-catalysed esterification of *Sapium sebiferum* oil-derived dimer acid with glycerol carbonate (He et al., *2018*), or applying an easily scalable catalytic procedure from levulinic acid biomass-derived diphenolic acid, leading to renewable WPU coatings (Ma, Z. et al., *2017*). On the other hand, Thébault et al. (*2017*) reported the preparation of PHUs with aminated and carbonated mimosa tannin extract, achieving a bio-sourced content above 70%. By contrast, Tryznowski et

al. (*2015*) attained a 79% yield in the synthesis of five-membered cyclic carbonate from diglycerol to further produce non-isocyanate polyurethanes via one-step protocol at high temperatures. Further on, the wettability of these NIPUs were subjected to a deeper investigation (Tryznowski et al., *2017a*), revealing that the low hydrophobicity of polyhydroxyurethanes may have a detrimental effect on their performance under high moisture conditions. Besides, these systems typically exhibit reduced hardness and glass transition temperatures, giving rise to an inefficient chain mobility (He et al., *2018*). Although Cornille et al. (*2016b*) were capable of increasing the movement of the molecular chains with the utilization of a blowing agent, that methodology applies only for foams.

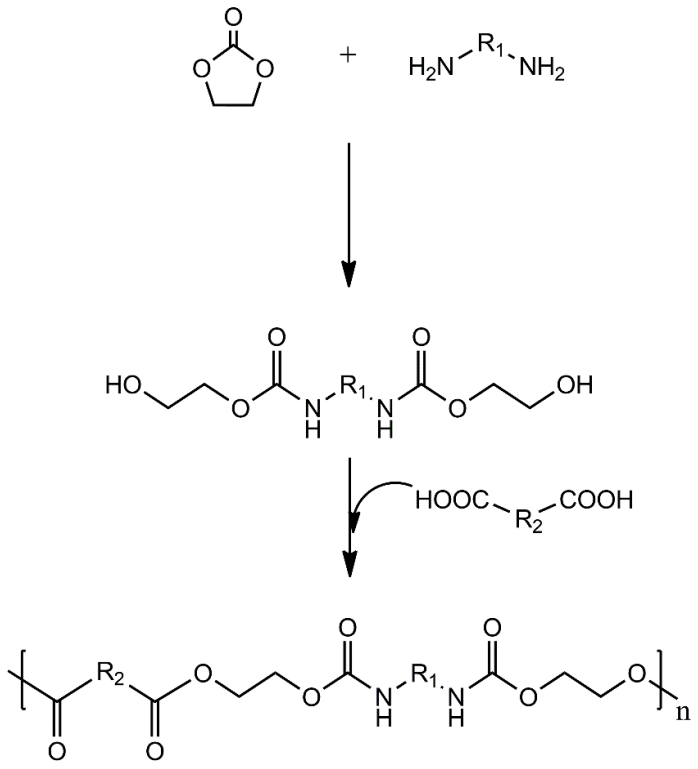

Figure 2.24 Non-isocyanate poly(ester urethane) synthesis (Wang et al., 2016)

Therefore, other methodologies, essentially hybridisation, have been considered. Thus, in an attempt to replace traditionally isocyanate-based polyurethane adhesives, Leitsch et al. (*2016*) claimed to report the pioneering production of PU/PHU hybrids first conducting a conventional NCO-OH condensation, followed by chain extension with

diamines, thanks to the previously grafted 1,2-carbonate glycerol. Although, according to Leitsch et al., the presence of free isocyanates is avoided during adhesive application, they still participate at the early stages of the synthesis. In this sense, the preparation of PHU hybrids with epoxy (Cornille et al., *2016a*), polyhedral oligomeric silsesquioxane (Liu, G. et al., *2016*) and amide (Tryznowski et al., *2017b*) groups appears to provide a safer way to tailor the PHU properties while preventing the use of isocyanates. More interestingly, Wang et al. (*2016*) completely averted pendant hydroxyl groups in NIPU's chemical structure by the reaction between diamines and monocyclic carbonates, and a further esterification with dicarboxylic acids, as shown in Figure 2.24.

3. Fundamentals of adhesion and adhesives

3.1. General concepts

Since their inception, polyurethanes have become widespread in the adhesive field, being applied on an extensive array of surfaces (glass, wood, plastics, ceramics, etc.). Thus, starting with the urethane prepolymers during the fifties, followed by the waterborne polyurethanes patented by DuPont (Mallonee, *1961*) and ending with the most recent pressure sensitive and hot melt adhesion techniques, polyurethane adhesives have carved out a well-established market niche.

Adhesion can be defined as the phenomenon of joining two substrates, so that it is not an exclusive property of adhesives but, in general terms, also of coatings, paints, varnishes, etc., or in other words, whenever two solids are put together (Baldan, *2012*). Though adhesive joining is not the only bonding technology, polymeric adhesives exhibit prominently better properties than traditional mechanical joints (rivets or fasteners), since they are capable of dissipating large amount of energy by a proper stress distribution along the whole adhesion area, with a reduced weight and enhanced resistance to corrosion and fatigue (Casdorff et al., *2018*). Consequently, adhesive joints play a key role in an extensive array of areas including microelectronics, medicine, aeronautics, construction, etc.

Adhesion is the result of a several-step process in which the adhesive flows and wets the surface, establishing certain physicochemical interactions in the adhesive mass (*cohesion*) and with the substrate (*adhesion*), including Van der Waals and dipole forces, along with stronger hydrogen and covalent bonds. Hence, a suitable wettability, thus promoting an intimate adhesive-substrate contact, is an important factor to take into consideration, which can be achieved whether the intermolecular forces of the adhesive are weaker than the corresponding interaction with the adhesion surface, meaning a surface energy lower than the corresponding to the adherends (Szycher, *2013*).

Additionally, the performance of an adhesive is not only determined by its properties, such as rheological behaviour or surface free energy, but also by the adhesion surface characteristics (pH, functional groups, roughness, presence of debris or extractives) and curing conditions (temperature, humidity, etc.). As a consequence, some investigations have revealed the relevant influence of parameters such as the relative humidity (Asahara et al., *2003*), artificial aging (Clerc et al., *2017*) and substrate modifications to improve the adhesive wettability (Boutar et al., *2016*) on the ultimate properties developed by the adhesive joints.

The already discussed heavy reliance of industrial production on crude oil, also concerning the adhesive field, has been the driving force for the removal of toxic volatile organic compounds (VOC) from adhesive formulations traditionally used as carrier fluids, such as urea formaldehyde, phenol formaldehyde, etc. (Kong et al., *2011*). As a result, in pursuit of environmental protection and the enforcement of the stringent governmental regulations, the feasibility of some natural adhesives, including starch, casein and other proteins, has been assessed. However, their characteristic low durability and hydrolytic resistance have led to the implementation of some modifications to improve the adhesion response of such natural adhesives. Thus, as examples Gumus and Wauton (*2014*) reported the preparation of yam and sweet potato starch with borax, while Liu, Y. and Li (*2007*) significantly enhanced the properties of soy protein-based adhesives by grafting maleic anhydride via amidification-esterification and a subsequent blend with polyethylenimine. Due to the great abundance of soy protein, its modification has been extensively reported as the object of many investigations, allowing for the incorporation to the adhesive formulations of oxirane rings (Chen et al., *2017*), tannins

(Ghahri et al., *2018*), phosphorus-bearing additives (Cheng et al., *2017*) or polyacrylate emulsions (Wang et al., *2018*). The development of other bio-based adhesives from natural sources, among others chitosan (Ji et al., *2017*) or quebracho tannin (Efhamisisi et al., *2016*), have been also addressed.

Nonetheless, the well-known efficient wettability, hydrogen bonding and ability to establish chemical interactions associated to polyurethanes place them in a favourable position to suitably satisfy the requirements for the production of bioadhesives, overcoming the above described shortcomings. Additionally, bearing in mind the progress made in the manufacturing of bio-sourced polyurethanes, as described in preceding sections, these "*greener*" adhesives seem to be increasingly meeting the definition of "*bio-based adhesive*" coined by Pizzi (*2006*), which states that *"bio-based adhesives include those materials of natural, non-mineral, origin which can be used as such or after small modifications to reproduce the behaviour and performance of synthetic resins*".

3.2. Adhesion theories and models

The response of an adhesive strongly depends on several factors, all of them necessarily related to the establishment of interaction forces between adhesive and substrate. Moreover, owing to the multidisciplinary character of adhesion, comprising chemistry, physics, rheology, stress analysis, etc., in conjunction with the different nature of adhesive and substrate, different theoretical models have been developed to explain the adhesion process (Awaja et al., *2009*; Baldan, *2012*; van der Leeden and Frens, *2002*). However, as there is still not a single adhesion theory capable of accurately explaining all the phenomena occurring during bonding, rather each one can be applied to some extent under certain circumstances, some researchers have devoted their investigations to gain a better understanding of the adhesion mechanisms (Casdorff et al., *2018*; Lavalette et al., *2016*).

The main adhesion theories and models, namely *adsorption*, *mechanical interlocking*, *electrostatic adhesion*, *interdiffusion*, *weak-boundary layer* and *chemical bonding*, are briefly described below.

3.2.1. Adsorption theory

This model states that adhesion is the result of the adsorption of adhesive molecules onto the solid surface, leading to the establishment of primary (covalent, ionic or metallic bonds), secondary (van der Waals, hydrogen bonds) and donor-acceptor interactions, upon achieving a proper surface wetting. Adsorption theory puts forward a thermodynamic approach to analyse the substrate wetting by the adhesive and the resulting work of adhesion on the basis of an equilibrium of interfacial parameters, more specifically related to the surface free energies of substrate and adhesive, allowing for the preparation of an appropriate adhesive. Thus, according to Dupre (*1869*), the work of adhesion (W_a) can be estimated as followed:

$$W_a = \gamma_S + \gamma_L - \gamma_{SL} \qquad (2.1)$$

where γ_S, γ_L and γ_{SL} represent the interfacial tensions of solid-air, liquid-air and solid-liquid respectively (Figure 2.25.a), whilst the relationship between these surface tensions is governed by the Young equation (2.2):

$$\gamma_L \cdot cos(\theta) = \gamma_S - \gamma_{SL} \qquad (2.2)$$

Therefore, the so-called Young-Dupre equation can be inferred (2.3):

$$W_a = \gamma_L \cdot (cos(\theta) + 1) \qquad (2.3)$$

In this sense, a suitable wettability will be achieved when the adhesive surface tension is lower than the corresponding to the solid substrate, thus obtaining a smaller contact angle, θ, see Figure 2.25.a.

3.2.1. Mechanical interlocking

Mechanical coupling is the oldest and simplest model, which considers the adhesion as a process in which the adhesive flows into the substrate asperities, then solidifying within those cavities. In accordance with this model, whose significance level has been rediscovered at the microscopic scale (Allen, *2003*; van der Leeden and Frens, *2002*), the adhesion response strongly depends on the direction of the applied force, as a

consequence of the occurrence of different sort of asperities (Figure 2.25.b). Despite appropriately working on surfaces rough enough, this mechanism fails in the explanation of the adhesion between perfectly smooth substrates (Baldan, *2012*).

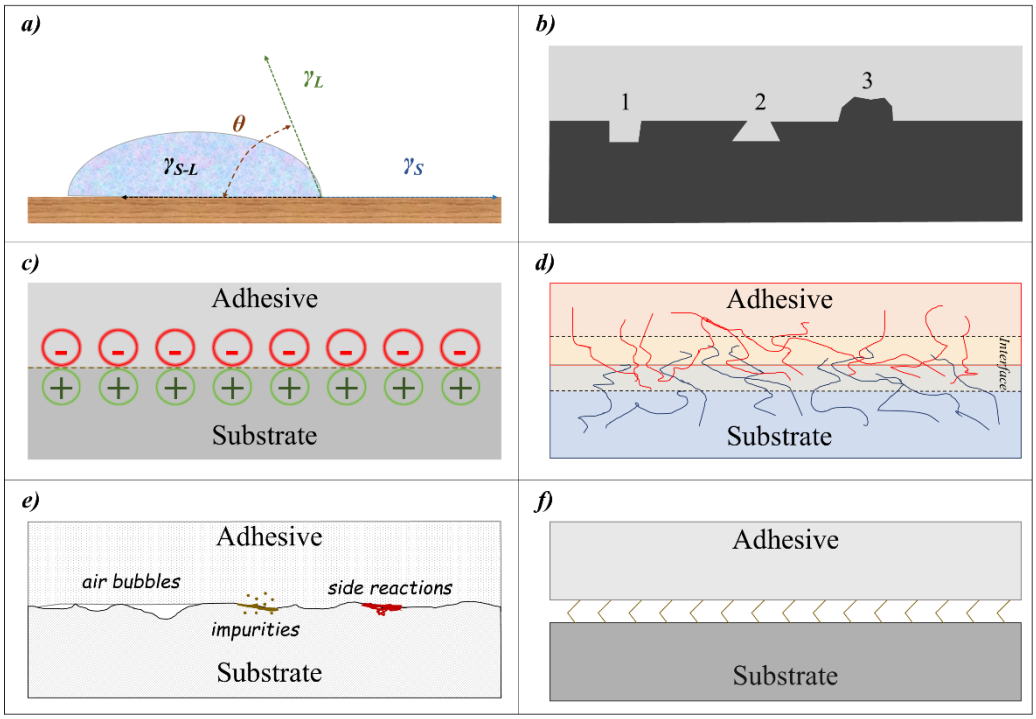

Figure 2.25 Scheme of the main adhesion theories: a) interfacial tension in andsorption theory; b) mechanical interlocking; c) electrostatic adhesion; d) interdiffusion model; e) weak boundary layer; f) chemical bonding

3.2.2. Electrostatic adhesion

In agreement with the electronic theory, an adhesive joint is formed as a result of a transfer of ionic charges across the adhesive-substrate interface, giving rise to an electrical double layer (Figure 2.25.c). However, even though this sort of adhesion is mainly limited to the bonding of metallic surfaces, it is unlikely the predominant mechanism of the resulting adhesive joint (Yang et al., *2001*).

3.2.3. Interdiffusion theory

The diffusion theory can solely be applicable when adhesive and substrate comprise thermodynamically compatible polymer chains, whose sufficient mobility, gained

through a temperature above their glass transition points, allows their macromolecules to diffuse into one another at the interface (Figure 2.25.d). Nevertheless, this model fails in case of restricted molecular motion, meaning either crystalline or highly crosslinked polymers, or at temperatures lower than their corresponding T_gs ($T<T_g$).

3.2.4. Weak boundary layer

According to this model, committed to elucidating the interfacial detachment origins, the failure of an adhesive joint is located in a mechanically weaker interfacial layer, which can arise from substrate, adhesive or environment as a consequence of the presence of impurities or air cavities, the occurrence of side reactions or diffusion of substances such as environmental moisture during the different stages of application, curing and performance of an adhesive bond, respectively (Figure 2.25.e).

3.2.5. Chemical bonding theory

This theory postulates that adhesion takes place as a consequence of the formation of interfacial linkages, entailing primary (*ionic, covalent and metallic*) and secondary (*dipole-dipole, van der Waals, hydrogen bonding*) bonds, thus requiring and intimate contact between adhesive and adhesion surface (Figure 2.25.f).

3.3. Analysis of the adhesion performance

In order to properly design an adhesive for a given substrate, the assessment of the critical stress that is capable of withstanding is of key importance. However, not only the ultimate adhesion performance of the fully cured adhesive is of interest, but also its evolution with time, what is also known as "*green strength*" (Desai et al., *2003a*).

Overall, adhesion strength is regarded as the stress required to detach two surfaces bonded by an adhesive under certain test conditions. At this point, it is necessary to differentiate between "*intrinsic adhesion*" and "*measured adhesion*", since the former refers to the intermolecular forces joining adhesive and substrate, while the latter is related to not only the energy associated to the intrinsic adhesion, but also the energy dissipated due to the viscoelastic and plastic deformation of the adhesive joint (Baldan,

2012). Consequently, the inaccuracy in the estimation of the adhesion strength from a thermodynamic standpoint makes the empirical analysis of the *measured adhesion* a key factor in the formulation of adhesives.

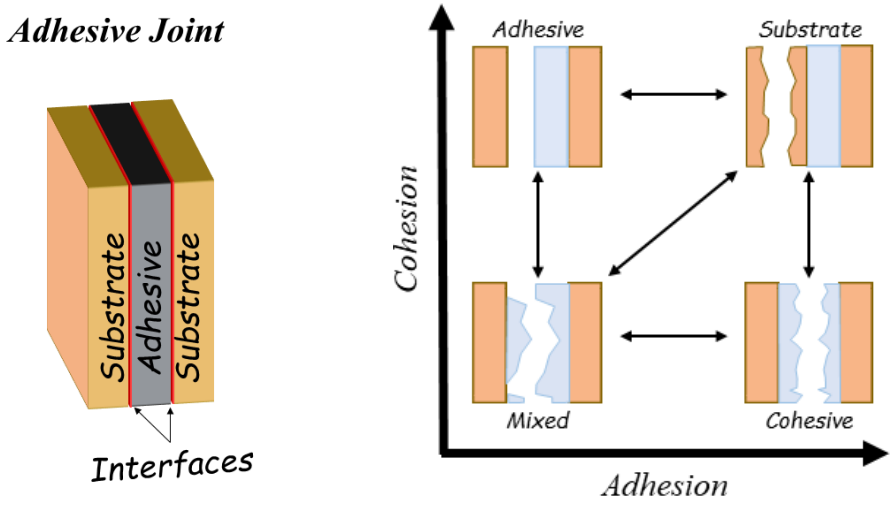

Figure 2.26 Adhesive joint layout (a) and type of failures as a function of the adhesion-cohesion forces (b)

Moreover, an adhesive joint typically comprises three main areas, viz. *substrate*, *adhesive* and *substrate-adhesive interfaces*, as shown in Figure 2.26.a. Given that an adhesive bond fails at the mechanically weakest point, the type of failure appearing upon detachment relies on a balance between cohesion and adhesion forces, corresponding to the intermolecular interactions within the adhesive bulk, and between adhesive and substrate, respectively (Khanlari and Dubé, *2013*). Therefore, an enhancement in the cohesion forces can move the location of the failure from the adhesive bulk (*cohesive failure*), obtaining a residual adhesive layer on each adhesion surface, to the substrate-adhesive interfaces (*adhesive failure*), so that a clean surface is eventually released (Figure 2.26.b). Finally, in case of overpassing the mechanical resistance of the adherend owing to improved adhesive and cohesive interactions, *substrate failure* is attained. Otherwise, a *mixed failure*, resulting from the combination of the former ones, could occur.

On the other hand, the assembly design of the adhesive joint modifies the direction in which an external stress is applied, in such a way that an early joint failure can be obtained, provided a non-uniform stress distribution along the adhesion area. Figure 2.27 depicts the most common joint designs below described:

- *Tensile and compression* specimens are subjected to normal forces (perpendicular to the adhesion area), but in opposite directions. These stresses are measured as force per bonded area, *[Pa]*.
- *Shear* stresses act tangentially on the plane of the adhesive joint and the resulting shear strength are typically measured as force per unit adhesion area, *[Pa]*.
- The *flexural* stress, in *[Pa]*, developed by an adhesive joint is obtained as a result of the application of a bending deformation in the specimens' midpoint.
- *Tear or cleavage*. In this case, the stress is applied at one end of the rigid bonded assembly in order to put the substrates apart, so that a heterogeneous stress distribution is created as the load is mainly concentrated at only one of the specimen extremes. The resulting tear strengths are commonly expressed as force per linear length, essentially the width of the bonding line, *[N/m]*.
- *Peeling* strength is similar to cleavage, but in this case at least one of the substrates present a flexible structure, meaning that the angle in which the substrates are separated is much larger than in the former tear tests.

In any of these mechanical tests, a load cell records the evolution of the specimen strength in response to an applied debonding rate or force increment until failure, which indicates the end of the test. However, as already pointed out, the resulting values are strongly influenced by different parameters (humidity, temperature, debonding rate, etc.). As a consequence, with the aim to overcome such issue, normalized methods have been developed to perform the assessment of the adhesion strength under comparable conditions. To this respect, different organisations, such as the American Society for Testing Materials (ASTM) or the International Organization for Standarization (ISO), among others (NASA, SAE, TAPPI, etc.) have collected a series of standard norms solely useful for comparison purposes, since they may not accurately simulate the real service conditions.

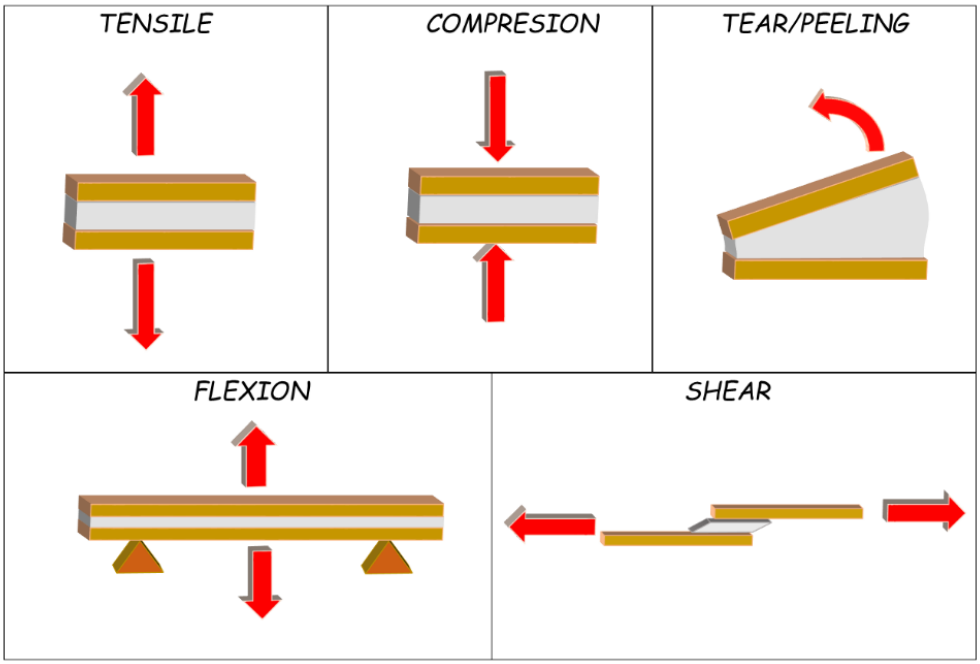

Figure 2.27 Typical joint assemblies

Generally, these normalized tests can be categorized into fundamental properties analysis (viscosity, hardness, etc.) and end-use tests (peeling, shear), so that the former consider the basic adhesive characteristics, while the latter try to simulate the service conditions of the adhesive joints. Some of the most remarkable standard tests specified by ASTM are as follows:

- *Lap-shear tests*. The evaluation of the shear strength can be conducted on wood (ASTM D906, D2339), metal (ASTM D1002) or plastic (ASTM D3163), although there are some other variations in order to avoid poor specimen's alignment or to prepare high-quality assemblies with an improved adhesion response (ASTM D3165, D3528, D3164, D4501).
- As for *peeling tests*, it is possible to apply different stripping angles, viz. 90º or 180º (ASTM D6862 and D1876, respectively), although the analysis of the peeling resistance when either both (ASTM D1876) or only one of the substrates (ASTM D3167, D1781, D903) is flexible can be considered, as well. When both substrates exhibit a rigid structure, the *cleavage* strength is determined by applying the following standard norms, ASTM D1062, D3807, D5041.

- *Others* tests can be applied to measure fatigue strength at specific frequencies and amplitude of the load (ASTM D3166), impact strength (ASTM D950), creep (ASTM D2293, D2294), flexural strength (ASTM D1184) and environmental influence on the adhesion response (ASTM D896).

3.4. Rheology of adhesives

The sensitivity of rheology to the intrinsic properties of polymeric adhesives, along with the utilization of simpler standard instruments compared to the conventional analytical methods, has made rheological tests essential in characterizing adhesives (Deplace et al., *2009*). Indeed, as it can be inferred from the study of Hicks et al. (*2015*) on automotive adhesives, the rheological properties of adhesives exert considerable influence not only on their application, but also during their handling and storage (Gumus and Wauton, *2014*). Polymeric adhesives should generally exhibit enough viscosity to minimize settling effects during storage or sagging after substrate wetting, while reasonably facilitating their flowability for the processing and application steps (Orgiles-Calpena et al., *2009*).

Adhesives commonly present a viscoelastic behaviour, whose elastic and viscous components may be estimated from small-amplitude shear stress (SAOS) in terms of the storage (*G'*) and loss (*G''*) moduli, respectively, together with their relative contribution (*G''/G'*), known as the loss tangent (*tan* δ). Frequency sweeps performed in the linear viscoelastic regime provide the mechanical spectrum of the analysed adhesive, that denotes the state (crosslinking degree, curing stage, etc…) and properties of the adhesive under almost unperturbed conditions (Zhang et al., *2011*), in such a way that its response at low frequencies are especially associated to their behaviour during bonding, while high frequencies results are more related to the debonding process (Mazzeo, *2002*).

Nevertheless, in order to assess the materials response under experimentally unattainable conditions, i.e. extremely high and/or low frequencies , the well-known time-Temperature superposition principle may be considered for application, as reported Van Ekeren and Carton (*2011*) when analysing polyurethanes potentially employed as transparent armour in ballistics. Therefore, given that time can be exchanged with

temperature, the *master curve* of a thermorheologically simple material can be achieved by horizontally shifting the results obtained at different temperatures using thermally dependant shift factors (a_T).

Furthermore, bearing in mind the reactive character of adhesives, dynamic time sweeps are of particular interest in order to analyse the evolution of their rheological properties with time, i.e. during curing (Głowińska and Datta, *2014*). Consequently, Jaruchattada et al. (*2012*) proposed the application of oscillatory time sweeps to assess the cure kinetics under isothermal conditions of polyurethane acrylate systems, thus determining the basic crosslinking polymerization parameters, namely gelation and vitrification times, that mark the structural transitions from liquid to rubber and from rubber to glass states, respectively (Figure 2.28).

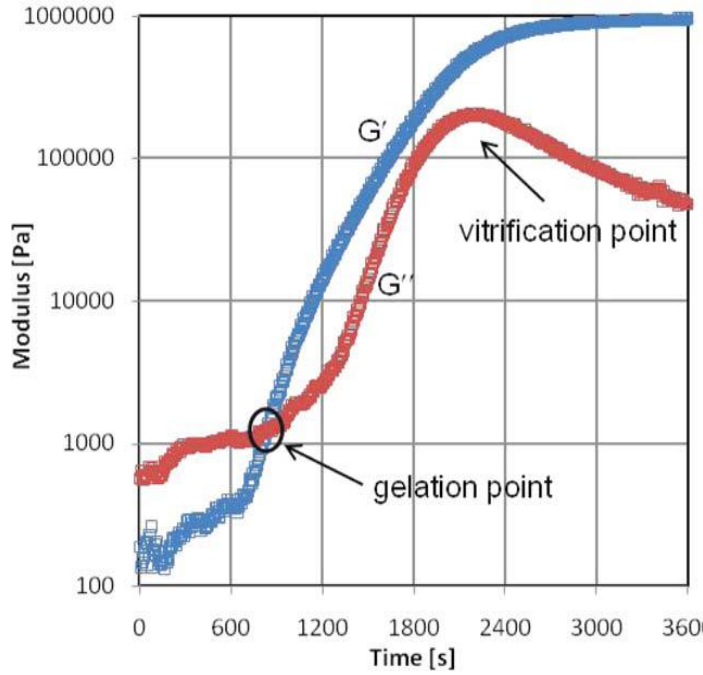

Figure 2.28 Rheological parameters during crosslinking polymerization (Jaruchattada et al., 2012)

Similarly, besides curing time, other parameters can allow to sensibly control the curing degree of adhesives, as is the case of adhesives containing thermoreversible Diels-Alder compounds, in which the rheological response as a function of temperature is of great importance. Hence, Turkenburg et al. (*2017*) proved the exceptional tunability of

temperature-susceptible polyester urethane adhesives conducting the analysis of the adhesive viscosity throughout heating and cooling ramps, thus monitoring the crosslinking and disruption of the polymer chains as a result of the reversible Diels-Alder reaction.

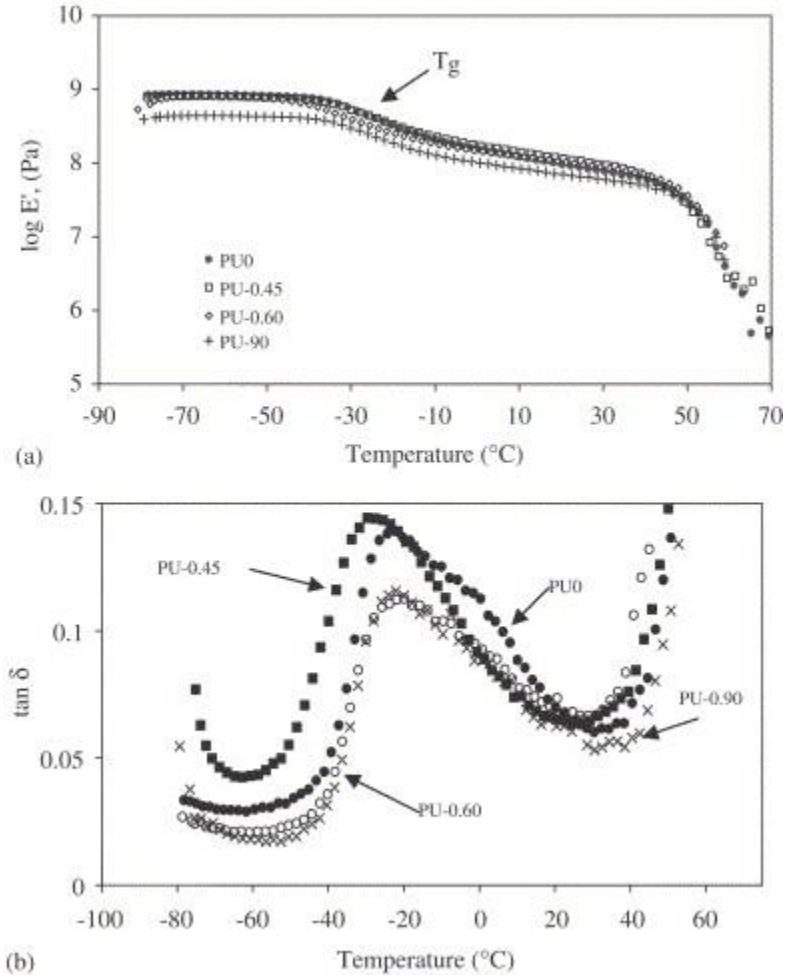

Figure 2.29 DMTA results of fully cured PU adhesives (Vega-Baudrit et al., 2007)

Upon curing elastomeric adhesives generally present a well-developed rubbery plateau region of the mechanical spectrum at room conditions, significantly noticeable not only in frequency sweeps, but also in dynamic mechanical thermal analysis (DMTA) (Bahattab et al., *2011*; Vega-Baudrit et al., *2007*), in which the oscillatory viscoelastic functions are obtained during the application of a certain heating rate at a constant frequency (Figure 2.29).

Given the change of state occurring as a consequence of the curing process (Figure 2.28), the rheological geometries and type of deformations may range from conventional shear of uncured liquid-like adhesives using geometries like plate-plate, cone-plate or concentric cylinders, to appropriate deformations of rod or rectangular solid specimens, including torsion (Hablot et al., *2008*), tensile (Choi et al., *2015*) or bending (single (Fuensanta et al., *2017*) and dual (Chen et al., *2011*) cantilever and three-point bending (Rueda-Larraz et al., *2009*)), as shown in Figure 2.30. However, depending on the deformation mode, viscoelastic moduli may vary from shear (G, G', G'', etc.) to tensile/bending (E, E', E'', etc.) functions, whose relationship in case of elastic solids, is given by Equation (2.4:

$$E = 2 \cdot G \cdot (\nu + 1) \qquad (2.4)$$

where ν is the Poisson's ratio, whose values associated to simple materials typically fall within the range 0-0.5 (Van Oosten et al., *2016*), so that incompressible solid samples are characterized by an E/G ratio of 3, as it has been widely reported (Ciesielski, *1999*). Regardless the deformation mode employed, the application of the previously described dynamic mechanical thermal analysis over cured adhesives allows to ensure that the synthesized adhesives show a glass transition temperature within the appropriate limits, commonly identified as the temperature at which a maximum in the loss tangent is achieved (Valero and Gonzalez, *2012*), see Figure 2.29. Thus, above this temperature the chain motion is promoted, drastically modifying the mechanical properties of the adhesives.

Moreover, apart from the estimation of the T_gs, DMTA results can provide more information such as the activation energy of the glass transition (Abdalla et al., *2016*) or more importantly the crosslinking density (γ) of the polymer network (Equation (2.5) as a function of the rubber plateau region temperature (T), as recently reported by Ling et al. (*2018*) when analysing the evolution of WPU adhesives in the post-cure stage. The direct proportionality between crosslinking density and glass transition temperature was evinced by Kong et al. (*2011*), when increasing both parameters by raising the NCO:OH ratio in the synthesis of canola-based polyurethane adhesives.

$$E' = 3\gamma RT = \frac{3\rho RT}{M_c} \quad (2.5)$$

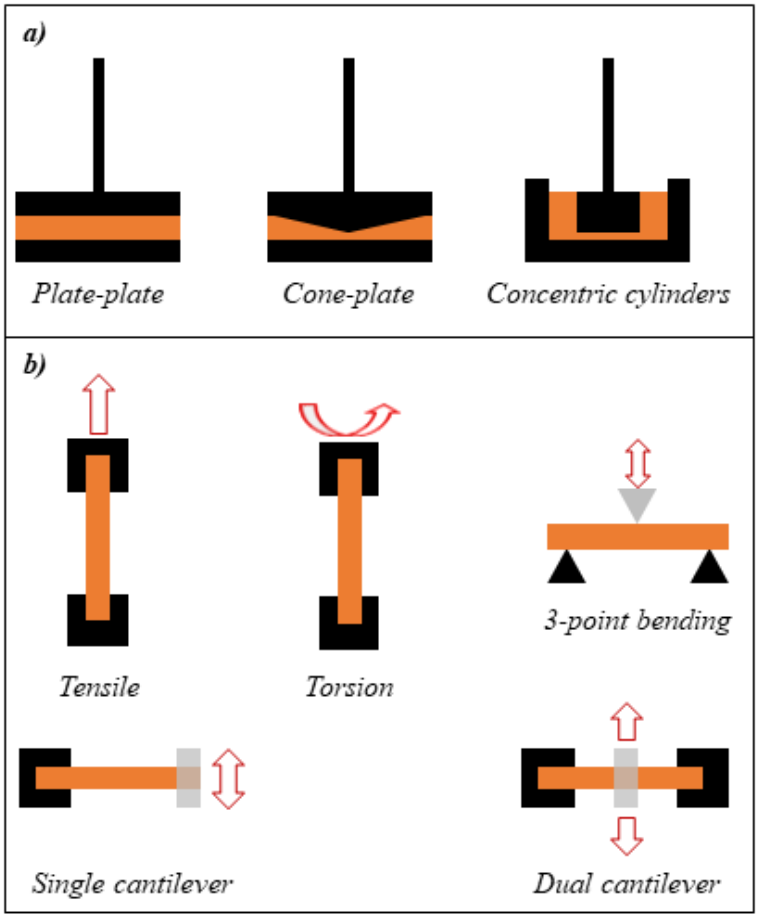

Figure 2.30 Rheological geometries and deformations for a) uncured and b) fully cured adhesives

Additionally, segmentation, especially significant in polyurethane systems, can be easily analysed, since such microphase separation make an impact on the viscoelastic response. Therefore, poorer chain interactions, arising from reduced phase separation, can lead to a reduced elastic modulus and modifying the temperature and number of the glass transitions (Sánchez-Adsuar et al., *1997*). Thus, this technique enables the identification of polyurethane adhesives whose structure can range from an enhanced phases-mixing with only one T_g, as the IPDI/castor oil-based adhesives reported by Ferreira et al. (*2007a*), to highly segmented polyurethanes with several glass transition temperatures corresponding to each microdomain, like the WPUs recently studied by Li et al. (*2018*).

Furthermore, the rheological analysis can be complemented by the estimation of the glass transition temperatures obtained under static conditions, such as from differential scanning calorimetric analysis (DSC), although some deviations can be found between both of them as a consequence of the dynamic nature of the DMTA tests.

Furthermore, there is a group of adhesives whose main viscoelastic response is located in the flow region of the mechanical spectrum, denoting their liquid-like appearance (G''>G') (Fonseca et al., *2016*). This is the case of pressure sensitive adhesives (PSA), which have to show permanent stickiness and the ability to adhere a surface under low-pressures and during short contact times, without taking place any phase transition or chemical reaction (Maassen et al., *2016*). Consequently, PSAs must meet an array of requirements at some degree contradictory, since they should hold enough elasticity to exhibit a high cohesion strength, so that they are capable of withstanding high degree of stress and enabling a clean removal, while exhibiting a low viscosity in order to present an appropriate flowability ($T_g<T_{g,Room}$), achieving a suitable surface wetting. The balance of these properties can be tailored by judicious microstructure modifications, inter alia their glass transition, molecular weight distribution, crosslinking density, etc. (Degrandi-Contraires et al., *2013*).

Among other types of analysis to evaluate the instant adhesion performance of PSAs, probe-tack tests, based on the extensional deformation of an adhesive film, are typically applied. In a probe-tack test an adhesive layer is submitted to small contact time and pressure, subsequently releasing the stress at a constant debonding rate, leading to the stretching of the adhesive in the tensile direction (Figure 2.31). The work of adhesion (W_{adh}), maximum nominal stress (σ_{max}) and strain (ε_{max}) are the main parameters resulting from the stress-strain curves, greatly influenced by the tests conditions, such as contact time/pressure, temperature, debonding rate, etc. (Baron et al., *2003*). As a consequence, Creton and coworkers (Creton and Leibler, *1996*; Creton, and Lakrout, *2000*) studied the impact of time and pressure of contact on the adhesion energy of soft viscoelastic polymeric pressure sensitive adhesives, describing a micromechanical debonding mechanism for the detachment procedure, confirming the first formation and growth of cavities followed by the appearance and further elongation of filaments until breakdown.

Generally, as depicted in Figure 2.31, during the debonding process, the first maximum stress (σ_{max}) marks the end of the adhesive elastic deformation, followed by the viscous region characterized by cavitation and, in most cases, fibrillation. The formation of such filaments and their subsequent disentanglement during detachment is the responsible for the appearance of a plateau region in the stress-strain plots. Owing to the importance of the formation of fibrils to improve the energy dissipation, Zosel (*1998*) devoted his study to get a better understanding of the relationships between the test conditions and the formation of fibrils. Indeed, the study of Mehravar et al. (*2017*), comprising the synthesis of polyurethane/acrylic hybrids to evaluate the impact of the polymer microstructure on the immediate adhesion performance, revealed the efficient improvement of adhesion energy on account of a well-defined fibrillation mechanism during detachment.

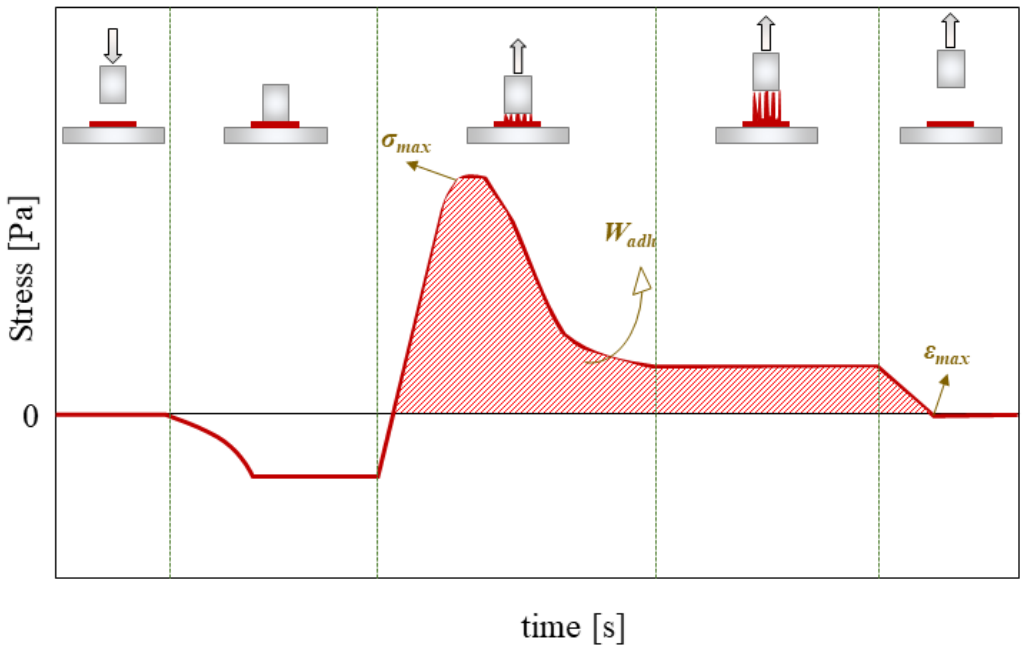

Figure 2.31 Probe-tack test scheme

3.5. Bio-polyurethanes in the adhesion field

As reviewed throughout the previous sections, the widely flexible composition of polyurethanes adhesives has made them such versatile materials that they can be applied in many areas, such as in automotive (Hicks et al., *2015*), footwear (Che et al., *2017*), woodworking (Aung et al., *2014*), etc. In general, as a consequence of such extensive array of polyurethane adhesives, several classifications can be found on the basis of different criteria, whether physical state (*solid or liquid*), number of components to blend to promote the adhesion (*single or two components*), curing mechanism (*thermosetting or thermoplastic*) or carrier (*solvent-borne, water-borne or solvent-free*) (Szycher, *2013*). These classifications meeting different approaches are summarised in Table 2.4.

Table 2.4 Polyurethane adhesives classifications

Physical State \ Components		One Component	Two Components
Liquid like	Solvent-borne	TPS	TS
	Water-borne	TPS	TS
	Solvent-free	TS	TS
Solid like	Hot melt	TP	
	Reactive hot melt	TS	
	Powder	TPS	

TP: Thermoplastic; TS: Thermosetting; TPS: Thermoplastic or Thermosetting

Two-component polyurethanes represent those adhesives traditionally produced whose components are delivered in separate compartment given their commonly high reaction rate. In these systems, whether *solvent-* or *water-based*, the curing process is mainly occasioned by carrier release after urethane linkages formation, while *solvent-free* polyurethane yield adhesive joints exclusively due to NCO-OH reaction. Conversely, ***one-component adhesives***, when *reactive*, consist of NCO-terminated prepolymers, in

which the reaction with proton donor groups on the substrate and/or with atmospheric humidity (*moisture curable polyurethanes*) is the driving force for curing, whereas those containing a carrier, like in two-component PUs, the curing comprises the coalescence of precipitated particles owing the removal of the carrier fluid. Moreover, *hot melt* PU adhesives are solid typically melted, thus acquiring appropriate wettability, leading to the adhesive bond by cooling from molten state, although on some occasions combined with moisture reactions (*reactive hot melt adhesives*) (Szycher, *2013*).

As reflected by extensive research production on moisture curable adhesives (Daniel da Silva et al., *2006*; Daniel-da-Silva et al., *2008*; Ferreira et al., *2007b*; Malucelli et al., *2005*), such type of one component polyurethanes has been widely applied. Notwithstanding, as stated above, the main obstacle of the consequent curing step is the production of CO_2 (Figure 2.3), what may diminish the adhesion performance as a result of the appearance of bubbles or pores. In this regard, some studies have avoided the carbon dioxide production by synthesizing silane-modified PU, releasing ethanol instead of CO_2 as a result of the curing reaction with environmental humidity (Yuan, Y. et al., *2017*), while Yuan, L. et al. (*2017*) reported the implementation of oxazolidines as latent curing agent, since their hydrolysis leads to alkanolamines as intermediate products, further reacting with free isocyanate groups (Figure 2.32). The ketones, produced as byproducts, are easily volatilized. With this modification, the authors succeeded in raising the shear strength eight times, while attaining twenty-fold greater adhesion forces via addition of $CaCO_3$ as a filler at a 23% of content. Filler incorporation allowed them to prepare smoother adhesive surfaces with reduced pores content as a consequence of the reinforcing water absorption effect of $CaCO_3$ particles. Therefore, these authors successfully produced more environmentally-friendly polyurethane adhesives, in a broader sense than the one associated to the definition of "*bio-based adhesives*" given by Pizzi (*2006*) (see section 3.1). Indeed, as previously mentioned, according to the *Green Chemistry* principles (Dubé and Salehpour, *2014*), the "*sustainability*" of adhesives lies not only in their provenance, i.e. their chemical constituents, but also in all aspects associated to their synthesis and application, such as the reduction of the CO_2 release related to the adhesive end use.

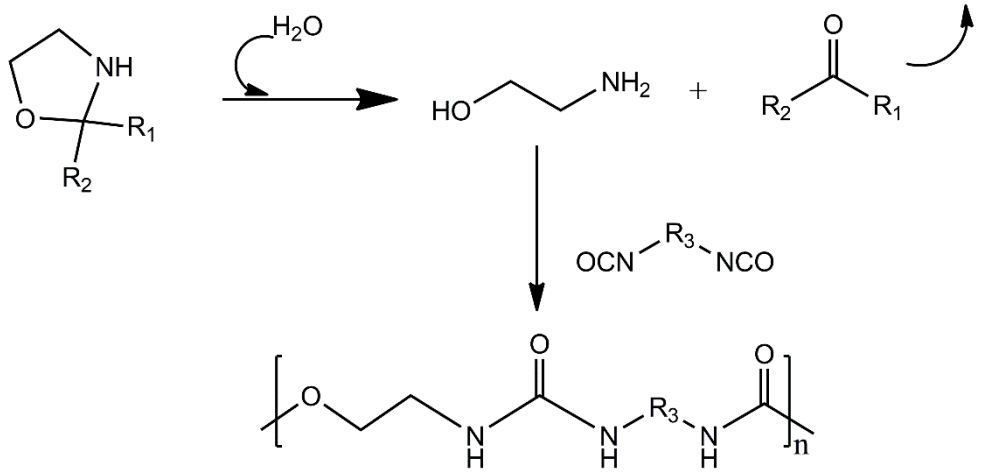

Figure 2.32 Latent curing mechanism of oxazolidines (Yuan, L. et al., 2017)

Furthermore, the great versatility of urethane polymer network has unleashed a myriad of investigations (Cui et al. *2017a*; Desai et al., *2003a*; Moghadam et al., *2016*; Sahoo et al., *2017*; Somani et al., *2003*) dealing with judicious variations in the NCO:OH molar ratio in order to optimize the PU adhesion response. Even though some scholars achieved optimal properties at higher NCO:OH ratios (Norazwani et al., *2013*; Silva et al., *2010*), most of them reported a generalized value of 1.3 to obtain more appropriate adhesion performance, giving rise to not only more interesting type of failure, i.e. substrate (Moghadam et al., *2016*), but also to improved lap-shear strengths, as described by Cui et al. (*2017b*; *2017a*) who developed PU adhesives with shear strengths of around 36 MPa, fairly competitive with the 29-37.7 MPa shown by commercial benchmarks based on petrochemical raw materials. Cui and coworkers succeeded in synthesizing fast-curing adhesives from crude-glycerol, whose curing times have proven to be below one hour, even shorter than those accomplished by PU adhesives based on castor (Somani et al., *2003*) or canola (Kong et al., *2011*) oils.

On the other hand, the adjustment of adhesion properties of polyurethanes has been also addressed by changing other parameters, such as polyol hydroxyl value (Cui et al., *2017a*) or chemical structure of chain extenders (Orgilés-Calpena et al., *2012*). Particularly significant is Somani's investigation (Somani et al., *2003*), which revealed the superior properties of aromatic isocyanates over their analogous aliphatic, leading to aromatic polyurethane with lap-shear strengths around seven times greater. Overall,

larger polyol functionalities promote greater crosslinking densities, resulting in improved T_g, chemical and hydrolysis resistance (Cui et al., *2017a*; Moghadam et al., *2016*).

With the aim to design high quality joint adhesives, as above stated, the characteristics of the substrates to be bonded deserve attention as well. Indeed, the application of mechanical pretreatment on the adhesion surfaces, mainly polishing with sandpaper to increase the adhesive penetration, is generally acknowledged (Desai et al., *2003a*). Besides that, Norazwani et al. (*2013*) assessed the modification of aluminium alloy by either alkaline etching or warm water followed by silanization. The improved adhesive wettability resulting from greater surface roughness achieved through either case, was especially noticeable in the significant contact angle reduction (20-30º) and the development of shear strengths three times higher than that shown by the untreated aluminium surface.

Moreover, given the natural compatibility between isocyanate and hydroxyl bearing compounds, polyurethane adhesives have been extensively applied for bonding wood (Aung et al., *2014*; Moghadam et al., *2016*; Silva et al., *2010*). However, on this substrate the adhesive mobility into the substrate porous is strongly influenced by wood moisture, owing to the side reaction occurring between NCO groups with water (free or bound) instead of with substrate reacting sites. Therefore, Bastani et al. (Bastani et al., *2017*) thermally modified Scots wood pine to control its moisture content, while Lavalette et al. (*2016*) revealed the greater influence of moisture content on the ultimate shear strength than the amount of one-component polyurethane adhesive in the production of green-glued plywood. Hence the considerable influence of water contact is apparent, although it can be also extended to curing and storage steps as shown by Chattopadhyay et al. (*2005*) or Asahara et al. (*2003*) when analysing the curing kinetics under moisture conditions. Because of the critical importance of correctly understanding the adhesive aging, Huacuja-Sánchez et al. (*2016*) has studied the long-term adhesion performance of crosslinked PU adhesives by conducting different maturation conditions, namely conditioning under 90% of relative humidity at 60 ºC and immersion in water at different temperatures. The plasticizing effect of water, more pronounced at greater temperatures, was proved to undermine the shear modulus in a 40% and T_g in 16.7 ºC due to the

substitution of free urethane and inter-urethane hydrogen bonding by hydrogen bridging with water molecules. Similarly, Raghunanan et al. (*2018*) submitted castor oil-based PU adhesives to different controlled relative humidities, pointing out that a greater environmental moisture allowed to achieve an improved mechanical resistance, owing to the stronger hydrogen bridging associated to a larger urea content.

In order to enhance the behaviour of polyurethane adhesives, among other properties adhesion strength, durability and thermomechanical resistance, the addition of modifiers have been proposed. Accordingly, Arán-Aís et al. (*2002*) added rosin acid to the polyurethane-urea formulation as an internal tackifier to bestow a proper immediate adhesion to PVC. Malik and Kaur (*2016*) reported the preparation of nanocomposites with the addition of titanium dioxide (TiO_2) in castor oil-based PU adhesives, entailing remarkable enhancements in adhesion strength and chemical resistance with only a 3% wt of nanoparticles, while the addition of a more moderate content of 2.5% wt of organically modified nanosilicas into hyperbranched polyurethane obtained from *Mesua ferrea* L. seed oil (Deka and Karak, *2011*) almost doubled the lap shear strength results on wood (from 6.5 up to 10.8 MPa) also raising tensile strength in 10 MPa.

In an effort to further increase the sustainability of polyurethane adhesives, as stated above (see section 2), petrochemical derivatives traditionally used in the PU production have been substituted by more eco-friendly alternatives, such as polyols resulting from liquefaction of polysaccharides (Desai et al., *2003a*; Mishra and Sinha, *2010*) or from the modification of vegetable oils, mainly epoxidation with further oxirane ring opening (Ang et al., *2014*; Norhisham et al., *2017*) or transesterification (Cakić et al., *2016*), thus designing polyurethane adhesives with fairly competitive or even superior adhesion properties than commercial benchmarks. Furthermore, the production of polyhydroxyurethanes through the already detailed non-isocyanate pathway has also been applied to synthesize PU adhesives, thus improving their renewability due to the utilization of sustainable materials, such as CO_2 (Orgilés-Calpena et al., *2016b*; Orgilés-Calpena et al., *2016a*), while at the same time avoiding the utilization of isocyanates during their synthesis. This technique also promotes the adhesion to the substrates via secondary interactions (van der Waals forces, hydrogen bonding, etc.) due to the

presence of hydroxyl groups in their chemical structure, outperforming not only the previous solvent-borne, but also WPU adhesive dispersions (Liu, H. et al., *2017*).

Finally, bearing in mind the likely reaction between free isocyanates with amine groups located in the proteins, the polyurethane adhesive field has also spread to the biomedical area, requiring quick curing process and biocompatible building blocks to be applied as bioadhesives in living tissues (Ferreira et al., *2007a*; Ferreira et al., *2007b*; Sheikh et al., *2000*). In response to the growing need for rapid curing process, photocrosslinkable technique emerges to satisfy such requirements (Li, C. et al., *2014*), enabling the reduction of the curing times till one minute as Abdalla et al. (*2016*) pointed out, obtaining morphologically homogeneous and biocompatible photocrosslinkable biomedical polyurethane adhesives from polycaprolactone-diol and 2-isocyanatoethylmethacrylate.

4. References

Abdalla, S., Al-Aama, N., Al-Ghamdi, M. A., 2016. A bio polymeric adhesive produced by photo cross-linkable technique, Polymers 8(8), 292; 10.3390/polym8080292.

Abdolhosseini, F., Givi, M. K. B., 2016. Characterization of a biodegradable polyurethane elastomer derived from castor oil, American Journal of Polymer Science 6(1), 18-27; 10.5923/j.ajps.20160601.03.

Abdollahi, M. F., Zandi, M., Shokrollahi, P., Ehsani, M., 2015. Synthesis and characterization of curcumin segmented polyurethane with induced antiplatelet activity, Journal of Polymer Research 22(9), 1-10.

Akintayo, C., Akintayo, E., Ziegler, T., Babalola, B., 2013. Newly developed epoxy-polyol and epoxy-polyurethane from renewable resources, British Journal of Applied Science & Technology 3(4), 984.

Alagi, P., Choi, Y. J., Hong, S. C., 2016a. Preparation of vegetable oil-based polyols with controlled hydroxyl functionalities for thermoplastic polyurethane, European Polymer Journal 78, 46-60.

Alagi, P., Choi, Y. J., Seog, J., Hong, S. C., 2016b. Efficient and quantitative chemical transformation of vegetable oils to polyols through a thiol-ene reaction for thermoplastic polyurethanes, Industrial Crops and Products 87, 78-88.

Alagi, P., Ghorpade, R., Jang, J. H., Patil, C., Jirimali, H., Gite, V., Hong, S. C., 2018. Functional soybean oil-based polyols as sustainable feedstocks for polyurethane coatings, Industrial Crops and Products 113, 249-258.

Alagi, P., Hong, S. C., 2015. Vegetable oil-based polyols for sustainable polyurethanes, Macromolecular Research 23(12), 1079-1086.

Ali, A., Yusoh, K., Hasany, S., 2014. Synthesis and physicochemical behaviour of polyurethane-multiwalled carbon nanotubes nanocomposites based on renewable castor oil polyols, Journal of Nanomaterials 2014, 1-9; 10.1155/2014/564384.

Allauddin, S., Narayan, R., Raju, K., 2013. Synthesis and properties of alkoxysilane castor oil and their polyurethane/urea–silica hybrid coating films, ACS Sustainable Chemistry & Engineering 1(8), 910-918; 10.1021/sc3001756.

Allen, K., 2003. “At forty cometh understanding”: A review of some basics of adhesion over the past four decades, International Journal of Adhesion and Adhesives 23(2), 87-93.

Alvarez, G. A., Fuensanta, M., Orozco, V. H., Giraldo, L. F., Martín-Martínez, J. M., 2018. Hybrid waterborne polyurethane/acrylate dispersion synthesized with bisphenol A-glicidylmethacrylate (Bis-GMA) grafting agent, Progress in Organic Coatings 118, 30-39; 10.1016/j.porgcoat.2018.01.016.

Ang, K. P., Lee, C. S., Cheng, S. F., Chuah, C. H., 2014. Synthesis of palm oil-based polyester polyol for polyurethane adhesive production, Journal of Applied Polymer Science 131(6), 39967 (1)-39967 (8); 10.1002/app.39967.

Arán-Aís, F., Torró-Palau, A. M., Orgilés-Barceló, A. C., Martín-Martínez, J. M., 2002. Characterization of thermoplastic polyurethane adhesives with different hard/soft segment ratios containing rosin as an internal tackifier, Journal of Adhesion Science and Technology 16(11), 1431-1448; 10.1163/156856102320252886.

Araujo, R. C. S., Pasa, V. M. D., 2003. Mechanical and thermal properties of polyurethane elastomers based on hydroxyl-terminated polybutadienes and biopitch, Journal of Applied Polymer Science 88(3), 759-766.

Asahara, J., Sano, A., Hori, N., Takemura, A., Ono, H., 2003. Crosslinked acrylic pressure-sensitive adhesives. II. Effect of humidity on the crosslinking reaction, Journal of Applied Polymer Science 89(11), 3039-3045.

Aung, M. M., Yaakob, Z., Kamarudin, S., Abdullah, L. C., 2014. Synthesis and characterization of Jatropha (Jatropha curcas L.) oil-based polyurethane wood adhesive, Industrial Crops and Products 60, 177-185.

Awaja, F., Gilbert, M., Kelly, G., Fox, B., Pigram, P. J., 2009. Adhesion of polymers, Progress in polymer science 34(9), 948-968.

Ayres, E., Oréfice, R. L., Yoshida, M. I., 2007. Phase morphology of hydrolysable polyurethanes derived from aqueous dispersions, European Polymer Journal 43(8), 3510-3521; 10.1016/j.eurpolymj.2007.05.014.

Badri, K. H., Ujar, A. H., Othman, Z., Hani Sahaldin, F., 2006. Shear strength of wood to wood adhesive based on palm kernel oil, Journal of Applied Polymer Science 100(3), 1759-1764.

Bahattab, M. A., Donate-Robles, J., García-Pacios, V., Martín-Martínez, J. M., 2011. Characterization of polyurethane adhesives containing nanosilicas of different particle size, International Journal of Adhesion and Adhesives 31(2), 97-103.

Bajsić, E. G., Filipan, V., Bulatović, V. O., Mandić, V., 2017. The influence of filler treatment on the mechanical properties and phase behavior of thermoplastic polyurethane/polypropylene blends, Polymer Bulletin 74(8), 2939-2955.

Baldan, A., 2012. Adhesion phenomena in bonded joints, International Journal of Adhesion and Adhesives 38, 95-116; 10.1016/j.ijadhadh.2012.04.007.

Balgude, D., Sabnis, A., Ghosh, S. K., 2016. Synthesis and Characterization of Cardanol based Aqueous 2K Polyurethane Coatings, European Polymer Journal 85, 620-634.

Baron, A., Cloutet, E., Cramail, H., Papon, E., 2003. Relationship between Architecture and Adhesive Properties of Macromolecular Materials, 1, Macromolecular Chemistry and Physics 204(13), 1616-1620.

Bastani, A., Adamopoulos, S., Militz, H., 2017. Effect of open assembly time and equilibrium moisture content on the penetration of polyurethane adhesive into thermally modified wood, The Journal of Adhesion 93(7), 575-583.

Basterretxea, A., Haga, Y., Sanchez-Sanchez, A., Isik, M., Irusta, L., Tanaka, M., Fukushima, K., Sardon, H., 2016. Biocompatibility and hemocompatibility evaluation of polyether urethanes synthesized using DBU organocatalyst, European Polymer Journal 84, 750-758.

Bayer, O., 1947. Das Di-Isocyanat-Polyadditionsverfahren (Polyurethane), Angewandte Chemie 59(9), 257-272; 10.1002/ange.19470590901.

Benhamou, K., Kaddami, H., Magnin, A., Dufresne, A., Ahmad, A., 2015. Bio-based polyurethane reinforced with cellulose nanofibers: a comprehensive investigation on the effect of interface, Carbohydrate Polymers 122, 202-211.

Berta, M., Lindsay, C., Pans, G., Camino, G., 2006. Effect of chemical structure on combustion and thermal behaviour of polyurethane elastomer layered silicate nanocomposites, Polymer Degradation and Stability 91(5), 1179-1191.

Bistričić, L., Baranović, G., Leskovac, M., Bajsić, E. G., 2010. Hydrogen bonding and mechanical properties of thin films of polyether-based polyurethane–silica nanocomposites, European Polymer Journal 46(10), 1975-1987; 10.1016/j.eurpolymj.2010.08.001.

Borrero-López, A. M., Valencia, C., Franco, J., 2017. Rheology of lignin-based chemical oleogels prepared using diisocyanate crosslinkers: Effect of the diisocyanate and curing kinetics, European Polymer Journal 89, 311-323; 10.1016/j.eurpolymj.2017.02.020.

Boutar, Y., Naïmi, S., Mezlini, S., Ali, M. B. S., 2016. Effect of surface treatment on the shear strength of aluminium adhesive single-lap joints for automotive applications, International Journal of Adhesion and Adhesives 67, 38-43.

Caillol, S., Desroches, M., Carlotti, S., Auvergne, R., Boutevin, B., 2013. Synthesis of new polyurethanes from vegetable oil by thiol-ene coupling, Green Materials 1(1), 16-26.

Cakić, S. M., Ristić, I. S., Cincović, M. M., Nikolić, N. Č, Nikolić, L. B., Cvetinov, M. J., 2017. Synthesis and properties biobased waterborne polyurethanes from glycolysis product of PET waste and poly (caprolactone) diol, Progress in Organic Coatings 105, 111-122; 10.1016/j.porgcoat.2016.10.038.

Cakić, S. M., Ristić, I. S., Milena, M., Nikolić, N. Č, Ilić, O. Z., Stojiljković, D. T., B-Simendić, J. K., 2012. Glycolyzed products from PET waste and their application in synthesis of polyurethane dispersions, Progress in organic coatings 74(1), 115-124.

Cakić, S. M., Ristić, I. S., Milena, M., Stojiljković, D. T., Jaroslava, B., 2016. Preparation and characterization of waterborne polyurethane/silica hybrid dispersions from castor oil polyols obtained by glycolysis poly (ethylene terephthalate) waste, International Journal of Adhesion and Adhesives 70, 329-341.

Cakić, S. M., Ristić, I. S., Stojiljković, D. T., Nikolić, N. N., Todorović, B. Ž, Radosavljević-Stevanović, N. V., 2018. Effect of the silica nanofiller on the properties of castor oil-based waterborne polyurethane hybrid dispersions based on recycled PET waste, Polymer Bulletin , 1-22.

Cakić, S. M., Špírková, M., Ristić, I. S., B-Simendić, J. K., Milena, M., Poręba, R., 2013. The waterborne polyurethane dispersions based on polycarbonate diol: Effect of ionic content, Materials Chemistry and Physics 138(1), 277-285; 10.1016/j.matchemphys.2012.11.057.

Calvo-Correas, T., Martin, M. D., Retegi, A., Gabilondo, N., Corcuera, M. A., Eceiza, A., 2016. Synthesis and characterization of polyurethanes with high renewable carbon content and tailored properties, ACS Sustainable Chemistry & Engineering 4(10), 5684-5692; 10.1021/acssuschemeng.6b01578.

Calvo-Correas, T., Santamaria-Echart, A., Saralegi, A., Martin, L., Valea, Á, Corcuera, M. A., Eceiza, A., 2015. Thermally-responsive biopolyurethanes from a biobased diisocyanate, European Polymer Journal 70, 173-185; 10.1016/j.eurpolymj.2015.07.022.

Campanella, A., Bonnaillie, L., Wool, R., 2009. Polyurethane foams from soyoil-based polyols, Journal of Applied Polymer Science 112(4), 2567-2578; 10.1002/app.29898.

Carothers, W. H., Hill, J. W., 1933. Studies of polymerization and ring formation. XXII. Stereochemistry and mechanism in the formation and stability of large rings, Journal of the American Chemical Society 55(12), 5043-5052.

Casdorff, K., Kläusler, O., Gabriel, J., Amen, C., Lehringer, C., Burgert, I., Keplinger, T., 2018. About the influence of a water-based priming system on the interactions between wood and one-component polyurethane adhesive studied by atomic force microscopy and confocal Raman spectroscopy imaging, International Journal of Adhesion and Adhesives 80, 52-59; 10.1016/j.ijadhadh.2017.10.001.

Casper, D. M., Newbold, T., 2006. Methods of preparing hydroxy functional vegetable oils, Patent US7893287B2, US.

Çaylı, G., Küsefoğlu, S., 2008. Biobased polyisocyanates from plant oil triglycerides: Synthesis, polymerization, and characterization, Journal of Applied Polymer Science 109(5), 2948-2955.

Cervantes-Uc, J., Espinosa, J. M., Cauich-Rodriguez, J., Avila-Ortega, A., Vázquez-Torres, H., Marcos-Fernández, A., San Román, J., 2009. TGA/FTIR studies of segmented aliphatic polyurethanes and their nanocomposites prepared with commercial montmorillonites, Polymer Degradation and Stability 94(10), 1666-1677.

Chattopadhyay, D., Prasad, P., Sreedhar, B., Raju, K., 2005. The phase mixing of moisture cured polyurethane-urea during cure, Progress in organic coatings 54(4), 296-304.

Chattopadhyay, D., Raju, K., 2007. Structural engineering of polyurethane coatings for high performance applications, Progress in Polymer Science 32(3), 352-418; 10.1016/j.progpolymsci.2006.05.003.

Che, J., Cheon, J., Chun, J., Park, C., Lee, Y., Kim, H., 2017. Preparation and properties of emulsifier-/solvent-free slightly crosslinked waterborne polyurethane-acrylic hybrid emulsions for footwear adhesives (III)–effect of trimethylol propane (TMP)/ethylene diamine (EDA) content, Journal of Adhesion Science and Technology 31(17), 1-16.

Chen, G., Guan, X., Xu, R., Tian, J., He, M., Shen, W., Yang, J., 2016. Synthesis and characterization of UV-curable castor oil-based polyfunctional polyurethane acrylate via photo-click chemistry and isocyanate polyurethane reaction, Progress in Organic Coatings 93, 11-16.

Chen, N., Zheng, P., Zeng, Q., Lin, Q., Rao, J., 2017. Characterization and performance of soy-based adhesives cured with epoxy resin, Polymers 9(10), 514.

Chen, S., Wang, Q., Wang, T., 2011. Hydroxy-terminated liquid nitrile rubber modified castor oil based polyurethane/epoxy IPN composites: Damping, thermal and mechanical properties, Polymer Testing 30(7), 726-731.

Cheng, H., Ford, C., Dowd, M. K., He, Z., 2017. Effects of phosphorus-containing additives on soy and cottonseed protein as wood adhesives, International Journal of Adhesion and Adhesives 77, 51-57.

Cherng, J. Y., Hou, T. Y., Shih, M. F., Talsma, H., Hennink, W. E., 2013. Polyurethane-based drug delivery systems, International journal of pharmaceutics 450(1), 145-162.

Chien, Y., Chuang, W., Jeng, U., Hsu, S., 2017. Preparation, Characterization, and Mechanism for Biodegradable and Biocompatible Polyurethane Shape Memory Elastomers, ACS Applied Materials & Interfaces 9(6), 5419-5429.

Choi, K. K., Park, S. H., Oh, K. W., Kim, S. H., 2015. Effect of castor oil/polycaprolactone hybrid polyols on the properties of biopolyurethane, Macromolecular Research 23(4), 333-340.

Ciecierska, E., Jurczyk-Kowalska, M., Bazarnik, P., Gloc, M., Kulesza, M., Kowalski, M., Krauze, S., Lewandowska, M., 2016. Flammability, mechanical properties and structure of rigid polyurethane foams with different types of carbon reinforcing materials, Composite Structures 140, 67-76.

Ciesielski, A., 1999. An Introduction to Rubber Technology. iSmithers Rapra Publishing.

Clerc, G., Brülisauer, M., Affolter, S., Volkmer, T., Pichelin, F., Niemz, P., 2017. Characterization of the ageing process of one-component polyurethane moisture curing wood adhesive, International Journal of Adhesion and Adhesives 72, 130-138; 10.1016/j.ijadhadh.2016.09.008.

Coleman, M. M., Lee, K. H., Skrovanek, D. J., Painter, P. C., 1986. Hydrogen bonding in polymers. 4. Infrared temperature studies of a simple polyurethane, Macromolecules 19(8), 2149-2157.

Coleman, M. M., Skrovanek, D. J., Hu, J., Painter, P. C., 1988. Hydrogen bonding in polymer blends. 1. FTIR studies of urethane-ether blends, Macromolecules 21(1), 59-65.

Corcuera, M., Rueda, L., d'Arlas, B. F., Arbelaiz, A., Marieta, C., Mondragon, I., Eceiza, A., 2010. Microstructure and properties of polyurethanes derived from castor oil, Polymer Degradation and Stability 95(11), 2175-2184; 10.1016/j.polymdegradstab.2010.03.001.

Corcuera, M., Rueda, L., Saralegui, A., Martín, M., Fernández-d'Arlas, B., Mondragon, I., Eceiza, A., 2011. Effect of diisocyanate structure on the properties and microstructure of polyurethanes based on polyols derived from renewable resources, Journal of Applied Polymer Science 122(6), 3677-3685.

Cornille, A., Auvergne, R., Figovsky, O., Boutevin, B., Caillol, S., 2017. A perspective approach to sustainable routes for non-isocyanate polyurethanes, European Polymer Journal 87, 535-552.

Cornille, A., Serres, J., Michaud, G., Simon, F., Fouquay, S., Boutevin, B., Caillol, S., 2016a. Syntheses of epoxyurethane polymers from isocyanate free oligo-polyhydroxyurethane, European Polymer Journal 75, 175-189.

Cornille, A., Guillet, C., Benyahya, S., Negrell, C., Boutevin, B., Caillol, S., 2016b. Room temperature flexible isocyanate-free polyurethane foams, European Polymer Journal 84, 873-888.

Cornille, A., Michaud, G., Simon, F., Fouquay, S., Auvergne, R., Boutevin, B., Caillol, S., 2016c. Promising mechanical and adhesive properties of isocyanate-free poly (hydroxyurethane), European Polymer Journal 84, 404-420; 10.1016/j.eurpolymj.2016.09.048.

Creton, C., Leibler, L., 1996. How does tack depend on contact time and contact pressure, Journal of Polymer Science B Polymer Physics 34, 545-554.

Creton, C., Lakrout, H., 2000. Micromechanics of flat-probe adhesion tests of soft viscoelastic polymer films, Journal of Polymer Science Part B: Polymer Physics 38(7), 965-979.

Cui, S., Luo, X., Li, Y., 2017a. Synthesis and properties of polyurethane wood adhesives derived from crude glycerol-based polyols, International Journal of Adhesion and Adhesives 79, 67-72; 10.1016/j.ijadhadh.2017.04.008.

Cui, S., Liu, Z., Li, Y., 2017b. Bio-polyols synthesized from crude glycerol and applications on polyurethane wood adhesives, Industrial Crops and Products 108, 798-805.

Culin, J., Andreis, M., Smit, I., Veksli, Z., Anzlovar, A., Zigon, M., 2004. Motional heterogeneity and phase separation of functionalized polyester polyurethanes, European polymer journal 40(8), 1857-1866.

Daniel da Silva, A. L., Martín-Martínez, J. M., Bordado, J. C. M., 2006. Influence of the free isocyanate content in the adhesive properties of reactive trifunctional polyether urethane quasi-prepolymers, International Journal of Adhesion and Adhesives 26(5), 355-362; 10.1016/j.ijadhadh.2005.06.001.

Daniel-da-Silva, A. L., Bordado, J. C. M., Martín-Martínez, J. M., 2008. Moisture curing kinetics of isocyanate ended urethane quasi-prepolymers monitored by IR spectroscopy and DSC, Journal of Applied Polymer Science 107(2), 700-709.

Das, B., Konwar, U., Mandal, M., Karak, N., 2013. Sunflower oil based biodegradable hyperbranched polyurethane as a thin film material, Industrial Crops and Products 44, 396-404; 10.1016/j.indcrop.2012.11.028.

Datta, J., Głowińska, E., 2014a. Chemical modifications of natural oils and examples of their usage for polyurethane synthesis, Journal of Elastomers & Plastics 46(1), 33-42.

Datta, J., Głowińska, E., 2014b. Effect of hydroxylated soybean oil and bio-based propanediol on the structure and thermal properties of synthesized bio-polyurethanes, Industrial Crops and Products 61, 84-91.

Degrandi-Contraires, E., Lopez, A., Reyes, Y., Asua, J. M., Creton, C., 2013. High-Shear-Strength Waterborne Polyurethane/Acrylic Soft Adhesives, Macromolecular Materials and Engineering 298(6), 612-623.

Deka, H., Karak, N., 2011. Bio-based hyperbranched polyurethane/clay nanocomposites: adhesive, mechanical, and thermal properties, Polymers for Advanced Technologies 22(6), 973-980.

Deka, H., Karak, N., 2009. Bio-based hyperbranched polyurethanes for surface coating applications, Progress in Organic Coatings 66(3), 192-198; 10.1016/j.porgcoat.2009.07.005.

Deplace, F., Carelli, C., Mariot, S., Retsos, H., Chateauminois, A., Ouzineb, K., Creton, C., 2009. Fine tuning the adhesive properties of a soft nanostructured adhesive with rheological measurements, The Journal of Adhesion 85(1), 18-54.

Desai, S. D., Patel, J. V., Sinha, V. K., 2003a. Polyurethane adhesive system from biomaterial-based polyol for bonding wood, International Journal of Adhesion and Adhesives 23(5), 393-399.

Desai, S. D., Emanuel, A. L., Sinha, V. K., 2003b. Biomaterial based polyurethane adhesive for bonding rubber and wood joints, Journal of Polymer Research 10(4), 275-281.

Desroches, M., Caillol, S., Lapinte, V., Auvergne, R., Boutevin, B., 2011. Synthesis of biobased polyols by thiol− ene coupling from vegetable oils, Macromolecules 44(8), 2489-2500.

Desroches, M., Escouvois, M., Auvergne, R., Caillol, S., Boutevin, B., 2012. From vegetable oils to polyurethanes: Synthetic routes to polyols and main industrial products, Polymer Reviews 52(1), 38-79; 10.1080/15583724.2011.640443.

Du, H., Zhao, Y., Li, Q., Wang, J., Kang, M., Wang, X., Xiang, H., 2008. Synthesis and characterization of waterborne polyurethane adhesive from MDI and HDI, Journal of Applied Polymer Science 110(3), 1396-1402.

Dubé, M. A., Salehpour, S., 2014. Applying the principles of green chemistry to polymer production technology, Macromolecular Reaction Engineering 8(1), 7-28; 10.1002/mren.201300103.

Dupre, A., 1869. Theorie mecanique de la Chaleur, Chapter IX, Actions moleculaires (suite), Paris: Gauthier-Villars.

Dutta, N., Karak, N., Dolui, S., 2004. Synthesis and characterization of polyester resins based on Nahar seed oil, Progress in organic coatings 49(2), 146-152.

Dutta, S., Karak, N., 2005. Synthesis, characterization of poly (urethane amide) resins from Nahar seed oil for surface coating applications, Progress in organic coatings 53(2), 147-152.

Dutta, S., Karak, N., 2006. Effect of the NCO/OH ratio on the properties of Mesua Ferrea L. seed oil-modified polyurethane resins, Polymer International 55(1), 49-56.

Eckert, H., Forster, B., 1987. Triphosgene, a crystalline phosgene substitute, Angewandte Chemie International Edition in English 26(9), 894-895.

Efhamisisi, D., Thevenon, M., Hamzeh, Y., Karimi, A., Pizzi, A., Pourtahmasi, K., 2016. Induced tannin adhesive by boric acid addition and its effect on bonding quality and biological performance of poplar plywood, ACS Sustainable Chemistry & Engineering 4(5), 2734-2740.

EU Publications, 2010. Commission Regulation (EU) No 276/2010 of 31 March 2010 amending Regulation (EC) No 1907/2006 of the European Parliament and of the Council on the Registration, Evaluation, Authorisation and Restriction of Chemicals (REACH) as regards Annex XVII (dichloromethane, lamp oils and grill lighter fluids and organostannic compounds), 2018, (09/18); https://publications.europa.eu/en/publication-detail/-/publication/dfe232f5-9002-4375-b4d4-00a85251525b/language-en/format-RDF.

Evtiouguina, M., Barros-Timmons, A., Cruz-Pinto, J., Neto, C. P., Belgacem, M., Gandini, A., 2002. Oxypropylation of cork and the use of the ensuing polyols in polyurethane formulations, Biomacromolecules 3(1), 57-62.

Fernández d'Arlas, B., Rueda, L., De la Caba, K., Mondragon, I., Eceiza, A., 2008. Microdomain composition and properties differences of biodegradable polyurethanes based on MDI and HDI, Polymer Engineering & Science 48(3), 519-529; 10.1002/pen.20983.

Fernández, M., Landa, M., Muñoz, M. E., Santamaría, A., 2010. Tackiness of an electrically conducting polyurethane–nanotube nanocomposite, International Journal of Adhesion and Adhesives 30(7), 609-614; 10.1016/j.ijadhadh.2010.05.011.

Ferreira, P., Pereira, R., Coelho, J., Silva, A. F., Gil, M., 2007a. Modification of the biopolymer castor oil with free isocyanate groups to be applied as bioadhesive, International journal of biological macromolecules 40(2), 144-152.

Ferreira, P., Coelho, J., Pereira, R., Silva, A. F., Gil, M., 2007b. Synthesis and characterization of a poly (ethylene glycol) prepolymer to be applied as a bioadhesive, Journal of Applied Polymer Science 105(2), 593-601.

Fonseca, L. R., Bergman, J. A., Kessler, M. R., Madbouly, S. A., Lima-Neto, B. S., 2016. Self-metathesis of 10-undecen-1-ol with Ru-amine-based complex for preparing the soft segment and chain extender of novel castor oil-based polyurethanes, Macromolecular Symposia 368(1), 30-39; 10.1002/masy.201500173.

Fridrihsone, A., Stirna, U., Lazdiņa, B., Misāne, M., Vilsone, D., 2013. Characterization of polyurethane networks structure and properties based on rapeseed oil derived polyol, European Polymer Journal 49(6), 1204-1214.

Fu, H., Wang, Y., Li, X., Chen, W., 2016. Synthesis of vegetable oil-based waterborne polyurethane/silver-halloysite antibacterial nanocomposites, Composites Science and Technology 126, 86-93.

Fuensanta, M., Jofre-Reche, J. A., Rodríguez-Llansola, F., Costa, V., Iglesias, J. I., Martín-Martínez, J. M., 2017. Structural characterization of polyurethane ureas and waterborne polyurethane urea dispersions made with mixtures of polyester polyol and polycarbonate diol, Progress in Organic Coatings 112, 141-152; 10.1016/j.porgcoat.2017.07.009.

Gabriel, L. P., dos Santos, Maria Elizabeth M, Jardini, A. L., Bastos, G. N., Dias, C. G., Webster, T. J., Maciel Filho, R., 2016. Bio-based polyurethane for tissue engineering applications: How hydroxyapatite nanoparticles influence the structure, thermal and biological behavior of polyurethane composites, Nanomedicine: Nanotechnology, Biology and Medicine 13(1), 201-208.

Gallego, R., Arteaga, J. F., Valencia, C., Díaz, M. J., Franco, J. M., 2015a. Gel-like dispersions of HMDI-cross-linked lignocellulosic materials in castor oil: Toward completely renewable lubricating grease formulations, ACS Sustainable Chemistry & Engineering 3(9), 2130-2141; 10.1021/acssuschemeng.5b00389.

Gallego, R., Arteaga, J., Valencia, C., Franco, J., 2015b. Thickening properties of several NCO-functionalized cellulose derivatives in castor oil, Chemical Engineering Science 134, 260-268; 10.1016/j.ces.2015.05.007.

Gallego, R., Arteaga, J., Valencia, C., Franco, J., 2013a. Chemical modification of methyl cellulose with HMDI to modulate the thickening properties in castor oil, Cellulose 20(1), 495-507; 10.1007/s10570-012-9803-4.

Gallego, R., Arteaga, J., Valencia, C., Franco, J., 2013b. Rheology and thermal degradation of isocyanate-functionalized methyl cellulose-based oleogels, Carbohydrate Polymers 98(1), 152-160; 10.1016/j.carbpol.2013.04.104.

Gallego, R., Cidade, T., Sánchez, R., Valencia, C., Franco, J., 2016. Tribological behaviour of novel chemically modified biopolymer-thickened lubricating greases investigated in a steel–steel rotating ball-on-three plates tribology cell, Tribology International 94, 652-660.

Gandini, A., 2008. Polymers from renewable resources: a challenge for the future of macromolecular materials, Macromolecules 41(24), 9491-9504.

Ghahri, S., Pizzi, A., Mohebby, B., Mirshokraie, A., Mansouri, H. R., 2018. Soy-based, tannin-modified plywood adhesives, The Journal of Adhesion 94(3), 218-237.

Głowińska, E., Datta, J., 2016. Bio polyetherurethane composites with high content of natural ingredients: Hydroxylated soybean oil based polyol, bio glycol and microcrystalline cellulose, Cellulose 23(1), 581-592; 10.1007/s10570-015-0825-6.

Głowińska, E., Datta, J., 2015. Structure, morphology and mechanical behaviour of novel bio-based polyurethane composites with microcrystalline cellulose, Cellulose 22(4), 2471-2481; 10.1007/s10570-015-0685-0.

Głowińska, E., Datta, J., 2014. A mathematical model of rheological behavior of novel bio-based isocyanate-terminated polyurethane prepolymers, Industrial Crops and Products 60, 123-129.

Gogoi, S., Karak, N., 2014. Biobased biodegradable waterborne hyperbranched polyurethane as an ecofriendly sustainable material, ACS Sustainable Chemistry & Engineering 2(12), 2730-2738; 10.1021/sc5006022.

Griffini, G., Passoni, V., Suriano, R., Levi, M., Turri, S., 2015. Polyurethane coatings based on chemically unmodified fractionated lignin, ACS Sustainable Chemistry & Engineering 3(6), 1145-1154.

Groszos, S. J., Drechsel, E. K., 1957. Method of preparing a polyurethane .

Gumus, R. H., Wauton, I., 2014. Rheological Characterization of Yam and Potato Paste (Dioscorea rotundata) and (Ipomea batata) for Adhesive Purpose, Advances in Chemical Engineering and Science 2014.

Güney, A., Hasirci, N., 2014. Properties and phase segregation of crosslinked PCL-based polyurethanes, Journal of Applied Polymer Science 131(1), 1-13; 10.1002/APP.39758.

Guo, A., Cho, Y., Petrović, Z. S., 2000. Structure and properties of halogenated and nonhalogenated soy-based polyols, Journal of Polymer Science Part A: Polymer Chemistry 38(21), 3900-3910.

Guo, A., Demydov, D., Zhang, W., Petrovic, Z. S., 2002. Polyols and polyurethanes from hydroformylation of soybean oil, Journal of Polymers and the Environment 10(1-2), 49-52.

Guo, Z., Kim, T. Y., Lei, K., Pereira, T., Sugar, J. G., Hahn, H. T., 2008. Strengthening and thermal stabilization of polyurethane nanocomposites with silicon carbide nanoparticles by a surface-initiated-polymerization approach, Composites Science and Technology 68(1), 164-170.

Gurunathan, T., Chung, J. S., 2016. Physicochemical oroperties of amino–silane-terminated vegetable oil-based waterborne polyurethane nanocomposites, ACS Sustainable Chemistry & Engineering 4(9), 4645-4653; 10.1021/acssuschemeng.6b00768.

Gurunathan, T., Mohanty, S., Nayak, S. K., 2015. Isocyanate terminated castor oil-based polyurethane prepolymer: Synthesis and characterization, Progress in Organic Coatings 80, 39-48; 10.1016/j.porgcoat.2014.11.017.

Hablot, E., Zheng, D., Bouquey, M., Avérous, L., 2008. Polyurethanes based on castor oil: kinetics, chemical, mechanical and thermal properties, Macromolecular Materials and Engineering 293(11), 922-929.

He, W., Fang, Z., Ji, D., Chen, K., Wan, Z., Li, X., Gan, H., Tang, S., Zhang, K., Guo, K., 2013. Epoxidation of soybean oil by continuous micro-flow system with continuous separation, Organic Process Research & Development 17(9), 1137-1141.

He, X., Wu, G., Xu, L., Yan, J., Yan, Y., 2018. Lipase-Catalyzed Synthesis, Properties Characterization, and Application of Bio-Based Dimer Acid Cyclocarbonate, Polymers 10(3), 262.

Heck, C. A., dos Santos, João Henrique Z, Wolf, C. R., 2015. Waterborne polyurethane: the effect of the addition or in situ formation of silica on mechanical properties and adhesion, International Journal of Adhesion and Adhesives 58, 13-20.

Hicks, C. R., Carlson, B. E., Mallick, P., 2015. Rheological study of automotive adhesives: Influence of storage time, temperature and shear rate on viscosity at dispensing, International Journal of Adhesion and Adhesives 63, 108-116.

Hojabri, L., Kong, X., Narine, S. S., 2010. Novel long chain unsaturated diisocyanate from fatty acid: Synthesis, characterization, and application in bio-based polyurethane, Journal of Polymer Science Part A-1: Polymer Chemistry 48(15), 3302-3310.

Hojabri, L., Kong, X., Narine, S. S., 2009. Fatty acid-derived diisocyanate and biobased polyurethane produced from vegetable oil: synthesis, polymerization, and characterization, Biomacromolecules 10(4), 884-891.

Honarkar, H., 2017. Waterborne Polyurethanes: A Review, Journal of Dispersion Science and Technology (just-accepted).

Hu, Y., Feng, G., Shang, Q., Bo, C., Jia, P., Liu, C., Xu, F., Zhou, Y., 2018. Bio-based reactive diluent derived from cardanol and its application in polyurethane acrylate (PUA) coatings with high performance, Journal of Coatings Technology and Research , 1-11; 10.1007/s11998-018-0128-6.

Huacuja-Sánchez, J., Müller, K., Possart, W., 2016. Water diffusion in a crosslinked polyether-based polyurethane adhesive, International Journal of Adhesion and Adhesives 66, 167-175; 10.1016/j.ijadhadh.2016.01.005.

Isikgor, F. H., Becer, C. R., 2015. Lignocellulosic biomass: a sustainable platform for the production of bio-based chemicals and polymers, Polymer Chemistry 6(25), 4497-4559.

Jaruchattada, J., Fuongfuchat, A., Pattamaprom, C., 2012. Rheological investigation of cure kinetics and adhesive strength of polyurethane acrylate adhesive, Journal of Applied Polymer Science 123(4), 2344-2350.

Javni, I., Petrović, Z. S., Guo, A., Fuller, R., 2000. Thermal stability of polyurethanes based on vegetable oils, Journal of Applied Polymer Science 77(8), 1723-1734.

Jeong, H., Park, J., Kim, S., Lee, J., Ahn, N., Roh, H., 2013. Preparation and characterization of thermoplastic polyurethanes using partially acetylated kraft lignin, Fibers and Polymers 14(7), 1082-1093.

Ji, D., Fang, Z., He, W., Zhang, K., Luo, Z., Wang, T., Guo, K., 2015. Synthesis of soy-polyols using a continuous microflow system and preparation of soy-based polyurethane rigid foams, ACS Sustainable Chemistry & Engineering 3(6), 1197-1204; 10.1021/acssuschemeng.5b00170.

Ji, X., Li, B., Yuan, B., Guo, M., 2017. Preparation and characterizations of a chitosan-based medium-density fiberboard adhesive with high bonding strength and water resistance, Carbohydrate Polymers 176, 273-280.

Jiao, Z., Yang, Q., Wang, X., Wang, C., 2016. UV-curable hyperbranched urethane acrylate oligomers modified with different fatty acids, Polymer Bulletin 74(12), 5049-5063.

Kavanaugh, T. E., Clark, A. Y., Chan-Chan, L. H., Ramírez-Saldaña, M., Vargas-Coronado, R. F., Cervantes-Uc, J. M., Hernández-Sánchez, F., García, A. J., Cauich-Rodríguez, J. V., 2016. Human mesenchymal stem cell behavior on segmented polyurethanes prepared with biologically active chain extenders, Journal of Materials Science: Materials in Medicine 27(2), 1-11.

Khanlari, S., Dubé, M. A., 2013. Bioadhesives: a review, Macromolecular Reaction Engineering 7(11), 573-587.

Kim, K. H., Yu, J., Lee, E. Y., 2016. Crude glycerol-mediated liquefaction of saccharification residues of sunflower stalks for production of lignin biopolyols, Journal of Industrial and Engineering Chemistry 38, 175-180.

Kim, M., Kim, H., Ha, C., Park, D., Lee, J., 2001. Syntheses and thermal properties of poly (hydroxy) urethanes by polyaddition reaction of bis (cyclic carbonate) and diamines, Journal of Applied Polymer Science 81(11), 2735-2743.

Kong, X., Liu, G., Curtis, J. M., 2012. Novel polyurethane produced from canola oil based poly (ether ester) polyols: Synthesis, characterization and properties, European Polymer Journal 48(12), 2097-2106; 10.1016/j.eurpolymj.2012.08.012.

Kong, X., Liu, G., Curtis, J. M., 2011. Characterization of canola oil based polyurethane wood adhesives, International Journal of Adhesion and Adhesives 31(6), 559-564; 10.1016/j.ijadhadh.2011.05.004.

Kong, X., Yue, J., Narine, S. S., 2007. Physical properties of canola oil based polyurethane networks, Biomacromolecules 8(11), 3584-3589; 10.1021/bm0704018.

Kong, X., Zhao, L., Curtis, J. M., 2016. Polyurethane nanocomposites incorporating biobased polyols and reinforced with a low fraction of cellulose nanocrystals, Carbohydrate Polymers 152, 487-495; 10.1016/j.carbpol.2016.07.032.

Krol, P., 2007. Synthesis methods, chemical structures and phase structures of linear polyurethanes. Properties and applications of linear polyurethanes in polyurethane elastomers, copolymers and ionomers, Progress in materials science 52(6), 915-1015.

Kultys, A., Pikus, S., 2001. Polyurethanes containing sulfur. III. New thermoplastic HDI-based segmented polyurethanes with diphenylmethane unit in their structure, Journal of Polymer Science Part A: Polymer Chemistry 39(10), 1733-1742.

Kupka, V., Vojtova, L., Fohlerova, Z., Jancar, J., 2016. Solvent free synthesis and structural evaluation of polyurethane films based on poly (ethylene glycol) and poly (caprolactone). Express Polymer Letters 10(6), 479-492; 10.3144/expresspolymlett.2016.46.

Lamarzelle, O., Durand, P., Wirotius, A., Chollet, G., Grau, E., Cramail, H., 2016. Activated lipidic cyclic carbonates for non-isocyanate polyurethane synthesis, Polymer Chemistry 7(7), 1439-1451.

Lavalette, A., Cointe, A., Pommier, R., Danis, M., Delisée, C., Legrand, G., 2016. Experimental design to determine the manufacturing parameters of a green-glued plywood panel, European Journal of Wood and Wood Products , 1-9.

Lee, H. S., Wang, Y. K., Hsu, S. L., 1987. Spectroscopic analysis of phase separation behavior of model polyurethanes, Macromolecules 20(9), 2089-2095.

Lee, J., Lee, J. H., Kim, D., Park, C., Yu, J., Lee, E. Y., 2016. Crude glycerol-mediated liquefaction of empty fruit bunches saccharification residues for preparation of biopolyurethane, Journal of Industrial and Engineering Chemistry 34, 157-164.

Lee, S., Hahn, Y. B., Nahm, K. S., Lee, Y., 2005. Synthesis of polyether-based polyurethane-silica nanocomposites with high elongation property, Polymers for Advanced Technologies 16(4), 328-331.

Lei, L., Xia, Z., Lin, X., Yang, T., Zhong, L., 2015. Synthesis and adhesion properties of waterborne polyurethane dispersions with long-branched aliphatic chains, Journal of Applied Polymer Science 132(12).

Lei, L., Zhang, Y., Ou, C., Xia, Z., Zhong, L., 2016. Synthesis and characterization of waterborne polyurethanes with alkoxy silane groups in the side chains for potential application in waterborne ink, Progress in Organic Coatings 92, 85-94.

Leitsch, E. K., Heath, W. H., Torkelson, J. M., 2016. Polyurethane/polyhydroxyurethane hybrid polymers and their applications as adhesive bonding agents, International Journal of Adhesion and Adhesives 64, 1-8.

Li, C., Wang, T., Hu, L., Wei, Y., Liu, J., Mu, X., Nie, J., Yang, D., 2014. Photocrosslinkable bioadhesive based on dextran and PEG derivatives, Materials Science and Engineering: C 35, 300-306.

Li, X., Li, W., Wang, X., Guo, H., Wang, R., Guo, X., Li, C., Jia, X., 2018. Enhanced adhesion force based on microphase separation induced by complexation of ferric ions and polyurethane matrix, Journal of Applied Polymer Science 135(17), 46069.

Li, Y., Luo, X., Hu, S., 2015. Bio-Based Polyols and Polyurethanes. Springer briefs in molecular science: Green chemistry for sustainabiliy: Springer.

Li, Y., Noordover, B. A., van Benthem, R. A., Koning, C. E., 2014. Reactivity and regio-selectivity of renewable building blocks for the synthesis of water-dispersible polyurethane prepolymers, ACS Sustainable Chemistry & Engineering 2(4), 788-797.

Liang, L., Mao, Z., Li, Y., Wan, C., Wang, T., Zhang, L., Zhang, L., 2007. Liquefaction of crop residues for polyol production, BioResources 1(2), 248-256.

Ling, Z., Omura, Y., Hori, N., Iwata, T., Takemura, A., 2018. In-situ chemical structure analysis of aqueous vinyl polymer solution-isocyanate adhesive in post-cure process by using Fourier transform near infrared spectroscopy, International Journal of Adhesion and Adhesives 81, 56-64.

Liu, B., Nie, J., He, Y., 2016. From rosin to high adhesive polyurethane acrylate: synthesis and properties, International Journal of Adhesion and Adhesives 66, 99-103.

Liu, G., Wu, G., Chen, J., Kong, Z., 2016. Synthesis, modification and properties of rosin-based non-isocyanate polyurethanes coatings, Progress in Organic Coatings 101, 461-467.

Liu, H., Li, C., Sun, X. S., 2017. Soy-oil-based waterborne polyurethane improved wet strength of soy protein adhesives on wood, International Journal of Adhesion and Adhesives 73, 66-74; 10.1016/j.ijadhadh.2016.09.006.

Liu, K., Miao, S., Su, Z., Sun, L., Ma, G., Zhang, S., 2016a. Castor oil-based waterborne polyurethanes with tunable properties and excellent biocompatibility, European Journal of Lipid Science and Technology 118, 1-9; 10.1002/ejlt.201500595.

Liu, K., Su, Z., Miao, S., Ma, G., Zhang, S., 2016b. UV-curable enzymatic antibacterial waterborne polyurethane coating, Biochemical engineering journal 113, 107-113.

Liu, S., Wang, X., 2017. Polymers from carbon dioxide: Polycarbonates, polyurethanes, Current Opinion in Green and Sustainable Chemistry 3, 61-66.

Liu, T., Ye, L., 2010. Synthesis and properties of fluorinated thermoplastic polyurethane elastomer, Journal of Fluorine Chemistry 131(1), 36-41.

Liu, X., Xu, K., Liu, H., Cai, H., Su, J., Fu, Z., Guo, Y., Chen, M., 2011. Preparation and properties of waterborne polyurethanes with natural dimer fatty acids based polyester polyol as soft segment, Progress in Organic Coatings 72(4), 612-620.

Liu, Y., Li, K., 2007. Development and characterization of adhesives from soy protein for bonding wood, International Journal of Adhesion and Adhesives 27(1), 59-67; 10.1016/j.ijadhadh.2005.12.004.

Lligadas, G., Ronda, J., Galia, M., Biermann, U., Metzger, J., 2006. Synthesis and characterization of polyurethanes from epoxidized methyl oleate based polyether polyols as renewable resources, Journal of Polymer Science Part A: Polymer Chemistry 44(1), 634-645.

Lligadas, G., Ronda, J. C., Galià, M., Cádiz, V., 2010. Oleic and undecylenic acids as renewable feedstocks in the synthesis of polyols and polyurethanes, Polymers 2(4), 440-453.

Lluch, C., Ronda, J. C., Galià, M., Lligadas, G., Cádiz, V., 2010. Rapid Approach to Biobased Telechelics through Two One-Pot Thiol− Ene Click Reactions, Biomacromolecules 11(6), 1646-1653.

Lopez, A., Degrandi-Contraires, E., Canetta, E., Creton, C., Keddie, J. L., Asua, J. M., 2011. Waterborne Polyurethane− Acrylic Hybrid Nanoparticles by Miniemulsion Polymerization: Applications in Pressure-Sensitive Adhesives, Langmuir 27(7), 3878-3888.

Ma, G., Shen, Y., Gao, R., Wang, X., 2017. Micromorphology and adhesive properties of sulfonated polyurethane/polyacrylate emulsions prepared by surfactant-free polymerization, Journal of Polymer Research 24(3), 36-47; 10.1007/s10965-017-1200-0.

Ma, Z., Li, C., Fan, H., Wan, J., Luo, Y., Li, B., 2017. Polyhydroxyurethanes (PHUs) Derived from Diphenolic Acid and Carbon Dioxide and Their Application in Solvent-and Water-Borne PHU Coatings, Industrial & Engineering Chemistry Research 56(47), 14089-14100.

Maassen, W., Meier, M. A., Willenbacher, N., 2016. Unique adhesive properties of pressure sensitive adhesives from plant oils, International Journal of Adhesion and Adhesives 64, 65-71.

Maciel, V. G., Bockorny, G., Domingues, N., Scherer, M. B., Zortea, R. B., Seferin, M., 2017. Comparative Life Cycle Assessment among Three Polyurethane Adhesive Technologies for the Footwear Industry, ACS Sustainable Chemistry & Engineering 5(9), 8464-8472.

Mahapatra, S. S., Karak, N., 2004. Synthesis and characterization of polyesteramide resins from Nahar seed oil for surface coating applications, Progress in organic coatings 51(2), 103-108.

Malik, M., Kaur, R., 2016. Mechanical and Thermal Properties of Castor Oil–Based Polyurethane Adhesive: Effect of TiO2 Filler, Advances in Polymer Technology 00, 1-7; 10.1002/adv.21637.

Mallonee, J. E., 1961. Stable polyurethane latex and process of making same, Patent US2968575, US.

Malucelli, G., Priola, A., Ferrero, F., Quaglia, A., Frigione, M., Carfagna, C., 2005. Polyurethane resin-based adhesives: curing reaction and properties of cured systems, International Journal of Adhesion and Adhesives 25(1), 87-91.

Manjula, K., 2007. Transport characteristics of carboxylic acids based chain extended PU membranes with n-alkane penetrants, Polymer Engineering & Science 47(12), 2057-2064.

Manjula, K., Kumar, S., Soare, B. G., Picciani, P., 2010. Biobased chain extended polyurethane and its composites with silk fiber, Polymer Engineering & Science 50(4), 851-856; 10.1002/pen.21604.

Mattia, J., Painter, P., 2007. A comparison of hydrogen bonding and order in a polyurethane and poly (urethane− urea) and their blends with poly (ethylene glycol), Macromolecules 40(5), 1546-1554; 10.1021/ma0626362.

Mazzeo, F. A., 2002. Characterization of pressure sensitive adhesives by rheology, TA Instruments report RH082, 1-8.

Mehravar, S., Ballard, N., Agirre, A., Tomovska, R., Asua, J. M., 2017. Relating polymer microstructure to adhesive performance in blends of hybrid polyurethane/acrylic latexes, European Polymer Journal 87, 300-307.

Mekewi, M. A., Ramadan, A. M., ElDarse, F. M., Rehim, M. H. A., Mosa, N. A., Ibrahim, M. A., 2017. Preparation and characterization of polyurethane plasticizer for flexible packaging applications: Natural oils affirmed access, Egyptian Journal of Petroleum 26(1), 9-15; 10.1016/j.ejpe.2016.02.002.

Miao, S., Zhang, S., Su, Z., Wang, P., 2010. A novel vegetable oil–lactate hybrid monomer for synthesis of high-Tg polyurethanes, Journal of Polymer Science Part A-1: Polymer Chemistry 48(1), 243-250.

Mishra, D., Sinha, V. K., 2010. Eco-economical polyurethane wood adhesives from cellulosic waste: Synthesis, characterization and adhesion study, International Journal of Adhesion and Adhesives 30(1), 47-54; 10.1016/j.ijadhadh.2009.08.003.

Moghadam, P. N., Yarmohamadi, M., Hasanzadeh, R., Nuri, S., 2016. Preparation of polyurethane wood adhesives by polyols formulated with polyester polyols based on castor oil, International Journal of Adhesion and Adhesives 68, 273-282; 10.1016/j.ijadhadh.2016.04.004.

Mohamed, H., Morsi, S., Badran, B., Rabie, A., 2017. Eco-friendly protective coatings based on poly (urethane sulfone amide) dispersions for carbon steel, Journal of Coatings Technology and Research 14(2), 437-446.

Monteavaro, L. L., da Silva, E. O., Costa, A. P. O., Samios, D., Gerbase, A. E., Petzhold, C. L., 2005. Polyurethane networks from formiated soy polyols: synthesis and mechanical characterization, Journal of the American Oil Chemists' Society 82(5), 365-371.

More, A. S., Lebarbé, T., Maisonneuve, L., Gadenne, B., Alfos, C., Cramail, H., 2013. Novel fatty acid based di-isocyanates towards the synthesis of thermoplastic polyurethanes, European Polymer Journal 49(4), 823-833.

Narine, S. S., Yue, J., Kong, X., 2007. Production of polyols from canola oil and their chemical identification and physical properties, Journal of the American Oil Chemists' Society 84(2), 173-179.

Narute, P., Palanisamy, A., 2016. Study of the performance of polyurethane coatings derived from cottonseed oil polyol, Journal of Coatings Technology and Research 13(1), 171-179; 10.1007/s11998-015-9741-9.

Ning, L., De-Ning, W., Sheng-Kang, Y., 1997. Hydrogen-bonding properties of segmented polyether poly (urethane urea) copolymer, Macromolecules 30(15), 4405-4409; 10.1021/ma951386e.

Ning, L., De-Ning, W., Sheng-Kang, Y., 1996. Hydrogen bonding between urethane and urea: band assignment for the carbonyl region of FTi. r. spectrum, Polymer 37(14), 3045-3047.

Nohra, B., Candy, L., Blanco, J., Guerin, C., Raoul, Y., Mouloungui, Z., 2013. From petrochemical polyurethanes to biobased polyhydroxyurethanes, Macromolecules 46(10), 3771-3792.

Norazwani, M. Z., Ahmad, S. H., Ali, E. S., 2013. Green Polyurethane Adhesive Bonding of Aluminum: Effect of Surface Treatments, Applied Mechanics and Materials 393, 51.

Norhisham, S. M., Maznee, T. T. N., Ain, H. N., Devi, P. K., Srihanum, A., Norhayati, M., Yeong, S., Hazimah, A., Schiffman, C. M., Sendijarevic, A., 2017. Soft polyurethane elastomers with adhesion properties based on palm olein and palm oil fatty acid methyl ester polyols, International Journal of Adhesion and Adhesives 73, 38-44; 10.1016/j.ijadhadh.2016.10.012.

Octave, S., Thomas, D., 2009. Biorefinery: toward an industrial metabolism, Biochimie 91(6), 659-664.

Ogunniyi, D., 2006. Castor oil: A vital industrial raw material, Bioresource technology 97(9), 1086-1091; 10.1016/j.biortech.2005.03.028.

Oprea, S., Potolinca, V. O., Gradinariu, P., Joga, A., Oprea, V., 2016. Synthesis, properties, and fungal degradation of castor-oil-based polyurethane composites with different cellulose contents, Cellulose 23, 2515-2526; 10.1007/s10570-016-0972-4.

Orgilés-Calpena, E., Arán-Aís, F., Torró-Palau, A. M., Montiel-Parreño, E., Orgilés-Barceló, C., 2016a. Synthesis of polyurethanes from CO2-based polyols: A challenge for sustainable adhesives, International Journal of Adhesion and Adhesives 67, 63-68.

Orgilés-Calpena, E., Arán-Aís, F., Torró-Palau, A. M., Orgilés-Barceló, C., 2016b. Novel polyurethane reactive hot melt adhesives based on polycarbonate polyols derived from CO 2 for the footwear industry, International Journal of Adhesion and Adhesives 70, 218-224.

Orgilés-Calpena, E., Arán-Aís, F., Torró-Palau, A. M., Orgilés-Barceló, C., 2012. Influence of the chain extender nature on adhesives properties of polyurethane dispersions, Journal of Dispersion Science and Technology 33(1), 147-154.

Orgiles-Calpena, E., Aran-Ais, F., Torró-Palau, A. M., Orgilés-Barceló, C., Martín-Martínez, J. M., 2009. Addition of different amounts of a urethane-based thickener to waterborne polyurethane adhesive, International Journal of Adhesion and Adhesives 29(3), 309-318.

Otieno, G., Kim, J., 2008. Conductive graphite/polyurethane composite films using amphiphilic reactive dispersant: Synthesis and characterization, Journal of Industrial and Engineering Chemistry 14(2), 187-193.

Otorgust, G., Dodiuk, H., Kenig, S., Tenne, R., 2017. Important insights into polyurethane nanocomposite-adhesives; a comparative study between INT-WS 2 and CNT, European Polymer Journal 89, 281-300; 10.1016/j.eurpolymj.2017.02.027.

Park, S. H., Oh, K. W., Kim, S. H., 2013. Reinforcement effect of cellulose nanowhisker on bio-based polyurethane, Composites Science and Technology 86, 82-88.

Patel, C. M., Barot, A. A., Kumar Sinha, V., 2016. Sequential liquefaction of Nicotiana tabacum stems biomass by crude polyhydric alcohols for the production of polyols and rigid polyurethane foams, Journal of Applied Polymer Science 133(38).

Patel, M. M., Patel, K. I., Patel, H. B., Parmar, J. S., 2009. UV-curable polyurethane coatings derived from cellulose, Iranian Polymer Journal 18(11), 903-915.

Patil, C. K., Rajput, S. D., Marathe, R. J., Kulkarni, R. D., Phadnis, H., Sohn, D., Mahulikar, P. P., Gite, V. V., 2017. Synthesis of bio-based polyurethane coatings from vegetable oil and dicarboxylic acids, Progress in Organic Coatings 106, 87-95.

Pavličević, J., Špírková, M., Bera, O., Jovičić, M., Pilić, B., Baloš, S., Budinski-Simendić, J., 2014. The influence of ZnO nanoparticles on thermal and mechanical behavior of polycarbonate-based polyurethane composites, Composites Part B: Engineering 60, 673-679.

Pawar, M. S., Kadam, A. S., Yemul, O. S., 2015. Development of polyetheramide based corrosion protective polyurethane coating from mahua oil, Progress in Organic Coatings 89, 143-149.

Paz, R. J. G., 2010. A green approach toward oleic and undecylenic acids-derived polyurethanes, Journal of Polymer Science Part A: Polymer Chemistry 49(11), 2407-2416.

Pechar, T. W., Wilkes, G. L., Zhou, B., Luo, N., 2007. Characterization of soy-based polyurethane networks prepared with different diisocyanates and their blends with petroleum-based polyols, Journal of Applied Polymer Science 106(4), 2350-2362.

Pérez-Limiñana, M. Á, Arán-Aís, F., Torró-Palau, A. M., Orgilés-Barceló, C., Martín-Martínez, J. M., 2006. Structure and properties of waterborne polyurethane adhesives obtained by different methods, Journal of Adhesion Science and Technology 20(6), 519-536.

Petrović, Z. S., 2008. Polyurethanes from vegetable oils, Polymer Reviews 48(1), 109-155.

Petrović, Z. S., Javni, I., Waddon, A., Bánhegyi, G., 2000. Structure and properties of polyurethane–silica nanocomposites, Journal of Applied Polymer Science 76(2), 133-151.

Petrović, Z. S., Yang, L., Zlatanić, A., Zhang, W., Javni, I., 2007. Network structure and properties of polyurethanes from soybean oil, Journal of Applied Polymer Science 105(5), 2717-2727.

Petrovic, Z. S., Zhang, W., Javni, I., 2005. Structure and properties of polyurethanes prepared from triglyceride polyols by ozonolysis, Biomacromolecules 6(2), 713-719.

Petrovic, Z., Javni, I., Guo, A., Zhang, W., 2002. Method of making natural oil-based polyols and polyurethanes therefrom, Patent US10176214, US.

Pizzi, A., 2006. Recent developments in eco-efficient bio-based adhesives for wood bonding: Opportunities and issues, Journal of Adhesion Science and Technology 20(8), 829-846; 10.1163/156856106777638635.

Queiroz, D. P., de Pinho, M. N., Dias, C., 2003. ATR− FTIR studies of poly (propylene oxide)/polybutadiene bi-soft segment urethane/urea membranes, Macromolecules 36(11), 4195-4200; 10.1021/ma034032t.

Raghunanan, L. C., Fernandez-Prieto, S., Martínez, I., Valencia, C., Sánchez, M. C., Franco, J. M., 2018. Molecular insights into the mechanisms of humidity-induced changes on the bulk performance of model castor oil derived polyurethane adhesives, European Polymer Journal 101, 291-303; 10.1016/j.eurpolymj.2018.02.041.

Raquez, J., Deléglise, M., Lacrampe, M., Krawczak, P., 2010. Thermosetting (bio) materials derived from renewable resources: a critical review, Progress in Polymer Science 35(4), 487-509.

Rezayan, A. H., Firoozi, N., Kheirjou, S., Tabatabaei Rezaei, S. J., Nabid, M. R., 2017. Synthesis and Characterization of Biodegradable Semi-Interpenetrating Polymer Networks Based on Star-Shaped Copolymers of varepsilon-Caprolactone and Lactide, Iranian journal of pharmaceutical research : IJPR 16(1), 63-73.

Rogulska, M., Kultys, A., Puszka, A., 2017. New thermoplastic poly (carbonate-urethane) s based on chain extenders with sulfur atoms, Chemical Papers 71(7), 1195-1204.

Rojek, P., Prociak, A., 2012. Effect of different rapeseed-oil-based polyols on mechanical properties of flexible polyurethane foams, Journal of Applied Polymer Science 125(4), 2936-2945; 10.1002/app.36500.

Ruanpan, S., Manuspiya, H., 2018. Synthesized amino-functionalized porous clay heterostructure as an effective thickener in waterborne polyurethane hybrid adhesives for lamination processes, International Journal of Adhesion and Adhesives 80, 66-75; 10.1016/j.ijadhadh.2017.10.005.

Rueda-Larraz, L., d'Arlas, B. F., Tercjak, A., Ribes, A., Mondragon, I., Eceiza, A., 2009. Synthesis and microstructure–mechanical property relationships of segmented polyurethanes based on a PCL–PTHF–PCL block copolymer as soft segment, European Polymer Journal 45(7), 2096-2109; 10.1016/j.eurpolymj.2009.03.013.

Saetung, A., Rungvichaniwat, A., Tsupphayakorn-ake, P., Bannob, P., Tulyapituk, T., Saetung, N., 2016. Properties of waterborne polyurethane films: effects of blend formulation with hydroxyl telechelic natural rubber and modified rubber seed oils, Journal of Polymer Research 23(12), 264.

Sahoo, S., Kalita, H., Mohanty, S., Nayak, S. K., 2017. Synthesis and characterization of vegetable oil based polyurethane derived from low viscous bio aliphatic isocyanate: Adhesion strength to wood-wood substrate bonding, Macromolecular Research 25(8), 1-7; 10.1007/s13233-017-5080-2.

Sánchez-Adsuar, M., Pastor-Blas, M., Martín-Martínez, J., Villenave, J., 1997. Properties of elastomeric polyurethanes obtained with ϵ-caprolactone macroglycol, International Journal of Adhesion and Adhesives 17(2), 155-161.

Santamaria-Echart, A., Ugarte, L., García-Astrain, C., Arbelaiz, A., Corcuera, M. A., Eceiza, A., 2016. Cellulose nanocrystals reinforced environmentally-friendly waterborne polyurethane nanocomposites, Carbohydrate Polymers 151, 1203-1209; 10.1016/j.carbpol.2016.06.069.

Saravari, O., Praditvatanakit, S., 2013. Preparation and properties of urethane alkyd based on a castor oil/jatropha oil mixture, Progress in Organic Coatings 76(4), 698-704.

Saunders, J., 1959. The reactions of isocyanates and isocyanate derivatives at elevated temperatures, Rubber Chemistry and Technology 32(2), 337-345.

Septevani, A. A., Evans, D. A., Chaleat, C., Martin, D. J., Annamalai, P. K., 2015. A systematic study substituting polyether polyol with palm kernel oil based polyester polyol in rigid polyurethane foam, Industrial Crops and Products 66, 16-26.

Sharma, C., Kumar, S., Unni, A. R., Aswal, V. K., Rath, S. K., Harikrishnan, G., 2014. Foam stability and polymer phase morphology of flexible polyurethane foams synthesized from castor oil, Journal of Applied Polymer Science 131(17), 40668 (1)-40668 (8); 10.1002/app.40668.

Sharma, V., Kundu, P., 2006. Addition polymers from natural oils—A review, Progress in Polymer Science 31(11), 983-1008.

Sheikh, N., Katbab, A., Mirzadeh, H., 2000. Isocyanate-terminated urethane prepolymer as bioadhesive base material: synthesis and characterization, International Journal of Adhesion and Adhesives 20(4), 299-304.

Shirke, A., Dholakiya, B., Kuperkar, K., 2015. Novel applications of castor oil based polyurethanes: a short review, Polymer Science Series B 57(4), 292-297.

Silva, B. B., Santana, R. M., Forte, M. M., 2010. A solventless castor oil-based PU adhesive for wood and foam substrates, International Journal of Adhesion and Adhesives 30(7), 559-565; 10.1016/j.ijadhadh.2010.07.001.

Soares, B., Gama, N., Freire, C. S., Barros-Timmons, A., Brandão, I., Silva, R., Neto, C. P., Ferreira, A., 2015. Spent coffee grounds as a renewable source for ecopolyols production, Journal of Chemical Technology & Biotechnology 90(8), 1480-1488.

Somani, K. P., Kansara, S. S., Patel, N. K., Rakshit, A. K., 2003. Castor oil based polyurethane adhesives for wood-to-wood bonding, International Journal of Adhesion and Adhesives 23(4), 269-275; 10.1016/S0143-7496(03)00044-7.

Stirna, U., Fridrihsone, A., Lazdiņa, B., Misāne, M., Vilsone, D., 2013. Biobased polyurethanes from rapeseed oil polyols: structure, mechanical and thermal properties, Journal of Polymers and the Environment 21(4), 952-962.

Strankowski, M., Strankowska, J., Gazda, M., Piszczyk, Ł, Nowaczyk, G., Jurga, S., 2012. Thermoplastic polyurethane/(organically modified montmorillonite) nanocomposites produced by in situ polymerization. Express Polymer Letters 6(8).

Su, S., Gu, J., Lee, H., Yu, S., Wu, C., Suen, M., 2016. Effects of an Aromatic Fluoro-Diol and Polycaprolactone on the Properties of the Resultant Polyurethanes, Advances in Polymer Technology 37(4), 1142-1152.

Sung, G., Gwon, J. G., Kim, J. H., 2016. Characteristics of polyurethane adhesives with various uretonimine contents in isocyanate and average alcohol functionalities, Journal of Applied Polymer Science 133(31).

Suresh, K. I., 2012. Rigid polyurethane foams from cardanol: synthesis, structural characterization, and evaluation of polyol and foam properties, ACS Sustainable Chemistry & Engineering 1(2), 232-242.

Szycher, M., 2013. Szycher's Handbook of Polyurethanes. New York: CRC press.

Tayfun, U., Dogan, M., Bayramli, E., 2015. Investigations of the flax fiber/thermoplastic polyurethane eco-composites: Influence of isocyanate modification of flax fiber surface, Polymer Composites 38(12), 2874-2880.

Thakur, S., Karak, N., 2014. Ultratough, ductile, castor oil-based, hyperbranched, polyurethane nanocomposite using functionalized reduced graphene oxide, ACS Sustainable Chemistry & Engineering 2(5), 1195-1202.

The Statistics Portal, 2018. Polyurethane Demand Worldwide, 2018, (7/13); https://www.statista.com/statistics/747004/polyurethane-demand-worldwide/.

Thébault, M., Pizzi, A., Santiago-Medina, F., Al-Marzouki, F., Abdalla, S., 2017. Isocyanate-free polyurethanes by coreaction of condensed tannins with aminated tannins, Journal of Renewable Materials 5(1), 21-29.

Tomita, H., Sanda, F., Endo, T., 2001. Model reaction for the synthesis of polyhydroxyurethanes from cyclic carbonates with amines: Substituent effect on the reactivity and selectivity of ring-opening direction in the reaction of five-membered cyclic carbonates with amine, Journal of Polymer Science Part A: Polymer Chemistry 39(21), 3678-3685.

Tran, P., Graiver, D., Narayan, R., 2005. Ozone-mediated polyol synthesis from soybean oil, Journal of the American Oil Chemists' Society 82(9), 653-659.

Tryznowski, M., Izdebska-Podsiadły, J., Żołek-Tryznowska, Z., 2017a. Wettability and surface free energy of NIPU coatings based on bis (2, 3-dihydroxypropyl) ether dicarbonate, Progress in Organic Coatings 109, 55-60.

Tryznowski, M., Świderska, A., Gołofit, T., Żołek-Tryznowska, Z., 2017b. Wood adhesive application of poly (hydroxyurethane) s synthesized with a dimethyl succinate-based amide backbone, RSC Advances 7(48), 30385-30391.

Tryznowski, M., Świderska, A., Żołek-Tryznowska, Z., Gołofit, T., Parzuchowski, P. G., 2015. Facile route to multigram synthesis of environmentally friendly non-isocyanate polyurethanes, Polymer 80, 228-236.

Turkenburg, D. H., van Bracht, H., Funke, B., Schmider, M., Janke, D., Fischer, H. R., 2017. Polyurethane adhesives containing Diels–Alder-based thermoreversible bonds, Journal of Applied Polymer Science 134(26).

Valero, M. F., Gonzalez, A., 2012. Polyurethane adhesive system from castor oil modified by a transesterification reaction, Journal of Elastomers and Plastics 44(5), 433-442; 10.1177/0095244312437155.

van der Leeden, Mieke C, Frens, G., 2002. Surface properties of plastic materials in relation to their adhering performance, Advanced Engineering Materials 4(5), 280-289.

Van Ekeren, P., Carton, E., 2011. Polyurethanes for potential use in transparent armour investigated using DSC and DMA, Journal of thermal analysis and calorimetry 105(2), 591-598; 10.1007/s10973-011-1665-8.

Van Oosten, A. S., Vahabi, M., Licup, A. J., Sharma, A., Galie, P. A., MacKintosh, F. C., Janmey, P. A., 2016. Uncoupling shear and uniaxial elastic moduli of semiflexible biopolymer networks: compression-softening and stretch-stiffening, Scientific reports 6, 19270.

Vega-Baudrit, J., Navarro-Banon, V., Vazquez, P., Martín-Martínez, J. M., 2006. Addition of nanosilicas with different silanol content to thermoplastic polyurethane adhesives, International Journal of Adhesion and Adhesives 26(5), 378-387.

Vega-Baudrit, J., Sibaja-Ballestero, M., Vázquez, P., Torregrosa-Maciá, R., Martín-Martínez, J. M., 2007. Properties of thermoplastic polyurethane adhesives containing nanosilicas with different specific surface area and silanol content, International Journal of Adhesion and Adhesives 27(6), 469-479.

Velankar, S., Cooper, S. L., 1998. Microphase separation and rheological properties of polyurethane melts. 1. Effect of block length, Macromolecules 31(26), 9181-9192.

Waldman, T. E., McGhee, W. D., 1994. Isocyanates from primary amines and carbon dioxide:'dehydration'of carbamate anions, Journal of the Chemical Society, Chemical Communications (8), 957-958.

Wang, F., Wang, J., Hu, L., Chu, F., Wang, C., Pang, J., Cheng, Z., 2018. Combinations of soy protein and polyacrylate emulsions as wood adhesives, International Journal of Adhesion and Adhesives 82, 160-165; 10.1016/j.ijadhadh.2018.01.002.

Wang, G., Fang, B., Zhang, Z., 1994. Study of the domain structure and mechanical properties of the ethylene oxide endcapped poly (propylene oxide) polyol/4, 4′-diphenylmethane diisocyanate/ethylenediol polyurethane system, Polymer 35(15), 3178-3183.

Wang, T., Mu, X., Li, H., Wu, W., Nie, J., Yang, D., 2013. The photocrosslinkable tissue adhesive based on copolymeric dextran/HEMA, Carbohydrate Polymers 92(2), 1423-1431.

Wang, T., Nie, J., Yang, D., 2012. Dextran and gelatin based photocrosslinkable tissue adhesive, Carbohydrate Polymers 90(4), 1428-1436.

Wang, Z., Zhang, X., Zhang, L., Tan, T., Fong, H., 2016. Nonisocyanate biobased poly (ester urethanes) with tunable properties synthesized via an environment-friendly route, ACS Sustainable Chemistry & Engineering 4(5), 2762-2770; 10.1021/acssuschemeng.6b00275.

Webster, D. C., Crain, A. L., 2000. Synthesis and applications of cyclic carbonate functional polymers in thermosetting coatings, Progress in organic coatings 40(1-4), 275-282.

Worldometers, 2018. 2018, (10/03); http://www.worldometers.info/world-population/europe-population/.

Wu, C., Tsou, C., Tseng, Y., Lee, H., Suen, M., Gu, J., Tsou, C., Chiu, S., 2016. Preparation and characterization of biodegradable polyurethanes composites filled with silver nanoparticles-decorated graphene, Journal of Polymer Research 23(12), 263.

Xiao, Y., Jiang, L., Liu, Z., Yuan, Y., Yan, P., Zhou, C., Lei, J., 2017. Effect of phase separation on the crystallization of soft segments of green waterborne polyurethanes, Polymer Testing 60, 160-165.

Xiong, J., Liu, Y., Yang, X., Wang, X., 2004. Thermal and mechanical properties of polyurethane/montmorillonite nanocomposites based on a novel reactive modifier, Polymer Degradation and Stability 86(3), 549-555.

Xu, Y., Petrovic, Z., Das, S., Wilkes, G. L., 2008. Morphology and properties of thermoplastic polyurethanes with dangling chains in ricinoleate-based soft segments, Polymer 49(19), 4248-4258; 10.1016/j.polymer.2008.07.027.

Yakushin, V., Stirna, U., Bikovens, O., Misane, M., Sevastyanova, I., Vilsone, D., 2013. Synthesis and Characterization of Novel Polyurethanes Based on Tall Oil, Materials Science 19(4), 390-396; 10.5755/j01.ms.19.4.2666.

Yang, S., Gu, L., Gibson, R. F., 2001. Nondestructive detection of weak joints in adhesively bonded composite structures, Composite Structures 51(1), 63-71.

Yarmohammadi, M., Shahidzadeh, M., 2018. Evaluation of disulfide chain extender effect on the mechanical properties of unsaturated polyurethane-urea networks, Journal of Applied Polymer Science 135(21), 46309.

Yeganeh, H., Mehdizadeh, M. R., 2004. Synthesis and properties of isocyanate curable millable polyurethane elastomers based on castor oil as a renewable resource polyol, European polymer journal 40(6), 1233-1238.

Yildiz, Z., Onen, H. A., 2017. Dual-curable PVB based adhesive formulations for cord/rubber composites: The influence of reactive diluents, International Journal of Adhesion and Adhesives 78, 38-44.

Yilgör, E., Burgaz, E., Yurtsever, E., Yilgör, I., 2000. Comparison of hydrogen bonding in polydimethylsiloxane and polyether based urethane and urea copolymers, Polymer 41(3), 849-857; 10.1016/S0032-3861(99)00245-1.

Yong, Q., Nian, F., Liao, B., Huang, L., Wang, L., Pang, H., 2015. Synthesis and characterization of solvent-free waterborne polyurethane dispersion with both sulfonic and carboxylic hydrophilic chain-extending agents for matt coating applications, RSC Advances 5(130), 107413-107420.

Yuan, L., Qiang, P., Gao, J., Shi, Y., 2017. Synthesis of oxazolidines as latent curing agents for single-component polyurethane adhesive and its properties study, Journal of Applied Polymer Science 135(4), 45722.

Yuan, Y., Zhang, Y., Fu, X., Kong, W., Liu, Z., Hu, K., Jiang, L., Lei, J., 2017. Molecular design for silane-terminated polyurethane applied to moisture-curable pressure-sensitive adhesive, Journal of Applied Polymer Science 134(37).

Zabalov, M., Tiger, R., Berlin, A., 2012. Mechanism of urethane formation from cyclocarbonates and amines: a quantum chemical study, Russian Chemical Bulletin 61(3), 518-527.

Zhang, C., Ding, R., Kessler, M. R., 2014. Reduction of Epoxidized Vegetable Oils: A Novel Method to Prepare Bio-Based Polyols for Polyurethanes, Macromolecular rapid communications 35(11), 1068-1074.

Zhang, C., Vennerberg, D., Kessler, M. R., 2015. In situ synthesis of biopolyurethane nanocomposites reinforced with modified multiwalled carbon nanotubes, Journal of Applied Polymer Science 132(36).

Zhang, C., Xia, Y., Chen, R., Huh, S., Johnston, P. A., Kessler, M. R., 2013. Soy-castor oil based polyols prepared using a solvent-free and catalyst-free method and polyurethanes therefrom, Green Chemistry 15(6), 1477-1484.

Zhang, X., Ding, Y., Zhang, G., Li, L., Yan, Y., 2011. Preparation and rheological studies on the solvent based acrylic pressure sensitive adhesives with different crosslinking density, International Journal of Adhesion and Adhesives 31(7), 760-766.

Zhou, X., Fang, C., Yu, Q., Yang, R., Xie, L., Cheng, Y., Li, Y., 2017. Synthesis and characterization of waterborne polyurethane dispersion from glycolyzed products of waste polyethylene terephthalate used as soft and hard segment, International Journal of Adhesion and Adhesives 74, 49-56; 10.1016/j.ijadhadh.2016.12.010.

Zhu, R., Wang, Y., Zhang, Z., Ma, D., Wang, X., 2016. Synthesis of polycarbonate urethane elastomers and effects of the chemical structures on their thermal, mechanical and biocompatibility properties, Heliyon 2(6), e00125.

Zieleniewska, M., Auguścik, M., Prociak, A., Rojek, P., Ryszkowska, J., 2014. Polyurethane-urea substrates from rapeseed oil-based polyol for bone tissue cultures intended for application in tissue engineering, Polymer Degradation and Stability 108, 241-249; 10.1016/j.polymdegradstab.2014.03.010.

Zimmer, B., Nies, C., Schmitt, C., Possart, W., 2017. Chemistry, polymer dynamics and mechanical properties of a two-part polyurethane elastomer during and after crosslinking. Part I: dry conditions, Polymer 115, 77-95; 10.1016/j.polymer.2017.03.020.

Zlatanić, A., Lava, C., Zhang, W., Petrović, Z. S., 2004. Effect of structure on properties of polyols and polyurethanes based on different vegetable oils, Journal of Polymer Science Part B: Polymer Physics 42(5), 809-819.

Zlatanic, A., Petrovic, Z. S., Dušek, K., 2002. Structure and properties of triolein-based polyurethane networks, Biomacromolecules 3(5), 1048-1056.

Zosel, A., 1998. The effect of fibrilation on the tack of pressure sensitive adhesives, International Journal of Adhesion and Adhesives 18(4), 265-271; http://dx.doi.org/10.1016/S0143-7496(98)80060-2.

Chapter 3
Materials and Methods

1. Materials

1.1. Cellulose acetate

Cellulose acetate (CA), supplied by Sigma-Aldrich (St. Louis, MO, USA) and characterized by an average molecular weight (M_n) of $3 \cdot 10^4$ g·mol^{-1}, obtained by GPC, was used as hydroxyl group bearing polymer. This cellulose derivative, containing 39.8 wt.% acetyl groups, is a powdery material with a density of 1.3 g·ml^{-1} at 25 ºC. Figure 3.1 depicts the cellulose acetate common structure, where *R* substituents can be ascribed to either hydrogen or acetyl groups.

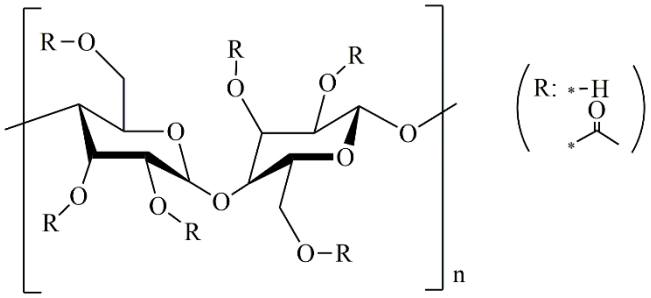

Figure 3.1 Generalized chemical structure of cellulose acetate

This naturally occurring biopolymer was subjected to a drying pre-treatment at 100 ºC for 30 min prior utilization.

1.2. Diisocyanates

The impact of the isocyanate chemical structure on the cellulose acetate modification and ultimate properties of the ensuing bio-sourced adhesives was evaluated by testing different, aliphatic and aromatic, difunctional isocyanates, namely 1,6-hexamethylene diisocyanate, a liquid like NCO-containing reactive material (bp: 82-85 ºC/0.1 mmHg, ρ: 1.047 g·ml^{-1}/20 ºC) and solid diphenylmethane-4,4'-diisocyanate (mp: 38-42 ºC, bp: 200 ºC/5 mmHg, ρ: 1.18 g·ml^{-1}/25 ºC) (see Table 2.1.b,e), respectively. Both isocyanates, with 11.89 and 7.99 mmol NCO equivalent/g and ≥98.0 % purum grade, were kindly provided by Sigma-Aldrich (St. Louis, MO, USA) and used without further purification.

1.3. Castor oil

The renewability of the synthesized bio-based adhesives was increased via castor oil addition. This non-edible pale yellow-coloured vegetable oil belongs to the coveted group of OH-bearing plant oils (Ali et al., *2014*; Ogunniyi, *2006*), owing to the hydroxyl functionality of the ricinoleic fatty acid chains (see Table 2.3) (Sharma and Kundu, *2006*). Even though castor oils chemical structure comprises not only hydroxyl, but also double bonds and ester functional groups (see Figure 3.2), giving the opportunity to perform a myriad of chemical modifications (see section 2.1.2), in this investigation a simple synthetic pathway, dealing with the favourable and rather specific reaction of isocyanates with nucleophiles such as the pendant –OH groups of castor oil, has been adopted. Thus, unnecessary additional steps and the employment of environmentally hazardous materials have been avoided by using castor oil in its original form (211 cSt at 40 ºC, av. 2.84 mmol OH equivalent/g), provided by Guinama (Valencia Spain), whose fatty acid profile can be found elsewhere (Quinchia et al., *2012*).

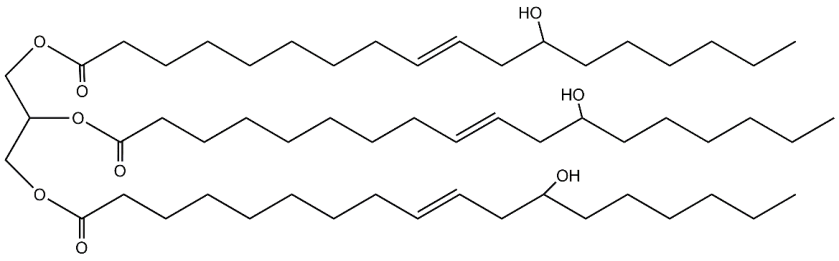

Figure 3.2 Schematic castor oil chemical structure

1.4. Other chemical reagents

Other common materials and solvents were purchased from Sigma–Aldrich (St Louis, MO, USA). More specifically, toluene (ACS reagent, reag. ISO. Ph. Eur., ≥99.7%) and triethylamine (TEA, analytical grade, 99.5%, 0.725 $g \cdot ml^{-1}$/20 ºC), if required, were considered as reaction solvent and catalyst, respectively, and used without further purification.

*Table 3.1 Basic information about the commercial adhesives**

Adhesive	***Berner® fast curing***	***UHU® Montakit®***	***U-Bond® 309 TFC***	***Revin® B3***
Composition	Neoprene	Rosin resin (colophony)	Polyurethane	Single-component vinyl adhesive (aqueous dispersion)
Curing	Solvent release	Solvent release	Moisture- based	–
Applications	Wood, PVC, stone, concrete, brick	Wood, concrete, brick, metal, plastic, synthetic materials	Wood, cement, metal, plastic, stones	Wood
Curing time	2–3 days	24 h	20 min	–
Application temperature	5–30 ºC	–	–	10–30 ºC
Open time	5 min (23 ºC/55 % RH)	–	–	8–12 min (20 ºC)
Thermal resistance	–20–70 ºC	–20–100 ºC	–40–100 ºC	–

**As provided by the manufacturers*

Table 3.2 Description of the adhesion substrates for the preparation of adhesion joints

Substrate	*Designation*	*Supplier*	*Qualitative stiffness*
Polyester fabric	PF	Local store	Flexible
Poplar wood	PW	Local store	Rigid
Sycamore wood	SyW	Local store	
Spruce wood	SW	Local store	
Oak wood	OW	Local store	
Plywood	PlyW	Local store	
Medium density fibreboard	MDF	Local store	
Austenitic stainless steel (AISI 316L)	SS	Local store	
Polyethylene	PE	Repsol-YPF (Madrid, Spain)	

1.5. Benchmark commercial adhesives

For comparison purposes, an extensive variety of commercial adhesives has been regarded as benchmarks, handled following the supplier guidelines and properly tested. Adhesives marketed under the brands Berner® Fast Curing, UHU Montakit®, U-Bond® 309-TFC and Revin® B3, hereinafter called CAdh1, CAdh2, CAdh3 and CAdh4, respectively, were acquired at local stores. Basic information related to adhesives' main composition, along with other practical data (recommended surface application and temperature, curing time, etc.) provided by the manufacturers are collected in Table 3.1.

1.6. Adhesion substrates

In order to assess the adhesion response of the synthesized bio-sourced polyurethanes and benchmarks described above, the materials listed in Table 3.2, which can be classified into flexible and rigid, have been considered as adhesion substrates.

2. Synthesis protocols

The preparation of bio-sourced polyurethanes has been accomplished through two different approaches: a two-step protocol derived from previous studies (Gallego et al., 2013), and by means of a proposed greener straight-through procedure, which is the object of investigation in the study presented in Chapter 4, Block 3. These synthetic routes are described in detail here below.

2.1. Two-step protocol

Firstly, according to preceding investigations (Gallego et al., 2013), a certain amount of solvent was introduced in a three-neck round-bottom flask and bubbled for half an hour with Argon to displace the air with its associated moisture. Then, pre-dried cellulose acetate was added into the reaction medium and totally or partially modified with diisocyanate (HMDI or MDI), with the aid of triethylamine as catalyst after 24 hours of vigorous stirring (≈500 rpm) with a magnetic stirrer at room temperature (Figure 3.3).

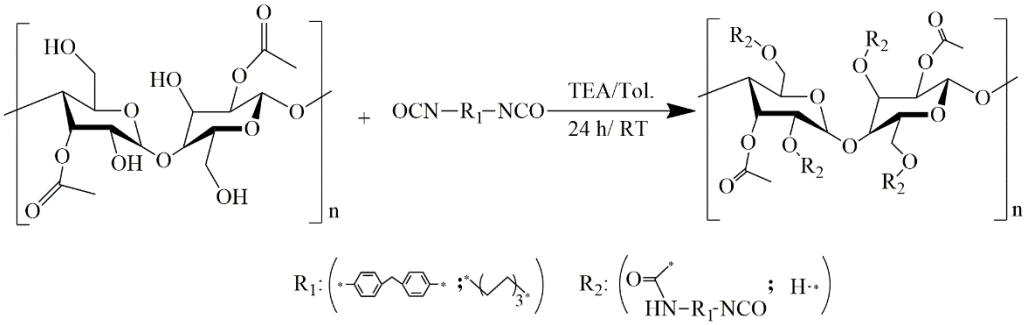

Figure 3.3 Cellulose acetate modification

Upon solvent and catalyst removal under vacuum evaporation at 80 ºC, the resulting NCO-terminated prepolymer was mechanically blended with castor oil in an open vessel at 65-70 rpm, using a controlled-rotational speed mixing apparatus RW 20 from Ika (Staufen, Germany) equipped with an anchor impeller. Vegetable oil and bio-based prepolymer were mixed at certain weight ratios (see Table 3.3 for detailed compositions) at ambient conditions for either 24 hours or 40 minutes, depending on whether initial CA-modification was conducted with aliphatic or aromatic diisocyanate, respectively.

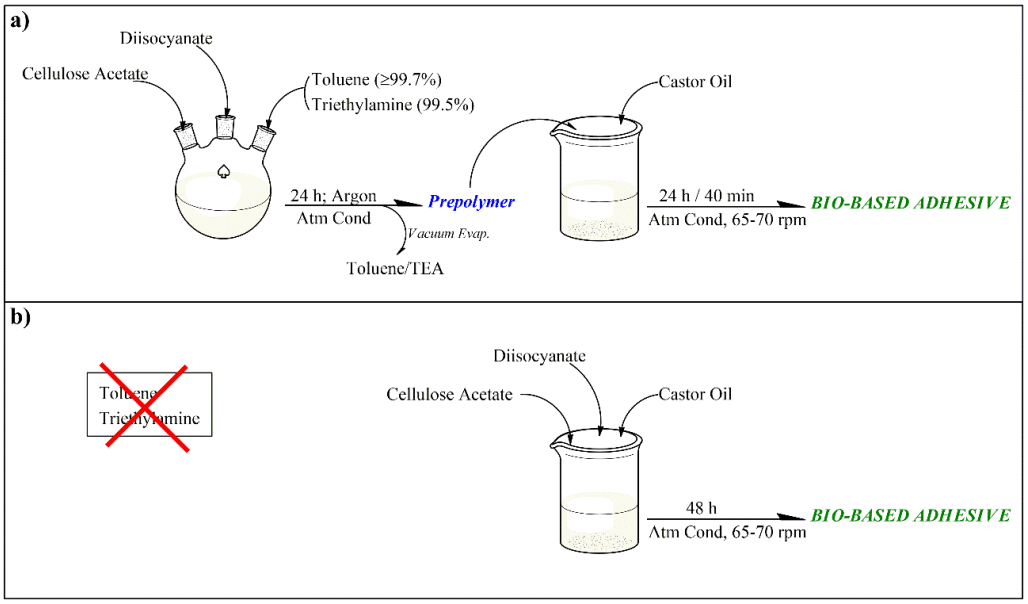

Figure 3.4 Schematic representation for a) two- and b) single-step protocols

Finally, the ensuing products were homogenized with an Ultra-Turrax T50 rotor-stator turbine (Ika, Staufen, Germany) at 10000 rpm for 60 s. Although this homogenization

step has been initially applied (Chapter 4, Block 1), it has been discarded in subsequent synthetic protocols (Blocks 2 and 3) inasmuch as it has been proven in a complementary study to exert a negligible influence on the final polyurethane properties. The bio-sourced adhesives thus developed (Figure 3.4.a) were ready to be applied onto the adhesion substrates and left for curing.

2.2. Single-step protocol

In the straight through protocol (Figure 3.4.b) all the reagents (CA, HMDI or MDI and CO) are blended in an open reactor and stirred at 65-70 rpm for 48 h at room conditions, so that the use of other environmentally hazardous materials is avoided, while reducing the synthetic pathway-steps.

Table 3.3 Weight proportions of the components used in the preparation of natural-based PU adhesives

	Sample	Processing Sequence	Weight [%] (w/w)				NCO:OH molar ratio*
			CA	HMDI	MDI	CO	
Block 1	PU20.80	2-Step	**18.9**	**61.1**	-	**20**	3.35
	PU50.50	2-Step	**11.8**	**38.2**	-	**50**	1.87
	PU70.30	2-Step	**7.1**	**22.9**	-	**70**	1.05
Block 2	PU2	2-Step	**16.0**	-	**34.0**	**50**	0.98
	PU2.5	2-Step	**13.7**	-	**36.3**	**50**	1.12
	PU3	2-Step	**12.0**	-	**38.0**	**50**	1.25
	PU3.5	2-Step	**10.6**	-	**39.4**	**50**	1.36
	PU4	2-Step	**9.5**	-	**40.5**	**50**	1.45
	PU4.53	2-Step	**8.6**	-	**41.4**	**50**	1.54
Block 3	PU2	2-Step	**11.8**	**38.2**	-	**50**	1.87
	PU1a	1-Step	**11.8**	**38.2**	-	**50**	1.87
	PU1b	1-Step	-	**30.9**	-	**60.1**	1.87
	PU1c	1-Step	-	**43.3**	-	**56.7**	3.20

**Values estimated taking into account the fatty acid profile given by Quinchia et al. (2012)*

3. Characterization techniques

3.1. Fourier transform infrared – attenuated total reflectance (FTIR-ATR) spectroscopy

The chemical structure of the synthesized bio-based PUs at different curing stages was characterized by means of Fourier transform infrared spectroscopy (FTIR), using a FT/IR-4200 apparatus (JASCO Inc., Easton, MD, EEUU). An attenuated total reflectance (ATR) accessory, provided with monolithic diamond crystal as prism, was used to acquire the IR spectra in transmittance mode at room temperature as a result of an average of around 70-100 scans with a resolution of 4 cm^{-1} and a 45° incidence angle of the laser beam, in the spectral range 4000–400 cm^{-1}, with the aid of the Spectra Manager software.

Aiming to monitor the curing process of the studied PU adhesives, the progress of the peak area attributable to the free isocyanate functional group (-NCO), at 2261 cm^{-1}, (Zieleniewska et al., 2014), was followed. Therefore, when required, the quantification of the reaction conversion (*X*) was evaluated as follows (Abdolhosseini and Givi, 2016):

$$X_{NCO}^{t} = \frac{[A]_{NCO}^{t_0} - [A]_{NCO}^{t}}{[A]_{NCO}^{t_0}} \qquad (3.1)$$

where $[A]_{NCO}^{t_0}$ and $[A]_{NCO}^{t}$, as described further down, represent the areas assigned to free isocyanates at times *0* and *t*, respectively, taking the unchanging -CH_3/-CH_2 stretching vibrational band (2924 cm^{-1}) as reference.

3.2. Thermogravimetric analysis (TGA)

The thermal stability of bio-sourced PUs was assessed by means of thermogravimetric analysis. Approximately 10-20 mg of PU sample were placed in open aluminium crucibles and subjected to a heating rate of 10 ºC·min^{-1}, from 30 to 600 ºC, under inert atmosphere of Nitrogen (purge flow of 60 mL·min^{-1}). Two different thermogravimetric analysers were used to evaluate the weight loss and decomposition rate during the

heating process as a function of temperature: a Thermogravimetry/Differential Thermal Analyzer (TG/DTA) 6200 (Seiko Instruments Inc., Chiba, Japan) and Thermogravimetric Analyzer Q50 (TA Instruments, New Castle, DE, USA).

3.3. Standard and temperature modulated differential scanning calorimetry (DSC & MDSC)

Standard DSC analysis were carried out over hermetically sealed aluminium pans loaded with 3-10 mg of PU samples. These specimens were submitted to a heating speed of 10 $^{o}C \cdot min^{-1}$, in the temperature range from -85 up to 250-320 ºC with a Nitrogen purge flow of 50 $mL \cdot min^{-1}$. In this case, DSC tests were performed by using Q100 or DSC250 Differential Scanning Calorimeters (TA Instruments, New Castle, DE, USA).

Moreover, owing to the well-known limitations of standard DSC analysis, i.e. likely overlapping of several thermal transitions arising from the contribution of different constituents in the polymer network, temperature-modulated DSC (MDSC) analyses, also under Nitrogen environment, were performed using the Differential Scanning Calorimeter DSC250. According to Thomas (2005), the MDSC tests were conducted with a heating rate of 2 $^{o}C \cdot min^{-1}$, in the range of 0-300 ºC, with modulation amplitude and period of 0.32 ºC and 60 s, respectively. Data analysis was performed by using TRIOS and Universal Analysis softwares.

3.4. Rheological characterization

Linear viscoelastic measurements of PU specimens were carried out in a controlled-stress Physica MCR301 rheometer (Anton Paar, Graz, Austria), equipped with a Convection Temperature Device CTD600, in the torsional mode. In order to prepare rectangular specimens 50 × 10 × 2 mm^3 in size, fresh bio-sourced PU adhesives were poured into metal moulds and left for curing under room conditions till completion. The linear viscoelastic region (LVR) was determined through the application of stress sweep tests at 1 Hz and throughout the entire temperature range considered in the subsequent rheological tests. Afterwards, small-amplitude frequency sweep tests were performed within 0.01–100 $rad \cdot s^{-1}$ at different constant temperatures (25-200 ºC), although such

range was extended to lower temperatures of around -10 ºC when characterizing MDI-based polyurethanes (Chapter 4, Block 2).

Finally, continuous upward temperature ramps were applied at 1 Hz by imposing a gradient of 2 ºC·min^{-1}, from 25 up to 200 ºC. This temperature range was particularly expanded until minimum temperatures of -30 ºC in the case of PU adhesives prepared from MDI-functionalized cellulose acetate (Chapter 4, Block 2).

All the rheological data shown in this study were the result of an average of at least three replicates.

3.5. Adhesion measurements

The adhesion performance of the synthesized bio-based adhesives and the benchmarks was evaluated on the substrates previously detailed in section 1.6 by performing Standard Tests Methods for the determination of 180º-peeling (ASTM D903), single-lap shear (ASTM D906, D1002, D3163), lap-shear sandwich joints (ASTM D3164) and 3-point flexural (ASTM D1184) strengths.

Most substrates required an additional pre-treatment process prior to adhesive application. First, pelletized polyethylene was subjected to a compression–moulding treatment at 200 ºC at 100 bar for 10 min, obtaining rectangular specimens of 190 × 25 × 1.5 mm^3 in size that were unmolded, trimmed, if needed, to the required dimensions and hand-abraded with 280 grit CarbiMet™ abrasive paper [P320]. Moreover, stainless steel metal substrates were cleaned with ethanol and acetone to remove surface impurities and subsequently dried, while polyester fabrics sheets were also wiped and cut to fulfil the requirements for peeling tests (25 × 300 × 0.7 mm^3). Regarding wooden materials, such as poplar wood, supplied in individual sterilized packages, along with spruce wood, oak wood, plywood and medium density fibreboard were cut, if required, into smaller pieces to meet the peeling and shear strength standard methods (ASTM D903 and D906). Moreover, sycamore wooden boards, whose particularly unusual thickness of 0.25 mm allowed it to meet the test requirements, were also cut into rectangular pieces (38 × 19 × 0.25 mm^3), following the guidelines of ASTM D1184.

All the mechanical measurements were conducted in an AG-IS Universal Testing Machine (Shimadzu, Kyoto, Japan), equipped with load cells with capacities of 1 and 10 kN, selected in accordance with the requirements of the strength to be measured. Prior to adhesive application, all the substrates were again gently wiped to remove likely impurities and dust from their surfaces. Afterwards, the still fresh adhesives were generally spread over the substrate surfaces to a film thickness of 0.5 ± 0.1 mm by using a stainless steel spatula. By exception, the films for the flexural tests were 0.2 mm thick and used to join 8 wooden plies to one another, giving rise to sycamore-adhesive bonded laminated assemblies to be analysed under 3-point flexural test according to the standard norm ASTM D1184. Upon adhesive application (see bonding areas in Table 3.4) the substrates to be joined were put together immediately and allowed to stand without applying pressure under atmospheric conditions (av. 64 % RH and room temperature). Although the adhesive thicknesses for shear and peeling tests were set to 0.5 mm with the aid of silicon spacers (see Figure 3.5), the curing process provoked in MDI-based PU adhesives an increase in the bonding line-thickness up to around 1 mm.

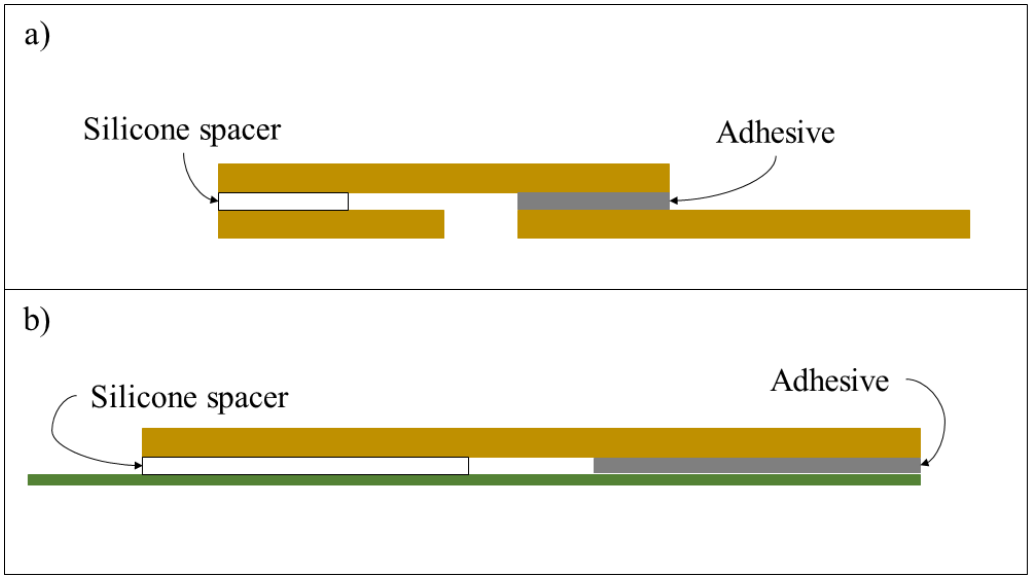

Figure 3.5 Assembly of samples for mechanical characterization in a) shear and b) peeling tests during the curing process

Table 3.4 Mechanical test conditions and bonding line dimensions

ASTM Test	Sample	Procedure conditions		Adhesive line dimensions		
		Strain rate (mm·min^{-1})	*Force rate (kN·min^{-1})*	*Area (mm^2)*	*Width (mm)*	*Thickness (mm)*
D903	PF-PPW	152.4	-	-	18.2	0.5
	PF-PlyW				19.2	
	PF-MDF				17.3	
	PF-SW				26.3	
	PF-OW				25.8	
	PF-SS				23.0	
	PF-PE				25.0	
D906	PPW/PPW	-	3.56	18.2 × 18.2	-	0.5
	PlyW/PlyW			19.2 × 14.2		
	MDF/MDF			17.3 × 15.7		
	SW/SW			26.3 × 15.7		
	OW/OW			25.8 × 14.2		
D3163	PE-PE	1.3	-	25.0 × 25.0	-	0.5
D3164	SS-PE-SS	1.3	-	23.0 × 23.0	-	0.5
D1002	SS-SS	1.3	-	23.0 × 23.0	-	0.5
D1184	SyW (x8)	0.74	-	38.0 × 19.0	-	0.25

Shear strengths were calculated as the maximum stress throughout the whole debonding process (MPa), while peeling strengths were recorded as the average load per bonding width (kN/m) as shown in Equations (3.2) and (3.3) respectively. In addition, flexural strengths, as detailed in ASTM D1184, were evaluated in accordance with Equation (3.4).

$$S_{Shear} = \frac{F_{Shear}}{A} \tag{3.2}$$

$$S_{Peel} = \frac{F_{Av}}{W} \tag{3.3}$$

$$S_{Flexural} = \frac{3 \cdot F \cdot L}{2 \cdot W \cdot T^2} \tag{3.4}$$

where S_{Shear} [Pa], F_{Shear} [N] and A [m^2] denote the shear strength, maximum shear force and the adhesion area (Figure 3.6.a), S_{Peel} [N/m], F_{Av} [N] and W [m] are the peeling strength, the average peeling force and the sample width (Figure 3.6.b), whilst $S_{Flexural}$ [Pa], F [N], L [m] and T [m] correspond to the flexural strength, maximum flexural force, the distance between supports and the thickness of the beams in three-point bending tests respectively (Figure 3.6.c).

Each adhesive specimen was subjected to an appropriate cross-head speed or force ramp (see Table 3.4) at room temperature, except for aromatic isocyanate-based PU adhesives whose adhesion study was also analysed at higher temperature (100 ºC). All mechanical experiments were performed at least ten times repeatedly, and the resulting data were submitted to a statistical analysis by conducting the Generalized Extreme Studentized Deviated (ESD) test, aimed to track down likely outliers with a level of significance of $\alpha<0.05$. The reported data were expressed as an arithmetic mean ± standard deviation, after removing the identified outliers, and the type of failures and their percentages were assessed by means of photographic image analysis of the tested specimens. Additionally, one-way analysis of variance (ANOVA) followed by a post-hoc analysis (Scheffé test), based on a level of significance of $\alpha<0.05$, were conducted to assess whether, within the same mechanical test and conditions, the differences found between the studied adhesives were statistically significant.

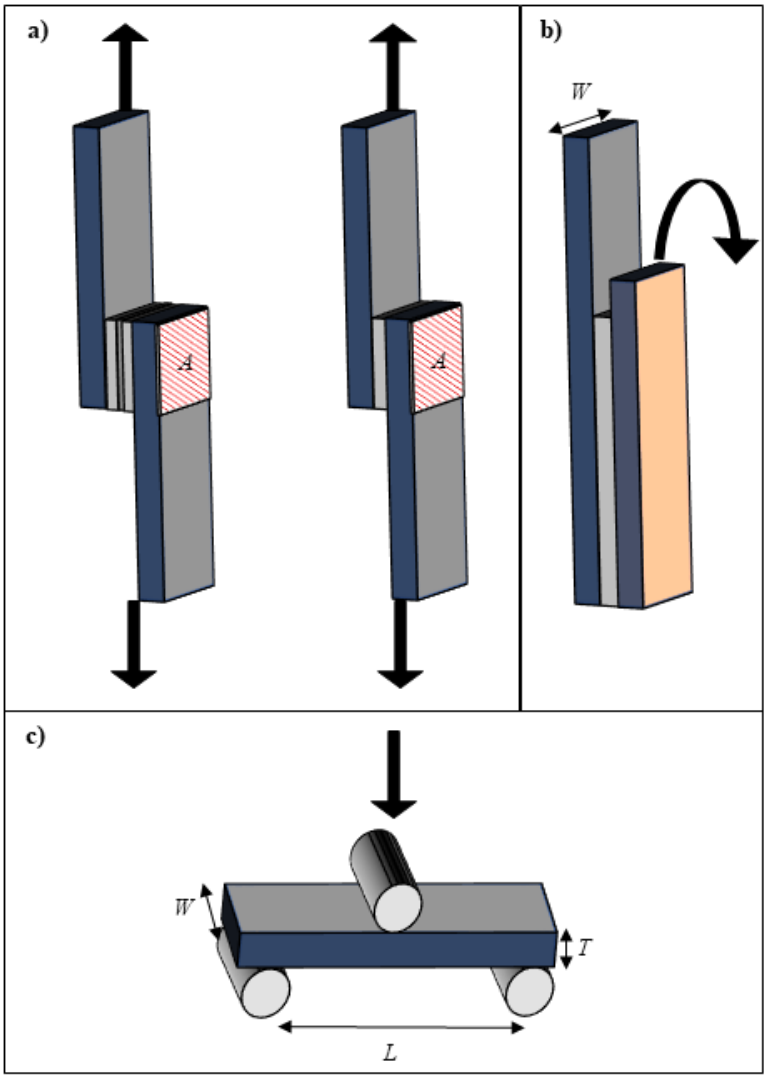

Figure 3.6 Scheme of the force application in (a) shear, (b) peeling and (c) flexural tests

4. References

Abdolhosseini, F., Givi, M. K. B., 2016. Characterization of a biodegradable polyurethane elastomer derived from castor oil, American Journal of Polymer Science 6(1), 18-27; 10.5923/j.ajps.20160601.03.

Ali, A., Yusoh, K., Hasany, S., 2014. Synthesis and physicochemical behaviour of polyurethane-multiwalled carbon nanotubes nanocomposites based on renewable castor oil polyols, Journal of Nanomaterials 2014, 1-9; 10.1155/2014/564384.

Gallego, R., Arteaga, J., Valencia, C., Franco, J., 2013. Chemical modification of methyl cellulose with HMDI to modulate the thickening properties in castor oil, Cellulose 20(1), 495-507; 10.1007/s10570-012-9803-4.

Ogunniyi, D., 2006. Castor oil: A vital industrial raw material, Bioresource technology 97(9), 1086-1091; 10.1016/j.biortech.2005.03.028.

Quinchia, L., Delgado, M., Franco, J., Spikes, H., Gallegos, C., 2012. Low-temperature flow behaviour of vegetable oil-based lubricants, Industrial Crops and Products 37(1), 383-388.

Sharma, V., Kundu, P., 2006. Addition polymers from natural oils—A review, Progress in Polymer Science 31(11), 983-1008.

Thomas, L. C., 2005. Modulated DSC® Paper# 3 Modulated DSC® Basics; Optimization of MDSC® Experimental Conditions, Technical Report, TA Instruments (8), 1-10.

Zieleniewska, M., Auguścik, M., Prociak, A., Rojek, P., Ryszkowska, J., 2014. Polyurethane-urea substrates from rapeseed oil-based polyol for bone tissue cultures intended for application in tissue engineering, Polymer Degradation and Stability 108, 241-249; 10.1016/j.polymdegradstab.2014.03.010.

Chapter 4

Results and Discussion

Block 1: Synthesis and characterization of aliphatic crosslinker-based polyurethane adhesives

1. Preparation, characterization and mechanical properties of bio-based polyurethane adhesives from isocyanate-functionalized cellulose acetate and castor oil for bonding wood

1.1. Abstract

Nowadays, different types of natural carbohydrates such as sugars, starch, cellulose and their derivatives are widely used as renewable raw materials. Vegetable oils are also considered as promising raw materials to be used in the synthesis of high quality products in different applications, including in the adhesive field. According to this, several bio-based formulations with adhesion properties were synthesized first by inducing the functionalization of cellulose acetate with 1,6-hexamethylene diisocyanate and then mixing the resulting biopolymer with a variable amount of castor oil, from 20% to 70% (wt). These bio-based adhesives were mechanically characterized by means of small-amplitude oscillatory torsion measurements, at different temperatures, and standardized tests to evaluate tension loading (ASTM-D906) and peel strength (ASTM-D903). In addition, thermal properties and stability of the synthesized bio-polyurethane formulations were also analyzed through differential scanning calorimetry and thermal gravimetric analysis. As a result, the performance of these bio-polyurethane products as wood adhesives were compared and analyzed. Bio-polyurethane formulations exhibited a simple thermo-rheological behavior below a critical temperature of around 80–100 °C depending on the castor oil/cellulose acetate weight ratio. Formulation with medium castor oil/biopolymer weight ratio (50:50 % wt.) showed the most suitable mechanical properties and adhesion performance for bonding wood.

1.2. Introduction

In the 21st century, sustainable development has become one of the main objectives in industrial activity. The approaching exhaustion of petroleum supplies, their fluctuating and rising prices, along with the stringent regulations as a consequence of the increasing environmental concerns have propelled scientists towards using renewable natural resources in order to replace total or partially petroleum-based raw materials, with the aim of overcoming these issues (Desroches et al., *2012*; Moubarik et al., *2010*).

In the adhesive field, traditional formulations are petro-based (Kong et al., *2011*; Moubarik et al., *2010*), containing some volatile organic compounds (VOC) and other toxic substances, such as formaldehyde derivatives. Those materials are hazardous to the environment and detrimental to the human health, which encourages the adhesive industry to develop adhesives from renewable raw materials with suitable functional properties (Gogoi and Karak, *2014*; Liu and Li, *2007*). The use of eco-friendly alternatives in this field can help to overcome those problems. In fact, some natural adhesives like starch, casein and other proteins were used at the start of the 20th century (Pizzi, *1994*). Nevertheless, their utilization is limited as they exhibit low durability and low water resistance. In the past few years, as recently reviewed by Ferdosian et al. (*2017*), some bio-based adhesives have been developed from a range of natural resources, including lignin (Pizzi, *2006*), starch (Moubarik et al., *2010*), tannin (Santiago-Medina et al., *2016*), vegetable oils (Kong et al., *2011*), soy flour and soy protein (Liu and Li, *2007*). However, there are still some properties to be sharpened to make those natural-based adhesives competitive in comparison to the traditional ones (Muttil et al., *2014*). In this sense, bio-based polyurethanes seem to be an excellent alternative to petroleum-based products, overcoming the environmental drawbacks but, at the same time, providing suitable properties.

Since their discovery by Otto Bayer and co-workers in 1937 (Bayer, *1947*), polyurethanes have become one of the most outstanding polymers as they exhibit a high performance and versatility, being employed in a vast range of industrial and engineering applications such as foams (Ji et al., *2015*; Pan et al., *2016*), coatings (Bakhshi et al., *2014*), medicinal products (Abdalla et al., *2016*; Ali et al., *2014*) or adhesives (Daniel da

Silva et al., *2006*), among others. This wide variety of applications is associated to their superior properties, including excellent corrosion, solvent and chemical resistance, high mechanical strength, low temperature flexibility, adhesion, suitable curing rates, chemical structure versatility, etc. (Chattopadhyay and Raju, *2007*; Manjula et al., *2010*; Silva et al., *2010*). As it is well known, polyurethanes are polymers containing urethane linkages (NHCOO) in the main polymer chain (Sharma and Kundu, *2008*). In most cases, the synthesis of polyurethanes is accomplished through the reaction taking place between isocyanates (NCO) and active hydroxyl groups (OH) and using a chain extender (low molecular weight glycol or amine) (Chattopadhyay and Raju, *2007*; Desroches et al., *2012*; Kong et al., *2011*). Typical polyurethanes are multiblock copolymers whose structure comprises two domains, called "*soft*" and "*hard*" segments, which provide them with their characteristic exceptional versatility (Calvo-Correas et al., *2016*; Xu et al., *2008*).

In the polyurethane synthesis, an extensive variety of diisocyanates might be employed, including toluene diisocyanate (TDI), 4,4′-methylene diphenyl diisocyanate (MDI), 1,6-hexamethylene diisocyanate (HMDI) and isophorone diisocyanate (IPDI), among others (Chattopadhyay and Raju, *2007*). Moreover, although traditional polyols consist of polyether or polyester, some approaches have been made to replace this source of hydroxyl groups by eco-friendly materials, for instance natural oils (Desroches et al., *2012*; Ronda et al., *2011*), or biopolymers (Gallego et al., *2015a*; Gallego et al., *2014*). In particular, castor oil (Allauddin et al., *2013*; Silva et al., *2010*) and cellulose derivatives (Gallego et al., *2015b*; Głowińska and Datta, *2016*) have been proposed as eco-friendly polyols. Vegetable oils are considered one of the most important types of renewable feed stock for the petroleum-based industrial products due to their noteworthy and favourable properties, since they are a copious resource, biodegradable, inexpensive, sustainable, non-toxic, easy to handle, structurally versatile, highly pure, flexible for chemical transformations, high physically and chemically stable, etc. (Deka and Karak, *2009*; Gurunathan and Chung, *2016*). Polyurethane production from vegetable oils is not a new approach. In fact, a wide range of natural oils have been considered as feasible choices to synthesized segmented polyurethanes (Campanella et al., *2009*; Ferrer et al., *2008*), such as linseed or rapeseed (Rojek and Prociak, *2012*), sunflower (Das et al.,

2013), canola (Kong et al., *2012*), but principally soybean (Głowińska and Datta, *2016*) and castor oil (Ali et al., *2014*; Bakhshi et al., *2014*). Castor oil belongs to the vegetable oil minority that exhibits bearing hydroxyl group (Ali et al., *2014*), which, along with double bond presence (Ogunniyi, *2006*), makes it an appealing resource for producing polyurethanes. In particular, some castor oil-based polyurethane formulations have been previously proposed as eco-friendly solventless adhesives (Silva et al., *2010*; Somani et al., *2003*). On the other hand, due to the vast abundance of cellulose in nature, this carbohydrate and its derivatives have also drawn great interest in industrial production. For instance, different cellulose derivatives, i.e., methylcellulose, α-cellulose, 2-hydroxyethylcellulose, methyl 2-hydroxyethylcellulose and cellulose acetate propionate have been successfully employed in previous investigations (Gallego et al., *2015b*), promoting the reaction between the hydroxyl groups located in the cellulose backbone and active diisocyanate crosslinkers to synthesize functionalized biopolymers which were further dispersed in vegetable oils. This study demonstrated that the rheological response, and therefore the application field, of the different oleogels achieved basically depends on the balance between the polarity and the size of cellulose substituents.

In the present section, novel bio-based polyurethane adhesive formulations have been prepared in two steps by combining a carbohydrate polymer like cellulose acetate and castor oil. Cellulose acetate was first functionalized by inducing the reaction with 1,6-hexamethylene diisocyanate. Then, the resulting product was blended with different proportions of castor oil producing bio-based polyurethanes with adhesion properties. The main objective of this section was to evaluate the influence of the castor oil/functionalized biopolymer ratio on the rheological, thermal and adhesion performance properties of these eco-friendly formulations.

1.3. Results and discussion

1.3.1. Chemical and thermal characterization

The Fourier transform infrared spectroscopic attenuated total reflectance (FTIR-ATR) technique was used to evaluate the preparation of polyurethanes with different castor oil/biopolymer weight ratio (PU20.80, PU50.50 and PU70.30). Figure 4.1.1.1 shows the

infrared spectra for castor oil/cellulose acetate-based polyurethanes after seven days of curing (Figure 4.1.1.1.b), in comparison to those obtained with the raw materials, i.e., 1,6-hexamethylene diisocyanate, cellulose acetate and castor oil (Figure 4.1.1.1.a). Figure 4.1.1.1.a also includes the FTIR spectrum of the functionalized biopolymer which was further blended with castor oil to get the final bio-based polyurethanes. As can be seen, the characteristic peak attributed to the O–H stretching vibration has almost disappeared by around 3330 cm^{-1}, thus confirming the total functionalization of cellulose acetate as intended. On the other hand, bio-based polyurethanes (Figure 4.1.1.1.b) also exhibit the absorption band centered at 3330 cm^{-1} due, in this case, to both the O–H and N–H stretching vibrations (Calvo-Correas et al., *2016*; Corcuera et al., *2010*; Stuart, *2004*; Ugarte et al., *2015*; Wang et al., *2016*) as well as the band at 1741 cm^{-1} corresponding to the aliphatic carbonyl group (C=O) (Stuart, *2004*), which are in concordance with those found in the castor oil spectrum (Figure 4.1.1.1.a). Besides, the absorption bands at 2919–2931 and 2851–2860 cm^{-1} correspond to the C–H asymmetric and symmetric stretching vibration, respectively, due to existing methylene groups in the polyurethane backbones, which can be observed in all IR spectra. Those peaks are accompanied by the bands at 1462 cm^{-1}, corresponding to CH_2 bending vibration (Stuart, *2004*).

Furthermore, the almost disappearance in the peak intensity at approximately 2260 cm^{-1}, attributable to free N=C=O groups (*Figure 4.1.1*.1.b) (Calvo-Correas et al., *2016*; Gallego et al., *2013a*; Stuart, *2004*), confirms the complete reaction of N=C=O groups for sample with the lower biopolymer content (PU70.30), due to the excess of hydroxyl groups. This fact is corroborated by means of the reduction in the intensity of peak located at 1354 cm^{-1}, attributable to C–N stretching vibration in free isocyanate groups. However, the intensity of the peak associated to the stretching vibration of the N=C=O group clearly increases as biopolymer content does. Moreover, the extensive formation of urethane linkages is confirmed by their characteristic bands apparent at 3330 cm^{-1}, which appears to overlap the O–H stretching vibration but as a sharper peak, 1715, 1697 and 1580 cm^{-1} attributed to N–H stretching, amorphous and crystalline hydrogen bonded C=O stretching, and N–H bending vibrations, respectively (Corcuera et al., *2010*; Gurunathan and Chung, *2016*; Stuart, *2004*). Finally, no evidence of free isocyanate groups was found after one month of curing, as illustrated in *Figure 4.1.1*.1.b for the 50:50

CO/biopolymer weight ratio. However, despite the fact that total curing process requires around one month, the bio-polyurethane mechanical properties remain almost unchanged after one week.

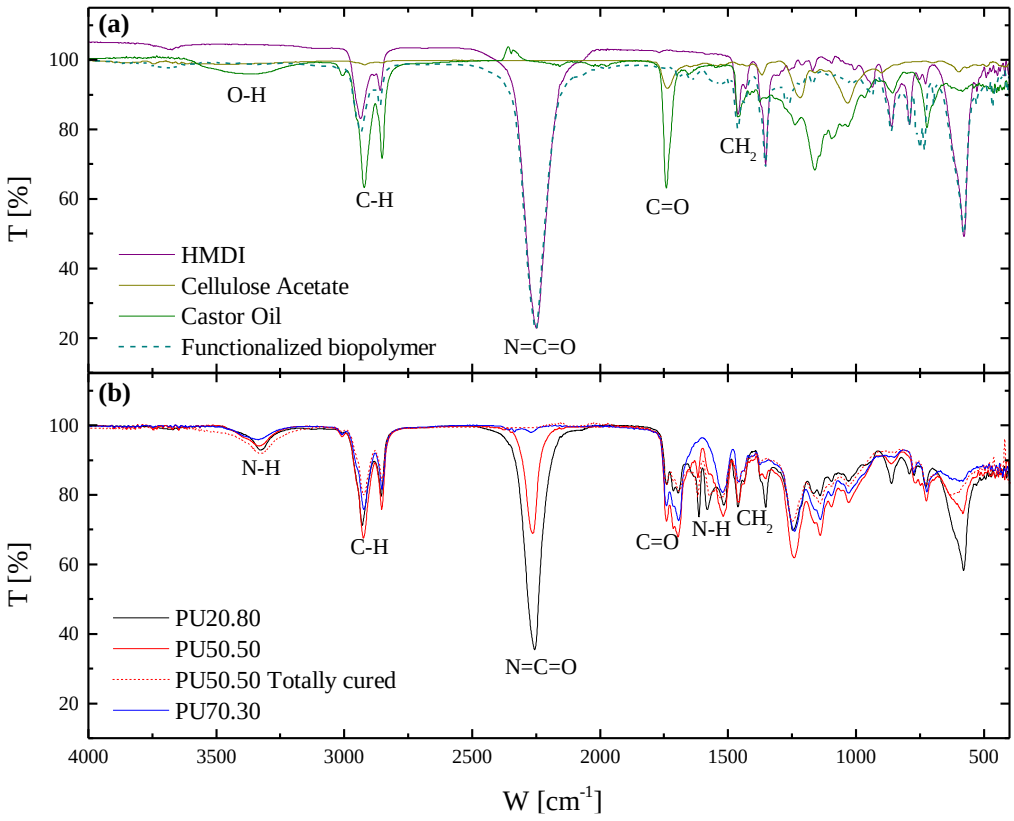

Figure 4.1.1.1 Fourier transform infrared spectroscopic attenuated total reflectance (FTIR-ATR) spectra for: (a) 1,6-hexamethylene diisocyanate, cellulose acetate, castor oil and functionalized biopolymer; (b) formulation PU20.80, PU50.50, PU70.30 and totally cured PU50.50

The thermal stability and decomposition behavior of bio-based adhesives were studied with the aid of thermogravimetric analysis after one week of curing. Figure 4.1.1.2 displays TGA curves for the different formulations studied, showing the weight loss percentage and the derivative curve versus temperature. Those results were also compared to those obtained with the corresponding reactants, i.e., cellulose acetate, 1,6-hexamethylene diisocyanate and castor oil (Figure 4.1.1.3). Table 4.1.1.1 collects the characteristic thermal parameters determined from the thermograms, such as, the onset temperature (T_{onset}), the temperature for the maximum decomposition rate (T_{max}) and the

final temperature in each decomposition step (T_{final}), along with the weight-loss percentage corresponding to each step and the percentage of non-degraded residue (R) at the end of the process.

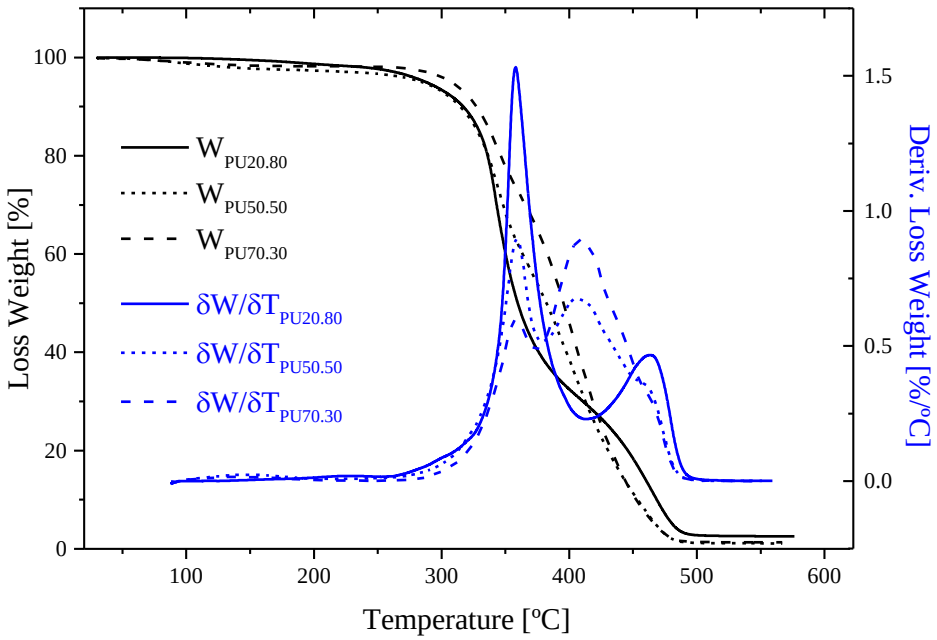

Figure 4.1.1.2 Thermogravimetric analysis (TGA) analysis for all bio-based adhesives

For cellulose acetate, thermal decomposition under nitrogen atmosphere took place in one single step, as can be deduced from Figure 4.1.1.3, ranging from 335 to 373 °C, yielding an almost complete weight loss (≈82%) after this temperature. In comparison to pure cellulose acetate, bio-based polyurethanes prepared from this polymer experienced a slight decrease in thermal stability as a consequence of the polymerization process. As can be seen in Table 4.1.1.1, all synthesized bio-based polyurethanes generally start to decompose at lower temperatures, experiencing a not very significant weight loss (≈1–2%) within the range of 60–204 °C, which can be attributed to the loss of some free remaining NCO segments (Gallego et al., 2013b), but also residual solvent and moisture. Moreover, as a result of the urethane linkages, the biopolymer degradation started at lower temperatures. As previously reported, the isocyanate functionalization of cellulose derivatives generally expands the degradation temperature range (Gallego et al., 2013b; Gallego et al., 2015b).

Table 4.1.1.1 Thermal parameters obtained from thermogravimetric analysis curves

Sample	T_{onset} **[°C]**	T_{max} **[°C]**	T_{final} **[°C]**	**Weight loss [%]**	**Residue [%]**
20% CO	130/326/426	193/343/465	204/372/493	1.6/67.5/28.5	2.6
50% CO	63/314/374	98/344/397	158/358/442	2.3/39.2/47.2	1.2
70% CO	60/307/370	93/343/402	155/357/453	1.6/26.9/63.1	1.4
HMDI	138	171	176	99.7	0.3
CA	335	358	373	82	18
CO	367	395	416	99.4	0.6

Besides this, for castor oil, a single step thermal decomposition took place between 367 and 416 °C (see Figure 4.1.1.3), which is clearly noticeable in the thermograms of bio-polyurethane samples PU50.50 and PU70.30 (Figure 4.1.1.2). Interestingly, the formulation with 20% CO did not show this degradation peak due to the low oil content in its structure. As a consequence, the lower castor oil content, the less intense peak appeared at around 395 °C, and also the higher intensity in the event located at 343 °C, corresponding to cellulose acetate, was observed.

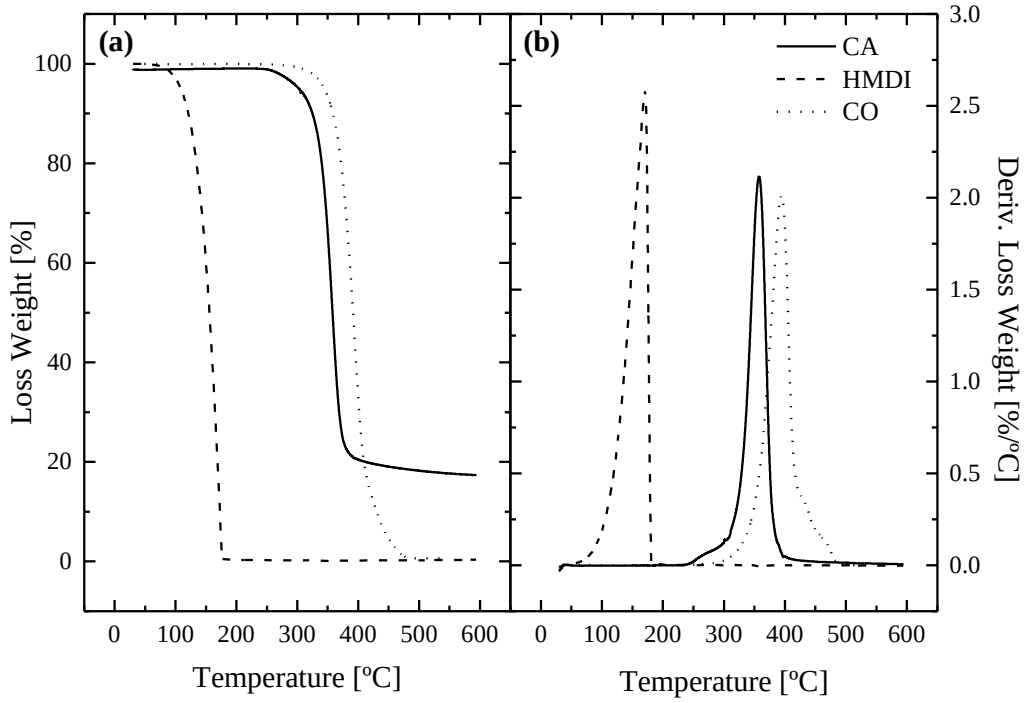

*Figure 4.1.1.3 (**a**) Loss weight and (**b**) derivative loss weight curves for cellulose acetate, 1,6-hexamethylene diisocyanate (HMDI) and CO raw materials*

Finally, the bio-adhesive PU20.80 exhibited a clear peak centered at 465 °C, which does not correspond to the degradation of urethane groups. According to Gurunathan and coworkers (Gurunathan et al., *2015*; Gurunathan and Chung, *2016*) and Corcuera et al. (*2010*), this event takes place at around 320–370 °C, overlapped in this case with the degradation of cellulose acetate backbone. At around that temperature (450–470 °C), a shoulder in the last decomposition peak was also detected in samples containing 50% and 70% CO as well (Figure 4.1.1.2). As a consequence, the degradation peaks found at these temperatures in the bio-based polyurethanes studied must be assigned to

excessively crosslinked polyurethane networks. These more rigid domains, logically favoured by the higher biopolymer content, i.e., higher density of urethane linkages, are more thermally stable (Gallego et al., *2014*).

The different structural thermal events taking place in the synthesized cellulose-based polyurethane were evaluated by means of differential scanning calorimetry (DSC). Generally, only one thermal event, corresponding to the glass transition of soft segments domains ($T_{g,SS}$), was detected in the temperature range applied (Figure 4.1.1.4), whereas no glass transition attributable to hard segments was observed (Bagdi et al., *2011*). Moreover, melting transitions of the crystalline domains were also not observed below 200 °C. The temperature of the glass transition values ($T_{g,SS}$) were taken at the midpoint of the transition, and inserted in Figure 4.1.1.4. According to these results, $T_{g,SS}$ increases with the biopolymer content in the formulation. Nevertheless, because of the low vegetable oil content, $T_{g,SS}$ became unnoticeable in the formulation with the 20% CO content.

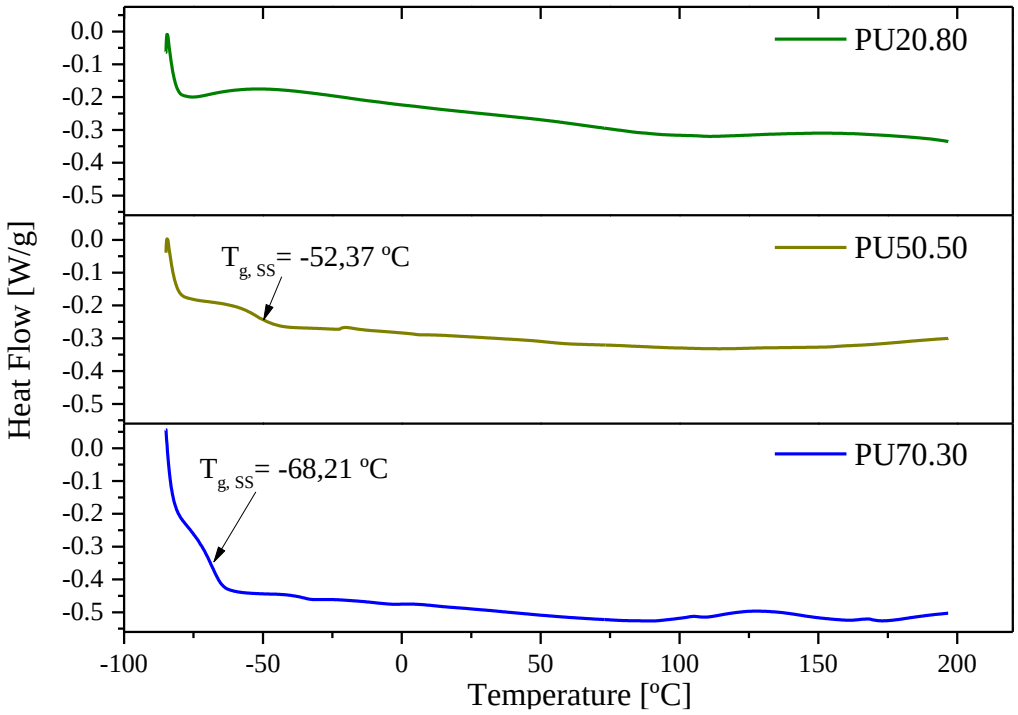

Figure 4.1.1.4 Differential scanning calorimetry (DSC) thermograms for bio-based polyurethane samples studied

1.3.2. Rheological properties

Figure 4.1.1.5 shows the evolution of viscoelastic moduli (*G′* and *G″*) with frequency for sample PU50.50, at different selected temperatures, measured under oscillatory torsional deformations. As can be noticed, a well-developed plateau region of the mechanical spectrum was always obtained, independently of the temperature, characterized by a predominant elastic behavior throughout the whole frequency range studied. Moreover, *G′* decreases with temperature, slightly up to 80–100 °C and then more dramatically. The same influence can be observed in *G″* at medium and high frequencies. However, the most remarkable effect of temperature on the viscous modulus is the change in the frequency dependence.

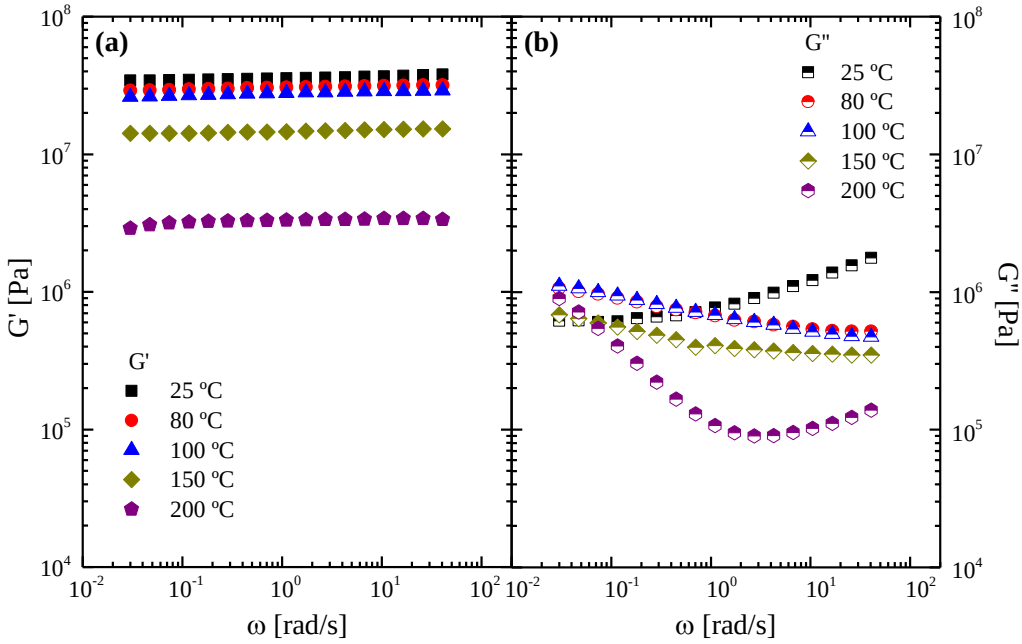

*Figure 4.1.1.5 Evolution of (**a**) elastic, G'; and (**b**) viscous moduli, G", with frequency, within the linear viscoelastic range, for formulation PU50.50 at different temperatures*

With the aim to extend the mechanical spectrum of the synthesized formulations, the time–temperature principle was applied (Figure 4.1.1.6), with the aid of suitable shift factors (a_T). This principle can be properly applied to bioadhesives with 50:50 and 70:30 castor oil/biopolymer weight ratio, until approximately 100 and 80 °C, respectively, but no longer. Nonetheless, bio-based polyurethane with the lowest oil content (PU20.80)

showed an extreme brittleness, which hindered the torsional frequency response. The values of the empirical shift factors applied in the time–temperature principle are included in Figure 4.1.1.7.a as a function of the reciprocal temperature, taking 25 °C as the reference temperature. The evolution of the shift factor with temperature can be described by means of the Arrhenius model as follow:

$$a_T = A \cdot e^{\frac{E_a}{R}\left(\frac{1}{T} - \frac{1}{T_0}\right)} \qquad (4.1.1.1)$$

where R is the ideal gas constant (8.31434 $J \cdot mol^{-1} \cdot K^{-1}$), T the absolute temperature (K), T_0 is the reference temperature (K), A is the pre-exponential factor and E_a is the activation energy ($J \cdot mol^{-1}$). Fitting values for the activation energy are shown in Figure 4.1.1.7.a for each sample.

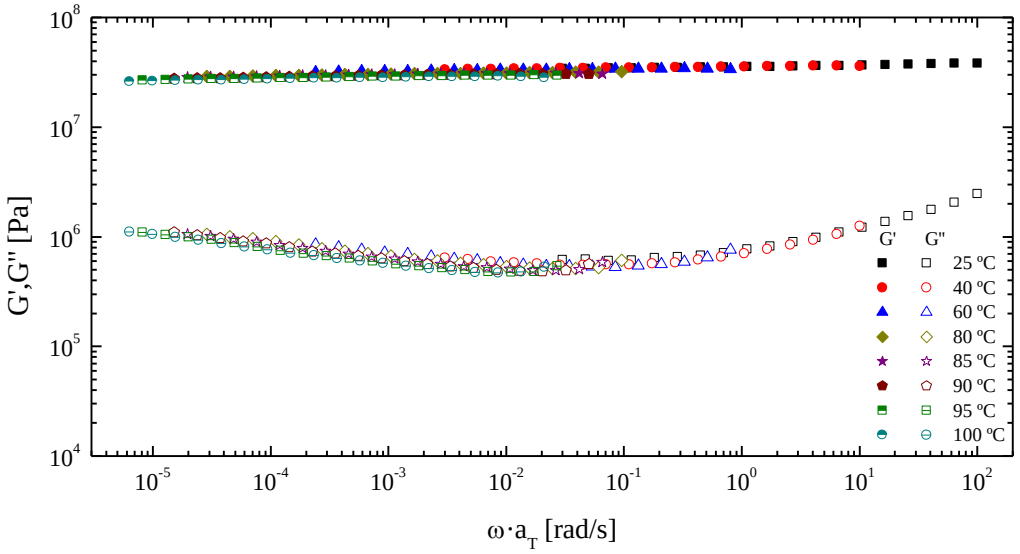

Figure 4.1.1.6 t–T superposition for formulation with 50% CO from 25 up to 100 °C temperature

As can be noticed, an increase in activation energy was found when CO content is reduced, meaning a bio-based adhesive characterized by a higher thermal susceptibility. The values of the plateau modulus, G_N^0, the characteristic parameter of the plateau region, estimated as the value of G' at the frequency for which the loss tangent ($\tan\delta = G''/G'$) is minimum, were also plotted versus the reciprocal temperature (Figure 4.1.1.7.b). As expected, G_N^0 values do not significantly change in the temperature range

where the *t–T* superposition principle was applied, but dramatically decrease afterwards. The Arrhenius equation can be also applied to evaluate the temperature dependence on G_N^0 in the two above referred regions, below and above the critical temperature for a significant softening, as shown elsewhere (Gallego et al., *2015a*). Fitting values for the activation energy are included in Figure 4.1.1.7.b. This behaviour reflects the thermo-rheological simplicity of those bio-based polyurethanes, from room temperature up to the mentioned critical temperatures, above which a different evolution of the rheological functions with both temperature and frequency was observed. This change in thermo-rheological response might be associated to the initial weight loss found in TGA tests, attributable to the loss of free isocyanate content.

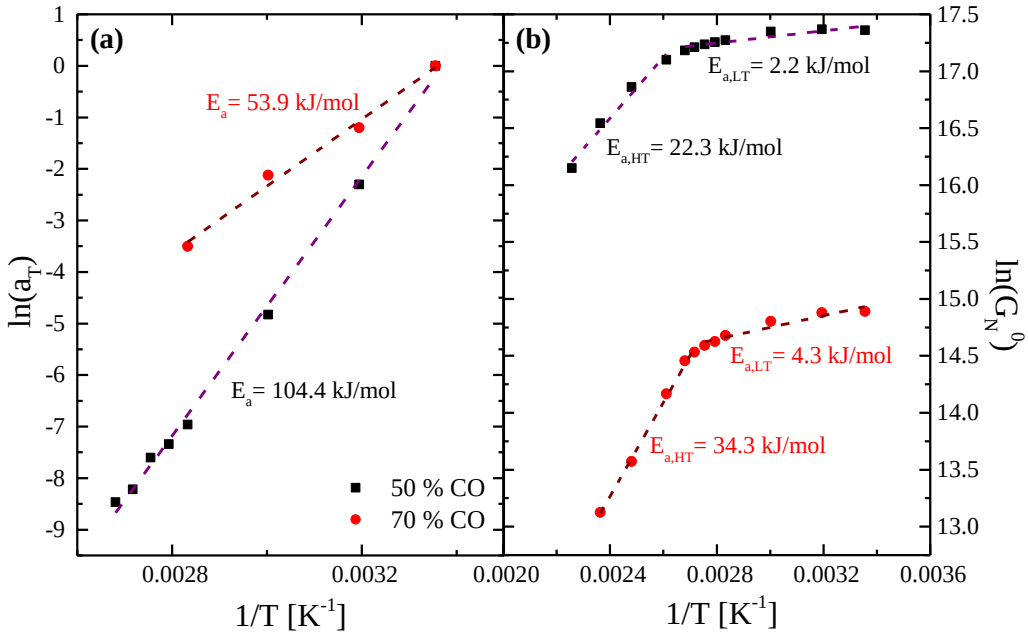

*Figure 4.1.1.7 (**a**) Shift factors (a_T) and (**b**) plateau moduli (G_N^0) for formulations PU50.50 and PU70.30*

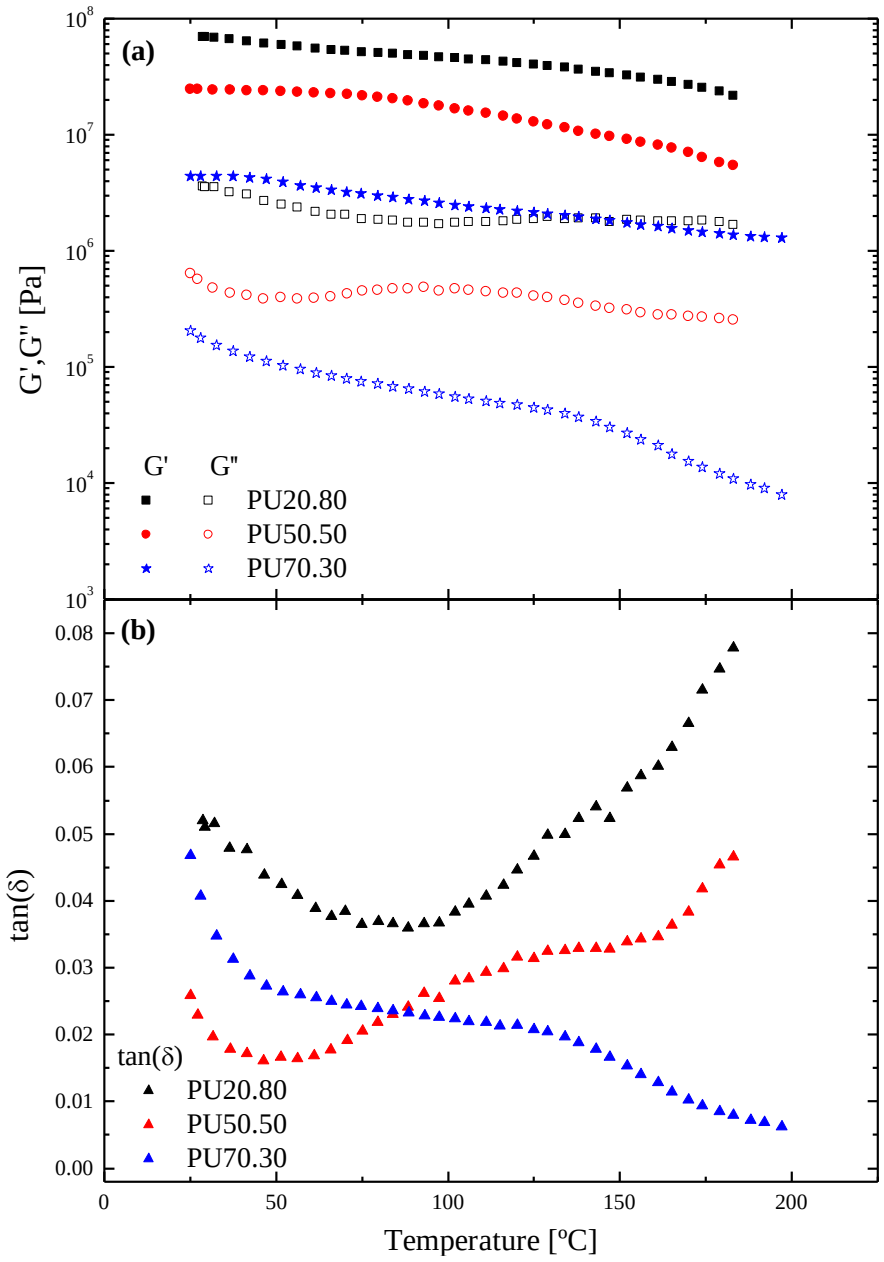

*Figure 4.1.1.8 Temperature ramps for all ecofriendly bioadhesives at 2 °C/min of heating rate within the linear viscoelastic region: **(a)** elastic (G') and viscous (G") moduli; **(b)** loss tangent (tanδ)*

In addition, Figure 4.1.1.8 depicts the evolution of viscoelastic functions when applying continuous temperature ramps for all formulations studied. Generally, in bio-based polyurethane systems PU20.80, PU50.50 and PU70.30 a slight temperature influence

over the storage moduli (*G'*) was found up to a critical temperature of around 120, 80 and 40 °C, respectively. Above these temperatures, a more important softening was noticed, similarly to the evolution found in frequency sweep tests. The evolution of *G''* is more complex since the frequency dependence is also affected by temperature as previously discussed. Nevertheless, the sample with the highest castor oil content (or lower biopolymer concentration) undergoes a continuous and much more important decrease in both viscoelastic functions within all temperature ranges evaluated. Moreover, attending to the evolution of the loss tangent, bio-polyurethanes with 20% and 50% CO exhibit a well extended plateau region in the range from 25 to 180 °C, with increasing values related to the melting transition of the crystalline microdomains, which is expected to be found at higher temperatures. Overall, the higher biopolymer content in the formulation, the higher values of the viscoelastic moduli and critical temperature for the softening were found.

1.3.3. Adhesion performance on wood substrates

Adhesion performance of the synthesized bio-based formulations was studied by applying standardized mechanical tests. Table 4.1.1.2 shows the different mechanical parameters obtained from these tests. According to these, polyurethane with a medium CO content exhibits more important peeling strength in comparison to the other samples, although still slightly lower than the commercial polyurethane used as benchmark. Moreover, concerning shear tests results, adhesives PU20.80 and PU50.50 present comparable shear strengths, almost three times higher than the sample containing 70:30 castor oil/biopolymer weight ratio (Table 4.1.1.2). These samples also undergo a substrate failure, which seems to be a more appropriate and desirable sort of failure. The values of the shear strength provided by the ASTM D906 test are almost twice as those reported by Somani et al. (*2003*) for castor oil-based adhesives prepared using aliphatic diisocyanates, and slightly higher than those reported by Silva et al. (*2010*) for castor oil-based adhesives including TDI as crosslinking agent. Moreover, the lap shear strength values for adhesives PU20.80 and PU50.50 are very similar to that obtained with the commercial sample. Finally, as judged by flexural results, all formulations showed similar failing loads, even though, once again, the sample with the highest castor

oil/biopolymer weight ratio exhibited a stress value which is significantly lower than those obtained with the rest of samples, while the commercial adhesive provided, in this case, a significantly lower flexural strength.

Table 4.1.1.2 Peeling, shear and flexural strengths on bonding wood substrate

Sample	Peeling Strength [g–f/mm]	Shear strength [MPa]	Flexural strength [MPa]
PU20.80	59.8 ± 10.9 [a]	2.37 ± 0.03 [b,c]	21.9 ± 6.0 [e,f]
PU50.50	169.4 ± 19.6 [b]	2.84 ± 0.36 [b,c]	21.6 ± 4.9 [e,f]
PU70.30	76.9 ± 4.9 [b]	0.94 ± 0.24 [b]	14.5 ± 0.9 [e]
Commercial polyurethane adhesive	228.6 ± 28.3 [b]	2.50 ± 0.40 [b]	11.0 ± 3.0 [e,f]

Failure classification: [a] Adhesion; [b] Cohesion; [c] Substrate; [d] Delamination; [e] Breaking; [f] Buckling.

1.4. Conclusions

In this research, a cellulose derivative was first functionalized by inducing the reaction with 1,6-hexamethylene diisocyanate, and then the biopolymer was blended with castor oil to obtain bio-based polyurethane adhesives. The influence of the castor oil/biopolymer weight ratio in bio-based adhesive was evaluated with the aid of rheological, standardized mechanical, thermal and spectroscopic analysis. The results demonstrated that the formulation with medium castor oil/biopolymer weight ratio (PU50.50) showed more suitable mechanical properties with more appealing failures for bonding wood, comparable to those exhibited by a well-known commercial polyurethane-based adhesive. The rheological response of all synthesized polyurethanes corresponds to strong crosslinked gels characterized by the plateau region of the mechanical spectrum. Moreover, the storage and loss moduli increased with biopolymer content. A slight decrease in viscoelastic moduli was detected with the increase in temperature, becoming more important above a critical temperature, which increases with the biopolymer/castor oil weight ratio. Below this critical temperature, a simple thermo-rheological response was found, being able to apply the t–T superposition principle. Finally, thermal analysis, supported by rheological and spectroscopic results,

suggests a chemical structure based on soft and crystalline hard segments, characterized by a several-stage thermal decomposition pattern.

2. Assessing the rheological properties and adhesion performance on different substrates of a novel green polyurethane based on castor oil and cellulose acetate: a comparison with commercial adhesives

2.1. Abstract

Interest in replacing petroleum-based adhesives with more environmentally friendly materials has grown enormously in recent decades. In this section, a novel bio-sourced polyurethane was synthesized by functionalizing cellulose acetate with 1,6-hexametylene di-isocyanate (HMDI) and then blending the resulting biopolymer with castor oil in a 1:1 weight ratio to obtain a chemical oleogel which was left for curing. The rheological properties and adhesion performance of this new bio-based formulation were compared with those of commercially available adhesives by using small-amplitude oscillatory torsional tests and standardized mechanical tests to evaluate shear (ASTM D906, D1002, D3163) and peeling (ASTM D903) strengths in single-lap and lap-joint assemblies (ASTM D3164) on various substrates including wood, polyethylene and stainless steel, as well as flexural strength (ASTM D1184) on wood. As shown here, the new adhesive is suitable for most of the adherends examined, thus exhibiting mechanical strengths comparable to or even better than that of the benchmarks in wood–wood and steel–steel contacts, similarly good rheological response and significantly higher relative elasticity. On the other hand, the adhesion performance of the new adhesive on polyethylene was worse than that of the commercial adhesives.

2.2. Introduction

Most currently available adhesive formulations are based on volatile organic compounds (VOCs) that are used as vehicles for their application and subsequently evaporate before the adhesive bonds to the adherent. The solvents contribute some adhesive features such as fluidity, drying time and instantaneous tackiness. However, most of the VOCs and main components in solventless adhesives are petrochemical derivatives and thus pose health and environmental risks (Packham, *2009*). Crude oil is becoming an increasingly scant and expensive resource, and also one of the main culprits of environmental pollution, global warming and climate change. The need to preserve the environment and the increasing shortage of petroleum have led a number of researchers to develop alternative adhesives. Thus, for instance, Ferrer et al. (*2008*) and Santiago-Medina et al. (*2016*) have proposed a new generation of more environmentally friendly adhesives by reducing the use of petro-based materials or replacing them with renewable natural raw materials. Unfortunately, these natural systems typically possess a lower resistance to moisture, chemicals and biological organisms than synthetic adhesives, and also a lower mechanical strength in some cases (Kong et al., *2011*).

The exceptional physical properties of polyurethanes among commercially available adhesives, which include versatility, excellent flexibility, high chemical resistance and mechanical strength, acceptable curing speed, and very good adhesion performance (Strobech, *1990*), make them very effective alternatives to the widely used formaldehyde and epoxy resins. Polyurethanes are usually synthesized by reacting di-isocyanates with polyalcohols. The di-isocyanates most commonly used for this purpose are 4,4′-diphenylmethane di-isocyanate (MDI), toluene di-isocyanate (TDI), 1,6-hexamethylene di-isocyanate (HMDI), 1,5-naphthalene di-isocyanate (NDI) and isophorone di-isocyanate (IPDI); the polyols have traditionally been obtained from petrochemicals, but these are gradually being replaced with renewable materials such as carbohydrates, tannins and silanes, as Gallego et al. (*2013a*), Santiago-Medina et al. (*2016*), Ghahri et al. (*2017*) and Thébault et al. (*2016*) reported, or with vegetable oils and their derivatives, as Kong et al. (*2011*), Badri et al. (*2006*) and Campanella et al. (*2009*) described, in polyurethane synthetic procedures. Specifically, castor (Silva et al., *2010*; Valero and Gonzalez, *2012*), soybean (Głowińska and Datta, *2016*), sunflower (Ferrer et al., *2008*),

canola (Kong et al., *2011*), linseed and rapeseed (Rojek and Prociak, *2012*) oils are being increasingly used to prepare bio-polyurethane formulations. According to Valero and Gonzalez (*2012*), castor oil is to be preferred for end-use industrial products because it is an abundant, inexpensive, non-edible, low-toxicity renewable resource, and also, it is the main natural source of ricinoleic acid (12-hydroxy-9-octadecenoic acid), whose unsaturated double bonds and hydroxyl and carboxyl groups are efficient reaction sites. Moreover, as shown by Quinchia et al. (*2010*), the hydroxyl group content, chain length and extent of unsaturation of castor oil make it highly viscous in relation to other vegetable oils. Although Zhou et al. (*2003*) reported the preparation of films by blending castor oil-based polyurethane and cellulose acetate, the potential of this mixture as an adhesive remains largely unexplored.

Because adhesion involves interatomic and/or intermolecular interactions between the adhesive and two substrates, it is highly dependent on the surface free energy of the adhesive and adherend. However, the multidisciplinary nature of adhesion and its comprising chemical, mechanical and rheological concepts make a simple description of the phenomenon virtually impossible. Baldan (*2012*) has reviewed a wide range of mechanisms intended to explain adhesion over the last few decades, although each of them can be valid only to some extent. The chemical bonding mechanism, which assumes a chemical interaction between adhesive and substrate, in combination with various physical mechanisms, have rendered polyurethane-based adhesives especially attractive for bonding wood, as can be inferred from the results obtained in the investigations carried out by Aung et al. (*2014*) with bio-based polyurethanes, but not limited to this substrate, according to the results reported by Kim et al. (*2017*) or Zain et al. (*2016*) regarding the evaluation of the adhesion performance of polyurethane-based systems for the automotive industry, among others. Although validating specific adhesion mechanisms in novel bio-based adhesives is no easy task, destructive tests can provide useful information about the mechanical properties of adhesive bonds. As well known, ASTM and ISO have issued standards regulating tests for measuring bulk adhesion performance in terms of strength or toughness. Moreover, non-destructive rheological tests in torsion or bending modes can also be applied to characterize cured adhesive formulations though. The main aim of this section was to compare the adhesion

performance on different substrates of a novel eco-friendly adhesive based on castor oil and cellulose acetate with that of a wide spectrum of commercial adhesives involving a wide range of chemistry and applications through standardized mechanical tests and small-amplitude oscillatory torsional tests.

2.3. Results and discussion

2.3.1. Rheological behavior

Figure 4.1.2.1 compares the viscoelastic response to small-amplitude oscillatory torsional deformation of the proposed bio-based polyurethane (PU50.50) with that of commercial adhesives as evaluated at different temperatures. Generally, as can be observed, in all systems the values of the storage (elastic) modulus, G', were much higher than those of the loss (viscous) modulus, G'', throughout the frequency range examined. The G' and G'' frequency dependence, with relatively low slopes in their plots against frequency, corresponds to the so-called "*rubbery plateau region*" of the mechanical spectrum, which is typically observed in cured adhesives once a three-dimensional network has developed as a result of substantial cross-linking (Kong et al., *2011*; Leitsch et al., *2016*). Only sample CAdh4, which is an aqueous dispersion, exhibited a stronger frequency dependence of both moduli at 25 ºC in addition to a slight tendency for the two viscoelastic functions to cross over, which suggests that the glass transition temperature of this material is higher than those of the others. Moreover, the viscoelastic moduli for the commercial samples CAdh1 and CAdh3 invariably decreased with temperature. On the other hand, the moduli for CAdh2 were virtually temperature-independent and those for CAdh4 decreased with increasing temperature from 25 to 80 ºC and then increased markedly above 150 ºC —an obvious result of water evaporation. Therefore, adhesive CAdh4 was the most strongly affected by temperature and frequency for the above-described reasons; also, it exhibited greater values of the storage and loss moduli at the highest and lowest temperature studied. By contrast, the small-amplitude oscillatory torsional test for CAdh1 revealed that it exhibited the smallest values of the storage modulus throughout the temperature and frequency ranges. Overall, the loss tangent ($\tan\delta = G''/G'$) was similar for all commercial samples at 80 and 150 ºC,

where CAdh1 exhibited a slightly more relative viscous response (greater tanδ values) and sample CAdh3 the most relative elastic behaviour (smallest tanδ values). The results obtained at 25 ºC were much more variable, with CAdh4 as the most viscous sample as noted before.

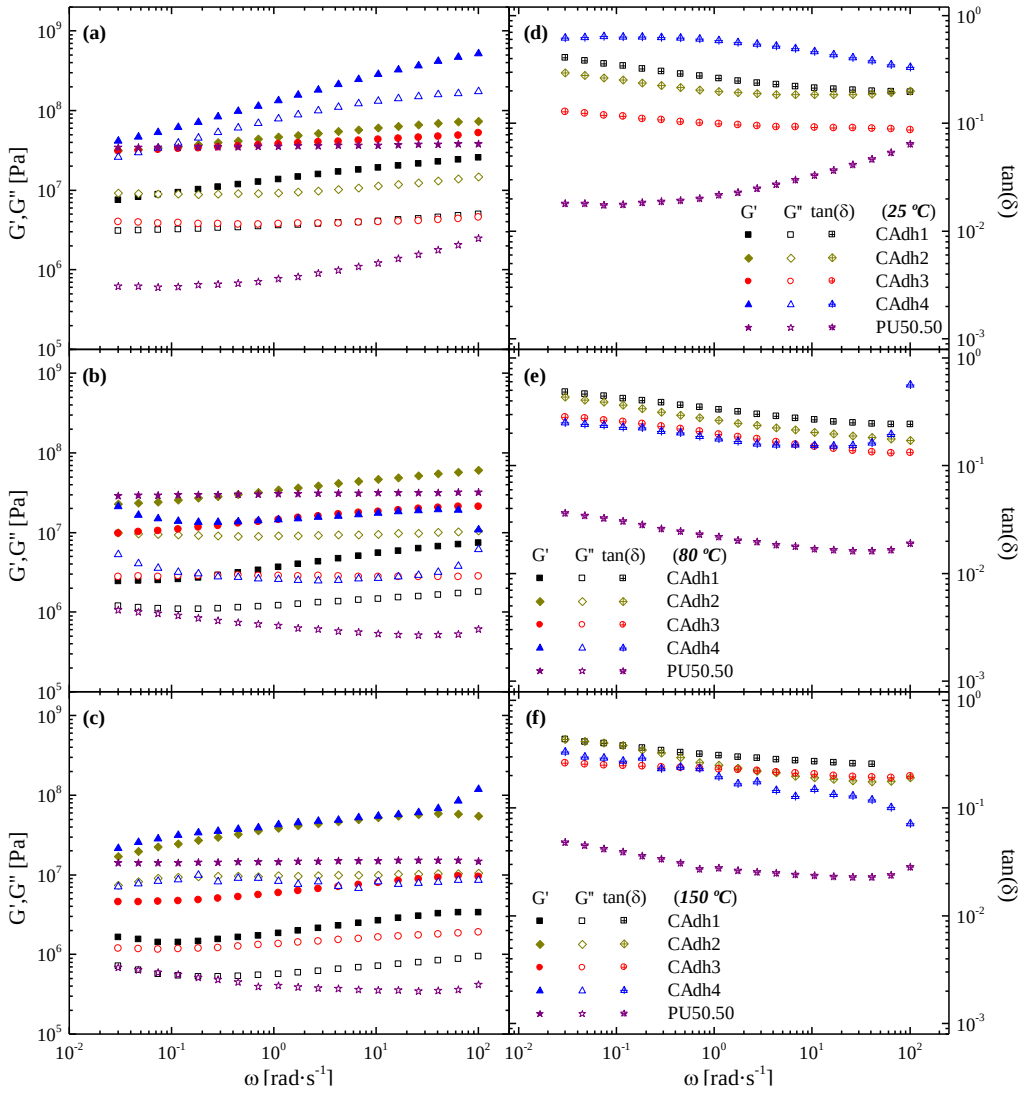

Figure 4.1.2.1 Variation of the storage and loss moduli (a–c) and loss tangen (d–f) with frequency at different temperatures

The frequency-dependence of the torsional viscoelastic functions for the bio-based polyurethane also exhibited a broad rubbery plateau region as a consequence of the extensive cross-linking achieved during the curing process. Whichever the temperature,

G' values fell in the range for the commercial samples, whereas G'' values were generally lower. As a result, the bio-based polyurethane PU50.50 exhibited a more marked relative elastic response, its loss tangent being roughly one decade smaller than the values for the commercial adhesives. On the other hand, the linear viscoelastic functions were only slightly affected by temperature, so the adhesives, similarly to CAdh2, exhibited a virtually identical mechanical response over a wide temperature range. The temperature dependence of the viscoelastic functions was explored by fitting the complex modulus, G^*, to the following power-law equation:

$$G^* = \sqrt{G'^2 + G''^2} = \mathrm{A} \cdot \omega^{1/\mathrm{n}} \qquad (4.1.2.1)$$

and analysing the dependence of the power-law parameters, *A* and *n*, on temperature. The figures of merit of the fitting are shown in Figure 4.1.2.2. As can be seen, CAdh2 and the model bio-polyurethane (PU50.50) were the two adhesives least markedly influenced by temperature —and the opposite held for CAdh1 and CAdh4. Moreover, parameter *n* for the bio-based urethane was always around one decade greater than those for the commercial adhesives, which is suggestive of a higher density of cross-linking points or a higher number of interacting structural units.

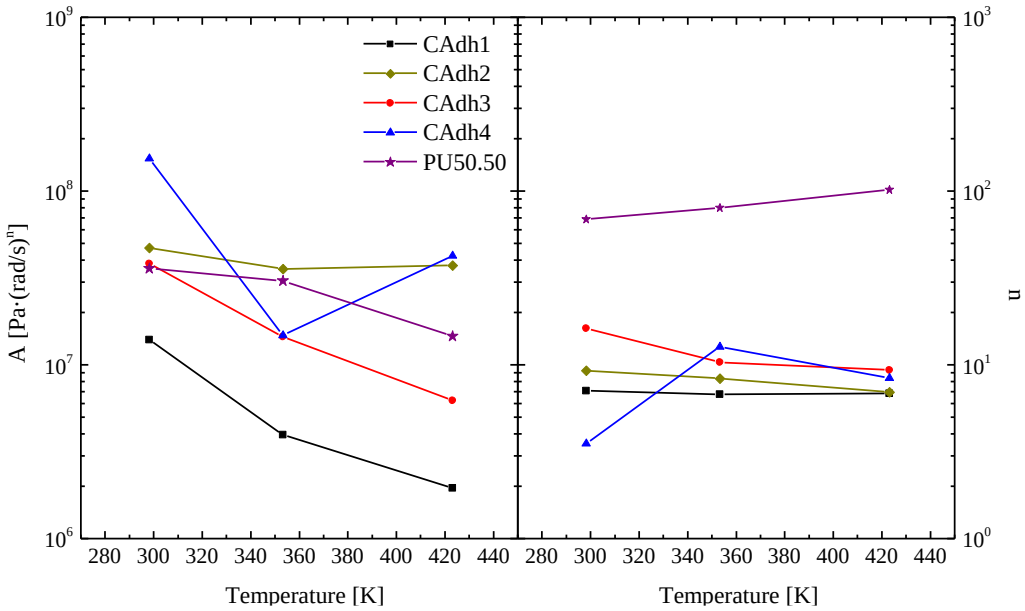

Figure 4.1.2.2 Power-law parameters for Equation (4.1.2.1) as a function of temperature

The temperature dependence of the rheological response was also examined, using a 2 C/min temperature ramp from room level to 200 ºC (Figure 4.1.2.3). As previously noted for the frequency sweep tests, *G′* exceeded *G″* throughout the temperature range in all samples. Also, the storage and loss moduli for CAdh1 and CAdh3 exhibited a steady fall as the temperature was raised. On the other hand, both moduli decreased with increasing temperature up to a critical level, and then increased at higher temperatures, in CAdh2 and CAdh4. Whereas the moduli for CAdh2 were seemingly scarcely influenced by temperature, CAdh4 exhibited a far more complex evolution owing to its previously noted increased thermal susceptibility; thus, it initially exhibited a dramatic drop by around one order of magnitude in both viscoelastic functions, reached the critical minimum value at ca. 80 ºC and increased beyond that point. Both linear functions peaked at around 150 ºC. Consistent with the foregoing, the storage and loss moduli for the bio-based polyurethane adhesive PU50.50 remained virtually constant or decreased slightly below 80–90 ºC, but exhibited a marked drop above this critical temperature level (Figure 4.1.2.3).

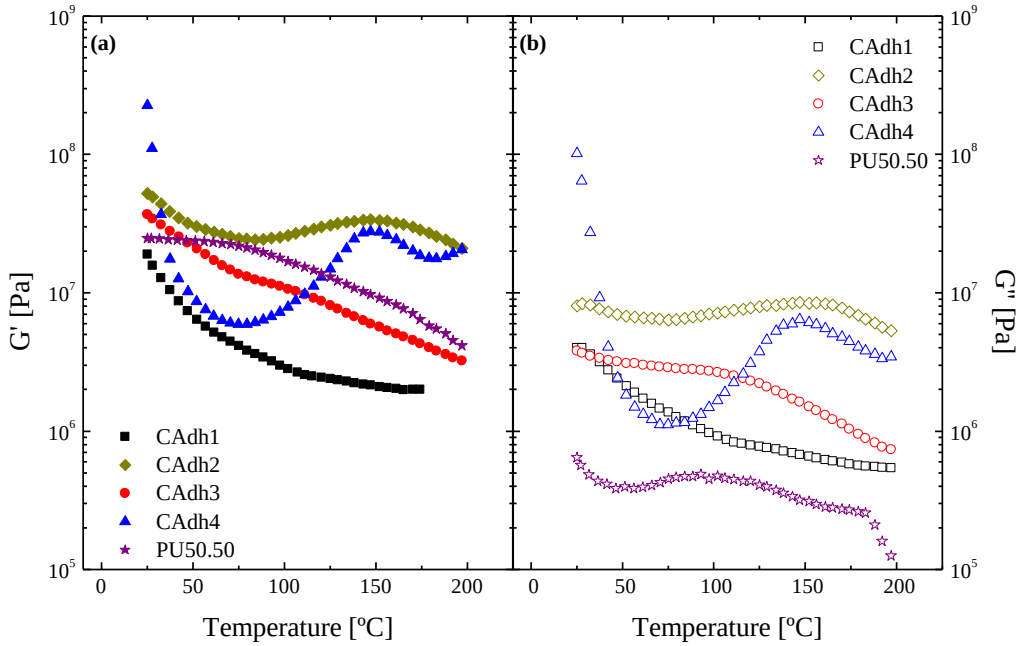

Figure 4.1.2.3 Temperature dependence of the storage (a) and loss (b) moduli for commercial and bio-based polyurethane adhesives PU50.50

2.3.2. Adhesion performance

The adhesion performance of the adhesives on different substrates was assessed by using the applicable ASTM tests for peeling strength, conventionally expressed as the force per unit width (ASTM D903), shear strength (ASTM D906, D1002, D3163 and D3164 for wood, steel, plastic and sandwich joint SS-PE-SS substrates, respectively) and flexural strength (ASTM D1184), typically expressed as stress values. The results of the tests are given in Table 4.1.2.1.

Benchmarks CAdh1 and CAdh4 exhibited the lowest and highest strength value, respectively, in the peeling tests on wood; on the other hand, the bio-based adhesive exhibited a fairly competitive stripping strength that even exceeded that for adhesives CAdh2 and CAdh1 by a factor of 2 or 3. The peeling strength values for the adhesives with polyethylene as the substrate were much lower; by exception, the values for CAdh1 were virtually identical with those obtained with wood , and so was the type of failure, so this is the most suitable adhesive for PE. Because of its especially low peeling strength, the bio-based adhesive does not seem very suitable for bonding to PE. With stainless steel, however, the bio-adhesive exhibited the best stripping performance, its peeling strength being higher than that on all other adherends. The peeling strength of CAdh3 and CAdh4 on SS was roughly one-half that on wood, whereas those of CAdh1 and CAdh2 were similar to their values on this substrate.

Bearing in mind the complexity of the mechanisms involved in adhesive bonding, the resulting mechanical response may have arisen from the combination of a wide range of interactions, including rheological, physical, chemical and mechanical phenomena, according to Baldan (*2012*) and Awaja et al. (*2009*). Obviously, the chemical nature of polyethylene precludes adhesion via mechanisms such as chemical bonding, interdiffusion and donor–acceptor interactions; rather, adhesion must occur through mechanical interlocking, and adsorption through dipole–dipole interaction and London dispersion forces, for example. Based on the foregoing, the peeling strength of CAdh4 and CAdh3 on polyethylene was 10 and 6 times lower than it is on wood and stainless steel, respectively. Moreover, these two adhesives produce "*adhesion failure*" on the metal and polyethylene substrates owing to their greater affinity for the flexible part. In

any case, other adhesion mechanisms such as covalent or hydrogen bonding seemingly act in their adhesion to wood surfaces that lead to higher stripping strengths —so much so that the adhesion of CAdh3 on wood finally resulted in a "*cohesive failure*". Similarly, an electrostatic mechanism might play a major important role in adhesion to metal substrates, even though it had a lower impact on the stripping strength of these benchmarks. The peeling strength of CAdh2 on PE was also smaller, albeit not so markedly —probably, apart from the different adhesion mechanisms involved, because of the apparent lower wettability of this commercial adhesive and its high viscoelastic moduli. Also, although the bio-based polyurethane exhibited cohesion failure on all solid materials, its stripping force was markedly higher on stainless steel and wood than it was on polyethylene as a result of the absence of Lewis acid–base and hydrogen bonding interactions with the PE surface. Moreover, the presence of free –NCO groups can be expected to result in covalent chemical interactions through urethane linkages with wood components such as lignocellulosic material, as described by Gallego et al. (*2015a*).

Similar to that found in the peeling test, adhesive CAdh1 exhibited the lowest maximum resistance to shearing deformation on any substrate in the lap shear strength tests; by exception, the bio-based polyurethane had the lowest adhesion strength of all adhesives on PE despite its shear strength on the other substrates being among the highest. Also, the bio-adhesive and CAdh4 exhibited a more suitable and desirable substrate failure on wood, onto which they adhered more strongly than the other adhesives —which in addition underwent cohesive rupture though. On the other hand, the strength of adhesion to stainless steel (SS–SS or sandwich joints) was rather low relative to wood–wood joints. With both substrates, the bio-polyurethane adhesive and benchmark CAdh3 (moisture-cured) exhibited increased mechanical adhesion (more than 20 times higher than that of CAdh1, for example). However, the shear strength of urethane-based adhesives (CAdh3 and the proposed formulation) in sandwich joints was much lower than that in stainless steel joints. As before, this result can be ascribed to the lack of chemical interactions on PE surfaces, where adhesion may be exclusively due to mechanical coupling and secondary molecular forces (e.g., van der Waals interactions (Baldan, *2012*)) on account of the chemical properties and mechanical pretreatment of the adherent. On the other hand, most of the commercial adhesives had higher lap shear

strength values than the bio-based system on PE, this result being a consequence of solvent release or fast moisture-induced curing favouring mechanical interlocking adhesion to such a rough surface. Despite this fact, the bio-based adhesive exhibited the highest shear strength in SS–PE–SS sandwich joints.

Regarding the flexural tests, the adhesive based on castor oil and cellulose acetate exhibited a high breaking strength on wood; its value doubled those of CAdh1 and CAdh3 and was only surpassed by those of CAdh2 and CAdh4. Also, all adhesives underwent a combination of breaking and buckling failure in this type of test.

The strength values of the new bio-based adhesive in the peeling (D903) and lap-shear (D906, D1002) tests on wood and stainless steel as adherends are similar to or even higher than those reported by Ho et al. (*1995*) for zwitterionic natural-based urethane adhesives, and Somani et al. (*2003*), Badri et al. (*2006*) and Zain et al. (*2016*), for caprolactone and/or vegetable oil-based urethane adhesives prepared from aliphatic and aromatic di-isocyanates. Also, the proposed bio-based adhesive exhibits a slightly higher flexural adhesion strength than the tannin-based wood adhesives studied by Barbosa et al. (*2000*).

Table 4.1.2.1 Strength values obtained in the standard mechanical tests

Sample		*Bio-adhesive*	*CAdh1*	*CA2*	*CA3*	*CAdh4*
Peeling strength [kN/m]	*PF-W*	1.7 ± 0.2^{b}	$0.6 \pm 0.1^{a,b\ (2)}$	$0.9 \pm 0.1^{a,b\ (3)}$	2.2 ± 0.3^{b}	2.8 ± 0.5^{a}
	PF-PE	0.024 ± 0.006^{b}	0.6 ± 0.2^{b}	$0.5 \pm 0.2^{a,b\ (4)}$	0.21 ± 0.04^{a}	0.27 ± 0.03^{a}
	PF-SS	2.4 ± 0.2^{b}	0.7 ± 0.1^{b}	0.8 ± 0.4^{a}	1.2 ± 0.3^{a}	1.6 ± 0.3^{a}
Shear strength [MPa]	*W-W*	$2.8 \pm 0.4^{b,c\ (1)}$	0.6 ± 0.1^{b}	3.2 ± 0.1^{b}	2.5 ± 0.4^{b}	2.9 ± 0.6^{c}
	PE-PE	0.037 ± 0.003^{b}	0.069 ± 0.008^{b}	0.19 ± 0.03^{b}	0.31 ± 0.08^{b}	0.17 ± 0.03^{b}
	SS-SS	2.0 ± 0.4^{b}	0.07 ± 0.02^{b}	0.32 ± 0.07^{b}	1.65 ± 0.04^{b}	0.11 ± 0.03^{b}
	SS–PE–SS	0.45 ± 0.08^{b}	0.06 ± 0.02^{a}	0.25 ± 0.04^{b}	0.3 ± 0.1^{b}	0.12 ± 0.04^{a}
Flexural strength [MPa]	*SyW(x8)*	$21.6 \pm 4.9^{e,f}$	$11.9 \pm 2.6^{e,f}$	$34.4 \pm 7.2^{e,f}$	$11.0 \pm 3.0^{e,f}$	$39.3 \pm 9.6^{e,f}$

Failure classification: [a] Adhesion; [b] Cohesion; [c] Substrate; [d] Delamination; [e] Breaking; [f] Buckling

(1)Cohesion/substrate failure 50/50 %; (2)Cohesion/Adhesion failure 5/95 %; (3)Cohesion/Adhesion failure 10/90 %; (4)Cohesion/Adhesion failure 70/30 %

2.4. Conclusions

A novel bio-based polyurethane adhesive was synthesized from castor oil and cellulose acetate previously functionalized with HMDI in a 1:1 weight ratio. The rheological response of the new adhesive under oscillatory torsional deformation and its adhesion performance on different substrates were compared with those of commercially available adhesives.

The bio-based polyurethane generally exhibited the same frequency dependence of its viscoelastic functions as the commercial adhesives, in addition to intermediate values of the storage modulus and lower values of the loss modulus. These properties confer the new adhesive a higher relative elasticity. Also, interestingly, its viscoelastic moduli are much less markedly affected by temperature.

Finally, the proposed bio-adhesive exhibited excellent adhesion performance on wood and stainless steel, and also in SS–PE–SS sandwich joints. It is thus an appealing alternative to existing commercial adhesives since it possesses similar or higher mechanical resistance to shear, peeling and flexure on these substrates. By contrast, its adhesion performance on polyethylene was inferior to that of most of the benchmarks.

Block 2: Synthesis and characterization of aromatic crosslinker-based polyurethane adhesives

1. Synthesis and mechanical properties of bio-sourced polyurethane adhesives obtained from castor oil and MDI-modified cellulose acetate: influence of cellulose acetate modification

1.1. Abstract

In this study, cellulose acetate and castor oil have been used to synthesize new eco-friendly alternatives to traditional polyurethane adhesives. First, cellulose acetate (CA) was modified with diphenylmethane-4,4'-diisocyanate (MDI) at different NCO:OH molar ratios, ranging from 2 to 4.53, and then the resulting biopolymers were mixed with castor oil (CO) at 1:1 weight ratio. The fully cured bio-sourced adhesives were rheologically characterized by applying dynamic oscillatory torsional tests at different temperatures (from -30 up to 200 ºC). Furthermore, their adhesion performance on stainless steel and poplar wood substrates was analyzed, by conducting standardized mechanical tests, namely single-lap shear and 180º peel strengths, at room temperature and 100 ºC. Fourier transform infrared spectroscopy-attenuated total reflectance along with differential scanning calorimetry and thermogravimetric analysis were also performed. Above a critical NCO:OH ratio, a thermo-rheological simplicity was found within the whole temperature range considered, being able to apply the t-T superposition principle. However, an increase in the temperature led to a depletion in their mechanical performance, thus reducing their temperature range of application. Thermal and spectroscopic analysis corroborated the complete disappearance of free isocyanate during the first few days of curing, and a segmented structure, typical of polyurethanes. Optimum thermo-rheological behaviour and adhesion performance on wood and stainless steel of the bio-sourced polyurethanes studied were found for NCO:OH molar ratios higher than 3.5, which was related to the higher compatibility between hard and soft microdomains.

1.2. Introduction

In the last years, renewable raw materials have attracted great attention as substitutes for petrochemical derivatives (Silva et al., *2010*). Since petroleum oil resources are becoming increasingly scarce and expensive to obtain, researchers have sought different resources and technologies to produce polymers, including polyurethanes (PU). Polyurethanes have received considerable attention due to their superior qualities like excellent strength and chemical resistance, but their production from fossil-fuel-based polyols and environmentally unfriendly materials is an issue to be solved.

The conventional synthesis of PUs is based on the reaction of isocyanates with compounds containing active hydroxyl groups such as polyols (Szycher, *1999*). With the increasing environmental awareness, the usage of sustainable raw materials as hydroxyl group-precursor sources has generated a great interest among researchers. Thus, the production of polyols from agricultural waste, sawdust, epoxidized methyl oleate and canola oil, among others, have been lately reported (Kong et al., *2007*; Liang et al., *2007*; Lligadas et al., *2007*; Schilling et al., *2005*; Yu et al., *2006*). Vegetable oils have shown great potential to produce different kinds of polymeric resins, such as lubricants (Borrero-López et al., *2018*; Gallego et al., *2015a*), foams (Sharma et al., *2014*) or adhesives (Raghunanan et al., *2018a*). With special interest in castor oil given its low cost and purity compared to traditional polyols produced from vegetable and animal fats (Gryglewicz et al., *2003*), it has drawn the attention in recent times. Castor oil, a triglyceride of ricinoleic acid, is a naturally-occurring and suitable monomer for PU production, whose particular high viscosity depends on the fatty acid profile (Scholz and da Silva, *2008*). The –NCO groups of diisocyanate compounds are able to react with the –OH groups of the castor oil, which become part of the network and will, therefore, not further vaporize out of the adhesive as a solvent does (Zhang and Ding, *1997*). In the literature, works regarding the relationships between the NCO:OH molar ratio and the mechanical properties of solvent-borne castor oil-based PU adhesives (Somani et al., *2003*; Zhang and Ding, *1997*) reported that an increase in the NCO:OH molar ratio up to 2.0 increases the chain cross-link density, which improved the adhesive bond strength.

Many other different options for replacing petrochemicals by renewable raw materials, such as carbohydrates, as shown by Gallego et al. (*2013a*; *2015b*), Santiago-Medina et al. (*2016*), Głowińska and Datta (*2015*; *2016*) and Oprea et al. (*2016*), have been also widely reported in the last decade. Among them, cellulose acetate modification with MDI has been addressed in previous investigations (Erdmann et al., *2014*; Li et al., *2015*; Penn et al., *1981*). However, to the best of our knowledge, the assessment of CA/MDI/CO mixtures with adhesion purposes still remains unexplored.

On the other hand, after the introduction in 1968 of the first structural adhesive by Goodyear initially used for truck hoods (Szycher, *2013*), polyurethane adhesives have gained high importance and have been continuously used to bond numerous substrates including glass, wood and plastics. Polyurethanes exhibit excellent adhesion performance, heat and chemical resistance, and fast curing. As the utilization of sustainable raw materials to produce PU adhesives provides evident environmental advantages over conventional petroleum-based counterparts, studies dealing with the development of eco-friendly and bio-sourced adhesives, especially for bonding wood, have acquired huge significance, like for instance the synthesis of wood adhesives by chemically modifying soy protein (Liu and Li, *2002*), Kraft lignin (Geng and Li, *2006*) or coffee bean shell (Khan and Ashraf, *2005*). In particular, in a previous work, cellulose acetate has been considered of great interest as raw material for the production of adhesives, for instance by promoting the reaction between the hydroxyl groups located in the cellulose backbone and active diisocyanate crosslinkers to synthesize functionalized biopolymers which were further blended with vegetable oils (Tenorio-Alfonso et al., *2017*). From the microstructural point of view, polyurethanes generally present a typical segmented structure, where "*soft*" and "*hard*" segment domains in the polymer matrix comprise the polyols and isocyanates, respectively, which are responsible of a several-stage thermal decomposition pattern. The hardness and rheological properties, in general, of polyurethanes may be controlled by the nature of the polyol and isocyanate used in their preparation, and the equivalent ratio of both of them (Javni et al., *2003*; Sharma et al., *2014*; Tenorio-Alfonso et al., *2017*; Zhang et al., *2007*).

Adhesion phenomena are concerned whenever different solid bodies or layers are brought into contact, for instance, in coatings, paints, varnishes, multi-layered sandwiches, polymer blends, filled polymers, adhesive joints and composite materials. Even though considerable research has been carried out during the last 60 years, the fundamental knowledge about adhesion phenomena is still not fully developed and no single global theory or model can explain all the mechanisms involved. This is mainly due to the fact that adhesion is a very complex phenomenon since it involves multidisciplinary knowledge of polymer and surface chemistry, fracture mechanism, mechanics of materials, rheology and other subjects (Baldan, *2012*; Silva et al., *2010*). Fourche (*1995*), in his review, described different adhesion models with the explanation of corresponding mechanisms in detail. Although viscoelastic polymeric materials are widely used for adhesive applications, the fundamental nature of the adhesion of these materials remains poorly understood. There are many factors that determine how a polymer adheres to a particular surface. Most important physical and chemical characteristics when adhesion performance is considered are its viscoelasticity nature, the molar mass distribution, the glass transition temperature T_g and the superficial distribution of functional groups (Pickering et al., *2001*). Other external factors could be temperature, humidity, surface roughness, the surface free energy of the substrates, and the total interfacial contact time. Despite the complexity to validate the different adhesion mechanisms in novel bio-sourced adhesives, destructive tests can provide relevant information related to mechanical properties of adhesive bonds. As well known, several standard test methods (ASTM or ISO), which regulate destructive tests, are proposed to measure bulk adhesion performance, i.e. strength, stress or toughness. Furthermore, non-destructive mechanical tests, such as torsional rheology can also be applied to characterize fully cured formulations.

In the present section, bio-based polyurethane adhesive formulations have been prepared by combining a carbohydrate polymer like cellulose acetate and castor oil. In the first step, cellulose acetate was modified by inducing the reaction with diphenylmethane-4,4'-diisocyanate, using six stoichiometric NCO:OH molar ratios. The resulting product was then blended with castor oil thus producing bio-based polyurethanes with adhesion properties. The main objective of this section was to evaluate the influence of the

cellulose acetate functionalization degree, i.e. the input NCO:OH molar ratio, over the rheological, thermal and adhesion properties of these bio-sourced PU formulations.

1.3. Results and discussion

1.3.1. Structural characterization

Infrared analysis was mainly employed to address the curing process of the synthesized bioadhesives by evaluating the decay of the characteristic absorption peak attributable to the asymmetric stretching vibration of free isocyanate functional groups (-NCO) at 2261 cm^{-1} (Tenorio-Alfonso et al., *2017*). Figure 4.2.1.1.a depicts the evolution of the reaction conversion, as defined in Equation (3.1). As can be noticed, the time required for the completion of the aging process ranged from 5 hours up to 6 days (Table 4.2.1.1), continuously increasing with the NCO:OH ratio. Moreover, it should be noted that the reaction rate (Figure 4.2.1.1.b) decreased as the curing proceeded, what it is in good agreement with previous studies (Borrero-López et al., *2017*; Raghunanan et al., *2018a*), since at the early stages of the crosslinking reaction the reagents are present in larger amounts and the system is characterized by a higher chain motion.

Table 4.2.1.1 Modification degrees and curing times of PU adhesives

Sample	NCO:OH* molar ratio	Curing time (d/(h))
PU2	2:1	0 (5 h)
PU2.5	2.5:1	3 (73 h)
PU3	3:1	5 (115 h)
PU3.5	3.5:1	6 (151 h)
PU4	4:1	6 (144 h)
PU4.53	4.53:1	6 (143 h)

**NCO:OH molar ratio in the first stage of the synthesis protocol*

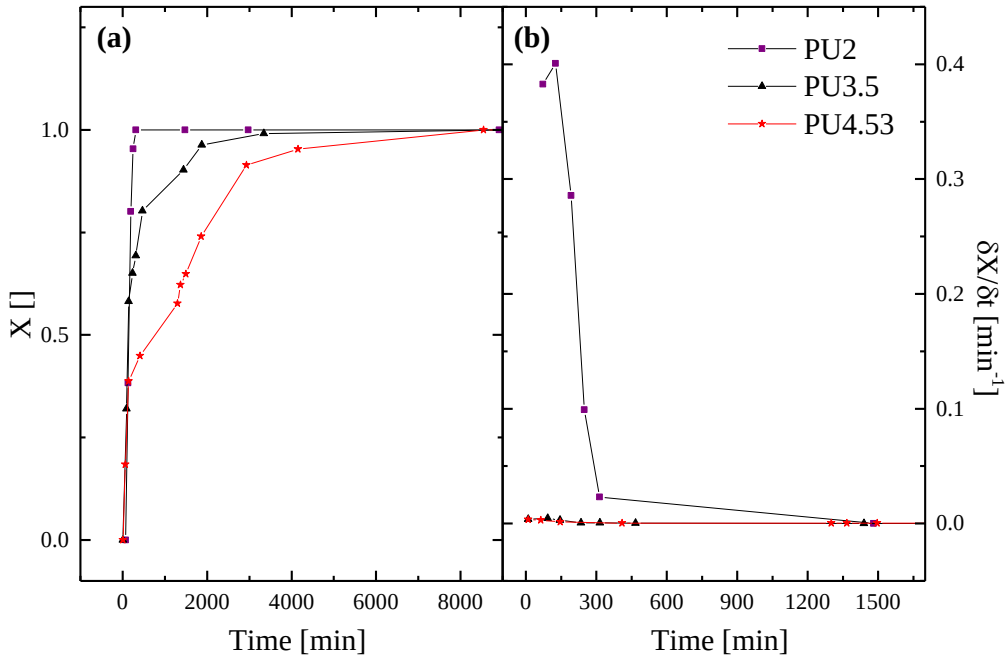

Figure 4.2.1.1 Evolution of the conversion factor (a) and reaction rate (b) of the curing process for selected formulations (PU2, PU3.5 and PU4.53)

Figure 4.2.1.2 shows a comparative of the IR spectra for fully cured polyurethanes with different NCO:OH molar ratio. In general, these spectra exhibit similar absorption bands ascribed to the cellulose acetate and castor oil backbones, i.e. -CH_2 asymmetric and symmetric stretching vibration, aromatic =C-H stretching, C=C stretching, CH_2 and CH_3 bending vibrations, out-of-plane deformation of CH_2 and -CH_2 rocking which may be correlated with the peaks centred at 2922, 2852, 3125-3193, 1647, 1411, 1377, 765 and 723 cm^{-1}, respectively (Bajsić et al., *2017*; Bistričić et al., *2010*; Otorgust et al., *2017*; Stuart, *2004*). Moreover, the peaks emerging due to the aromatic ring of the MDI are located at 3008 and 1595 cm^{-1} assigned to the stretching of =C-H and C=C, respectively. Furthermore, as a consequence of the second step of the synthesis protocol, along with the curing process at room conditions, free isocyanate groups are kept in direct contact with environmental moisture, yielding to the production of, not only urethane, but also urea (Raghunanan et al., *2018a*).

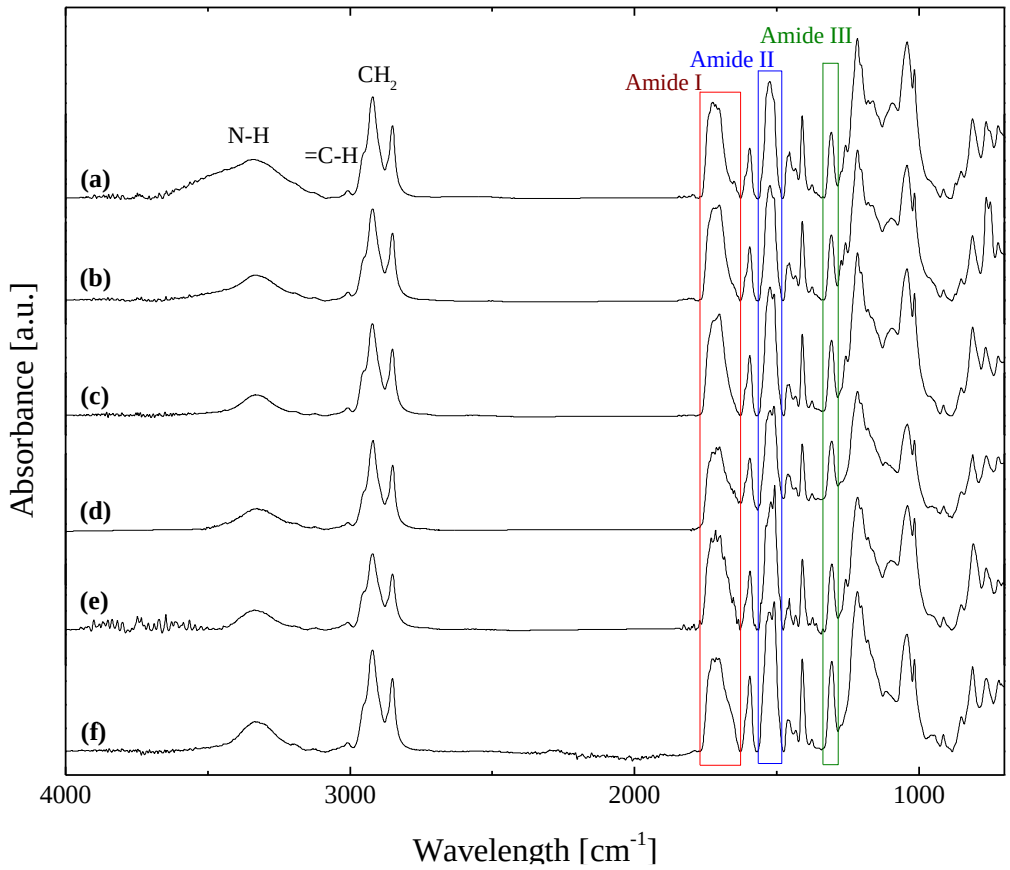

Figure 4.2.1.2 IR spectra for the MDI-based polyurethane formulations: a) PU2; b) PU2.5; c) PU3; d) PU3.5; e) PU4; f) PU4.53

On the other hand, polyurethane-urea systems are characterized by a segmented chemical structure, as denoted above, comprising soft and hard domains, capable of forming different kinds of hydrogen bonds. In this sense, hydrogen atom localized in the urethane and urea N-H may act as proton donator, while in turn the oxygen of its adjacent carbonyl group (Hard Segment, *HS*) or in the ester and ether functional groups in castor oil and cellulose acetate (Soft Segments, *SS*) as a proton acceptor. This competition in the formation of H-bonds is reflected in the appearance of shifted peaks in the N-H and C=O stretching regions to lower wavenumbers than their non-hydrogen bonded analogues.

Therefore, the distinguished peaks attributed to both urethane and urea linkages can be found in the infrared spectra, comprising stretching of N-H, C=O (Amide I band),

together with a mixed contribution of C-N stretching and N-H in-plane bending in the Amide bands II and III, assigned to the wavenumbers 3080-3500, 1637-1747, 1509-1554 and 1307 cm^{-1}, respectively. As can be inferred from Figure 4.2.1.2, the most noticeable difference when increasing the NCO:OH ratio lies in the disappearance of the shoulder overlapped with the single peak corresponding to the hydrogen bonded N-H absorption band, located at 3329 cm^{-1}. This fact can be explained by the likely fading of the overlapping with a broader O-H stretching band (3330 cm^{-1}) and/or the association of free N-H groups (3410-3450 cm^{-1}) with the aid of hydrogen bonding.

Obviously, hydrogen bonding provokes a remarkable influence over the macro and microscopic properties in these block-polymers and it can allow the estimation of the degree of phase separation (DPS). Thus, stronger hydrogen bonding between hard segments, restricting the chain motion, leads to improved separation of hard and soft segment phases, while increasing the electronic interaction between microphases causes an enhancement in the phase mixing. Hence, the determination of the DPS can be assessed by evaluating the extension of hydrogen bonding by FTIR as follows (Bistričić et al., *2010*; Zieleniewska et al., *2014*):

$$DPS = \frac{\sum A_{H-Bond}}{\sum A_{H-Bond} + \sum A_{non\ H-Bond}} \qquad (4.2.1.1)$$

where $A_{H\text{-}Bond}$ and $A_{non\ H\text{-}Bond}$ are the areas originated from the vibration of the hydrogen and non-hydrogen bonded contributions in the C=O or N-H regions.

Thus, in an effort to evaluate the relative contribution of the free and associated urethane and urea bonds, a mathematical procedure has been applied to perform the deconvolution of the carbonyl band (1600-1800 cm^{-1}) into individual Gaussian functions. The peaks overlapped in the C=O range were localized by analysing the second-derivative spectra (Queiroz et al., *2003*; Zimmer et al., *2017*). The peaks resulting from this decomposition are assigned to the ester C=O bands (1740-1747 cm^{-1}), in addition to the "*free*" (1725-1732 cm^{-1}), "*disordered H-bonded*" (1716 cm^{-1}) and "*ordered H-bonded*" (1697-1703 cm^{-1}) urethane, and also to the "*free*" (1677-1691 cm^{-1}), "*disordered H-bonded*" (1663-1670 cm^{-1}) and "*ordered H-bonded*" (1637-1653 cm^{-1}) urea (Ayres et al., *2007*; Ning et al., *1997*; Otorgust et al., *2017*; Queiroz et al., *2003*; Ruanpan and Manuspiya, *2018*;

Stuart, *2004*; Tenorio-Alfonso et al., *2017*; Yilgör et al., *2000*; Zimmer et al., *2017*). Figure 4.2.1.3 shows, as an example, the spectral components resulting from the deconvolution, reflecting the complexity of the hydrogen bonding in these polyurethane-urea systems. The appearance of different types of associated C=O arises from the possibility of forming H-bond by adjacent N-H (Huacuja-Sánchez et al., *2016*; Ruanpan and Manuspiya, *2018*). As Huacuja-Sánchez et al. (*2016*) and Zimmer et al. (*2017*) pointed out, this fact can usually be observed in semicrystalline polyurethanes, in which the amorphous and crystalline phases may be found (Huacuja-Sánchez et al., *2016*; Ning et al., *1997*; Queiroz et al., *2003*), so that strongly H-bonded (ordered) carbonyl groups may be related to the crystalline phase, while, weakly H-bonded (disordered) and free C=O groups may be associated to the amorphous phase. Thus, the ratio between them may be calculated. The relative contributions of urethane and urea linkages, together with the values obtained of DPS and amorphous/ordered phase ratio as a function of the modification degree are gathered in Table 4.2.1.2.

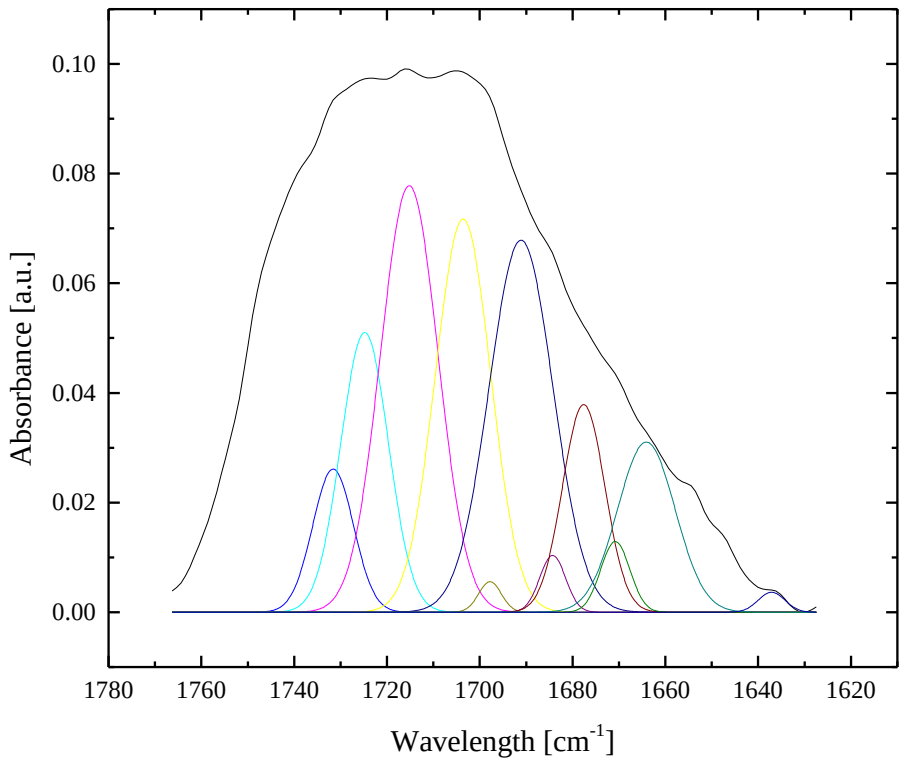

Figure 4.2.1.3 Deconvolution curves in the carbonyl region for a selected formulation (PU3.5)

Table 4.2.1.2 Deconvolution results in the Amide I region [%]

Sample	Urethane		Urea		$Urethane_{Tot}$	$Urea_{Tot}$	Urea/Urethane	DPS	Amorphous/Ordered
	free	H-bond	free	H-bond					
PU2	24.4	52.0	13.5	10.1	76.4	23.6	0.44	0.62	1.20
PU2.5	21.9	47.7	21.0	9.4	69.6	30.4	0.57	0.57	1.48
PU3	16.5	46.9	25.9	10.7	63.4	36.6	0.76	0.58	3.27
PU3.5	18.6	36.3	29.4	15.6	55.0	45.0	1.06	0.52	2.67
PU4	16.8	41.2	29.8	12.2	58.0	42.0	0.97	0.53	3.64
PU4.53	16.8	37.6	27.8	17.8	54.3	45.7	1.10	0.55	4.26

According to these results, the major contributions belonged to urethane bonds. However, the urea content rose with the NCO:OH ratio, since a greater CA modification degree involved longer curing process with atmospheric humidity. Notwithstanding the slight reduction in DPS, the relative amount of the amorphous phase in relation to the ordered domain became 3.5-fold larger when increasing the NCO:OH from 2 (PU2) up to 4.53 (PU4.53). As a result, a greater proportion of hard segment grains were better distributed in the soft domain, provoking a more extensive phase mixing, i.e. an enhancement in their thermodynamic compatibility.

1.3.2. Thermal characterization

The thermal transitions of the synthesized MDI-based polyurethanes were determined by means of DSC tests. The first thermal events perceptible in DSC thermograms (Figure 4.2.1.4) can be assigned to the glass transition of each microdomain, soft and hard segments ($T_{g,SS,}$ $T_{g,HS,1}$ and $T_{g,HS,2}$). As can be noticed, the higher the functionalization degree (i.e. higher input NCO:OH molar ratio), the greater the $T_{g,SS}$ value, ranging from -1.52 up to 25.88 ºC (see Table 4.2.1.3). The degree of phase separation of a block-copolymer is strongly related to its glass transition temperature, since an improved phase mixing may shift $T_{g,SS}$ to higher values, as a consequence of a more suitable hard segment dispersion into the soft phase (Bistričić et al., *2010*; Fernández d'Arlas et al., *2008*; Güney and Hasirci, *2014*; Ruanpan and Manuspiya, *2018*), what, in turn, provokes a hindrance to the chains mobility (Cakić et al., *2013*). This corroborates the tendency previously obtained for the DPS analysed with the aid of the ATR-FTIR results (Table 4.2.1.2). Furthermore, while $T_{g,SS}$ continuously increased with the isocyanate content, both glass transition temperatures ($T_{g,HS,1}$ and $T_{g,HS,2}$) attributed to the hard domains (viz. urethane/urea linkages and cellulose acetate backbone) first remained almost constant when increasing the functionalization degree up to around 3 (PU3), and raised, afterwards, reaching values in the range of 76-86 ºC and 158-160 ºC, respectively, which match fairly well those reported in the literature (Zhou et al., *2017*).

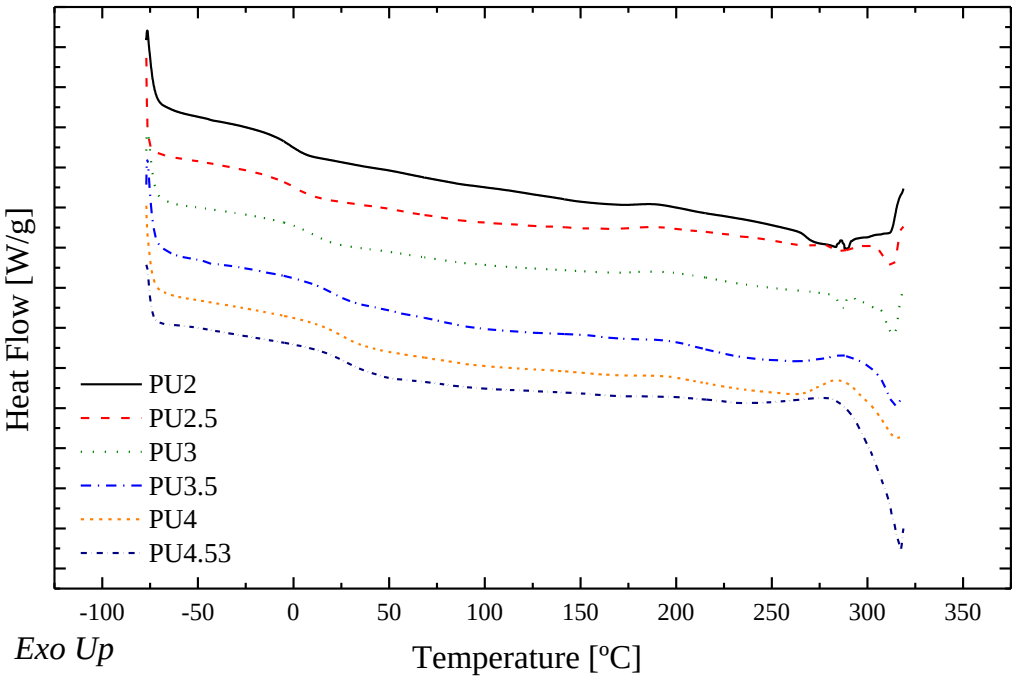

Figure 4.2.1.4 DSC thermograms for all bio-sourced polyurethane adhesives studied

On the other hand, an exothermic transition above 160 ºC (analysed in the range of 166-230 ºC) can be attributable to an annealing effect of the chains (Jung et al., *2000*). As Ning et al. (*1997*) reported, this thermal annealing may be associated to a rearrangement of hydrogen bonds, mainly arising from urea linkages, thus yielding to a higher ordered urea content and a reduction in $T_{g,SS}$ in a second heating step as a result of a higher tendency to phase segregation. Indeed, the enthalpy of the thermal annealing apparently rose up with the NCO:OH ratio (Table 4.2.1.3), but until a critical point (PU3.5) above which it lowered, likely because, regardless the increase in urea content (Table 4.2.1.2), the level of crosslinking in the polymer network might be considerably important, so that the rearrangement of the urea linkages with the subsequent formation of ordered domains resulted hampered.

Table 4.2.1.3 Transition temperatures in [ºC] and enthalpy in [J/g] of main thermal events deduced from DSC curves

Sample	$T_{g,Dyn.}$	$T_{g,SS}$	$T_{g,HS,1}$	$T_{g,HS,2}$	ΔH_{TA}	$T_{Max,TA}$
PU2	6.7	-1.52	58.96	148.10	1.773	189.87
PU2.5	15	2.71	56.62	143.46	1.784	190.84
PU3	25.1	12.40	57.55	158.86	2.356	196.72
PU3.5	34.9	18.79	76. 03	160.34	2.378	198.13
PU4	37.5	25.52	86.76	157.86	2.270	195.84
PU4.53	42.8	25.88	78.26	159.04	1.208	198.21

Finally, a multiple-peak transition at temperatures over 260 ºC (Figure 4.2.1.4) could correspond to the HS melting process (Bistričić et al., *2010*) and to the decomposition of the adhesives, as can be inferred from TGA results (Figure 4.2.1.5). The existence of several endothermic peaks has been extensively studied (Rueda-Larraz et al., *2009*) and may appear as a consequence of different types of domain and/or degrees of order, what would be supported by the identification of two glass transitions in the hard phase. In the same way, as Rueda-Larraz et al. (*2009*) concluded, when increasing the functionalization degree of the PU adhesives, the endothermic peaks underwent a displacement to higher temperatures, characteristic of better ordered hard domains. This is also indicative of a higher urea content due to its bifurcate chemical structure, corroborating the results obtained from the deconvolution of the C=O peak of the FTIR spectra (Table 4.2.1.2).

Thermal stability of the synthesized PU adhesives was evaluated by means of TGA analysis. Figure 4.2.1.5 shows the resulting weight loss vs. temperature plots, along with its derivative curve (DTGA), for selected samples. The characteristic temperature at 5% of loss weight ($T_{5\%}$), maximum (T_{max}) and onset (T_{onset}) temperatures, and loss weights (W) of each thermal event, along with the final residues (R) are gathered in Table 4.2.1.4. Thermal decomposition of polyurethane-urea systems generally exhibits a certain degree of complexity, due to their different features arising from interaction and stability differences between soft and hard segments (Cakić et al., *2013*; Ruanpan and Manuspiya,

2018). Therefore, according to the DTGA curves (Figure 4.2.1.5), fully cured PUs underwent a four-stage decomposition process, without taking into consideration the negligible initial vaporization of residual water and/or solvent retained in the polymer network (<2%, 20-110 ºC), thus remaining thermally stable till around 290 ºC. The first two steps may be attributed to rigid segments (Fuensanta and Martín-Martínez, *2018*). According to previous investigations (Cakić et al., *2013*; Zhou et al., *2017*), as a consequence of the higher resistance of the urea linkages, the contribution of these types of hard segment bonds (urethane and urea) might be distinguished in TGA results, thereby resulting in different peaks. However, when analysing the ratio of loss weights of these peaks (W_2/W_1), a clear lowering was noticed when increasing NCO:OH ratio, what, in turn, led to an increase in the urea proportion. This likely occurs owing to the reduction of ordered moiety content (Table 4.2.1.2), so ascribing the amorphous and crystalline highly ordered phases to the first and second thermal events, respectively.

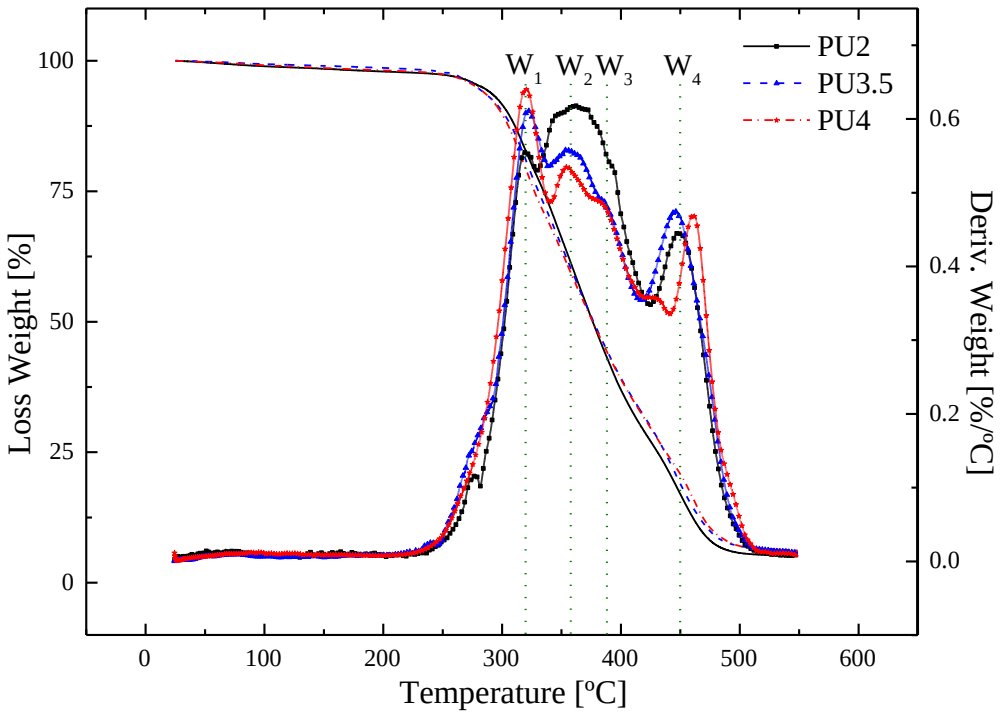

Figure 4.2.1.5 Loss weight and derivative function vs. temperature plots for selected formulations (PU2, PU3.5 and PU4)

Additionally, as can be subtracted from the evolution of $T_{5\%}$ (Table 4.2.1.4), the larger amount of more thermally instable isocyanate structure in the polymer matrix, arising from the increase in the NCO:OH ratio, yield to a slight reduction in the thermal stability of these adhesives, also noted in the shift in the T_{onset} attributable to the third decomposition step (380-390 ºC), associated to chain scission of soft segments (i.e. castor oil) (Ruanpan and Manuspiya, *2018*; Tenorio-Alfonso et al., *2017*). Finally, the last step, at around 450-480 ºC, corresponds to excessively crosslinked polymer networks and C-C bonds cleavage (Fuensanta et al., *2017*; Kong et al., *2016*; Tenorio-Alfonso et al., *2017*).

Table 4.2.1.4 Thermal degradation parameters resulted from the thermogravimetric analysis

Sample	$T_{5\%}$ [ºC]	T_{onset} [ºC]	T_{max} [ºC]	W [%]	R [%]	W_2/W_1
PU2	289	295/339/387/439	322/370/386/451	22/31/19/21	6	1.409
PU2.5	284	293/332/380/434	322/353/382/448	24/27/17/24	6	1.125
PU3	290	290/354/387/452	326/360/392/457	30/28/22/22	0	0.933
PU3.5	278	289/341/384/432	323/358/386/446	28/23/16/26	6	0.821
PU4	278	289/334/382/451	320/355/382/481	30/16/29/18	6	0.533
PU4.53	279	290/346/374/447	323/357/386/461	30/15/27/20	6	0.500

1.3.3. Rheological testing

Figure 4.2.1.6 shows the influence of temperature on the rheological response when applying a continuous temperature ramp, from -30 up to 200 ºC, at 1 Hz and heating rate of 2 ºC/min. As can be noticed, all the samples display two main regions in which the values of the storage (elastic) modulus, G', are much higher than those of the loss (viscous) modulus, G", related to the achievement of the glassy and rubbery regions of the mechanical spectrum, showing a similar dependence with temperature regardless the CA functionalization degree. However, between these two ranges, the glass transition region is apparent, in which both viscoelastic moduli presented cross over points for NCO:OH molar ratios lower than 3 (Figure 4.2.1.6.a). Nevertheless, when the CA modification degree was raised, the typical cross-over points were not attained, as a

consequence of the greater phase-compatibility, thus promoting a higher elastic response in the glass transition region (i.e. lower values of the loss tangent, Figure 4.2.1.6.b).

Moreover, from the maximum values in the loss tangent vs. temperature plots (Figure 4.2.1.6.b), the characteristic glass transition temperatures (T_g) can be obtained. Also, as previously discussed for $T_{g,SS}$ values obtained in DCS tests, T_g values deduced from temperature ramps under oscillatory torsional deformation, ranging from 6.7 up to 43 ºC (Figure 4.2.1.6 and Table 4.2.1.3), increases eventually as a consequence of a higher crosslinking density promoted by a larger CA functionalization degree (i.e. higher NCO:OH ratio), and remaining slightly higher than the calorimetric $T_{g,SS}$ counterparts. On account of the different basics of the techniques conducted to analysed the glass transition, along with the different heating rates applied, DSC and rheological analysis provide different T_g, values, under static and dynamic conditions respectively, as has been also reported in the literature (Calvo-Correas et al., *2015*; Liu et al., *2016*; Ma et al., *2017*). As it has been previously discussed, the degree of phase separation of a block-copolymer is strongly related to its glass transition temperature, so that an improved phase mixing may result in greater values of T_g, owing to a more suitable hard segments dispersion into the soft segment phase (Bistričić et al., *2010*; Fernández d'Arlas et al., *2008*; Güney and Hasirci, *2014*; Ruanpan and Manuspiya, *2018*). Therefore, an enhancement in the thermodynamic compatibility between both microdomains (SS and HS) leads to bio-polyurethanes characterized by a higher chain movement hindrance, thus broadening the peak in the loss tangent (Figure 4.2.1.6.b), as Rueda-Larraz et al. (*2009*) concluded when analysing polycaprolactone-polytetrahydrofurane-based segmented polyurethanes.

Furthermore, as can be inferred from the temperature ramps results (Figure 4.2.1.6.a), the storage and loss moduli underwent a sudden drop (α-relaxation) when temperature was raised, until a critical temperature from which both functions either remained fairly constant or slightly increased. However, this effect resulted more noticeable on the viscous moduli, which, in turn, presented a greater temperature dependence. This critical temperature was found to be around 100 ºC, or even higher when considering PUs with higher functionalization degrees. Thus, these MDI-based polyurethanes showed a good thermal stability at high temperatures, above this critical temperature, as may be also

deduced from the frequency sweep tests and the thermal analysis (DSC and TGA results).

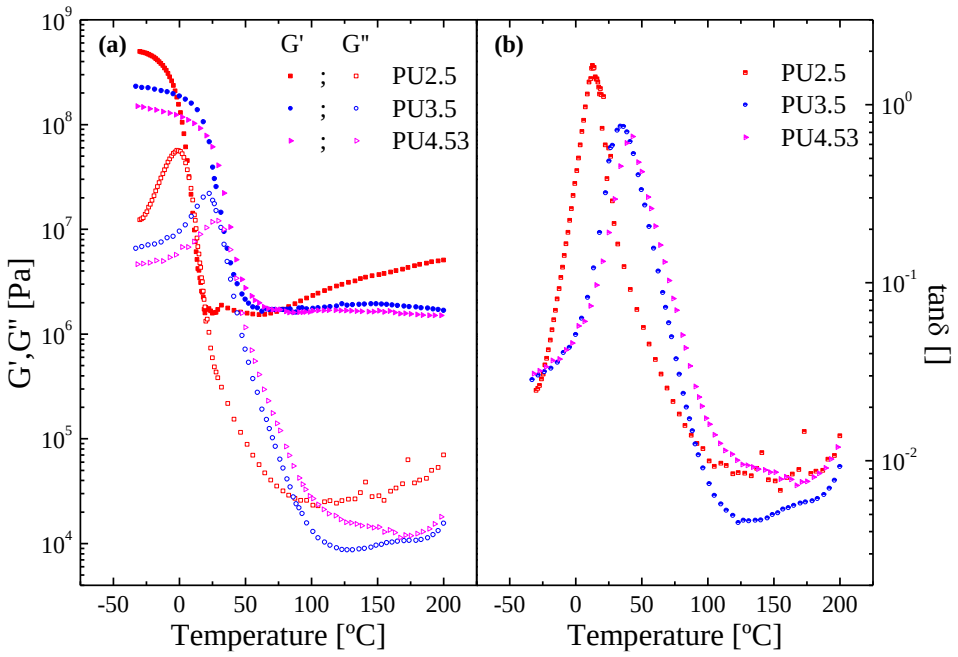

Figure 4.2.1.6 Evolution of the storage and loss moduli (a) and loss tangent (b) in temperature ramp tests for formulations PU2.5, PU3.5 and PU4.53

Figure 4.2.1.7.a,c show the evolution of the viscoelastic functions with frequency under small-amplitude oscillatory torsional deformation, at different temperatures, of two selected bio-based polyurethanes differing from each other in the input NCO:OH molar ratio applied in the CA modification, i.e., 2 and 3.5. With the aim of extending the mechanical spectrum and unifying the temperature dependence of the synthesized formulations, the time-temperature (T-t) superposition principle was applied by superimposing the viscoelastic functions obtained at the different temperatures (from -10 ºC to 200 ºC), with the aid of suitable shift factors (a_T), taking 25 ºC as the reference temperature. Generally, as can be observed, in the same way as in the temperature ramps, all systems showed two ranges in which a well-developed plateau region of the mechanical spectrum, characterized by a predominant elastic behaviour, was clearly apparent, namely the glassy and rubbery regions. However, both viscoelastic functions dramatically decrease above the glass transition temperature, until 2-3 orders of magnitude, as can be seen in the case of the PU3.5 sample (Figure 4.2.1.7.c).

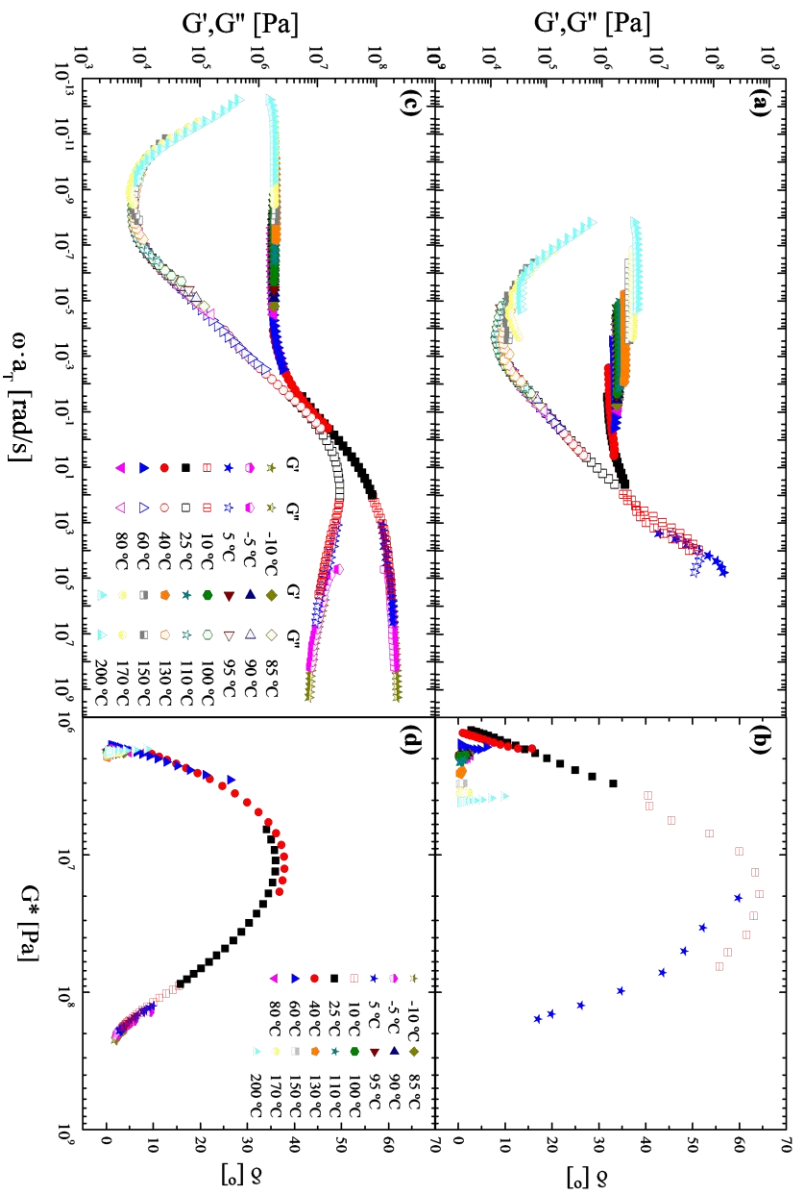

Figure 4.2.1.7 Application of the time-temperature superposition on selected formulations, PU2 (above) and PU3.5 (below): mechanical spectra (a, c) and van Gurp-Palmen plots (b, d)

On the other hand, as illustrated in Figure 4.2.1.7 for the selected samples (PU2 and PU3.5), the time-temperature superposition principle can be only satisfactorily applied over the samples prepared with NCO:OH ratios higher than 2.5. Therefore, the applicability of the T-t superposition principle is in good agreement with FTIR and DSC/TGA results, indicating an enhancement in the thermodynamic compatibility as NCO:OH ratio increases. The van Gurp–Palmen plots, which depict the phase angle (δ) versus the complex modulus (G*), were also included (Figure 4.2.1.7.b,d) in order to better verify the accuracy of the T-t superposition principle, since the effect of the shift factor is not considered in these plots (Van Gurp and Palmen, *1998*). Thus, as can be observed, PU 2 system does not hold the T-t superposition principle, due to the higher DPS which yields different relaxation patterns and temperature dependences characteristic of each domain. On the contrary, bio-based polyurethanes with higher input NCO:OH ratios clearly evinces a thermorheological simplicity in the wide range of temperatures evaluated (see Figure 4.2.1.7.c,d). In these cases, the shift factors followed the Williams-Landel-Ferry (WLF) equation (see Figure 4.2.1.8):

$$log(a_T) = \frac{-C_1 \cdot (T - T_{Ref})}{C_2 + (T - T_{Ref})} \qquad (4.2.1.2)$$

where the values of the constants, C_1 and C_2, were found to continuously increase with the NCO:OH ratio (see Table 4.2.1.5).

Table 4.2.1.5 Williams-Landel-Ferry fitting parameters for bio-sourced polyurethanes (PU3-PU4.53)

Sample	C_1	C_2 [K]
PU3	12.00	78.47
PU3.5	15.81	87.00
PU4	17.61	98.44
PU4.53	21.47	135.66

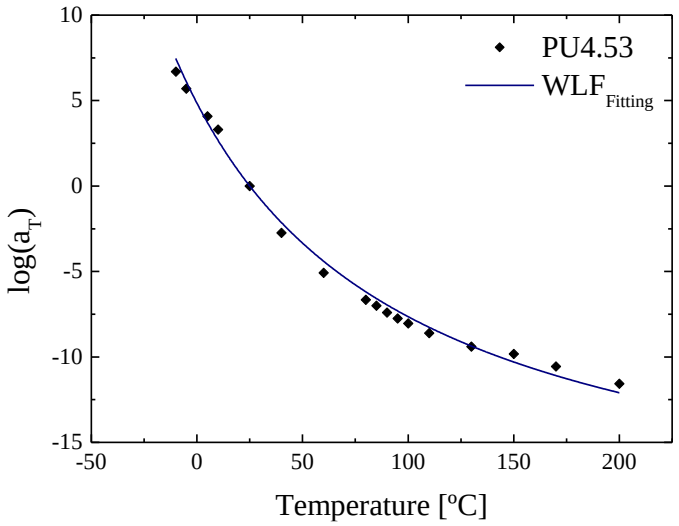

Figure 4.2.1.8 Example of fitting of the shift factor to the Williams-Landel Ferry equation for a selected formulation (PU4.53, Tref=25 ºC)

Arán-Aís et al. (*2002*) established that the molar ratio of reactive isocyanates to hydroxyl groups determines the thermal, rheological and mechanical properties of polyurethanes. So, when the NCO:OH ratio rises up from 2 to 4.53, modifies the degree of miscibility of hard and soft segments in the polyurethane chains. In this way, Sánchez-Adsuar and Martín-Martínez (*2000*) pointed out that for thermoplastic polyurethanes an increase in the hard segment content favoured the compatibility (i.e. reduced phase separation) between hard and soft segments. Thus, as a result of the higher thermodynamic compatibility between both microdomains, in the case of the synthesized polyurethane PU3-PU4.53, the T-t superposition principle was followed, at least, up to 200 ºC. Above this point, the softening associated to the thermal decomposition previously discussed of the sample hampered the measurement in torsional mode.

1.3.4. Adhesion performance on different substrates

The adhesion performance of all PU adhesives studied on different substrates has been analyzed by means of ASTM tests for determining the peeling (ASTM D903) and shear (ASTM D906 and D1002 for wood and steel, respectively) strengths. The results obtained in these mechanical tests are collected in Figure 4.2.1.9. At room temperature, an increase in the input NCO:OH molar ratio produced a rise in the hardness of the

adhesive, since a higher NCO concentration promotes a greater crosslinking degree, resulting in higher values of shear strength in both steel and wood substrates. This effect was more noticeable on wood, where there was a more than tenfold increase in shear strength when the NCO:OH ratio was doubled (i.e. PU2 vs. PU4). On the contrary, when the substrate was replaced by stainless steel, the influence of CA modification degree resulted less important, although values twice or three times higher were obtained for high NCO:OH ratios with respect to the formulation PU2. In this sense, it is well-known that the adhesion force varies considerably according to the wettability and chemical nature of the adhesive and substrate. The wettability of a given surface is a measure of its attraction towards a liquid, and is affected by the surface chemistry, energy, and texture. An ideal adhesive should spread easily and achieve good molecular contact with the surface (Davis, *1997*), which occurs more efficiently when the adhesive and substrate have similar polarities and/or chemical affinity (Rodrigues et al., *2005*; Silva et al., *2010*). In this study, wood substrate, which is composed of lignocellulosic material and therefore provides a significant amount of OH groups, contributes to an enhancement of the bonding strength between the substrate and the bioadhesives, since these groups are able to chemically interact with the free NCO groups of the uncured adhesives. In this sense, a rise in the NCO:OH molar ratio promoted a larger crosslinking density, what, in turn, led to both higher adhesive rigidity and bonding forces. With regard to stainless steel substrate, the values of the shear strength follow the same trend with the CA functionalization degree, but they are significantly lower than those obtained on wood, forasmuch as non-covalent bonds but only donor-acceptor interactions are expected.

With reference to peeling tests on wood, a gradual increment in the strength values was also observed, obtaining the highest strength value when increasing the NCO:OH ratio until 4.53 (Figure 4.2.1.9), in such a way that bio-polyurethanes PU4 and PU4.53 generated stripping strengths almost seven or eight times higher than the one developed by the formulation with the lowest input NCO:OH molar ratio (PU2). On the other hand, when considering stainless steel as substrate, a similar evolution can be noticed. However, when the functionalization degree was raised above 3.5, uniform values in the peeling strength were achieved, exceeding the results obtained on wood (Figure 4.2.1.9).

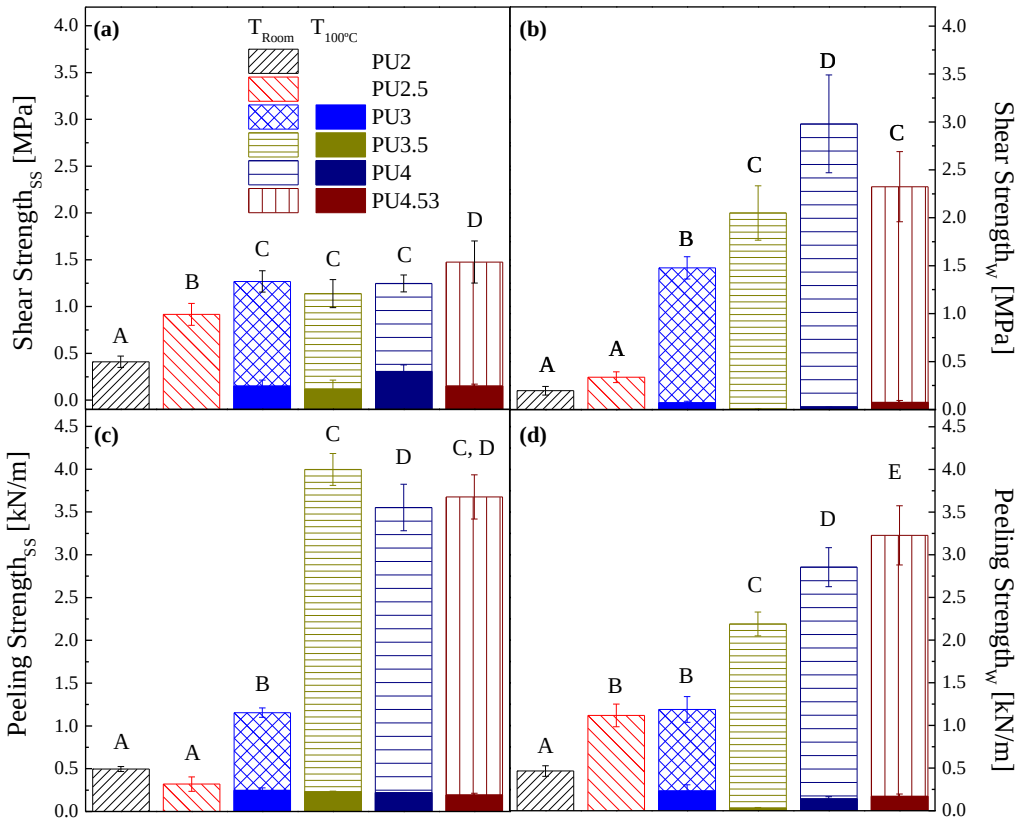

Figure 4.2.1.9 Strength values from mechanical standard tests results on stainless steel (a, c) and poplar wood (b, d), at room temperature and 100 ºC: shear (above) and peeling (below) strengths. Different letters between samples within the same test (a, b, c or d) denote mechanical results whose differences are considered statistically significant at a level of $\alpha<0.05$

When carrying out both mechanical tests at 100 ºC, i.e. well above the glass transition temperature, the adhesion performance decreased dramatically in all the cases. Bearing in mind the thermorheological behaviour previously discussed, these adhesion responses arise from the softening of the bioadhesives at those temperatures, leading also to a substantial change in the mechanical failure, principally in shear tests on stainless steel, thus obtaining the contribution, and in some cases the prevalence (PU3.5-PU4.53), of adhesion fracture instead of cohesion failure. This change in failure mechanism at 100 ºC was not however found in wood substrate, although a slight contribution of substrate fracture was obtained when NCO:OH ratio was raised up to 4.53 (PU4.53). On the contrary, the controlling sort of failure in peeling tests was cohesion, at both temperatures studied. Overall, these bio-sourced adhesives exhibit an appropriate

bonding behaviour on the substrates assessed in this research (wood and stainless steel) at temperatures lower than their critical softening point, which is enhanced by increasing the CA modification degree, obtaining shear and peeling strengths significantly higher with formulations PU4 and PU4.53, and providing in those cases, an adhesion performance fairly competitive with the benchmarks studied in previous investigations (Tenorio-Alfonso et al., *2018*).

1.4. Conclusions

In this research, bio-sourced polyurethane adhesives were successfully synthesized from cellulose acetate, castor oil and 4,4'-diphenylmethane diisocyanate by applying different input NCO:OH molar ratios (2-4.53) in the cellulose acetate modification. Afterwards, the resulting polyurethanes were left for curing. The impact of the cellulose acetate modification degree on the thermo-rheological, spectroscopic and adhesion response of these fully cured bio-adhesives were assessed. The results illustrated that these bio-sourced polyurethanes exhibited a segmented microstructure, showing a certain degree of phase separation, which decreased when the MDI modification degree was raised. Thus, a more suitable hard segment dispersion into the soft segment phase was obtained, provoking an enhancement in their thermodynamic compatibility and a rise of the static and dynamic glass transition temperatures. That improvement in the microdomain compatibility enabled the suitable application of the t-T superposition principle when the input NCO:OH ratio was raised over 2.5, where the shift factors followed the Williams-Landel-Ferry model. Moreover, the thermal analysis denoted a four-stage decomposition pattern for all polyurethane adhesives, whose thermal stability slightly decreased with the degree of cellulose acetate modification. Finally, mechanical response on the substrates studied was optimized for an input NCO:OH ratio greater than 3.5, resulting competitive shear and peeling adhesion strengths.

Block 3: Characterization of bio-inspired polyurethane adhesives through a greener synthetic route

1. Impact of the synthesis protocol on the properties of bio-sourced polyurethane adhesives for bonding wood

1.1. Abstract

During the last decades, the replacement of the traditionally petro-based raw materials by eco-friendly substances in the industrial production of polyurethanes has become a great challenge. The synthesis of polyurethanes is mainly conducted by means of a selective reaction between active isocyanate and hydroxyl groups, yielding to a characteristic segmented chemical structure. In this study, the traditional solvent-based polycondensation reaction for the synthesis of bio-based polyurethane adhesives, involving first cellulose acetate (CA) modification with 1,6-hexamethylene diisocyanate (HMDI) and subsequent crosslinking with castor oil, was evaluated and compared with a simpler solvent-free single-step processing protocol. The impact of the preparation procedure, along with the reagents proportion, on the chemical structure, thermo-mechanical behaviour and ultimate adhesion performance of the bio-based adhesives was evaluated. This research highlights the reinforcing and stabilizing effect of cellulose acetate on the bio-polyurethane performance, besides validating the feasibility of a novel and simple solvent-free synthetic route complying to a greater extent with the green chemistry standards, which also provides polyurethanes with improved rheological properties and adhesion performance.

1.2. Introduction

Wood materials have emerged as one of the main sources for the construction industry, due to their insulating and aesthetic characteristics, beside the low environmental impact they may entail. Nevertheless, in order to develop timber constructions, wooden pieces demand the application of joining mechanisms, among which polymer adhesives have proven to successfully exert such purpose (Otorgust et al., *2017*), since these binder systems allow to regularly distribute the stresses along the whole bonding line and reduce the weights and production costs of the bonding tools (Casdorff et al., *2018*; Otorgust et al., *2017*). In the last century, worldwide adhesive annual consumption amounted to 14 Mt, and it is thought to continue to grow by almost 4% per year in the next decade, according to the worldwide market study conducted by Ceresana (*2017*).

Since the advent of polymer adhesives, their production sharply hinged on conventional oil resources, leading to the production of the well-known solvent-borne adhesives, responsible for the release of volatile organic compounds (VOCs) during both, processing and application of these adhesives (Liu et al., *2016*). Therefore, the development of green adhesives for bonding wood, in pursuit of alternatives to traditional hazardous raw materials, has arisen as a prevailing environmental and economic commitment (Moghadam et al., *2016*). In particular, polyurethanes (PUs) have been generally considered as a promising choice for wood-joints, since the ultimate adhesion response relies not only on physical interactions, but also on chemical bonding between active isocyanate and pendant hydroxyl groups of the lignocellulosic substrates (Clerc et al., *2017*).

It is universally acknowledged the fact that PUs synthesis was traditionally accomplished by the so-called polyaddition reaction, in which the reaction between hydroxyl (OH) and isocyanate (NCO) groups bearing compounds (polyols and polyisocyanates) is promoted with the aid of chain extenders and catalysts (Abdolhosseini and Givi, *2016*), producing carbamate linkages, typically urethanes (NHCOO). Sensible modifications in molecular weight, branching, or chemical structure of the reagents, in general, as well as the NCO:OH ratio, may result in drastic changes in the ultimate polyurethane properties and, hence, in its application fields (Calvo-

Correas et al., *2016*). Such tunability is derived from the complex two-phase conformation, characterised by a wanting thermodynamic compatibility of both microdomains, namely soft (SS) and hard segment (HS) blocks (Norhisham et al., *2017*). Soft and hard segments, coming from the original polyols and polyisocyanates-chain extenders backbones respectively, can eventually compete for the formation of hydrogen bonds in a variety of ways (HS···HS, SS···HS, etc.), giving rise to a certain degree of microphase separation in the polymer network, what, in turn, results in an enhancement in the mechanical properties of the polyurethanes (Güney and Hasirci, *2014*; Yilgör et al., *2000*).

Furthermore, as Cui et al. (*2017*) reported, as a consequence of the apparent limitations when searching for sustainable biomaterials containing active NCO functional groups, the assessment of the likely natural alternatives to replace the former petrochemical polyols has been in the spotlight of the research in recent years. Natural sources including lignocellulosic materials (Oprea et al., *2016*), vegetable oils (Sahoo et al., *2017*), proteins (Liu et al., *2017*), agricultural wastes (Mishra and Sinha, *2010*), etc… have been lately proposed for PU synthesis, aiming to reduce the environmental impact and energy consumption.

Cellulose together with its different derivatives constitutes a natural hydroxyl-rich source. Their high availability, renewability, high reactivity with isocyanates and noticeably low environmental burden make these biomaterials especially appealing for polyurethane production (Santamaria-Echart et al., *2016*). Similarly, vegetable oils have drawn the attention for greener adhesive development, on account of their good functionality, technical versatility, large abundance and cost-effectivity (Sahoo et al., *2017*), so that at the beginning of the XXI century an extensive spectrum of vegetable oils such as palm (Norhisham et al., *2017*; Zain et al., *2016*), soybean (Liu et al., *2017*) or castor (Moghadam et al., *2016*; Sahoo et al., *2017*) oils, were used to manufacture bio-based PU adhesives.

Castor oil (CO) is a non-food grade natural feedstock obtained from *Ricinus communis* seeds (Allauddin et al., *2013*). Due to the fatty acid lengths and the particular arrangements of pendant chains in their structure (Raghunanan et al., *2018b*), hampering

the penetration of foreign substances, CO-based polyurethanes present an improved thermo-mechanical stability in combination with chemical and water resistance (Liu et al., *2016*; Valero and Gonzalez, *2012*). Moreover, its particularly high unsaturation degree, along with the fact that castor oil belongs to the limited group of hydroxylated plant oils, empowers it to suitably take part in the industrial production of polyurethanes (Moghadam et al., *2016*; Oprea et al., *2016*). Indeed, a wide variety of studies have been carried out promoting the development of castor oil-based PUs with apparent adhesion properties. More specifically, Fonseca et al. (*2016*) described the production of CO-based PU adhesives by developing chain extender via self-methatesis synthesis. Moghadam et al. (*2016*) in their research reported a simple procedure in line with the fundamentals of green chemistry to synthesize wood adhesive PUs from modified castor oil, whose lap shear strengths appeared to surpass the analogous benchmark. Patel et al. (*2009*) proposed the modification of castor oil to develop natural polyols as feedstock for polyurethane with adhesive applications on wood and metal substrates. Bio-sourced PUs obtained by Sahoo et al. (*2017*) when evaluating the influenced of the NCO:OH molar ratio, exhibited values almost fourfold greater than the commercial benchmark. Finally, in our previous investigations, adhesives from NCO-functionalized cellulose acetate and castor oil were synthesized (Tenorio-Alfonso et al., *2017*), and compared with a wide spectrum of commercialized adhesives, resulting in similar or even improved adhesion response on wood and stainless steel surfaces, in conjunction with a significantly higher elasticity (Tenorio-Alfonso et al., *2018*).

Castor oil has usually undergone different chemical modification processes to yield polyols, possessing higher hydroxyl content and ready availability (Fonseca et al., *2016*). The functionalization routes most frequently applied comprise transesterification (Moghadam et al., *2016*), along with epoxidation (Mekewi et al., *2017*). However, these additional treatments imply the utilization of supplementary solvents, catalysts or high temperatures and/or pressures which, according to the green chemistry tenets (Dubé and Salehpour, *2014*), could compromise the environmentally friendly character of the synthesis methodology inasmuch as an extra energy consumption arises from the requirement of a further removal of such substances from the adhesive system prior application (Güney and Hasirci, *2014*). Besides, aiming to attenuate the impact of PU

adhesives on the environment, it is required not only the replacement of hazardous raw materials and sources (Cornille et al., *2016*), but also some attention should be paid on the synthesis protocol (Kupka et al., *2016*; Moghadam et al., *2016*).

In order to delve further in this concern, this study analyses the feasibility of one-step solvent-free for the development of CO-based adhesives synthesis protocol, in comparison to that applied in previous investigations (Tenorio-Alfonso et al., *2018*; *2017*), aiming to simplify the PU manufacture and avoid the use of solvents, catalysts, intermediate modifications or complex reaction conditions thus, meeting to a larger extent the principles of green chemistry. Thence, bio-sourced PU wood adhesives were processed from mixtures of cellulose acetate, castor oil and 1,6-hexamethylene diisocyanate, through two different preparation methodologies, double- and single-step protocols. The influence of the synthetic routes on the adhesion performance, chemical structure and thermal and rheological properties of the resulting polyurethanes is analysed.

1.3. Results and discussion

1.3.1. Structural analysis

The influence of the synthetic route on the chemical structure of the natural polyurethane adhesives developed was approached by means of Fourier transform infrared spectroscopy in attenuated total reflection (ATR). Figure 4.3.1.1 plots the results obtained for the two-steps polyurethane adhesive (PU2) when recording the evolution of the NCO asymmetric stretching vibration (2261 cm^{-1}) (Tenorio-Alfonso et al., *2017*; Zieleniewska et al., *2014*) over time, estimating the moisture-cure conversion (X_{NCO}^{t}) as follows (Abdolhosseini and Givi, *2016*):

$$X_{NCO}^{t} = \frac{[A]_{NCO}^{t_0} - [A]_{NCO}^{t}}{[A]_{NCO}^{t_0}} \qquad (4.3.1.1)$$

where the normalized areas assigned to leftover isocyanates at time *0* and *t* refer to parameters $[A]_{NCO}^{t_0}$and $[A]_{NCO}^{t}$ respectively, taking as reference the peak associated to the carbohydrate backbone vibrational stretching (-CH_3/-CH_2, 2924 cm^{-1}).

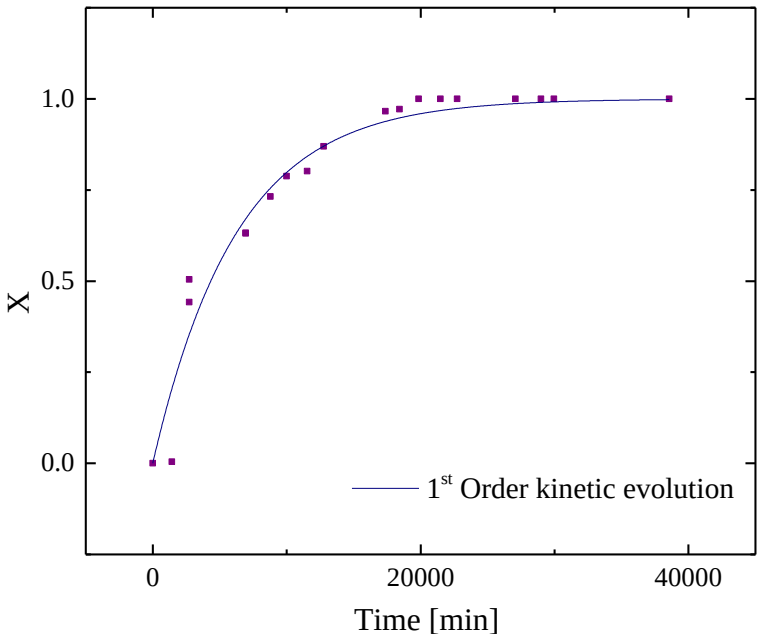

Figure 4.3.1.1 Monitoring of the humidity-driven curing process for PU2 sample

Therefore, an approximate kinetic study of the post-synthesis aging was performed, assuming that the reaction with environmental humidity was the predominant driving force for the free isocyanate consumption at stable conditions. The absence of the hydroxyl (-OH) characteristic peak centred at 3360 cm^{-1} during the first 30 minutes of curing for all bio-based polyurethanes (Figure 4.3.1.2.a), allows to bear out such assumption. Although the well-known nucleophilic addition taking place between NCO and OH active groups is typically a second order reaction (Raghunanan et al., *2018b*), as can be inferred from Figure 4.3.1.1, in this study the extent of the NCO conversion for all bio-sourced polyurethanes was well fitted to a first order equation (4.3.1.2), whose resulting constant kinetics (*k*) are gathered in Table 4.3.1.1.

$$X_{NCO}^{t} = 1 - e^{-kt} \qquad (4.3.1.2)$$

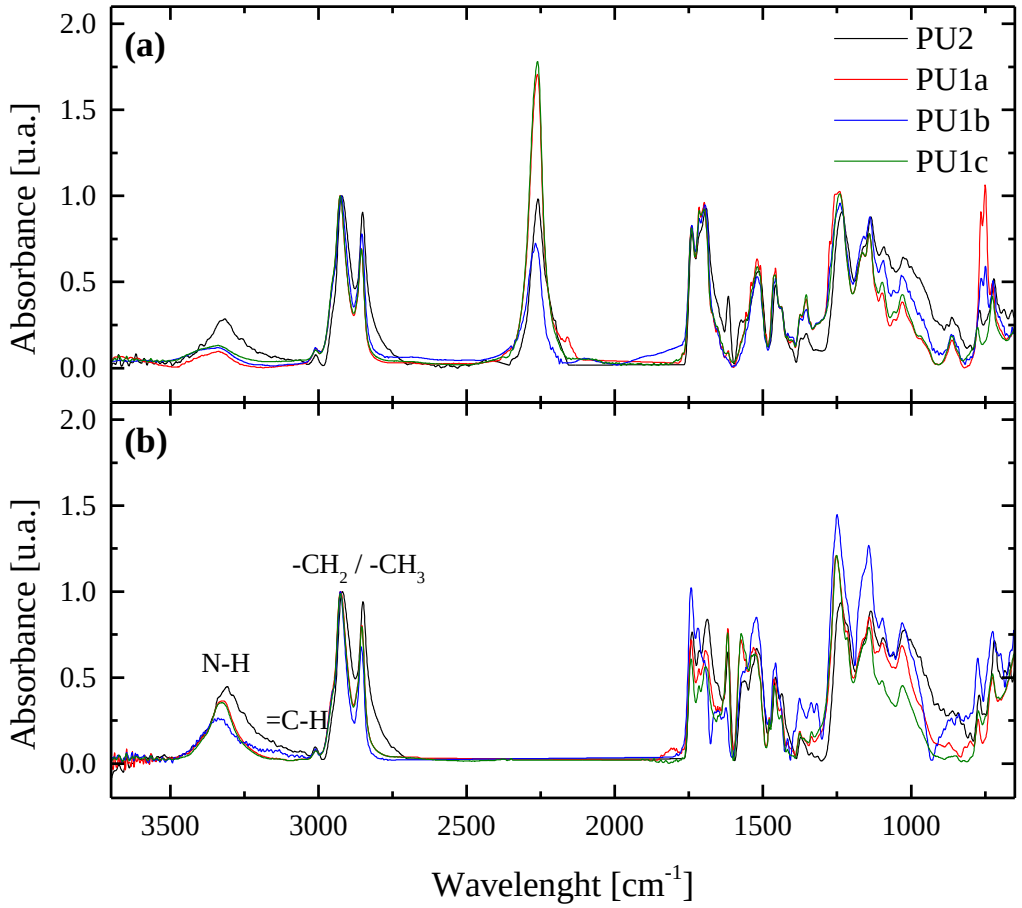

Figure 4.3.1.2 FTIR Spectra for all PU adhesives at different times: a) during the early stages of the curing process and b) fully-cured adhesives

This reaction order may have arisen from the fact that, under the same curing conditions, no any moisture dependence (i.e. [H_2O]) can be subtracted, since the limiting reagents were always the free NCO compounds. Furthermore, in terms of the reaction kinetics, the protocol optimisation (PU1a vs PU2) appears not to have brought about a significant impact on the curing rate. However, when analysing the influence of CA addition as an additional source of hydroxyl groups together with castor oil, CA-based polyurethane adhesives (PU2, PU1a), unlike the others (PU1b, PU1c), underwent a favoured curing process as can be concluded from the increase in the kinetic constants (Table 4.3.1.2), probably due to the chemical structure of the vegetable oil, which, as stated above, promotes a higher thermo-mechanical stability while hindering foreign compound

access, including moisture. Thus, a higher content in castor oil (PU1b and PU1c) may lead to lower constant kinetics, in other words, larger curing times.

Table 4.3.1.1 Kinetics constant and time needed for the completion of moisture-driven curing process

Sample	k [min^{-1}]	t_{Tot} [days]
PU2	$1.60 \cdot 10^{-4}$	13.8
PU1a	$1.39 \cdot 10^{-4}$	18.9
PU1b	$8.48 \cdot 10^{-5}$	24.0
PU1c	$9.90 \cdot 10^{-5}$	20.0

On the other hand, IR spectra for all polyurethane adhesives upon completion of the curing stage are depicted in Figure 4.3.1.2.b. Regardless of the procedure or their composition, infrared absorption bands attributed to polyols and diisocyanate backbones can be identified, including stretching of alkene =C-H (3010 cm^{-1}), in-phase and out-of-phase motions of methyl (-CH_3) and methylene (-CH_2) groups (2924 and 2853 cm^{-1}), aliphatic carbonyl (C=O) band (1742-1748 cm^{-1}), C=C absorption (1645 cm^{-1}) and ester C-O vibration (1141-1216 cm^{-1}), as well as absorption of asymmetrical (1479 cm^{-1}) and symmetrical (1375 cm^{-1}) -CH_3 bending, and -CH_2 scissoring (1463 cm^{-1}) and rocking (723 cm^{-1}) (Abdolhosseini and Givi, *2016*; Cui et al., *2017*; Stuart, *2004*; Zieleniewska et al., *2014*). Moreover, the production of secondary amides during the development of the natural adhesives was corroborated by the identification of their main absorption bands, such as N-H stretching and the Amide regions I (C=O band), II and III (mixed contribution of C-N stretching and N-H bending vibrations), and IV (N-H out-of-plane) attributable to the peaks centred at 3325, 1600-1735, 1509-1580, 1337 and 773 cm^{-1} respectively (Kantheti et al., *2013*; Stuart, *2004*).

Table 4.3.1.2 Infrared absorption band assignments in the Amide I vibrational region for bio-sourced PUs

Wavenumber [cm^{-1}]	Assignment of C=O
1722-1735	Free urethane
1717	Disordered H-bonded urethane
1698-1705	Ordered H-bonded urethane
1673-1694	Free urea
1652-1669	Disordered H-bonded urea
1635-1626	Ordered H-bonded urea

Given the strong dependence of segmented-polyurethane properties on the microdomain distribution and interaction of soft and hard segments and bearing in mind the high sensitivity of IR technique to the formation of hydrogen bonds (Mattia and Painter, *2007*; Mekewi et al., *2017*), the effect of modifying the synthesis methodology and polyols content on the degree of phase separation and the development of different urethane and urea linkages contributions was encompassed. Upon drawing a baseline in the range 1600-1770 cm^{-1} and locating the overlapped bands through the evaluation of the second-order derivative of the absorbance curves versus wavenumbers (Zimmer et al., *2017*), an Origin 9.0 Software was used to mathematically decompose the carbonyl region into Gaussian-shape functions. Owing to the variety of proton acceptor functional groups, including C-O-C_{SS}, C=O_{SS} and C=O_{HS}, competing with one another for hydrogen bridging with urea/urethane N-H proton donor (Mattia and Painter, *2007*), the resulting absorption bands, collected in Table 4.3.1.2, comprise not only free (1722-1735 cm^{-1}) and disordered (1717 cm^{-1}) and ordered (1698-1705 cm^{-1}) H-bonded urethane carbonyl groups developed during the adhesive synthesis, but also free (1673-1694 cm^{-1}), disordered (1652-1669 cm^{-1}) and ordered (1635-1626 cm^{-1}) H-bonded urea carbonyl groups appearing in the curing step (Otorgust et al., *2017*; Zimmer et al., *2017*). Consequently, as it has been previously reported (Huacuja-Sánchez et al., *2016*) ordered C=O entities are ascribed to carbonyl groups in hard domains connected to each other,

while in disordered carbonyl groups, by contrast, the adjacent N-H groups are associated to proton acceptor located in soft segments.

Moreover, an extra absorption band located at 1617 cm^{-1} arises from the Amide I range deconvolution assigned to N-H bending vibration for secondary amines (Stuart, *2004*), originated as a consequence of the moisture-cure in conjunction with the lack of the chains mobility due to the progress of the reaction. Thus, highly-diluted isocyanate groups in the polymer network may still react with environmental humidity, but their further interaction with additional NCO to produce a urea linkage could be inhibited (Zimmer et al., *2017*).

In addition, when analysing the advance of the aging till completion of curing (Figure 4.3.1.2), some differences can be perceived. A total disappearance of the NCO peak was noticed for all fully cured bioadhesives, while increasing the absorption of the N-H stretching and secondary-amine bending vibration bands (3325 and 1617 cm^{-1}). Besides that, the location of the N-H stretching peak suggests that all these functional groups are hydrogen bonded to a proton-acceptor entity. Moreover, the absence of some absorption bands, such as N-H bending at the wavelengths 1336 and 1617 cm^{-1}, at the early curing stages (Figure 4.3.1.2.a), along with the apparent intensity increase in the whole Amide I and II ranges, corroborate the assignments previously established.

Furthermore, according to previous investigations (Zieleniewska et al., *2014*), the degree of phase separation (DPS) of a block-polyurethane may be determined as the proportion of hydrogen bonded carbonyl groups resulting from a deconvolution of the carbonyl region (4.3.1.3):

$$DPS = \frac{\sum A_{H-Bond}}{\sum A_{H-Bond} + \sum A_{Free}} \qquad (4.3.1.3)$$

where $A_{H\text{-}Bond}$ and A_{Free} are the normalized areas attributable to hydrogen and non-hydrogen bonded C=O in urethane and urea linkages. Figure 4.3.1.3 shows the deconvoluted bands of the carbonyl functional groups in the amide I region and the proportions of free and hydrogen bonded urea and urethane contributions obtained from this mathematical procedure are collected in Table 4.3.1.3. As can be observed, when

applying the single-step protocol (PU1a), a higher urea/urethane ratio was achieved, owing to the fact that urea production is promoted under longer contact times with the environment. However, the simplified synthetic route allowed to reach lower values of DPS meaning a higher soft and hard domains compatibility, what unexpectedly enhanced the ultimate properties, as will be discussed below. Furthermore, when the NCO:OH molar ratio was kept constant (1.87), but castor oil was used as the only OH-source in the bio-based polyurethane production (PU1b vs PU1a), a noticeable rise in urea proportion was noticed, due to the steric hindrance of the secondary OH in the castor oil structure, thus promoting the reaction with environmental H_2O and increasing the degree of phase separation. In an effort to achieve a similar performance to the synthesized PU1a adhesive without using CA, the NCO:OH ratio was slightly rose, resulting in a bio-sourced polyurethane adhesives (PU1c) with a greater microphase separation, since hydrogen-bonded hard segments impede the segmental motion of the polymer network (Ayres et al., *2007*).

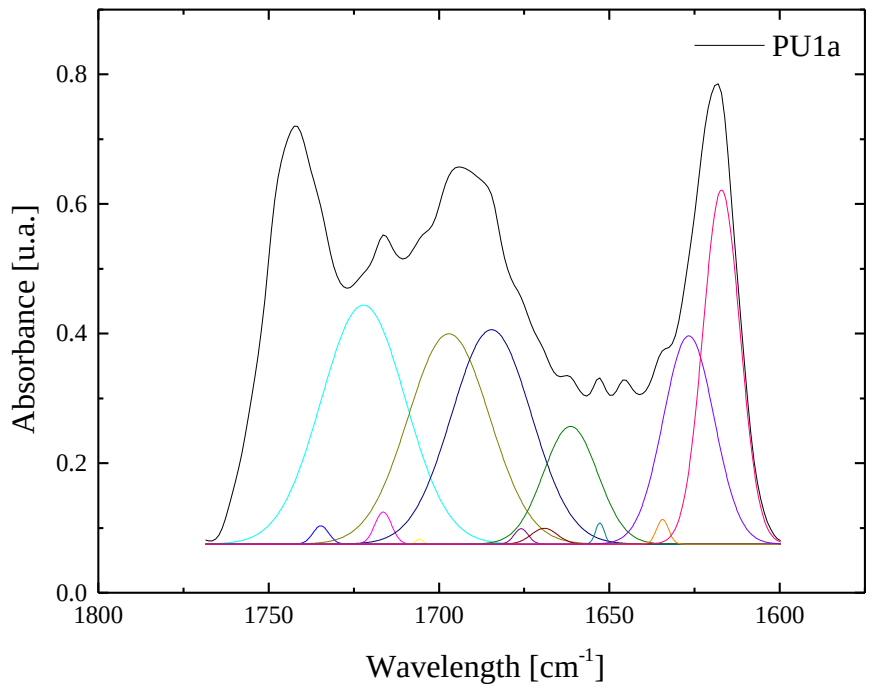

Figure 4.3.1.3 Deconvoluted FTIR absorption peaks in the Amide I region (urethane and urea) for adhesive PU1a

Table 4.3.1.3 Deconvolution results in terms of percentages of the different contributions in the C=O region

Sample		PU2	PU1a	PU1b	PU1c
Urethane	Free	13.67	27.85	18.74	9.03
	H-bond	54.20	24.16	31.76	36.79
Urea	Free	11.96	23.62	26.08	26.95
	H-bond	20.17	24.37	23.41	27.23
Urea/urethane		0.47	0.92	0.98	1.18
DPS		0.74	0.49	0.55	0.64

1.3.2. Thermal characterization

The impact of synthesis protocol and the role of CA on the thermal stability of the bio-based PU adhesives studied was explored by applying thermogravimetric analysis. The resulting thermograms and their derivative curves (DTA) are shown in Figure 4.3.1.4. Firstly, regardless of the synthetic route and CO/CA/HMDI proportions employed, a paltry weight loss (<0.6 %) centred at 100 ºC was observed, associated to water molecules retained during the curing stage (Kupka et al., *2016*).

Owing to the disparate stabilities of both microphases (SS and HS), along with the variable proportions of the reagents, it could be asserted that the synthesized bio-sourced polyurethanes are characterized by a complex thermal decomposition mechanism (Fuensanta et al., *2017*) inasmuch as DTA curves revealed several-step decomposition patterns (Figure 4.3.1.4.b). Furthermore, in previous studies (Yakushin et al., *2013*) the temperatures at which a 10 % mass is lost ($T_{10\%}$) were regarded as the beginning of the decomposition process. Therefore, the main degradation steps were evaluated and analysed in terms of the temperatures for maximum decomposition rate (T_{Max}), the onset and final temperatures (T_{Onset} and T_{Final}) of each step, together with the corresponding $T_{10\%}$ and the final char residue (R) (Table 4.3.1.4).

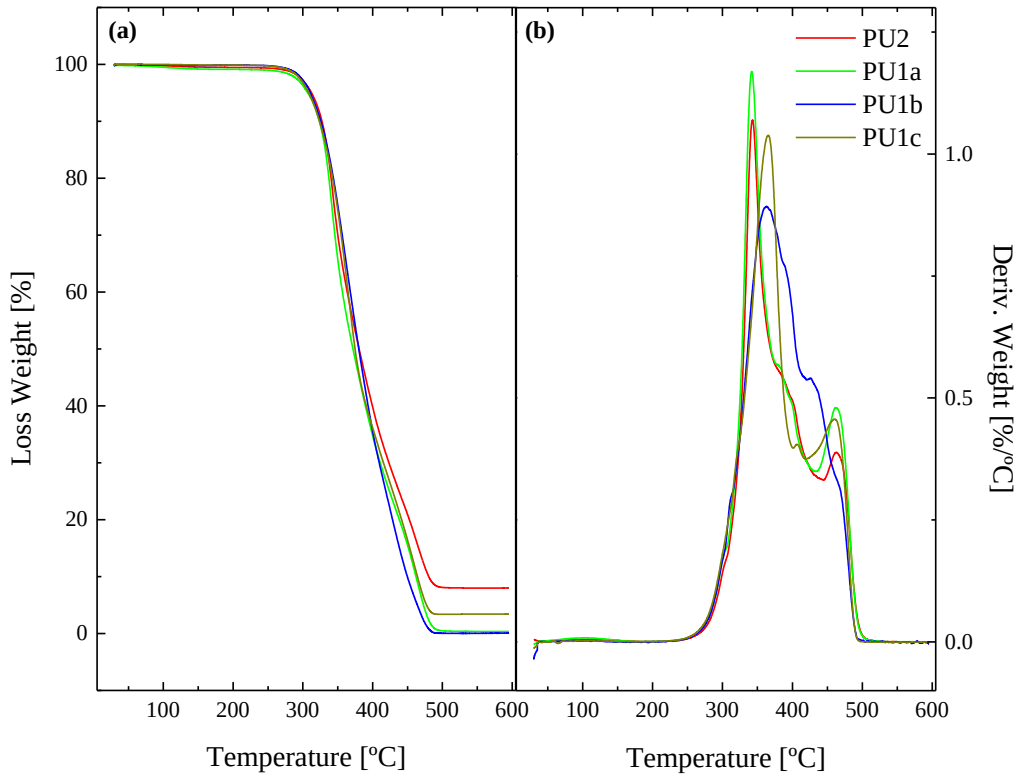

Figure 4.3.1.4 Loss weight thermograms (a) and corresponding derivative curves (b) for the different bio-based PU formulations studied

Disregarding free water removal, most of the polyurethanes, except for PU1b, decomposed in two steps, where the first thermal event (342-365 ºC) are associated to the hard segments domains, while the following peak (459-463 ºC) may be ascribed to soft segment backbones, i.e. the cleavage of the C-C bonds (Kong et al., *2016;* Puszka and Kultys, *2017*). Natural-based adhesive PU1b sample, however, presents a main peak in the range from 322 up to 479 ºC coupled with an apparent small shoulder at around 459 ºC, unambiguously attributed to the carbon-to-carbon scission.

On the other hand, some overlapping can be noticed in the temperature range of 300-450 ºC, due to the proximity of the decomposition steps of hard and soft segments domains, what impedes the identification of the loss weight for each event. Moreover, in most PU systems, two slight shoulders appeared at 380 and 394-425 ºC, likely attributed to the HS entities (Zieleniewska et al., *2014*) and the castor oil (Liu et al., *2016*; Zhou et al., *2003*) degradations, respectively. The appearance of several decomposition ranges

assigned to the hard segment phase emerges on account of the polyurethane synthesis conditions, which promotes the production of hard segment domains, comprising urethane and urea linkages, with a varying degree of organizational order (Alvarez et al., *2018*).

Table 4.3.1.4 Thermal decomposition steps' parameters obtained from thermogravimetric analysis

Sample	$T_{10\%}$ [ºC]	T_{Onset} [ºC]	T_{Max} [ºC]	T_{Final} [ºC]	R [%]
PU2	327	72/322/454	114/343/463	150/413/484	8.01
PU1a	324	55/321/449	105/342/462	143/409/482	0.38
PU1b	326	32/322	90/363	104/479	3.6
PU1c	324	30/326/443	93/365/460	128/411/479	3.4

As can be noticed from the TGA results, simplification of the synthesis protocol seemed to produce no impact on the thermal stability of the synthesized bio-based polyurethanes (PU2 vs PU1a). However, cellulose acetate removal from the adhesive formulation (PU1b and PU1c) led to a shift of 20 ºC in the second decomposition step assigned to hard domains (364 ºC), due to the fact that, according to a previous research (Tenorio-Alfonso et al., *2017*), the maximum decomposition rate of cellulose acetate (T_{Max}) is attained at 358 ºC, while suffering no detrimental effect on their thermal stability ($T_{10\%}$). Moreover, the increase of castor oil content in the natural adhesive PU1b, aimed to maintain the NCO:OH ratio at 1.87, resulted in an overlap of the degradation steps attributed to the natural oil and C-C splitting (Figure 4.3.1.4.b). When the oil content was once again reduced, thereby increasing the NCO:OH ratio (PU1c), the peak linked to C-C disruption could be differentiated, increasing the intensity of the peak associated to HS units and shifting the CO decomposition shoulder to lower temperatures.

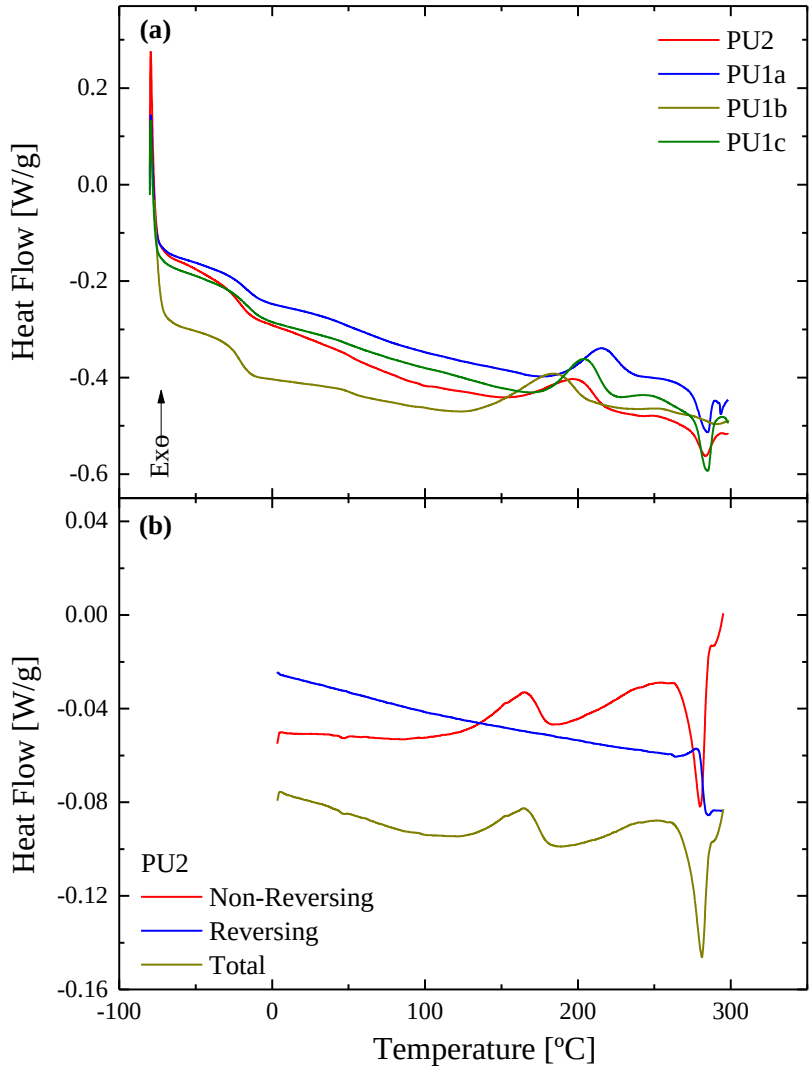

Figure 4.3.1.5 DSC curves for all bio-based PU adhesives (a) and curves from modulated temperature DSC test for a selected sample (PU2) (b)

The structure of the synthesized natural bio-adhesives was further analysed by means of DSC experiments. Figure 4.3.1.5.a illustrates the standard calorimetric results obtained in the temperature range from -80 up to 300 ºC. As can be inferred, the main thermal transitions identified for all PU adhesives comprise two glass transition temperatures (related to both soft and hard phases, T_g^{SS} and T_g^{HS}), an exothermic event followed by an endothermic peak. For comparative purposes in segmented polyurethanes, the location of the glass transition temperatures (T_gs) has been largely considered as an indicative

value to assess the degree of phase separation (Güney and Hasirci, *2014*), since T_gs are strongly influenced by the phase miscibility, so that the greater values of T_g^{SS}, the lower DPS as a consequence of tougher interaction between both microdomains. Therefore, comparing the natural polyurethanes PU2 and PU1a, regarding the synthesis protocol modification, an apparent reduction in the glass transition temperature difference of both segments was observed, indicating a reduction in the DPS, in agreement with the FTIR results. Furthermore, when replacing cellulose acetate with additional castor oil, despite the fact that the NCO:OH ratio remained unchanged, CO weight percentage increased in 10%, leading to a reduction in the T_g^{SS}, notwithstanding the DPS values (see Table 4.3.1.3). Afterwards, when raising the HMDI content (PU1c), a higher phase separation was obtained, also according to spectroscopic results, thus increasing the T_g^{SS} value, since a higher amount of aggregates of rigid units are more widely distributed in the soft phase, thus hindering the chains mobility (Fuensanta and Martín-Martínez, *2018*).

On the other hand, the exothermic peak located in the range of 130-250 ºC, in general, may be associated to different transitions implying an energy release due to curing steps, crystallization or other chain rearrangements. However, in this case, since PU adhesives were fully cured, this event may be related to either crystallization or a rearrangement process of the polymer chains, through which a more ordered polymer network may be obtained. In this sense, PU materials encompass a wide array of polymers, ranging from semicrystalline (Zieleniewska et al., *2014*) to totally amorphous structures (Puszka and Kultys, *2017*). Nevertheless, polyurethanes sometimes present a certain degree of organization, what should not be regarded as crystallites as such, but more ordered domains (Mattia and Painter, *2007*). As previously pointed out by Ning et al. (*1997*) and Van Ekeren and Carton (*2011*) at those temperatures, a typical thermal rearrangement of the disordered HS entities takes place. Regarding the energy associated to this thermal rearrangement (ΔH_{TA}), it apparently remained constant when the traditional protocol was substituted with the single-step procedure, despite showing a greater phase mixing. Nevertheless, the higher flexibility and length of the fatty acid chains in castor oil facilitated the chain annealing in bio-sourced adhesive PU1b. This effect was mitigated when increasing the NCO:OH molar ratio, so that a higher content of hard segment,

acting as crosslinking points, could hamper the molecular mobility, thus reducing the released energy during the thermal annealing (Table 4.3.1.5).

Table 4.3.1.5 Characteristic parameters associated to thermal events exhibited by bio-sourced PUs during DSC analyses

Sample	$T_{g,SS}$ [ºC]	$T_{g,HS}$ [ºC]	ΔH_{TA} [J/g]	$T_{Onset,TA}$ [ºC]	$T_{max,TA}$ [ºC]	$T_{Decomp.}$ [ºC]
PU2	-20.7	52.0	12.5	162.8	198.1	283.3
PU1a	-16.8	48.7	10.2	190.9	215.8	284.4
PU1b	-20.2	51.6	20.3	140.6	183.5	288.6
PU1c	-16.8	47.7	11.1	181.0	204.3	284.7

Finally, the last thermal transition involved an endothermic peak whose minimum temperatures were found in the range of 283-288 ºC, what may be ascribed to a melting of the likely crystalline region of the polyurethanes or polyurethane decomposition (Cakić et al., *2017*; Gurunathan and Chung, *2016*). Aiming to clarify the nature of this event, in addition to identify overlapping of different thermal events in block-polyurethanes, temperature modulated differential scanning calorimetry (MDSC) analysis was performed over all bio-sourced adhesives in the range from 0 up to 300 ºC. Figure 4.3.1.5.b shows selected MDSC results for PU2 adhesive. In all the cases, a similar behaviour was obtained, so that at around 280 ºC an endothermic peak was observed in the non-reversing heat flow curve. Subsequently, taking into consideration that most of the melting transitions appear in the reversing curve, along with the fact that, according to the TGA results (Figure 4.3.1.4), on average the 1.2 % of weight is lost at 280 ºC, this peak must be undoubtedly assigned to a thermal decomposition, instead of a melting process (Orgilés-Calpena et al., *2014*). Consequently, the previous exothermic peak is also attributed to the rearrangement of the polymer chains, instead of a crystallization, since no melting transition of those crystallites was obtained.

1.3.3. Rheology

Rheological response of the synthesized bio-inspired adhesives under torsional mode was evaluated after completion of the curing process. Thus, Figure 4.3.1.6 shows the influence of temperature on the evolution of the loss and storage moduli at 1 Hz, when a temperature ramp from 25-200 ºC is applied at a heating rate of 2 ºC/min. As in other bio-adhesives prepared from polyurethanes, the storage modulus values, G', are always higher than those of the loss moduli, G", showing once again the eminently elastic nature of these materials (Tenorio-Alfonso et al., *2018*). Generally, the temperature seems to exert a slight influence on the storage moduli, which levelled off till a critical value of around 80-120 ºC, depending on the preparation method and the inclusion of cellulose acetate in the formulation. Thus, the samples containing cellulose acetate in their composition show a good thermal stability up to temperature values around 80-100 ºC. However, when comparing samples PU1b and PU1c (without cellulose acetate), the temperature dependence of these samples is significantly different, especially when analysing the evolution of the loss modulus. Thus, the elastic component of the bio-adhesive that does not contain the biopolymer but the same NCO:OH ratio (PU1b) has a slightly lower thermal stability compared to that containing cellulose acetate, but the influence of temperature on the loss modulus is much more pronounced. The same evolution is exhibited by the sample containing a higher NCO:OH ratio (PU1c). These results support those obtained from TGA tests, which concluded that the protocol simplification seemed to produce no impact on the thermal stability of the synthesized bio-based polyurethanes (PU2 vs PU1a). However, cellulose acetate removal from the adhesive formulation (PU1b and PU1c) led a significant decrease in the SAOS functions and higher thermal dependence in the viscous component especially above 120 ºC.

Figure 4.3.1.7 shows the evolution of viscoelastic moduli (G', G" and tan δ) with frequency as a function of the preparation protocol and CA addition, at selected temperatures (25, 85 and 100 ºC). As can be noticed, G' values are much higher than those found for G", and hardly influenced by the frequency, thus showing a well-developed plateau region of the mechanical spectrum. This behaviour is independent of the temperature and again characterized by a predominant elastic behaviour throughout

the whole frequency range analysed. However, the most important effect of temperature is a clear change in G" frequency dependence at temperatures higher than 60 ºC (see Figure 4.3.1.7.a,b).

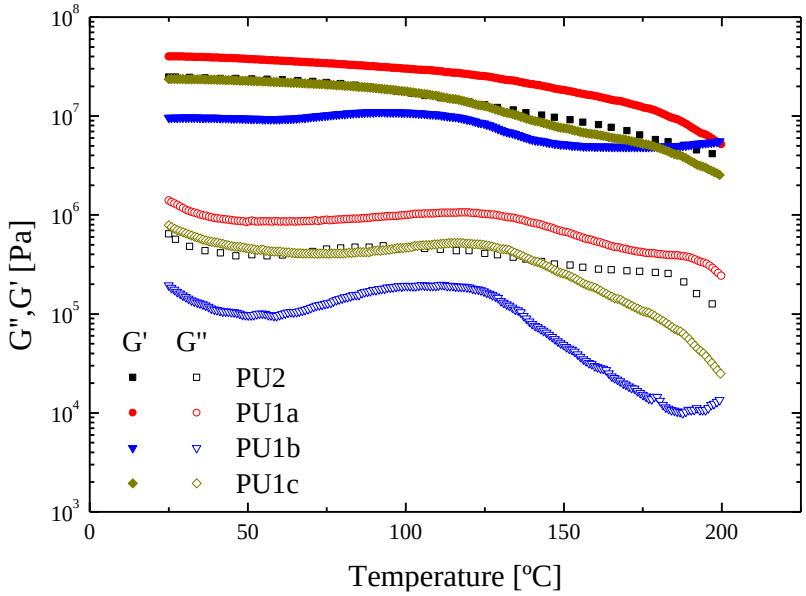

Figure 4.3.1.6 Evolution of the linear viscoelastic moduli with temperature during the application of an upward temperature ramp of 2 ºC/min

On the other hand, the lower values of the viscoelastic moduli shown by the CA-free sample (PU1b), despite the higher relative elasticity (lower values of the loss tangent) (Figure 4.3.1.7.d), reflects the reinforcing effect of cellulose acetate on the structure. Additionally, such an impact is also encouraged by the application of the single-step preparation protocol, as noticeable in the viscoelastic functions increase exhibited by sample PU1a in relation to bio-based adhesive PU2. This behaviour can be attributed to a reinforcing effect of cellulose acetate on the structure. Similar results have been previously obtained when studying the effect of cellulosic derivatives on the microstructure and thermomechanical properties of others bio-based polyurethane systems (Gallego et al., *2015b*; Głowińska and Datta, *2015*).

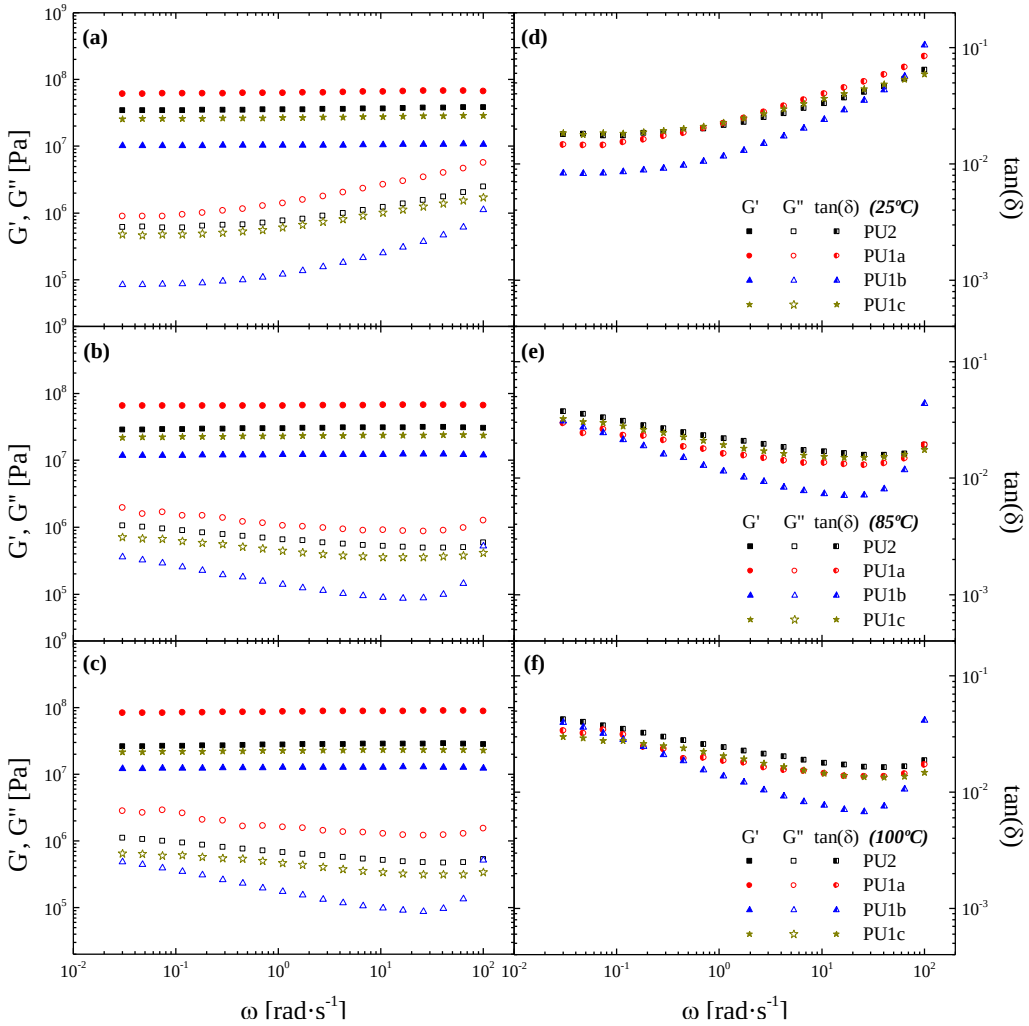

Figure 4.3.1.7 Frequency sweep dependence of G' and G'' (a–c) and tanδ (d–f) at selected temperatures (25, 85 and 100 ºC) of all PU adhesives

With the aim of unifying the temperature dependence of the synthesized formulations, the time-temperature (t-T) superposition principle was applied, from 25 to 110 ºC, by superimposing the above-mentioned viscoelastic functions with the aid of appropriate shift factors, a_T, taking 25 °C as the reference temperature. As can be inferred from Figure 4.3.1.8, the t-T superposition principle can only be successfully applied up to a temperature of around 110-130 °C, definitely failing above 150 ºC, which again suggests a temperature-induced change in structural arrangement, as previously discussed in DSC analysis (Table 4.3.1.5). Unlike previously reported results devoted to the preparation of

aromatic diisocyanate-based polyurethane adhesives (Tenorio-Alfonso et al., *2018*), the applicability of the t-T superposition principle is not restrained by the functionalization degree (NCO:OH ratio) or, in this case, by the addition of cellulose acetate and synthesis protocol, likely as a result of the improved compatibility between hard and soft segments arising from the aliphatic nature of the diisocyanate (HMDI) as well as the vegetable oil utilized in this research. The resulting shift factors for all systems have been fitted to the Williams-Landel-Ferry (WLF) model (inside Figure 4.3.1.8).

$$log(a_T) = \frac{-C_1 \cdot (T - T_{Ref})}{C_2 + (T - T_{Ref})} \qquad (4.3.1.4)$$

where C_1 and C_2, are the constant parameters of the WLF model, T is the temperature and T_{Ref} is the reference temperature (25ºC). The parameters resulting from the fitting are gathered in Table 4.3.1.6.

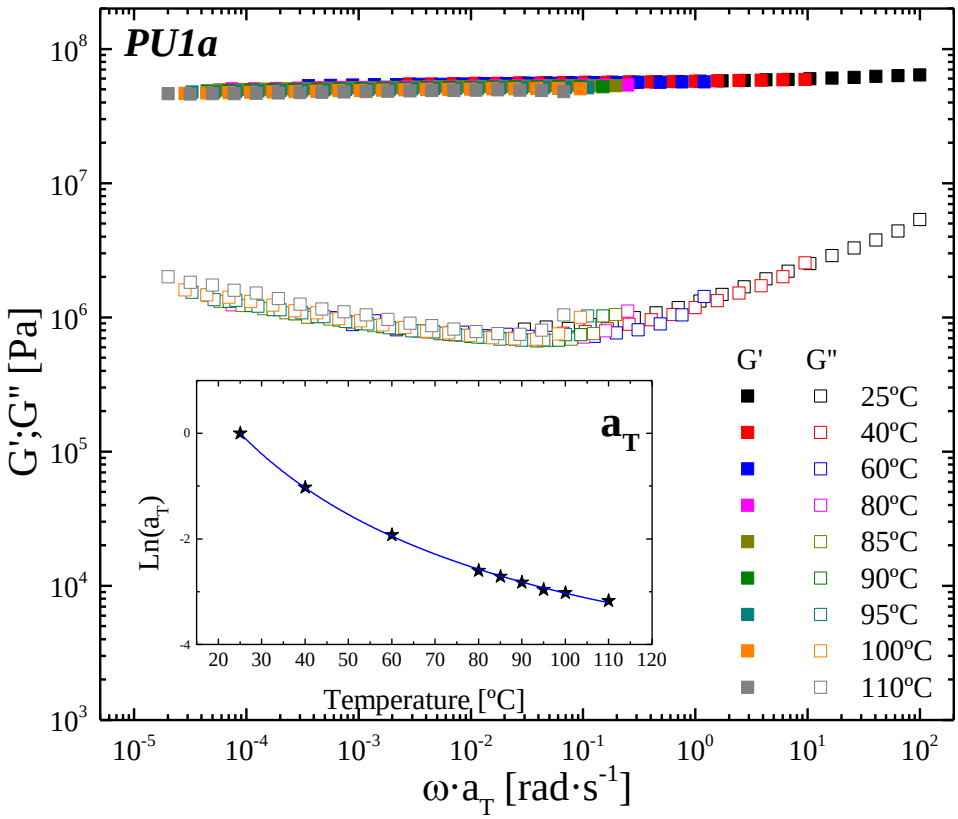

Figure 4.3.1.8 Time-temperature superposition for a selected formulation (PU1a) and fitting of the cortresponding shift factors to the William-Landel-Ferry equation (inside)

Table 4.3.1.6 Williams-Landel-Ferry fitting parameters

Sample	C_1	C_2 [K]
PU2	10.93	146.71
PU1a	5.87	70.41
PU1b	11.10	148.27
PU1c	5.85	68.09

As can be deduced from Table 4.3.1.6, these fitting parameters show the same evolution as the T_g^{SS} when analysing the effect of the synthesis protocol as well as the reagents proportions. Therefore, attending to Equation (4.3.1.4), higher values of parameters C_1 and C_2 entail, for a given temperature increment, a higher reduction in the shift factor, meaning a more pronounced thermal susceptibility. Thus, elastomers PU1a and PU1c showed a noticeably lower influence of temperature on the SAOS functions, thus diminishing the frequency range attainable with the application of the t-T superposition principle.

1.3.4. Adhesion performance

The adhesion response of an adhesive is, according to Baldan (*2012*), the resistance to the debonding process of an adhesive joint, arising from an array of adhesion phenomena, which may comprise interactions of rheological, physical, chemical and mechanical nature. However, more specifically, when considering wood as substrate, in terms of the surface nature, chemical interaction and mechanical interlocking appear to be the most likely adhesion phenomena. Therefore, the adhesion performance of the adhesives on different wooden substrates was assessed by using the applicable ASTM tests for peeling strength, conventionally expressed as the force per unit width (ASTM D903) and shear strength (ASTM D906 for wood). Table 4.3.1.7 collects the shear and peeling strength values for the different bio-adhesives on various types of wood substrates (poplar, spruce, plywood, DMF and oakwood). For comparison purposes regarding the synthetic route, the reference bio-polyurethane manufactured using the two-stage protocol was tested only on poplar wood, while when assessing the inclusion

of cellulose acetate and the HMDI:CO ratio, the adhesion analysis was extended to other wooden substrates (plywood, medium density fibreboard, spruce wood and oak wood). As a general rule, the cellulose acetate-free adhesive prepared using the simplified protocol (PU1b) is the one with the lowest shear and peeling strength in most wood substrates. Once again, the structural reinforcing action of cellulose acetate is evidenced. Moreover, regardless either the addition of cellulose derivative or the NCO:OH ratio, the simplified one-step synthesis procedure provided natural polyurethane adhesives whose shear strengths can't be significantly differentiated to each other considering the results obtained by ANOVA statistical tests with a 5% of significance level (see Table 4.3.1.8), despite the slight reduction in peeling strength. However, the adhesive manufactured with a higher NCO:OH ratio and free of cellulose acetate (PU1c), along with the formulation PU1a, had remarkable shear strength values on oak wood. In general, the higher adhesion performance found with PU1c must be attributed to the effect of the NCO:OH ratio on the mechanical properties of the adhesives, which in turn is similar to the CA reinforcing effect found with sample PU1a.

Regarding the sort of failure provided by polyurethanes adhesives synthesized through the single step protocol, except for the adhesion performance on oak wood in which a mixture of adhesive and cohesive failure was obtained, the failure is predominantly located at the substrate, which seems to be a more appropriate and desirable sort of failure. Thus, even though the adhesion strengths under shear deformation are not statistically different, when conducting the bio-sourced adhesive synthesis via the proposed single-step process, the failure becomes mainly substrate-based, so that the adhesion performance is clearly enhanced. Moreover, the values of the lap shear strength provided by the ASTM D906 test obtained with the synthesized PUs, particularly noticeable on oak wood, seem to meet the requirements for being considered as wood adhesives, since they appear to be fairly competitive with the values previously reported by Silva et al. (*2010*), Ang et al. (*2014*) and Sahoo et al. (*2017*), even exceeding those resulting from the investigations of Somani et al. (*2003*), Patel et al. (*2009*) or Wang et al. (*2018*), thus encompassing a wide range of polyurethane adhesives, most of them based on castor oil and both aromatic and aliphatic diisocyanates.

Table 4.3.1.7 Adhesion strengths developed by PU systems under shear and peeling deformation

Tests	Substrate	PU2	PU1a	PU1b	PU1c
Shear Strengths [MPa]	PW	3.321 ± 0.054[a,b,c]	4.297 ± 1.082[c]	3.773 ± 0.546[a,c]	4.422 ± 1.076[c]
	PlyW	-	1.523 ± 0.311[c]	1.706 ± 0.183[c]	1.726 ± 0.288[c]
	MDF	-	1.633 ± 0.204[c]	1.861 ± 0.474[c]	1.845 ± 0.537[c]
	SW	-	0.847 ± 0.001[c]	0.974 ± 0.215[c]	0.854 ± 0.159[c]
	OW	-	5.308 ± 0.489[a,b]	3.154 ± 0.153[a,b]	6.039 ± 0.716[a,b]
Peeling Strengths [kN/m]	PW	3.243 ± 0.194[b]	2.643 ± 0.045[b]	2.278 ± 0.303[b]	2.021 ± 0.411[b]
	PlyW	-	3.383 ± 0.190[a,b]	2.064 ± 0.411[a,b]	4.706 ± 0.368[b,c]
	MDF	-	3.435 ± 0.672[a,b]	1.952 ± 0.494[a,b]	3.241 ± 1.131[a,b,c]
	SW	-	3.070 ± 0.456[a]	2.381 ± 0.348[a,b]	3.159 ± 0.388[a]
	OW	-	3.438 ± 0.175[a,c]	1.956 ± 0.504[a,b]	2.826 ± 0.573[a,c]

Failures: [a] Cohesion; [b] Adhesion; [c] Substrate

Table 4.3.1.8 Failures' contributions in [%] and ANOVA+Scheffé significance results

Test	Surface	PU2				PU1a				PU1b				PU1c			
		Coh.	Adh.	Subst.		Coh.	Adh.	Subst.		Coh.	Adh.	Subst.		Coh.	Adh.	Subst.	
Shear	PW	21	78	1	A	0	0	100	A	20	0	80	A	0	0	100	A
	PlyW					0	0	100	A	0	0	100	A	0	0	100	A
	MDF					0	0	100	A	0	0	100	A	0	0	100	A
	SW					0	0	100	A	0	0	100	A	0	0	100	A
	OW					24	76	0	A	40	60	0	B	50	50	0	A
Peeling	PW	0	100	0	A	0	100	0	A,B	0	100	0	B,C	0	100	0	C
	PlyW					8	92	0	A	33	67	0	B	0	31	69	C
	MDF					22	78	0	A	41	59	0	A	10	7	83	A
	SW					100	0	0	A	15	85	0	B	100	0	0	A
	OW					0	75	25	A	43	57	0	B	20	0	80	A,B

Different group letters in raw denotes significantly different values with a significance level of α=0.05

In relation to the peeling tests carried out with the synthesized bio-polyurethanes, once again the adhesive prepared with the simplified one-step protocol and without cellulose acetate is the one that shows lower peeling strength values in all types of substrate; while the rest of the adhesives present values very close to those obtained with the polyurethane manufactured in two stages containing cellulose acetate. In agreement with thermal and rheological results, bio-based adhesives PU1a and PU1c showed a similar adhesive response, with peeling strengths statistically similar (see Table 4.3.1.8). Finally, regarding the type of failure, in most of the cases, the failure in peeling tests is mainly located in the interphase adhesive-substrate, with the exception of the system PU1c which, probably owing to the greater NCO:OH ratio, evidenced a significant substrate failure contribution at break (70-85 % of the failure).

1.4. Conclusions

In this study, a new synthetic solvent-free route for the production of bio-inspired polyurethane adhesives conforming the tenets of the green chemistry was properly addressed, and the resulting vegetable oil-based adhesives were compared to those obtained via a traditional solvent-borne protocol. This investigation also encompasses the impact of the reagents content, namely cellulose acetate, castor oil and 1,6-hexamethylene diisocyanate, on the ultimate adhesion properties. Thus, following the simplified one-step solvent-free processing protocol and the addition of cellulose acetate led to shorter moisture-curing steps and reinforced polymer networks with higher values of viscoelastic moduli and lower thermal dependence of the rheological functions. Furthermore, rheological results revealed a sharp elastomeric response, characterised by the rubbery region of the mechanical spectrum, within extensive temperature and frequency ranges. The application of the time-temperature superposition principle was solely limited by a critical temperature (of around 110-125 ºC), as a result of the temperature-induced structural rearrangements. Moreover, the complex nature of the bio-polyurethane chemical structure consisting of soft and hard segments and inter- and intra-domains hydrogen bonding, thus developing regions with different degrees of order, was identified from the thermal and spectroscopic results, in good agreement with the appearance of two glass transition temperatures and exothermic thermal

rearrangement. In this connection, the proposed single-step procedure fostered microphase mixing, yielding reduced DPS and increasing the T_g^{SS} accordingly. At the same time the straight through method allowed for the achievement of statistically indistinguishable shear strengths with much more appealing sort of failure located in the substrate through a cleaner and simpler approach, despite exhibiting similar thermal stability ($T_{10\%}$) and peeling resistance.

References

Abdalla, S., Al-Aama, N., Al-Ghamdi, M. A., 2016. A bio polymeric adhesive produced by photo cross-linkable technique, Polymers 8(8), 292; 10.3390/polym8080292.

Abdolhosseini, F., Givi, M. K. B., 2016. Characterization of a biodegradable polyurethane elastomer derived from castor oil, American Journal of Polymer Science 6(1), 18-27; 10.5923/j.ajps.20160601.03.

Ali, A., Yusoh, K., Hasany, S., 2014. Synthesis and physicochemical behaviour of polyurethane-multiwalled carbon nanotubes nanocomposites based on renewable castor oil polyols, Journal of Nanomaterials 2014, 1-9; 10.1155/2014/564384.

Allauddin, S., Narayan, R., Raju, K., 2013. Synthesis and properties of alkoxysilane castor oil and their polyurethane/urea–silica hybrid coating films, ACS Sustainable Chemistry & Engineering 1(8), 910-918; 10.1021/sc3001756.

Alvarez, G. A., Fuensanta, M., Orozco, V. H., Giraldo, L. F., Martín-Martínez, J. M., 2018. Hybrid waterborne polyurethane/acrylate dispersion synthesized with bisphenol A-glicidylmethacrylate (Bis-GMA) grafting agent, Progress in Organic Coatings 118, 30-39; 10.1016/j.porgcoat.2018.01.016.

Ang, K. P., Lee, C. S., Cheng, S. F., Chuah, C. H., 2014. Synthesis of palm oil-based polyester polyol for polyurethane adhesive production, Journal of Applied Polymer Science 131(6), 39967 (1)-39967 (8); 10.1002/app.39967.

Arán-Aís, F., Torró-Palau, A. M., Orgilés-Barceló, A. C., Martín-Martínez, J. M., 2002. Characterization of thermoplastic polyurethane adhesives with different hard/soft segment ratios containing rosin as an internal tackifier, Journal of Adhesion Science and Technology 16(11), 1431-1448; 10.1163/156856102320252886.

Aung, M. M., Yaakob, Z., Kamarudin, S., Abdullah, L. C., 2014. Synthesis and characterization of Jatropha (Jatropha curcas L.) oil-based polyurethane wood adhesive, Industrial Crops and Products 60, 177-185.

Awaja, F., Gilbert, M., Kelly, G., Fox, B., Pigram, P. J., 2009. Adhesion of polymers, Progress in polymer science 34(9), 948-968.

Ayres, E., Oréfice, R. L., Yoshida, M. I., 2007. Phase morphology of hydrolysable polyurethanes derived from aqueous dispersions, European Polymer Journal 43(8), 3510-3521; 10.1016/j.eurpolymj.2007.05.014.

Badri, K. H., Ujar, A. H., Othman, Z., Hani Sahaldin, F., 2006. Shear strength of wood to wood adhesive based on palm kernel oil, Journal of Applied Polymer Science 100(3), 1759-1764.

Bagdi, K., Molnár, K., Sajó, I., Pukánszky, B., 2011. Specific interactions, structure and properties in segmented polyurethane elastomers, Express Polymer Letters 5(5), 417-427; 10.3144/expresspolymlett.2011.41.

Bajsić, E. G., Filipan, V., Bulatović, V. O., Mandić, V., 2017. The influence of filler treatment on the mechanical properties and phase behavior of thermoplastic polyurethane/polypropylene blends, Polymer Bulletin 74(8), 2939-2955.

Bakhshi, H., Yeganeh, H., Yari, A., Nezhad, S. K., 2014. Castor oil-based polyurethane coatings containing benzyl triethanol ammonium chloride: Synthesis, characterization, and biological properties, Journal of Materials Science 49(15), 5365-5377; 10.1007/s10853-014-8244-x.

Baldan, A., 2012. Adhesion phenomena in bonded joints, International Journal of Adhesion and Adhesives 38, 95-116; 10.1016/j.ijadhadh.2012.04.007.

Barbosa, A., Mano, E., Andrade, C., 2000. Tannin-based resins modified to reduce wood adhesive brittleness, Forest Products Journal 50(9), 89.

Bayer, O., 1947. Das Di-Isocyanat-Polyadditionsverfahren (Polyurethane), Angewandte Chemie 59(9), 257-272; 10.1002/ange.19470590901.

Bistričić, L., Baranović, G., Leskovac, M., Bajsić, E. G., 2010. Hydrogen bonding and mechanical properties of thin films of polyether-based polyurethane–silica nanocomposites, European Polymer Journal 46(10), 1975-1987; 10.1016/j.eurpolymj.2010.08.001.

Borrero-López, A. M., Blánquez, A., Valencia, C., Hernández, M., Arias, M. E., Eugenio, M. E., Fillat, U., Franco, J. M., 2018. Valorization of Soda Lignin from Wheat Straw Solid-State Fermentation: Production of Oleogels, ACS Sustainable Chemistry & Engineering 6(4), 5198-5205; 10.1021/acssuschemeng.7b04846.

Borrero-López, A. M., Valencia, C., Franco, J., 2017. Rheology of lignin-based chemical oleogels prepared using diisocyanate crosslinkers: Effect of the diisocyanate and curing kinetics, European Polymer Journal 89, 311-323; 10.1016/j.eurpolymj.2017.02.020.

Cakić, S. M., Ristić, I. S., Cincović, M. M., Nikolić, N. Č, Nikolić, L. B., Cvetinov, M. J., 2017. Synthesis and properties biobased waterborne polyurethanes from glycolysis product of PET waste and poly (caprolactone) diol, Progress in Organic Coatings 105, 111-122; 10.1016/j.porgcoat.2016.10.038.

Cakić, S. M., Špírková, M., Ristić, I. S., B-Simendić, J. K., Milena, M., Poręba, R., 2013. The waterborne polyurethane dispersions based on polycarbonate diol: Effect of ionic content, Materials Chemistry and Physics 138(1), 277-285; 10.1016/j.matchemphys.2012.11.057.

Calvo-Correas, T., Martin, M. D., Retegi, A., Gabilondo, N., Corcuera, M. A., Eceiza, A., 2016. Synthesis and characterization of polyurethanes with high renewable carbon content and tailored properties, ACS Sustainable Chemistry & Engineering 4(10), 5684-5692; 10.1021/acssuschemeng.6b01578.

Calvo-Correas, T., Santamaria-Echart, A., Saralegi, A., Martin, L., Valea, Á, Corcuera, M. A., Eceiza, A., 2015. Thermally-responsive biopolyurethanes from a biobased diisocyanate, European Polymer Journal 70, 173-185; 10.1016/j.eurpolymj.2015.07.022.

Campanella, A., Bonnaillie, L., Wool, R., 2009. Polyurethane foams from soyoil-based polyols, Journal of Applied Polymer Science 112(4), 2567-2578; 10.1002/app.29898.

Casdorff, K., Kläusler, O., Gabriel, J., Amen, C., Lehringer, C., Burgert, I., Keplinger, T., 2018. About the influence of a water-based priming system on the interactions between wood and one-component polyurethane adhesive studied by atomic force microscopy and confocal Raman spectroscopy imaging, International Journal of Adhesion and Adhesives 80, 52-59; 10.1016/j.ijadhadh.2017.10.001.

Ceresana, 2017. Market Study: Adhesives - World 3rd Edition, 2018, (6/10); https://www.ceresana.com/en.

Chattopadhyay, D., Raju, K., 2007. Structural engineering of polyurethane coatings for high performance applications, Progress in Polymer Science 32(3), 352-418; 10.1016/j.progpolymsci.2006.05.003.

Clerc, G., Brülisauer, M., Affolter, S., Volkmer, T., Pichelin, F., Niemz, P., 2017. Characterization of the ageing process of one-component polyurethane moisture curing wood adhesive, International Journal of Adhesion and Adhesives 72, 130-138; 10.1016/j.ijadhadh.2016.09.008.

Corcuera, M., Rueda, L., d'Arlas, B. F., Arbelaiz, A., Marieta, C., Mondragon, I., Eceiza, A., 2010. Microstructure and properties of polyurethanes derived from castor oil, Polymer Degradation and Stability 95(11), 2175-2184; 10.1016/j.polymdegradstab.2010.03.001.

Cornille, A., Michaud, G., Simon, F., Fouquay, S., Auvergne, R., Boutevin, B., Caillol, S., 2016. Promising mechanical and adhesive properties of isocyanate-free poly (hydroxyurethane), European Polymer Journal 84, 404-420; 10.1016/j.eurpolymj.2016.09.048.

Cui, S., Luo, X., Li, Y., 2017. Synthesis and properties of polyurethane wood adhesives derived from crude glycerol-based polyols, International Journal of Adhesion and Adhesives 79, 67-72; 10.1016/j.ijadhadh.2017.04.008.

Daniel da Silva, A. L., Martín-Martínez, J. M., Bordado, J. C. M., 2006. Influence of the free isocyanate content in the adhesive properties of reactive trifunctional polyether urethane quasi-prepolymers, International Journal of Adhesion and Adhesives 26(5), 355-362; 10.1016/j.ijadhadh.2005.06.001.

Das, B., Konwar, U., Mandal, M., Karak, N., 2013. Sunflower oil based biodegradable hyperbranched polyurethane as a thin film material, Industrial Crops and Products 44, 396-404; 10.1016/j.indcrop.2012.11.028.

Davis, G., 1997. The performance of adhesive systems for structural timbers, International Journal of Adhesion and Adhesives 17(3), 247-255; 10.1016/S0143-7496(97)00010-9.

Deka, H., Karak, N., 2009. Vegetable oil-based hyperbranched thermosetting polyurethane/clay nanocomposites, Nanoscale research letters 4(7), 758-765; 10.1007/s11671-009-9313-y.

Desroches, M., Escouvois, M., Auvergne, R., Caillol, S., Boutevin, B., 2012. From vegetable oils to polyurethanes: Synthetic routes to polyols and main industrial products, Polymer Reviews 52(1), 38-79; 10.1080/15583724.2011.640443.

Dubé, M. A., Salehpour, S., 2014. Applying the principles of green chemistry to polymer production technology, Macromolecular Reaction Engineering 8(1), 7-28; 10.1002/mren.201300103.

Erdmann, R., Kabasci, S., Kurek, J., Zepnik, S., 2014. Study of Reactive Melt Processing Behavior of Externally Plasticized Cellulose Acetate in Presence of Isocyanate, Materials 7(12), 7752-7769.

Ferdosian, F., Pan, Z., Gao, G., Zhao, B., 2017. Bio-based adhesives and evaluation for wood composites application, Polymers 9(2), 70; 10.3390/polym9020070.

Fernández d'Arlas, B., Rueda, L., De la Caba, K., Mondragon, I., Eceiza, A., 2008. Microdomain composition and properties differences of biodegradable polyurethanes based on MDI and HDI, Polymer Engineering & Science 48(3), 519-529; 10.1002/pen.20983.

Ferrer, M. C. C., Babb, D., Ryan, A. J., 2008. Characterisation of polyurethane networks based on vegetable derived polyol, Polymer 49(15), 3279-3287; 10.1016/j.polymer.2008.05.017.

Fonseca, L. R., Bergman, J. A., Kessler, M. R., Madbouly, S. A., Lima-Neto, B. S., 2016. Self-metathesis of 10-undecen-1-ol with Ru-amine-based complex for preparing the soft segment and chain extender of novel castor oil-based polyurethanes,368(1), 30-39; 10.1002/masy.201500173.

Fourche, G., 1995. An overview of the basic aspects of polymer adhesion. Part I: Fundamentals, Polymer Engineering & Science 35(12), 957-967; 10.1002/pen.760351202.

Fuensanta, M., Jofre-Reche, J. A., Rodríguez-Llansola, F., Costa, V., Iglesias, J. I., Martín-Martínez, J. M., 2017. Structural characterization of polyurethane ureas and waterborne polyurethane urea dispersions made with mixtures of polyester polyol and polycarbonate diol, Progress in Organic Coatings 112, 141-152; 10.1016/j.porgcoat.2017.07.009.

Fuensanta, M., Martín-Martínez, J. M., 2018. Thermoplastic polyurethane coatings made with mixtures of polyethers of different molecular weights with pressure sensitive adhesion property, Progress in Organic Coatings 118, 148-156; 10.1016/j.porgcoat.2017.11.021.

Gallego, R., Arteaga, J., Valencia, C., Franco, J., 2013a. Chemical modification of methyl cellulose with HMDI to modulate the thickening properties in castor oil, Cellulose 20(1), 495-507; 10.1007/s10570-012-9803-4.

Gallego, R., Arteaga, J., Valencia, C., Franco, J., 2013b. Rheology and thermal degradation of isocyanate-functionalized methyl cellulose-based oleogels, Carbohydrate Polymers 98(1), 152-160; 10.1016/j.carbpol.2013.04.104.

Gallego, R., Arteaga, J. F., Valencia, C., Díaz, M. J., Franco, J. M., 2015a. Gel-like dispersions of HMDI-cross-linked lignocellulosic materials in castor oil: Toward completely renewable lubricating grease formulations, ACS Sustainable Chemistry & Engineering 3(9), 2130-2141; 10.1021/acssuschemeng.5b00389.

Gallego, R., Arteaga, J. F., Valencia, C., Franco, J. M., 2015b. Thickening properties of several NCO-functionalized cellulose derivatives in castor oil, Chemical Engineering Science 134, 260-268; 10.1016/j.ces.2015.05.007.

Gallego, R., González, M., Arteaga, J. F., Valencia, C., Franco, J. M., 2014. Influence of functionalization degree on the rheological properties of isocyanate-functionalized chitin-and chitosan-based chemical oleogels for lubricant applications, Polymers 6(7), 1929-1947; 10.3390/polym6071929.

Geng, X., Li, K., 2006. Investigation of wood adhesives from kraft lignin and polyethylenimine, Journal of Adhesion Science and Technology 20(8), 847-858; 10.1163/156856106777638699.

Ghahri, S., Mohebby, B., Pizzi, A., Mirshokraie, A., Mansouri, H. R., 2017. Improving water resistance of soy-based adhesive by vegetable tannin, Journal of Polymers and the Environment , 1-10.

Głowińska, E., Datta, J., 2016. Bio polyetherurethane composites with high content of natural ingredients: Hydroxylated soybean oil based polyol, bio glycol and microcrystalline cellulose, Cellulose 23(1), 581-592; 10.1007/s10570-015-0825-6.

Głowińska, E., Datta, J., 2015. Structure, morphology and mechanical behaviour of novel bio-based polyurethane composites with microcrystalline cellulose, Cellulose 22(4), 2471-2481; 10.1007/s10570-015-0685-0.

Gogoi, S., Karak, N., 2014. Biobased biodegradable waterborne hyperbranched polyurethane as an ecofriendly sustainable material, ACS Sustainable Chemistry & Engineering 2(12), 2730-2738; 10.1021/sc5006022.

Gryglewicz, S., Piechocki, W., Gryglewicz, G., 2003. Preparation of polyol esters based on vegetable and animal fats, Bioresource technology 87(1), 35-39; 10.1016/S0960-8524(02)00203-1.

Güney, A., Hasirci, N., 2014. Properties and phase segregation of crosslinked PCL-based polyurethanes, Journal of Applied Polymer Science 131(1), 1-13; 10.1002/APP.39758.

Gurunathan, T., Chung, J. S., 2016. Physicochemical oroperties of amino–silane-terminated vegetable oil-based waterborne polyurethane nanocomposites, ACS Sustainable Chemistry & Engineering 4(9), 4645-4653; 10.1021/acssuschemeng.6b00768.

Gurunathan, T., Mohanty, S., Nayak, S. K., 2015. Isocyanate terminated castor oil-based polyurethane prepolymer: Synthesis and characterization, Progress in Organic Coatings 80, 39-48; 10.1016/j.porgcoat.2014.11.017.

Ho, C., Xiao, H., Frisch, C., 1995. Zwitterionic urethane adhesives, Advances in Urethane Ionomers, 111.

Huacuja-Sánchez, J., Müller, K., Possart, W., 2016. Water diffusion in a crosslinked polyether-based polyurethane adhesive, International Journal of Adhesion and Adhesives 66, 167-175; 10.1016/j.ijadhadh.2016.01.005.

Javni, I., Zhang, W., Petrović, Z. S., 2003. Effect of different isocyanates on the properties of soy-based polyurethanes, Journal of Applied Polymer Science 88(13), 2912-2916; 10.1002/app.11966.

Ji, D., Fang, Z., He, W., Zhang, K., Luo, Z., Wang, T., Guo, K., 2015. Synthesis of soy-polyols using a continuous microflow system and preparation of soy-based polyurethane rigid foams, ACS Sustainable Chemistry & Engineering 3(6), 1197-1204.

Jung, H., Kang, S., Kim, W., Lee, Y., Choe, K., Hong, S., Kim, S., 2000. Properties of crosslinked polyurethanes synthesized from 4, 4′-diphenylmethane diisocyanate and polyester polyol, Journal of Applied Polymer Science 78(3), 624-630; 10.1002/1097-4628(20001017)78:33.0.CO;2-O.

Kantheti, S., Narayan, R., Raju, K., 2013. Development of moisture cure polyurethane–urea coatings using 1, 2, 3-triazole core hyperbranched polyesters, Journal of Coatings Technology and Research 10(5), 609-619; 10.1007/s11998-013-9494-2.

Khan, M., Ashraf, S., 2005. Development and characterization of a lignin-phenol-formaldehyde wood adhesive using coffee bean shell, Journal of Adhesion Science and Technology 19(6), 493-509; 10.1163/1568561054352577.

Kim, D., Lee, D. G., Kim, J. C., Lim, C. S., Kong, N. S., Kim, J. H., Jung, H. W., Noh, S. M., Park, Y. I., 2017. Effect of molecular weight of polyurethane toughening agent on adhesive strength and rheological characteristics of automotive structural adhesives, International Journal of Adhesion and Adhesives 74, 21-27.

Kong, X., Liu, G., Curtis, J. M., 2012. Novel polyurethane produced from canola oil based poly (ether ester) polyols: Synthesis, characterization and properties, European Polymer Journal 48(12), 2097-2106; 10.1016/j.eurpolymj.2012.08.012.

Kong, X., Liu, G., Curtis, J. M., 2011. Characterization of canola oil based polyurethane wood adhesives, International Journal of Adhesion and Adhesives 31(6), 559-564; 10.1016/j.ijadhadh.2011.05.004.

Kong, X., Yue, J., Narine, S. S., 2007. Physical properties of canola oil based polyurethane networks, Biomacromolecules 8(11), 3584-3589; 10.1021/bm0704018.

Kong, X., Zhao, L., Curtis, J. M., 2016. Polyurethane nanocomposites incorporating biobased polyols and reinforced with a low fraction of cellulose nanocrystals, Carbohydrate Polymers 152, 487-495; 10.1016/j.carbpol.2016.07.032.

Kupka, V., Vojtova, L., Fohlerova, Z., Jancar, J., 2016. Solvent free synthesis and structural evaluation of polyurethane films based on poly (ethylene glycol) and poly (caprolactone). Express Polymer Letters 10(6), 479-492; 10.3144/expresspolymlett.2016.46.

Leitsch, E. K., Heath, W. H., Torkelson, J. M., 2016. Polyurethane/polyhydroxyurethane hybrid polymers and their applications as adhesive bonding agents, International Journal of Adhesion and Adhesives 64, 1-8.

Li, R., Jiang, Q., Ren, X., Xie, Z., Huang, T., 2015. Electrospun non-leaching biocombatible antimicrobial cellulose acetate nanofibrous mats, Journal of Industrial and Engineering Chemistry 27, 315-321.

Liang, L., Mao, Z., Li, Y., Wan, C., Wang, T., Zhang, L., Zhang, L., 2007. Liquefaction of crop residues for polyol production, BioResources 1(2), 248-256.

Liu, H., Li, C., Sun, X. S., 2017. Soy-oil-based waterborne polyurethane improved wet strength of soy protein adhesives on wood, International Journal of Adhesion and Adhesives 73, 66-74; 10.1016/j.ijadhadh.2016.09.006.

Liu, K., Miao, S., Su, Z., Sun, L., Ma, G., Zhang, S., 2016. Castor oil-based waterborne polyurethanes with tunable properties and excellent biocompatibility, European Journal of Lipid Science and Technology 118, 0000-0000; 10.1002/ejlt.201500595.

Liu, Y., Li, K., 2007. Development and characterization of adhesives from soy protein for bonding wood, International Journal of Adhesion and Adhesives 27(1), 59-67; 10.1016/j.ijadhadh.2005.12.004.

Liu, Y., Li, K., 2002. Chemical modification of soy protein for wood adhesives, Macromolecular Rapid Communications 23(13), 739-742; 10.1002/1521-3927(20020901)23:133.0.CO;2-0.

Lligadas, G., Ronda, J. C., Galià, M., Cádiz, V., 2007. Poly (ether urethane) networks from renewable resources as candidate biomaterials: synthesis and characterization, Biomacromolecules 8(2), 686-692; 10.1021/bm060977h.

Ma, G., Shen, Y., Gao, R., Wang, X., 2017. Micromorphology and adhesive properties of sulfonated polyurethane/polyacrylate emulsions prepared by surfactant-free polymerization, Journal of Polymer Research 24(3), 36-47; 10.1007/s10965-017-1200-0.

Manjula, K., Kumar, S., Soare, B. G., Picciani, P., 2010. Biobased chain extended polyurethane and its composites with silk fiber, Polymer Engineering & Science 50(4), 851-856; 10.1002/pen.21604.

Mattia, J., Painter, P., 2007. A comparison of hydrogen bonding and order in a polyurethane and poly (urethane− urea) and their blends with poly (ethylene glycol), Macromolecules 40(5), 1546-1554; 10.1021/ma0626362.

Mekewi, M. A., Ramadan, A. M., ElDarse, F. M., Rehim, M. H. A., Mosa, N. A., Ibrahim, M. A., 2017. Preparation and characterization of polyurethane plasticizer for flexible packaging applications: Natural oils affirmed access, Egyptian Journal of Petroleum 26(1), 9-15; 10.1016/j.ejpe.2016.02.002.

Mishra, D., Sinha, V. K., 2010. Eco-economical polyurethane wood adhesives from cellulosic waste: Synthesis, characterization and adhesion study, International Journal of Adhesion and Adhesives 30(1), 47-54; 10.1016/j.ijadhadh.2009.08.003.

Moghadam, P. N., Yarmohamadi, M., Hasanzadeh, R., Nuri, S., 2016. Preparation of polyurethane wood adhesives by polyols formulated with polyester polyols based on castor oil, International Journal of Adhesion and Adhesives 68, 273-282; 10.1016/j.ijadhadh.2016.04.004.

Moubarik, A., Allal, A., Pizzi, A., Charrier, F., Charrier, B., 2010. Characterization of a formaldehyde-free cornstarch-tannin wood adhesive for interior plywood, European Journal of Wood and Wood Products 68(4), 427-433; 10.1007/s00107-009-0379-0.

Muttil, N., Ravichandra, G., Bigger, S. W., Thorpe, G. R., Shailaja, D., Singh, S. K., 2014. Comparative study of bond strength of formaldehyde and soya based adhesive in wood fibre plywood, Procedia Materials Science 6, 2-9; 10.1016/j.mspro.2014.07.002.

Ning, L., De-Ning, W., Sheng-Kang, Y., 1997. Hydrogen-bonding properties of segmented polyether poly (urethane urea) copolymer, Macromolecules 30(15), 4405-4409; 10.1021/ma951386e.

Norhisham, S. M., Maznee, T. T. N., Ain, H. N., Devi, P. K., Srihanum, A., Norhayati, M., Yeong, S., Hazimah, A., Schiffman, C. M., Sendijarevic, A., 2017. Soft polyurethane elastomers with adhesion properties based on palm olein and palm oil fatty acid methyl ester polyols, International Journal of Adhesion and Adhesives 73, 38-44; 10.1016/j.ijadhadh.2016.10.012.

Ogunniyi, D., 2006. Castor oil: A vital industrial raw material, Bioresource technology 97(9), 1086-1091; 10.1016/j.biortech.2005.03.028.

Oprea, S., Potolinca, V. O., Gradinariu, P., Joga, A., Oprea, V., 2016. Synthesis, properties, and fungal degradation of castor-oil-based polyurethane composites with different cellulose contents, Cellulose 23, 2515-2526; 10.1007/s10570-016-0972-4.

Orgilés-Calpena, E., Arán-Aís, F., Torró-Palau, A., Orgilés-Barceló, C., 2014. Biodegradable polyurethane adhesives based on polyols derived from renewable resources, Proceedings of the Institution of Mechanical Engineers, Part L: Journal of Materials: Design and Applications 228(2), 125-136; 10.1177/1464420713517674.

Otorgust, G., Dodiuk, H., Kenig, S., Tenne, R., 2017. Important insights into polyurethane nanocomposite-adhesives; a comparative study between INT-WS 2 and CNT, European Polymer Journal 89, 281-300; 10.1016/j.eurpolymj.2017.02.027.

Packham, D., 2009. Adhesive technology and sustainability, International Journal of Adhesion and Adhesives 29(3), 248-252.

Pan, Y., Zhan, J., Pan, H., Wang, W., Tang, G., Song, L., Hu, Y., 2016. Effect of fully biobased coatings constructed via layer-by-layer assembly of chitosan and lignosulfonate on the thermal, flame retardant, and mechanical properties of flexible polyurethane foam, ACS Sustainable Chemistry & Engineering 4(3), 1431-1438; 10.1021/acssuschemeng.5b01423.

Patel, M. R., Shukla, J. M., Patel, N. K., Patel, K. H., 2009. Biomaterial based novel polyurethane adhesives for wood to wood and metal to metal bonding, Materials Research 12(4), 385-393; 10.1590/S1516-14392009000400003.

Penn, B., Stannett, V., Gilbert, R., 1981. Biodegradable cellulose graft copolymers. I. Condensation-type graft reactions, Journal of Macromolecular Science-Chemistry 16(2), 473-479.

Pickering, J., Van Der Meer, D., Vancso, G. J., 2001. Effects of contact time, humidity, and surface roughness on the adhesion hysteresis of polydimethylsiloxane, Journal of Adhesion Science and Technology 15(12), 1429-1441; 10.1163/156856101753213286.

Pizzi, A., 2006. Recent developments in eco-efficient bio-based adhesives for wood bonding: Opportunities and issues, Journal of Adhesion Science and Technology 20(8), 829-846; 10.1163/156856106777638635.

Pizzi, A., 1994. Advanced Wood Adhesives Technology. New York, U.S.A.: CRC Press.

Puszka, A., Kultys, A., 2017. The influence of soft segments on some properties of new transparent segmented polyurethanes, Polymers for Advanced Technologies 28(12), 1937-1944; 10.1002/pat.4083.

Queiroz, D. P., de Pinho, M. N., Dias, C., 2003. ATR− FTIR studies of poly (propylene oxide)/polybutadiene bi-soft segment urethane/urea membranes, Macromolecules 36(11), 4195-4200; 10.1021/ma034032t.

Quinchia, L. A., Delgado, M. A., Valencia, C., Franco, J. M., Gallegos, C., 2010. Viscosity modification of different vegetable oils with EVA copolymer for lubricant applications, Industrial Crops and Products 32(3), 607-612; 10.1016/j.indcrop.2010.07.011.

Raghunanan, L. C., Fernandez-Prieto, S., Martínez, I., Valencia, C., Sánchez, M. C., Franco, J. M., 2018a. Molecular insights into the mechanisms of humidity-induced changes on the bulk performance of model castor oil derived polyurethane adhesives, European Polymer Journal 101, 291-303; 10.1016/j.eurpolymj.2018.02.041.

Raghunanan, L. C., Martínez, I., Valencia, C., Sánchez, M. C., Franco, J. M., 2018b. Unexpected selectivity in the functionalization of neat castor oil under benign catalyst-free conditions, ACS Sustainable Chemistry & Engineering 6(6), 7212-7215; 10.1021/acssuschemeng.8b00979.

Rodrigues, J., Pereira, M., De Souza, A., Carvalho, M., Neto, A. D., Dantas, T., Fonseca, J., 2005. DSC monitoring of the cure kinetics of a castor oil-based polyurethane, Thermochimica Acta 427(1), 31-36; 10.1016/j.tca.2004.08.010.

Rojek, P., Prociak, A., 2012. Effect of different rapeseed-oil-based polyols on mechanical properties of flexible polyurethane foams, Journal of Applied Polymer Science 125(4), 2936-2945; 10.1002/app.36500.

Ronda, J. C., Lligadas, G., Galià, M., Cádiz, V., 2011. Vegetable oils as platform chemicals for polymer synthesis, European journal of lipid science and technology 113(1), 46-58; 10.1002/ejlt.201000103.

Ruanpan, S., Manuspiya, H., 2018. Synthesized amino-functionalized porous clay heterostructure as an effective thickener in waterborne polyurethane hybrid adhesives for lamination processes, International Journal of Adhesion and Adhesives 80, 66-75; 10.1016/j.ijadhadh.2017.10.005.

Rueda-Larraz, L., d'Arlas, B. F., Tercjak, A., Ribes, A., Mondragon, I., Eceiza, A., 2009. Synthesis and microstructure–mechanical property relationships of segmented polyurethanes based on a PCL–PTHF–PCL block copolymer as soft segment, European Polymer Journal 45(7), 2096-2109; 10.1016/j.eurpolymj.2009.03.013.

Sahoo, S., Kalita, H., Mohanty, S., Nayak, S. K., 2017. Synthesis and characterization of vegetable oil based polyurethane derived from low viscous bio aliphatic isocyanate: Adhesion strength to wood-wood substrate bonding, Macromolecular Research 25(8), 1-7; 10.1007/s13233-017-5080-2.

Sánchez-Adsuar, M. S., Martín-Martínez, J. M., 2000. Structure, composition, and adhesion properties of thermoplastic polyurethane adhesives, Journal of Adhesion Science and Technology 14(8), 1035-1055; 10.1163/156856100743068.

Santamaria-Echart, A., Ugarte, L., García-Astrain, C., Arbelaiz, A., Corcuera, M. A., Eceiza, A., 2016. Cellulose nanocrystals reinforced environmentally-friendly waterborne polyurethane nanocomposites, Carbohydrate Polymers 151, 1203-1209; 10.1016/j.carbpol.2016.06.069.

Santiago-Medina, F., Foyer, G., Pizzi, A., Caillol, S., Delmotte, L., 2016. Lignin-derived non-toxic aldehydes for ecofriendly tannin adhesives for wood panels, International Journal of Adhesion and Adhesives 70, 239-248; 10.1016/j.ijadhadh.2016.07.002.

Schilling, C. H., Tomasik, P., Karpovich, D. S., Hart, B., Garcha, J., Boettcher, P. T., 2005. Preliminary studies on converting agricultural waste into biodegradable plastics—part IV: polysaccharide containing natural materials, Journal of Polymers and the Environment 13(3), 203-211; 10.1007/s10924-005-4755-5.

Scholz, V., da Silva, J. N., 2008. Prospects and risks of the use of castor oil as a fuel, Biomass and Bioenergy 32(2), 95-100; 10.1016/j.biombioe.2007.08.004.

Sharma, C., Kumar, S., Unni, A. R., Aswal, V. K., Rath, S. K., Harikrishnan, G., 2014. Foam stability and polymer phase morphology of flexible polyurethane foams synthesized from castor oil, Journal of Applied Polymer Science 131(17), 40668 (1)-40668 (8); 10.1002/app.40668.

Sharma, V., Kundu, P., 2008. Condensation polymers from natural oils, Progress in Polymer Science 33(12), 1199-1215; 10.1016/j.progpolymsci.2008.07.004.

Silva, B. B., Santana, R. M., Forte, M. M., 2010. A solventless castor oil-based PU adhesive for wood and foam substrates, International Journal of Adhesion and Adhesives 30(7), 559-565; 10.1016/j.ijadhadh.2010.07.001.

Somani, K. P., Kansara, S. S., Patel, N. K., Rakshit, A. K., 2003. Castor oil based polyurethane adhesives for wood-to-wood bonding, International Journal of Adhesion and Adhesives 23(4), 269-275; 10.1016/S0143-7496(03)00044-7.

Strobech, C., 1990. Polyurethane adhesives, International Journal of Adhesion and Adhesives 10(3), 225-228.

Stuart, B. H., 2004. Organic molecules, in: Ando, D. J. (Ed), Infrared Spectroscopy: Fundamentals and Applications. University of Technology, Sidney, Australia, Wiley Online Library, 71-93.

Szycher, M., 2013. Szycher's Handbook of Polyurethanes. New York: CRC press.

Szycher, M., 1999. End-stage renal disease (ESRD) and vascular access grafting: A critical review, Journal of Biomaterials Applications 13(4), 297-350; 10.1177/088532829901300403.

Tenorio-Alfonso, A., Pizarro, M., Sánchez, M., Franco, J., 2018. Assessing the rheological properties and adhesion performance on different substrates of a novel green polyurethane based on castor oil and cellulose acetate: A comparison with commercial adhesives, International Journal of Adhesion and Adhesives 82, 21-26; 10.1016/j.ijadhadh.2017.12.012.

Tenorio-Alfonso, A., Sánchez, M. C., Franco, J. M., 2018. Synthesis and mechanical properties of bio-sourced polyurethane adhesives from castor oil and MDI-

modified cellulose acetate: influence of cellulose acetate modification, International Journal of Adhesion and Adhesives (SUBMITTED).

Tenorio-Alfonso, A., Sánchez, M. C., Franco, J. M., 2017. Preparation, characterization and mechanical properties of bio-based polyurethane adhesives from isocyanate-functionalized cellulose acetate and castor oil for bonding wood, Polymers 9(4), 132-145; 10.3390/polym9040132.

Thébault, M., Pizzi, A., Santiago-Medina, F., Al-Marzouki, F., Abdalla, S., 2016. Isocyanate-free polyurethanes by coreaction of condensed tannins with aminated tannins, Journal of Renewable Materials 5(1), 21-29; 10.7569/JRM.2016.634116.

Ugarte, L., Gómez-Fernández, S., Peña-Rodríuez, C., Prociak, A., Corcuera, M. A., Eceiza, A., 2015. Tailoring mechanical properties of rigid polyurethane foams by sorbitol and corn derived biopolyol mixtures, ACS Sustainable Chemistry & Engineering 3(12), 3382-3387; 10.1021/acssuschemeng.5b01094.

Valero, M. F., Gonzalez, A., 2012. Polyurethane adhesive system from castor oil modified by a transesterification reaction, Journal of Elastomers and Plastics 44(5), 433-442; 10.1177/0095244312437155.

Van Ekeren, P., Carton, E., 2011. Polyurethanes for potential use in transparent armour investigated using DSC and DMA, Journal of thermal analysis and calorimetry 105(2), 591-598; 10.1007/s10973-011-1665-8.

Van Gurp, M., Palmen, J., 1998. Time-temperature superposition for polymeric blends, Rheology Bulletin 67(1), 5-8.

Wang, F., Wang, J., Hu, L., Chu, F., Wang, C., Pang, J., Cheng, Z., 2018. Combinations of soy protein and polyacrylate emulsions as wood adhesives, International Journal of Adhesion and Adhesives 82, 160-165; 10.1016/j.ijadhadh.2018.01.002.

Wang, Z., Zhang, X., Zhang, L., Tan, T., Fong, H., 2016. Nonisocyanate biobased poly (ester urethanes) with tunable properties synthesized via an environment-friendly route, ACS Sustainable Chemistry & Engineering 4(5), 2762-2770; 10.1021/acssuschemeng.6b00275.

Xu, Y., Petrovic, Z., Das, S., Wilkes, G. L., 2008. Morphology and properties of thermoplastic polyurethanes with dangling chains in ricinoleate-based soft segments, Polymer 49(19), 4248-4258; 10.1016/j.polymer.2008.07.027.

Yakushin, V., Stirna, U., Bikovens, O., Misane, M., Sevastyanova, I., Vilsone, D., 2013. Synthesis and Characterization of Novel Polyurethanes Based on Tall Oil, Materials Science 19(4), 390-396; 10.5755/j01.ms.19.4.2666.

Yilgör, E., Burgaz, E., Yurtsever, E., Yilgör, I., 2000. Comparison of hydrogen bonding in polydimethylsiloxane and polyether based urethane and urea copolymers, Polymer 41(3), 849-857; 10.1016/S0032-3861(99)00245-1.

Yu, H., Mhaisalkar, S., Wong, E., Teh, L., Wong, C., 2006. Investigation of cure kinetics and its effect on adhesion strength of nonconductive adhesives used in flip chip assembly, IEEE Transactions on Components and Packaging Technologies 29(1), 71-79; 10.1109/TCAPT.2005.850524.

Zain, N. M., Roslin, E. N., Ahmad, S., 2016. Preliminary study on bio-based polyurethane adhesive/aluminum laminated composites for automotive applications, International Journal of Adhesion and Adhesives 71, 1-9; 10.1016/j.ijadhadh.2016.08.001.

Zhang, L., Jeon, H. K., Malsam, J., Herrington, R., Macosko, C. W., 2007. Substituting soybean oil-based polyol into polyurethane flexible foams, Polymer 48(22), 6656-6667; 10.1016/j.polymer.2007.09.016.

Zhang, L., Ding, H., 1997. Study on the properties, morphology, and applications of castor oil polyurethane-poly (methyl methacrylate) IPNs, Journal of Applied Polymer Science 64(7), 1393-1401; 10.1002/(SICI)1097-4628(19970516)64:73.0.CO;2-Y.

Zhou, Q., Zhang, L., Zhang, M., Wang, B., Wang, S., 2003. Miscibility, free volume behavior and properties of blends from cellulose acetate and castor oil-based polyurethane, Polymer 44(5), 1733-1739; 10.1016/S0032-3861(02)00748-6.

Zhou, X., Fang, C., Yu, Q., Yang, R., Xie, L., Cheng, Y., Li, Y., 2017. Synthesis and characterization of waterborne polyurethane dispersion from glycolyzed products of waste polyethylene terephthalate used as soft and hard segment, International Journal of Adhesion and Adhesives 74, 49-56; 10.1016/j.ijadhadh.2016.12.010.

Zieleniewska, M., Auguścik, M., Prociak, A., Rojek, P., Ryszkowska, J., 2014. Polyurethane-urea substrates from rapeseed oil-based polyol for bone tissue cultures intended for application in tissue engineering, Polymer Degradation and Stability 108, 241-249; 10.1016/j.polymdegradstab.2014.03.010.

Zimmer, B., Nies, C., Schmitt, C., Possart, W., 2017. Chemistry, polymer dynamics and mechanical properties of a two-part polyurethane elastomer during and after crosslinking. Part I: dry conditions, Polymer 115, 77-95; 10.1016/j.polymer.2017.03.020.

Chapter 5
Conclusions

1. Conclusions

Next are described the main conclusions drawn from the accomplishment of the research activity previously outlined:

- Conventional two-step synthesis protocol has been successfully applied to functionalize cellulose acetate with aliphatic or aromatic diisocyanates –1,6-hexamethylene diisocyanate (HMDI) and 4,4'-diphenylmethane diisocyanate (MDI), respectively– yielding NCO-terminated biopolymers, which upon blending with castor oil led to bio-based polyurethane adhesives with NCO:OH molar ratios ranging from 1.05 up to 3.35.
- The assessment of the adhesion response as function of the weight ratio between castor oil and cellulose acetate modified with HMDI demonstrated that the adhesive with 1:1 weight ratio showed more suitable mechanical properties with more appealing failures for bonding wood. Such optimum polyurethane adhesive prepared with an aliphatic crosslinker encompassed a NCO:OH molar ratio of 1.87, slightly higher than the 1.45 obtained with their aromatic counterpart, using the same vegetable oil content.
- Synthesized bio-inspired polyurethanes developed adhesion strengths, under shear, peeling and flexural deformations, comparable or even superior to the examined benchmarks on wood and stainless steel, while failing in bonding non-polar surfaces (polyethylene), or at high temperatures of around 100 ºC.
- Viscoelastic results revealed the thermo-rheological simplicity of the cellulose acetate-based polyurethanes, extended to the whole temperature range analysed (from -10 up to 200 ºC) when using MDI, even achieving the glass region of the mechanical spectrum. On the contrary, this thermo-rheological simplicity was restricted to temperatures up to 110-125 ºC owing to temperature-induced structural rearrangements for HMDI-based systems, characterized by a sharp elastomeric response associated to an extensive rubbery plateau region. Moreover, in MDI-based polyurethanes the t-T superposition principle was only applicable above a critical NCO:OH molar ratio of 1.12.

- An increase in the isocyanate content, in the case of HMDI-based adhesives, resulted in enhanced viscoelastic moduli, which underwent a slight decrease with temperature, becoming more important above a critical point, strongly influenced by the biopolymer/castor oil ratio.
- Bio-sourced HMDI-based adhesives exhibited a rheological response very similar to the previously described benchmarks, albeit characterised by a greater relative elasticity and a less pronounced temperature dependence of the viscoelastic moduli.
- IR spectroscopic analyses allowed to monitor the curing process, corroborating the formation of urethane and urea linkages, besides the faster reaction between the MDI-based adhesives with the environmental humidity, as expected. Thereby those polyurethanes comprising aromatic crosslinkers demanded curing times ranging from 5 hours up to 6 days, rather than the 20 days required by their aliphatic crosslinker-based counterparts.
- A further examination of the carbonyl absorption band enabled to estimate the relative contribution of free and hydrogen-bonded carbonyl groups belonging to either urethane or urea linkages, by dint of a mathematical deconvolution procedure. Therefore, the establishment of inter- and intra-domains hydrogen bridges gave rise to regions with different degrees of order, allowing to evaluate the degree of phase separation (DPS), which underwent a decrease when the functionalization degree of cellulose acetate with MDI was raised. However, in the absence of cellulose acetate, greater contents of HMDI led to bio-inspired polyurethanes with reduced thermodynamic compatibility.
- Thermal results, supported by the spectroscopic analyses, suggested that synthesized polyurethanes exhibited the characteristic segmented chemical structure based on soft and hard segment domains, by identifying the glass transition temperatures attributed to each microdomain, beside an exothermic thermal rearrangement associated to the hard segments. Moreover, an increase of the NCO:OH molar ratio was proven to provoke a promotion of the thermodynamic compatibility between both phases, resulting in greater $T_{g,SS}$, since a greater amount of hard segments were more suitably dispersed in the soft domain, in good agreement with the evolution of the dynamic T_g shown by the MDI-based polyurethanes when performing oscillatory temperature ramps.

- Thermogravimetric analyses denoted a several-stage decomposition pattern for all polyurethane adhesives studied, whose thermal stability slightly decreased when raising the diisocyanate content, owing to the location of the hard segments decomposition step at lower temperatures than the corresponding to the more thermally stable soft segments.
- A new single-step and simple procedure which also avoids the use of any reaction solvent and catalyst has been properly implemented for the production of HMDI-based polyurethanes, giving rise to a more sustainable preparation of bio-sourced adhesives. This simplified synthetic route evinced the reinforcing effect of cellulose acetate on the polymer network, yielding adhesives with higher and less temperature-dependent viscoelastic moduli, also characterised by a shorter moisture curing process.
- The proposed straight-through protocol fostered microphase mixing, reducing the DPS of the ensuing polyurethanes and increasing the glass transition temperature of the soft segments accordingly. Moreover, the single-step procedure allowed for the achievement of adhesives which provided statistically indistinguishable shear strengths compared with the adhesives prepared with the traditional two-step protocol, despite exhibiting a much more appealing sort of failure located in the substrate, as well as similar thermal stability and peeling resistance through a cleaner and simpler approach.

2. Conclusiones

A continuación, se describen las principales conclusiones derivadas de la realización de los trabajos de investigación previamente descritos:

- El protocolo de síntesis convencional basado en dos etapas ha sido exitosamente aplicado con el objetivo de funcionalizar acetato de celulosa con diisocianatos alifáticos o aromáticos –diisocianatos de 1,6-hexametileno (HMDI) o 4,4'-metilendifenilo (MDI), respectivamente– produciendo biopolímeros funcionalizados con grupos NCO terminales, los cuales, tras una segunda etapa de mezclado con aceite de ricino, dan lugar a adhesivos de poliuretanos de origen natural con relaciones molares de NCO:OH que oscilan desde 1.05 hasta 3.35.
- La evaluación de las respuestas adhesivas en función de las concentraciones de aceite de ricino y acetato de celulosa modificado con HMDI reveló que el comportamiento mecánico más ventajoso en madera fue el desarrollado por el bio-adhesivo caracterizado por una relación 1:1 en peso de ambos componentes, exhibiendo tipos de fallos en las uniones adhesivas, localizados en el substrato, de mayor interés. Dicho adhesivo de poliuretano con propiedades óptimas, preparado con un agente entrecruzante alifático, comprendía una relación molar de NCO:OH de 1.87, ligeramente superior al 1.45 obtenido con su homólogo aromático, para el mismo contenido en aceite vegetal.
- Los poliuretanos naturales sintetizados desarrollaron fuerzas de adhesión en madera y acero inoxidable, bajo deformaciones de cizalla, pelado o flexión, equiparables o incluso superiores a los alcanzados por los adhesivos comerciales de referencia, a pesar de presentar una drástica reducción en sus rendimientos sobre superficies poliméricas apolares (polietileno) o a elevadas temperaturas (100 ºC).
- Los poliuretanos preparados con MDI manifestaron un comportamiento termoreológicamente simple, cuya extensión abarca todo el rango de temperaturas analizado (desde -10 a 200 ºC), alcanzando la región vítrea del espectro mecánico. Por el contrario, esta respuesta termoreológicamente simple está restringida a temperaturas de hasta 110-125 ºC, a causa de reorganizaciones estructurales inducidas por la temperatura, en el caso de los sistemas sintetizados a partir del

isocianato alifático (HMDI), caracterizados por una marcada respuesta elastomérica asociada a una extensa región plateau en el espectro mecánico. Por otra parte, en los poliuretanos sintetizados con MDI, el principio de superposición tiempo-temperatura resultó únicamente de aplicación para relaciones molares NCO:OH superiores a un valor crítico de 1.12.

- Un mayor contenido en isocianato causó un aumento significativo de los módulos viscoelásticos, los cuales, en el caso de adhesivos sintetizados a partir de HMDI, experimentaron una ligera disminución con la temperatura, llegando a ser de mayor importancia por encima de un punto crítico, altamente dependiente de la relación biopolímero/aceite de ricino.
- Los adhesivos naturales basados en HMDI exhibieron una respuesta reológica similar a los sistemas de referencia previamente descritos, aunque mostraron una mayor elasticidad relativa y módulos viscoelásticos menos dependientes de la temperatura.
- Los análisis espectroscopía de IR permitieron monitorizar el proceso de curado, corroborando la formación de enlaces uretano y urea, además de confirmar la mayor velocidad de curado con la humedad ambiental asociada a los adhesivos sintetizados a partir de MDI. Por consiguiente, tales poliuretanos, con agentes entrecruzantes aromáticos, precisaron unos tiempos de curado que oscilaron entre 5 horas y 6 días, al contrario de los 20 días alcanzados por los poliuretanos preparados con un agente entrecruzante alifático (HMDI).
- Un análisis más exhaustivo de la banda de absorción atribuida a los grupos funcionales carbonilos permitió realizar una estimación de las contribuciones individuales relativas de los grupos C=O libres y enlazados por puentes de hidrógeno, bien pertenecientes a enlaces uretanos o bien a ureas, a través de un procedimiento matemático de deconvolución. Así pues, el establecimiento de puentes de hidrógeno inter- o intra-dominios originó la constitución de regiones caracterizadas por diversos niveles de organización, posibilitando la evaluación del grado de separación de fases (DPS), que disminuyó con el aumento del grado de modificación del acetato de celulosa con MDI. No obstante, en ausencia del derivado celulósico, un mayor contenido de HMDI dió lugar a poliuretanos caracterizados por una compatibilidad termodinámica reducida.

- Los análisis térmicos, respaldados por los resultados espectroscópicos, sugirieron que los poliuretanos sintetizados presentan una estructura química segmentada, característica de poliuretanos, constituida por dominios duros y blandos, gracias a la identificación de las temperaturas de transición vítreas atribuidas a cada microdominio, además de un proceso exotérmico de reorganización asociado a los segmentos duros. Por otro lado, se demostró que un aumento en la relación NCO:OH fomenta la compatibilidad termodinámica entre fases, generando mayores $T_{g,SS}$, ya que un mayor número de segmentos duros se encuentran más adecuadamente distribuidos en los dominios blandos, conforme a la evolución de la T_g dinámica presentada por los adhesivos de poliuretanos basados en MDI al realizar rampas de temperatura en ensayos de torsión oscilatorios.
- Los análisis termogravimétricos revelaron que todos los adhesivos de poliuretanos sintetizados experimentaron un proceso de descomposición térmica constituido por varias etapas. Por otra parte, se advirtió una ligera disminución de la estabilidad térmica al incrementar el contenido de diisocianato, debido a que la etapa de descomposición asociada a los segmentos duros se sitúa a temperaturas inferiores a las relacionadas con los segmentos blandos, de mayor estabilidad térmica.
- Un nuevo procedimiento más simple, en una sola etapa, que además no necesita de disolvente ni de catalizador, fue concebido e implementado para la producción de poliuretanos basados en HMDI, dando lugar a un protocolo más sostenible para la preparación de adhesivos naturales. Dicha ruta sintética simplificada constató el efecto de refuerzo del acetato de celulosa sobre la estructura polimérica, produciendo adhesivos con mayores módulos viscoelásticos y menos dependientes de la temperatura, además de reducir el proceso de curado con la humedad.
- La aplicación del protocolo directo de preparación favorece la mezcla de fases, reduciendo el DPS de los poliuretanos resultantes e incrementando la temperatura de transición vítrea de los segmentos blandos en consecuencia. Por otro lado, dicho procedimiento permite obtener adhesivos que proporcionan fuerzas de cizalla estadísticamente indistinguibles comparados con los adhesivos preparados con el protocolo tradicional en dos etapas, a pesar de exhibir un tipo de fallo más atractivo, localizado en el substrato, además de una estabilidad térmica y una resistencia al pelado similares a través de un método más limpio y sencillo.

Annexe I

Published articles

Preparation, characterization and mechanical properties of bio-based polyurethane adhesives from isocyanate-functionalized cellulose acetate and castor oil for bonding wood

Adrián Tenorio-Alfonso[1], María del Carmen Sánchez[1,2] and José M. Franco[1,2]

[1] *Department of Chemical Engineering, University of Huelva, Campus El Carmen, Campus ceiA3, 21071 Huelva, Spain*

[2] *Pro[2]TecS-Chemical Process and Product Technology Research Center, University of Huelva, 21071 Huelva, Spain*

Published in: ***Polymers***

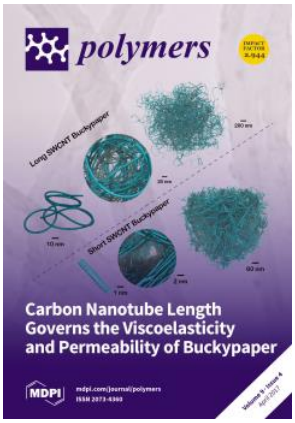

Publisher: MDPI AG
Editor-in-Chief: Prof. Dr. Alexander Böker
Volume 9, Issue 4, pp: 132
Year: 2017
DOI: 10.3390/polym9040132
ISSN: 2073-4360
eISSN: 2073-4360
JCR Impact Factor (2017): 2.935

JCR Category	Rank	Quartile
POLYMER SCIENCE	19/87	Q1

polymers

MDPI

Article

Preparation, Characterization and Mechanical Properties of Bio-Based Polyurethane Adhesives from Isocyanate-Functionalized Cellulose Acetate and Castor Oil for Bonding Wood

Adrián Tenorio-Alfonso [1], María Carmen Sánchez [1,2] and José M. Franco [1,2,*]

[1] Department of Chemical Engineering, University of Huelva, Campus El Carmen, Campus ceiA3, 21071 Huelva, Spain; adrian.tenorio@diq.uhu.es (A.T.-A.); mcarmen@uhu.es (M.C.S.)

[2] Pro²TecS-Chemical Process and Product Technology Research Center, University of Huelva, 21071 Huelva, Spain

* Correspondence: franco@uhu.es; Tel.: +34-959-219995

Academic Editor: Antonio Pizzi

Received: 6 March 2017; Accepted: 3 April 2017; Published: 5 April 2017

Abstract: Nowadays, different types of natural carbohydrates such as sugars, starch, cellulose and their derivatives are widely used as renewable raw materials. Vegetable oils are also considered as promising raw materials to be used in the synthesis of high quality products in different applications, including in the adhesive field. According to this, several bio-based formulations with adhesion properties were synthesized first by inducing the functionalization of cellulose acetate with 1,6-hexamethylene diisocyanate and then mixing the resulting biopolymer with a variable amount of castor oil, from 20% to 70% (wt). These bio-based adhesives were mechanically characterized by means of small-amplitude oscillatory torsion measurements, at different temperatures, and standardized tests to evaluate tension loading (ASTM-D906) and peel strength (ASTM-D903). In addition, thermal properties and stability of the synthesized bio-polyurethane formulations were also analyzed through differential scanning calorimetry and thermal gravimetric analysis. As a result, the performance of these bio-polyurethane products as wood adhesives were compared and analyzed. Bio-polyurethane formulations exhibited a simple thermo-rheological behavior below a critical temperature of around 80–100 °C depending on the castor oil/cellulose acetate weight ratio. Formulation with medium castor oil/biopolymer weight ratio (50:50 % wt) showed the most suitable mechanical properties and adhesion performance for bonding wood.

Keywords: biosourced adhesives; castor oil; cellulose acetate; isocyanate; polyurethane; rheology

1. Introduction

In the 21st century, sustainable development has become one of the main objectives in industrial activity. The approaching exhaustion of petroleum supplies, their fluctuating and rising prices, along with the stringent regulations as a consequence of the increasing environmental concerns have propelled scientists towards using renewable natural resources in order to replace total or partially petroleum-based raw materials, with the aim of overcoming these issues [1,2].

In the adhesive field, traditional formulations are petro-based [1,3], containing some volatile organic compounds (VOC) and other toxic substances, such as formaldehyde derivatives. Those materials are hazardous to the environment and detrimental to the human health, which encourages the adhesive industry to develop adhesives from renewable raw materials with suitable functional properties [4,5]. The use of eco-friendly alternatives in this field can help to overcome those

problems. In fact, some natural adhesives like starch, casein and other proteins were used at the start of the 20th century [6]. Nevertheless, their utilization is limited as they exhibit low durability and low water resistance. In the past few years, as recently reviewed by Ferdosian et al. [7], some bio-based adhesives have been developed from a range of natural resources, including lignin [8], starch [1], tannin [9], vegetable oils [3], soy flour and soy protein [4]. However, there are still some properties to be sharpened to make those natural-based adhesives competitive in comparison to the traditional ones [10]. In this sense, bio-based polyurethanes seem to be an excellent alternative to petroleum-based products, overcoming the environmental drawbacks but, at the same time, providing suitable properties.

Since their discovery by Otto Bayer and co-workers in 1937 [11], polyurethanes have become one of the most outstanding polymers as they exhibit a high performance and versatility, being employed in a vast range of industrial and engineering applications such as foams [12,13], coatings [14], medicinal products [15,16] or adhesives [17], among others. This wide variety of applications is associated to their superior properties, including excellent corrosion, solvent and chemical resistance, high mechanical strength, low temperature flexibility, adhesion, suitable curing rates, chemical structure versatility, etc. [18–20]. As is well known, polyurethanes are polymers containing urethane linkages (NHCOO) in the main polymer chain [21]. In most cases, the synthesis of polyurethanes is accomplished through the reaction taking place between isocyanates (NCO) and active hydroxyl groups (OH) and using a chain extender (low molecular weight glycol or amine) [2,3,19]. Typical polyurethanes are multiblock copolymers whose structure comprises two domains, called "soft" and "hard" segments, which provide them with their characteristic exceptional versatility [22,23].

In the polyurethane synthesis, an extensive variety of diisocyanates might be employed, including toluene diisocyanate (TDI), 4,4′-methylene diphenyl diisocyanate (MDI), 1,6-hexamethylene diisocyanate (HMDI) and isophorone diisocyanate (IPDI), among others [19]. Moreover, although traditional polyols consist of polyether or polyester, some approaches have been made to replace this source of hydroxyl groups by eco-friendly materials, for instance natural oils [2,24], or biopolymers [25,26]. In particular, castor oil [20,27] and cellulose derivatives [28,29] have been proposed as eco-friendly polyols. Vegetable oils are considered one of the most important types of renewable feed stock for the petroleum-based industrial products due to their noteworthy and favourable properties, since they are a copious resource, biodegradable, inexpensive, sustainable, non-toxic, easy to handle, structurally versatile, highly pure, flexible for chemical transformations, high physically and chemically stable, etc. [30,31]. Polyurethane production from vegetable oils is not a new approach. In fact, a wide range of natural oils have been considered as feasible choices to synthesized segmented polyurethanes [32,33], such as linseed or rapeseed [34], sunflower [35], canola [36], but principally soybean [29] and castor oil [14,15]. Castor oil belongs to the vegetable oil minority that exhibits bearing hydroxyl group [15], which, along with double bond presence [37], makes it an appealing resource for producing polyurethanes. In particular, some castor oil-based polyurethane formulations have been previously proposed as eco-friendly solventless adhesives [20,38]. On the other hand, due to the vast abundance of cellulose in nature, this carbohydrate and its derivatives have also drawn great interest in industrial production. For instance, different cellulose derivatives, i.e., methylcellulose, α-cellulose, 2-hydroxyethylcellulose, methyl 2-hydroxyethylcellulose and cellulose acetate propionate have been successfully employed in previous investigations [28], promoting the reaction between the hydroxyl groups located in the cellulose backbone and active diisocyanate crosslinkers to synthesize functionalized biopolymers which were further dispersed in vegetable oils. This study demonstrated that the rheological response, and therefore the application field, of the different oleogels achieved basically depends on the balance between the polarity and the size of cellulose substituents.

In the present work, novel bio-based polyurethane adhesive formulations have been prepared in two steps by combining a carbohydrate polymer like cellulose acetate and castor oil. Cellulose acetate was first functionalized by inducing the reaction with 1,6-hexamethylene diisocyanate. Then, the resulting product was blended with different proportions of castor oil producing bio-based

polyurethanes with adhesion properties. The main objective of this work was to evaluate the influence of the castor oil/functionalized biopolymer ratio on the rheological, thermal and adhesion performance properties of these eco-friendly formulations.

2. Materials and Methods

Materials. The raw material used to synthesize the biopolymers was cellulose acetate (CA, 40% acetyl groups, Mr, ~29,000), which was modified by inducing the reaction with 1,6-hexamethylene diisocyanate (HMDI, purity ≥98.0%) using toluene (purum grade ≥99.7%) as solvent, and triethylamine (TEA, purum grade of 99.5%) as a catalyst. All these compounds were supplied by Sigma-Aldrich (St. Louis, MO, USA). Moreover, castor oil purchased from Guinama (Valencia, Spain) was used to prepare the bio-based polyurethane together with the modified cellulose acetate. Poplar wood, polyester fabric and sycamore wooden sheets were employed as substrates and supplied by a local store. U-Bond® 309-TFC was selected as a commercial polyurethane-based adhesive and used as benchmark in the mechanical tests.

Synthesis of the bio-based polyurethanes. A two-step synthesis protocol was followed. Cellulose acetate functionalization was first performed following the protocol detailed in previous studies [39]. In the first step, the solvent was introduced into the flask and bubbled for half an hour with Argon, and then 15 g of CA, along with TEA and HMDI, were introduced into the flask in a molar proportion of 4.53:1:1 NCO:OH:TEA respectively. These reagents were vigorously mixed for 24 h at room temperature and under inert atmosphere. Finally, the solvent was removed from the mixture by means of a vacuum evaporation process, obtaining the functionalized biopolymer. Such a high NCO:OH molar ratio, i.e., excess of HMDI, and reaction time ensure the complete functionalization of available hydroxyl groups in cellulose acetate, as will be discussed below in Section 3.1.

Afterwards, the functionalized biopolymer and castor oil were placed together in an open vessel and blended using a controlled-rotational speed mixing device (RW 20, Ika, Staufen, Germany) provided with an anchor impeller. Castor oil/biopolymer ratio was varied, producing formulations with 20:80, 50:50 and 70:30 weight ratios. The excess of HMDI added in the CA functionalization step was estimated to theoretically counterbalance the amount of hydroxyl groups available for the highest castor oil/biopolymer weight ratio (70:30). These mixtures were agitated during 24 h, at room temperature. Afterwards, the resulting products were homogenized by using a rotor-stator turbine Ultra-Turrax T50 (Ika, Staufen, Germany), at 10,000 rpm, for 60 s.

Experimental Techniques. Bio-based polyurethanes studied were chemically, thermal and mechanically characterized by means of Fourier transform infrared (FTIR) spectroscopy, thermogravimetric analysis (TGA), differential scanning calorimetry (DSC) and rheological techniques as well as standardized mechanical testing. Characterization was carried out on cured samples one week after their preparation. After one week, properties remain unaltered.

The chemical structure of the synthesized polyurethanes was analyzed by FTIR spectroscopy in a FT/IR-4200 Spectrometer apparatus (JASCO Inc., Tokyo, Japan), equipped with an attenuated total reflectance (ATR) accessory provided with monolithic diamond crystal. Spectra were the result of an average of 73 scans with a resolution of 4 cm^{-1} and a 45° angle of incidence, in the spectral range 7800–350 cm^{-1}.

TGA measurements were also carried out by using a Q50 Thermogravimetric Analyzer (TA Instruments, New Castle, DE, USA). Ten to twenty milligrams of each sample were heated up from 30 up to 600 °C at a heating rate of 10 °C/min, under nitrogen environment (flow rate, 60 mL/min).

DSC analysis over the cured polyurethanes was performed by using a Q100 Calorimeter (TA Instruments, New Castle, DE, USA). Five to ten milligrams of each sample were placed on aluminum pans and submitted to a heating cycle from −85 up to 250 °C at a heating rate of 10 °C/min, under inert atmosphere of nitrogen (flow rate, 50 mL/min).

The rheological characterization of bio-based polyurethanes was carried out using a controlled-stress rheometer Physica MCR301 (Anton Paar Germany GmbH, Ostfildern, Germany). Small-amplitude oscillatory torsion tests were performed within the linear viscoelastic region, in a

frequency range 0.01–100 rad/s at different constant temperatures ranging from 25 up to 200 °C. The linear viscoelastic range was previously determined by performing stress sweep tests at 1 Hz. Furthermore, upward temperature ramps of 2 °C/min were applied from 25–200 °C at 1 Hz.

Mechanical properties for bonding wood were studied by means of Standard Test Methods ASTM D903, D906 and D1184, determining the stripping, shear and flexural strengths of the synthesized eco-friendly polyurethanes, using a Universal Testing Machine (Shimadzu, Kyoto, Japan), model AG-IS. Peeling strengths in poplar wood–polyester fabric joints (105 × 18 × 1 mm^3 bonding line) were evaluated by applying a constant separation rate of 152.4 mm/min at room conditions, thus obtaining the stripping strength as the arithmetic average load per millimeter of width. On the other hand, poplar wood-to-poplar wood lap-shear strengths (18 × 18 × 0.5 mm^3 adhesive volume) were obtained as the average maximum load per square centimeter of shear area when applying a force ramp of 3.56 kN/min. Finally, sycamore-adhesive bonded laminated assemblies, comprised of eight 38 × 19 × 0.25 mm^3 plies, underwent a 3-point flexural test, with a crosshead speed of 0.74 mm/min, and associated flexural strengths were calculated according to ASTM D1184 (ASTM International, West Conshohocken, PA, USA). All substrates were cut according to the required dimensions, joined without applying a permanent pressure or any other pretreatment, and were kept at room temperature and 50% relative humidity for 7 days, according to these test methods. All data were analyzed by means of statistical tests to identify and remove possible outliers (Grubbs and Generalized Extreme Studentized Deviate (ESD) tests).

3. Results and Discussion

3.1. Chemical and Thermal Characterization

The Fourier transform infrared spectroscopic attenuated total reflectance (FTIR-ATR) technique was used to evaluate the preparation of polyurethanes with different castor oil/biopolymer weight ratio. Figure 1 shows the infrared spectra for castor oil/cellulose acetate-based polyurethanes after seven days of curing (Figure 1b), in comparison to those obtained with the raw materials, i.e., 1,6-hexamethylene diisocyanate, cellulose acetate and castor oil (Figure 1a). Figure 1a also includes the FTIR spectrum of the functionalized biopolymer which was further blended with castor oil to get the final bio-based polyurethanes. As can be seen, the characteristic peak attributed to the O–H stretching vibration has almost disappeared by around 3330 cm^{-1}, thus confirming the total functionalization of cellulose acetate as intended. On the other hand, bio-based polyurethanes (Figure 1b) also exhibit the absorption band centered at 3330 cm^{-1} due, in this case, to both the O–H and N–H stretching vibrations [23,40–43] as well as the band at 1741 cm^{-1} corresponding to the aliphatic carbonyl group (C=O) [40], which are in concordance with those found in the castor oil spectrum (Figure 1a). Besides, the absorption bands at 2919–2931 and 2851–2860 cm^{-1} correspond to the C–H asymmetric and symmetric stretching vibration, respectively, due to existing methylene groups in the polyurethane backbones, which can be observed in all IR spectra. Those peaks are accompanied by the bands at 1462 cm^{-1}, corresponding to CH_2 bending vibration [40].

Furthermore, the almost disappearance in the peak intensity at approximately 2260 cm^{-1}, attributable to free N=C=O groups (Figure 1b) [23,39,40], confirms the complete reaction of N=C=O groups for the sample with the lower biopolymer content (Figure 1b), due to the excess of hydroxyl groups. This fact is corroborated by means of the reduction in the intensity of peak located at 1354 cm^{-1}, attributable to C–N stretching vibration in free isocyanate groups. However, the intensity of the peak associated to the stretching vibration of the N=C=O group clearly increases as biopolymer content does. Moreover, the extensive formation of urethane linkages is confirmed by their characteristic bands apparent at 3330 cm^{-1}, which appears to overlap the O–H stretching vibration but as a sharper peak, 1715, 1697 and 1580 cm^{-1} attributed to N–H stretching, amorphous and crystalline hydrogen bonded C=O stretching, and N–H bending vibrations, respectively [31,40,41]. Finally, no evidence of free isocyanate groups was found after one month of curing, as illustrated in Figure 1b for the 50:50 CO/biopolymer weight ratio. However, despite the fact that total curing

process requires around one month, the bio-polyurethane mechanical properties remain almost unchanged after one week.

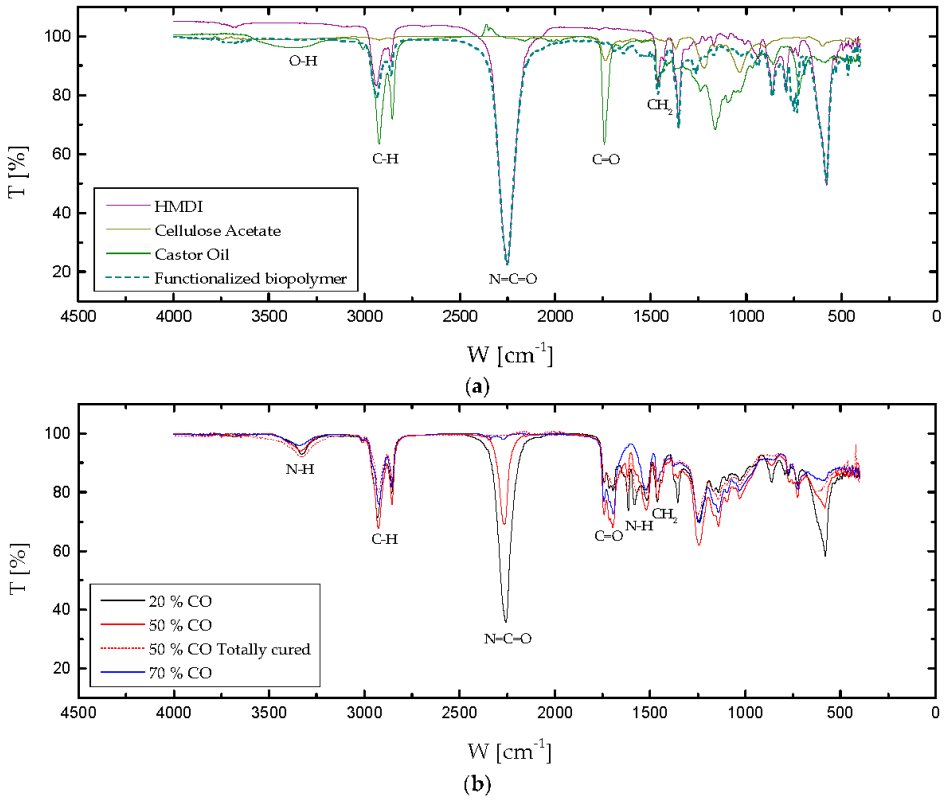

Figure 1. Fourier transform infrared spectroscopic attenuated total reflectance (FTIR-ATR) spectra for: (**a**) 1,6-hexamethylene diisocyanate, cellulose acetate, castor oil and functionalized biopolymer; (**b**) formulation with 20% CO, 50% CO, 70% CO and 50% CO totally cured.

The thermal stability and decomposition behavior of bio-based adhesives were studied with the aid of thermogravimetric analysis after one week of curing. Figure 2 displays TGA curves for the different formulations studied, showing the weight loss percentage and the derivative curve versus temperature. Those results were also compared to those obtained with the corresponding reactants, i.e., cellulose acetate, 1,6-hexamethylene diisocyanate and castor oil (Figure 3). Table 1 collects the characteristic thermal parameters determined from the thermograms, such as, the onset temperature (T_{onset}), the temperature for the maximum decomposition rate (T_{max}) and the final temperature in each decomposition step (T_{final}), along with the weight-loss percentage corresponding to each step and the percentage of non-degraded residue (R) at the end of the process.

For cellulose acetate, thermal decomposition under nitrogen atmosphere took place in one single step, as can be deduced from Figure 3, ranging from 335 to 373 °C, yielding an almost complete weight loss (≈82%) after this temperature. In comparison to pure cellulose acetate, bio-based polyurethanes prepared from this polymer experienced a slight decrease in thermal stability as a consequence of the polymerization process. As can be seen in Table 1, all synthesized bio-based polyurethanes generally start to decompose at lower temperatures, experiencing a not very significant weight loss (≈1–2%) within the range of 60–204 °C, which can be attributed to the loss of some free remaining NCO segments [44], but also residual solvent and moisture. Moreover, as a result of the urethane linkages, the biopolymer degradation started at lower temperatures. As

previously reported, the isocyanate functionalization of cellulose derivatives generally expands the degradation temperature range [28,44].

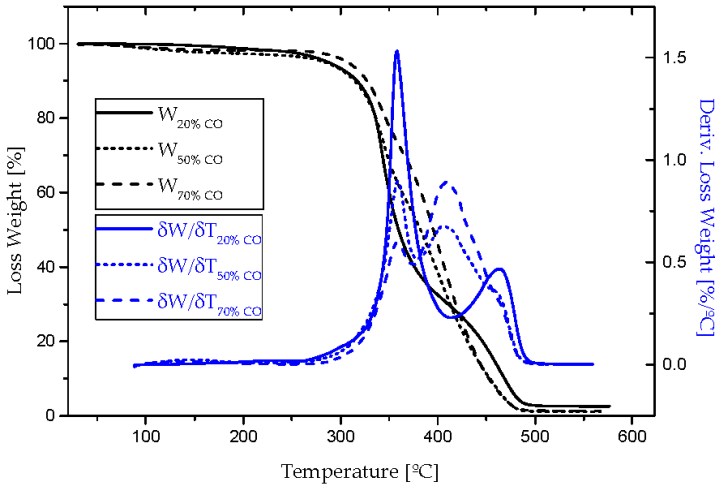

Figure 2. Thermogravimetric analysis (TGA) analysis for all bio-based adhesives.

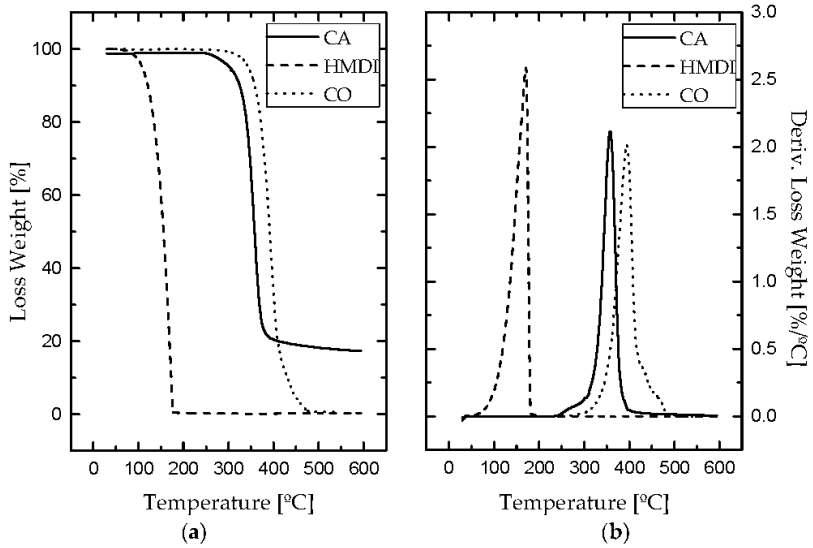

Figure 3. (**a**) Loss weight and (**b**) derivative loss weight curves for cellulose acetate, 1,6-hexamethylene diisocyanate (HMDI) and CO raw materials.

Table 1. Thermal parameters obtained from thermogravimetric analysis curves.

Sample	T_{onset} [°C]	T_{max} [°C]	T_{final} [°C]	Weight loss [%]	Residue [%]
20% CO	130/326/426	193/343/465	204/372/493	1.6/67.5/28.5	2.6
50% CO	63/314/374	98/344/397	158/358/442	2.3/39.2/47.2	1.2
70% CO	60/307/370	93/343/402	155/357/453	1.6/26.9/63.1	1.4
HMDI	138	171	176	99.7	0.3
Cellulose Acetate	335	358	373	82	18
Castor Oil	367	395	416	99.4	0.6

Besides this, for castor oil, a single step thermal decomposition took place between 367 and 416 °C (see Figure 3), which is clearly noticeable in the thermograms of bio-polyurethane samples containing 50% and 70% CO (Figure 2). Interestingly, the formulation with 20% CO did not show this degradation peak due to the low oil content in its structure. As a consequence, the lower castor oil content, the less intense peak appeared at around 395 °C, and also the higher intensity in the event located at 343 °C, corresponding to cellulose acetate, was observed.

Finally, the bio-adhesive with the highest biopolymer content exhibited a clear peak centered at 465 °C, which does not correspond to the degradation of urethane groups. According to Gurunathan et al. [31,45] and Corcuera et al. [41], this event takes place at around 320–370 °C, overlapped in this case with the degradation of cellulose acetate backbone. At around that temperature (450–470 °C), a shoulder in the last decomposition peak was also detected in samples containing 50% and 70% CO as well (Figure 2). As a consequence, the degradation peaks found at these temperatures in the bio-based polyurethanes studied must be assigned to excessively crosslinked polyurethanes networks. These more rigid domains, logically favoured by the higher biopolymer content, i.e., higher density of urethane linkages, are more thermally stable [25].

The different structural thermal events taking place in the synthesized cellulose-based polyurethane were evaluated by means of differential scanning calorimetry (DSC). Generally, only one thermal event, corresponding to the glass transition of soft segments domains ($T_{g,SS}$), was detected in the temperature range applied (Figure 4), whereas no glass transition attributable to hard segments was observed [46]. Moreover, melting transitions of the crystalline domains were also not observed below 200 °C. The temperature of the glass transition values ($T_{g,SS}$) were taken at the midpoint of the transition, and inserted in Figure 4. According to these results, $T_{g,SS}$ increases with the biopolymer content in the formulation. Nevertheless, because of the low vegetable oil content, $T_{g,SS}$ became unnoticeable in the formulation with the 20% CO content.

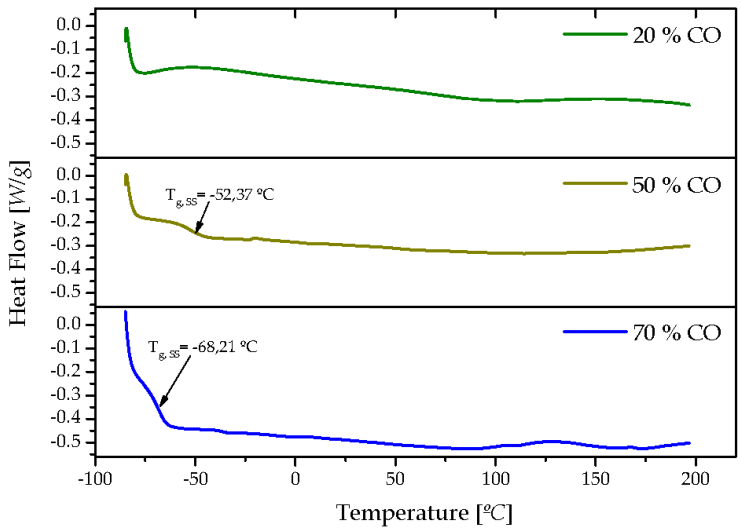

Figure 4. Differential scanning calorimetry (DSC) thermograms for bio-based polyurethane samples studied.

3.2. *Rheological Properties*

Figure 5 shows the evolution of viscoelastic moduli (G' and G'') with frequency for the sample containing 50:50 CO/biopolymer weight ratio, at different selected temperatures, measured under oscillatory torsional deformations. As can be noticed, a well-developed plateau region of the mechanical spectrum was always obtained, independently of the temperature, characterized by a predominant elastic behavior throughout the whole frequency range studied. Moreover, G'

decreases with temperature, slightly up to 80–100 °C and then more dramatically. The same influence can be observed in G'' at medium and high frequencies. However, the most remarkable effect of temperature on the viscous modulus is the change in the frequency dependence.

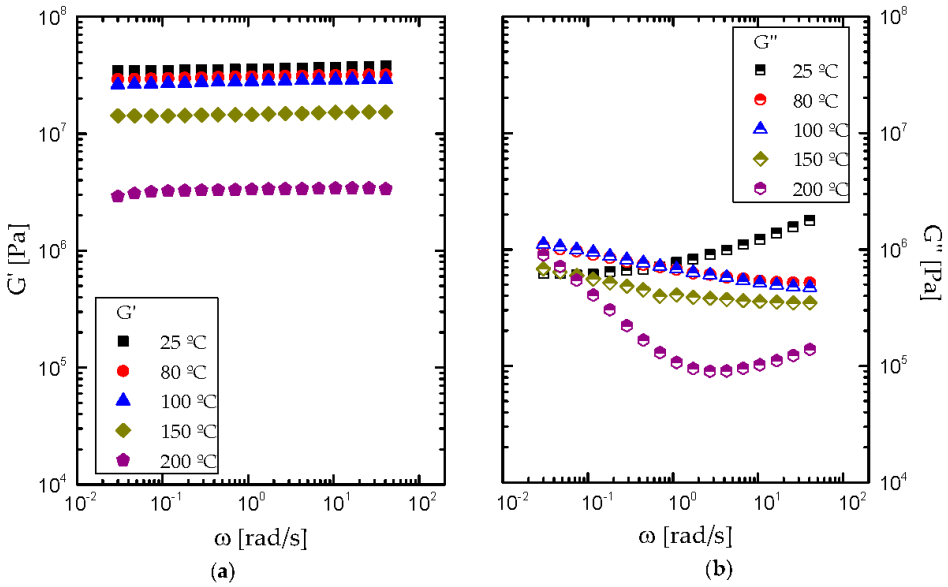

Figure 5. Evolution of (**a**) elastic, G', and (**b**) viscous moduli, G'', with frequency, within the linear viscoelastic range, for formulations containing 50% CO castor oil at different temperatures.

With the aim to extend the mechanical spectrum of the synthesized formulations, the time–temperature principle was applied (Figure 6), with the aid of suitable shift factors (a_T). This principle can be properly applied to bioadhesives with 50:50 and 70:30 castor oil/biopolymer weight ratio, until approximately 100 and 80 °C, respectively, but no longer. Nonetheless, bio-based polyurethane with the lowest oil content (20%) showed an extreme brittleness, which hindered the torsional frequency response. The values of the empirical shift factors applied in the time–temperature principle are included in Figure 7a as a function of the reciprocal temperature, taking 25 °C as the reference temperature. The evolution of the shift factor with temperature can be described by means of the Arrhenius model as follow:

$$a_T = A \cdot e^{\frac{E_a}{R}\left(\frac{1}{T}-\frac{1}{T_0}\right)}, \quad (1)$$

where R is the ideal gas constant (8.31434 J·mol^{-1}·K^{-1}), T the absolute temperature (K), T_0 is the reference temperature (K), A is the pre-exponential factor and E_a is the activation energy (J·mol^{-1}). Fitting values for the activation energy are shown in Figure 7a for each sample. As can be noticed, an increase in activation energy was found when CO content is reduced, meaning a bio-based adhesive characterized by a higher thermal susceptibility. The values of the plateau modulus, G_N^0, the characteristic parameter of the plateau region, estimated as the value of G' at the frequency for which the loss tangent ($\tan\delta = G''/G'$) is minimum, were also plotted versus the reciprocal temperature (Figure 7b). As expected, G_N^0 values do not significantly change in the temperature range where the t–T superposition principle was applied, but dramatically decrease afterwards. The Arrhenius equation can be also applied to evaluate the temperature dependence on G_N^0 in the two above referred regions, below and above the critical temperature for a significant softening, as shown elsewhere [26]. Fitting values for the activation energy are included in Figure 7b. This behaviour reflects the thermo-rheological simplicity of those bio-based polyurethanes, from room temperature up to the mentioned critical temperatures, above which a different evolution of the rheological

functions with both temperature and frequency was observed. This change in thermo-rheological response might be associated to the initial weight loss found in TGA tests, attributable to the loss of free isocyanate content.

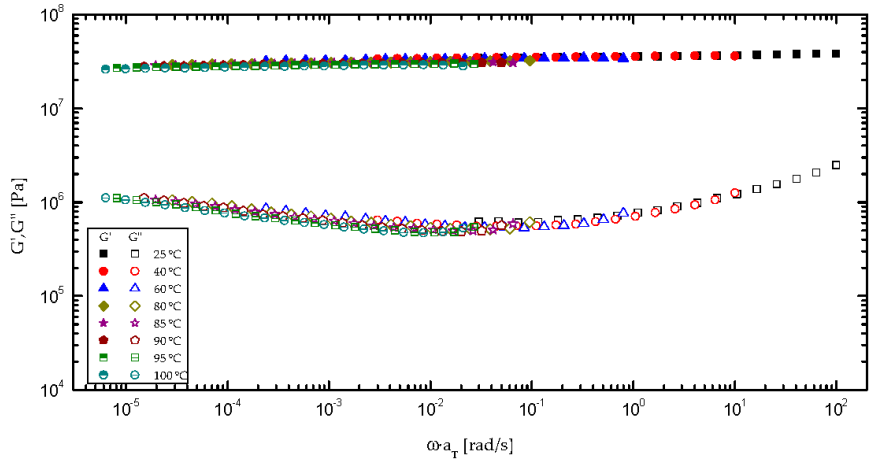

Figure 6. *t*–*T* superposition for formulation with 50% CO from 25 up to 100 °C temperature.

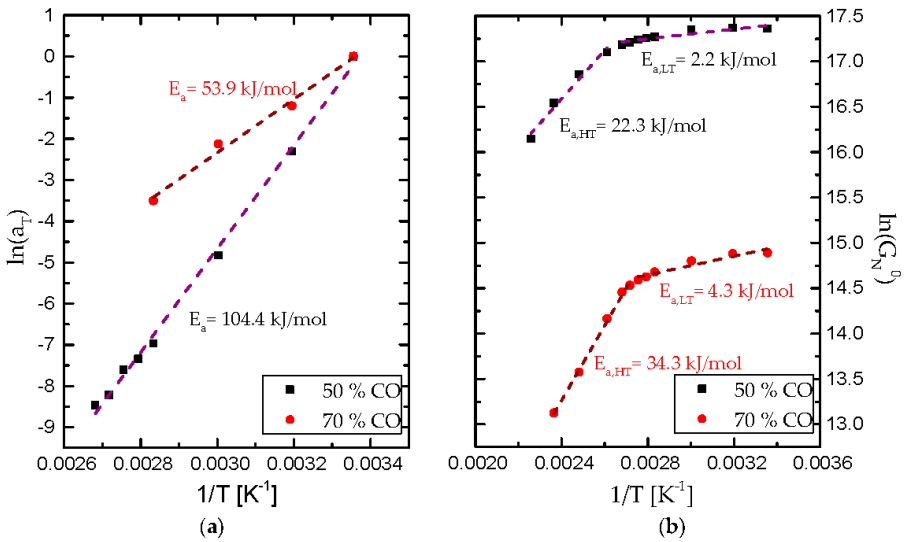

Figure 7. (**a**) Shift factors (a_T) and (**b**) plateau moduli (G_N^0) for formulations with 50:50 and 70:30 castor oil/biopolymer weight ratios.

In addition, Figure 8 depicts the evolution of viscoelastic functions when applying continuous temperature ramps for all formulations studied. Generally, in bio-based polyurethane systems with 20:80, 50:50 and 70:30 in castor oil/biopolymer weight ratios a slight temperature influence over the storage moduli (G') was found up to a critical temperature of around 120, 80 and 40 °C, respectively. Above these temperatures, a more important softening was noticed, similarly to the evolution found in frequency sweep tests. The evolution of G'' is more complex since the frequency dependence is also affected by temperature as previously discussed. Nevertheless, the sample with the highest castor oil content (or lower biopolymer concentration) undergoes a continuous and much more important decrease in both viscoelastic functions within all temperature ranges evaluated.

Moreover, attending to the evolution of the loss tangent, bio-polyurethanes with 20% and 50% CO exhibit a well extended plateau region in the range from 25 to 180 °C, with increasing values related to the melting transition of the crystalline microdomains, which is expected to be found at higher temperatures. Overall, the higher biopolymer content in the formulation, the higher values of the viscoelastic moduli and critical temperature for the softening were found.

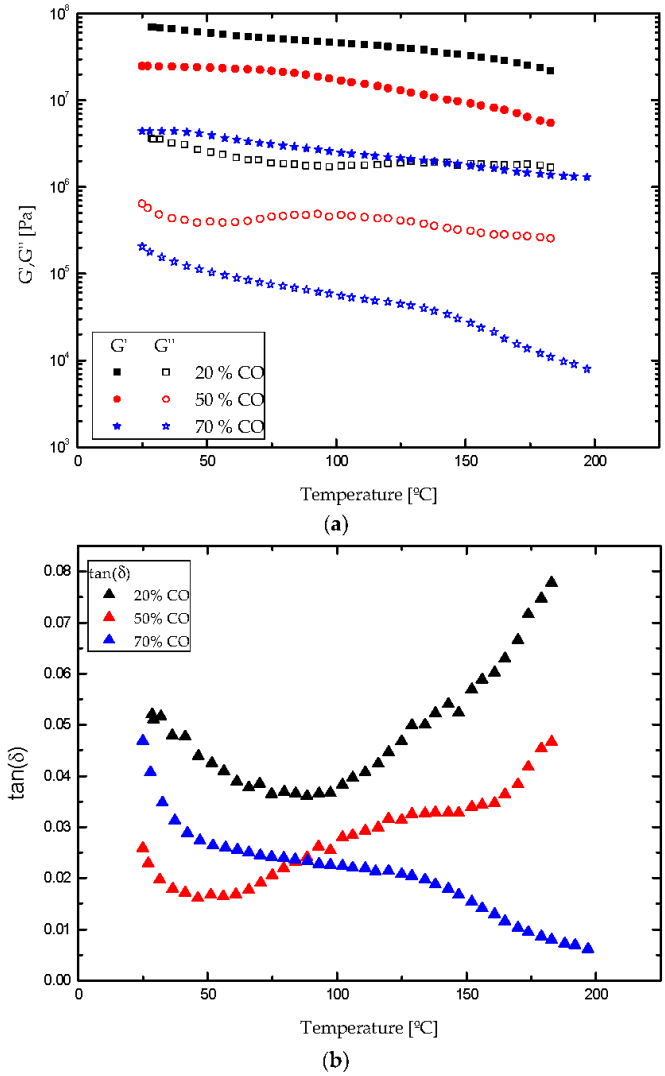

Figure 8. Temperature ramps for all ecofriendly bioadhesives at 2 °C/min of heating rate within the linear viscoelastic region: (**a**) elastic (*G'*) and viscous (*G''*) moduli; (**b**) loss tangent (tanδ).

3.3. *Adhesion Performance on Wood Substrates*

Adhesion performance of the synthesized bio-based formulations was studied by applying standardized mechanical tests. Table 2 shows the different mechanical parameters obtained from these tests. According to these, polyurethane with a medium CO content exhibits more important peeling strength in comparison to the other samples, although still slightly lower than the commercial polyurethane used as benchmark. Moreover, concerning shear tests results, the adhesive

with 20:80 and 50:50 castor oil/biopolymer weight ratio present comparable shear strengths, almost three times higher than the sample containing 70:30 castor oil/biopolymer weight ratio (Table 2). These samples also undergo a substrate failure, which seems to be a more appropriate and desirable sort of failure. The values of the shear strength provided by the ASTM D906 test are almost twice as those reported by Somani et al. [38] for castor oil-based adhesives prepared using aliphatic diisocyanates, and slightly higher than those reported by da Silva et al. [20] for castor oil-based adhesives including TDI as crosslinking agent. Moreover, the lap shear strength values for adhesives containing 20:80 and 50:50 castor oil/biopolymer weight ratios are very similar to that obtained with the commercial sample. Finally, as judged by flexural results, all formulations showed similar failing loads, even though, once again, the sample with the highest castor oil/biopolymer weight ratio exhibited a stress value which is significantly lower than those obtained with the rest of samples, while the commercial adhesive provided, in this case, a significantly lower flexural strength.

Table 2. Peeling, shear and flexural strengths on bonding wood substrate.

Sample	Peeling strength [g–f/mm]	Shear strength [MPa]	Flexural strength [MPa]
20% CO	59.8 ± 10.9 [a]	2.37 ± 0.03 [b,c]	21.9 ± 6.0 [d,e]
50% CO	169.4 ± 19.6 [b]	2.84 ± 0.36 [b,c]	21.6 ± 4.9 [d,e]
70% CO	76.9 ± 4.9 [b]	0.94 ± 0.24 [b]	14.5 ± 0.9 [d]
Commercial polyurethane adhesive	228.6 ± 28.3 [b]	2.50 ± 0.40 [b]	11.0 ± 3.0 [d,e]

Failure classification: [a] Adhesion; [b] Cohesion; [c] Substrate; [d] Breaking; [e] Buckling.

4. Conclusions

In this research, a cellulose derivative was first functionalized by inducing the reaction with 1,6-hexamethylene diisocyanate, and then the biopolymer was blended with castor oil to obtain bio-based polyurethane adhesives. The influence of the castor oil/biopolymer weight ratio in bio-based adhesive was evaluated with the aid of rheological, standardized mechanical, thermal and spectroscopic analysis. The results demonstrated that the formulation with medium castor oil/biopolymer weight ratio (50:50 % wt) showed more suitable mechanical properties with more desired type of failure in wood joints under the mechanical conditions studied, comparable to those exhibited by a well-known commercial polyurethane-based adhesive. The rheological response of all synthesized polyurethanes corresponds to strong crosslinked gels characterized by the plateau region of the mechanical spectrum. Moreover, the storage and loss moduli increased with biopolymer content. A slight decrease in viscoelastic moduli was detected with the increase in temperature, becoming more important above a critical temperature, which increases with the biopolymer/castor oil weight ratio. Below this critical temperature, a simple thermo-rheological response was found, being able to apply the t–T superposition principle. Finally, thermal analysis, supported by rheological and spectroscopic results, suggests a chemical structure based on soft and crystalline hard segments, characterized by a several-stage thermal decomposition pattern.

Acknowledgments: This work is part of two research projects (CTQ2014-56038-C3-1R and TEP-1499) sponsored by MINECO-FEDER and Junta de Andalucía programmes, respectively. One of the authors (Adrián Tenorio) has also received a PhD. Research Grant from 'Ministerio de Educación' (FPU13/01114). The authors gratefully acknowledge the financial support.

Author Contributions: All the authors conceived and designed the experiments; Adrián Tenorio-Alfonso performed the experiments and analyzed the data under the supervision of María Carmen Sánchez and José M. Franco.

Conflicts of Interest: The authors declare no conflict of interest.

References

1. Moubarik, A.; Allal, A.; Pizzi, A.; Charrier, F.; Charrier, B. Characterization of a formaldehyde-free cornstarch-tannin wood adhesive for interior plywood. *Eur. J. Wood Wood Prod.* **2010**, *68*, 427–433.
2. Desroches, M.; Escouvois, M.; Auvergne, R.; Caillol, S.; Boutevin, B. From vegetable oils to polyurethanes: Synthetic routes to polyols and main industrial products. *Polym. Rev.* **2012**, *52*, 38–79.
3. Kong, X.; Liu, G.; Curtis, J.M. Characterization of canola oil based polyurethane wood adhesives. *Int. J. Adhes. Adhes.* **2011**, *31*, 559–564.
4. Liu, Y.; Li, K. Development and characterization of adhesives from soy protein for bonding wood. *Int. J. Adhes. Adhes.* **2007**, *27*, 59–67.
5. Gogoi, S.; Karak, N. Biobased biodegradable waterborne hyperbranched polyurethane as an ecofriendly sustainable material. *ACS Sustain. Chem. Eng.* **2014**, *2*, 2730–2738.
6. Pizzi, A. *Advanced Wood Adhesives Technology*; CRC Press: New York, NY, USA, 1994.
7. Ferdosian, F.; Pan, Z.; Gao, G.; Zhao, B. Bio-based adhesives and evaluation for wood composites application. *Polymers* **2017**, *9*, 70.
8. Pizzi, A. Recent developments in eco-efficient bio-based adhesives for wood bonding: Opportunities and issues. *J. Adhes. Sci. Technol.* **2006**, *20*, 829–846.
9. Santiago-Medina, F.; Foyer, G.; Pizzi, A.; Caillol, S.; Delmotte, L. Lignin-derived non-toxic aldehydes for ecofriendly tannin adhesives for wood panels. *Int. J. Adhes. Adhes.* **2016**, *70*, 239–248.
10. Muttil, N.; Ravichandra, G.; Bigger, S.W.; Thorpe, G.R.; Shailaja, D.; Singh, S.K. Comparative study of bond strength of formaldehyde and soya based adhesive in wood fibre plywood. *Procedia Mater. Sci.* **2014**, *6*, 2–9.
11. Bayer, O. Das Di-Isocyanat-Polyadditionsverfahren (Polyurethane). *Angew. Chem.* **1947**, *59*, 257–272.
12. Ji, D.; Fang, Z.; He, W.; Zhang, K.; Luo, Z.; Wang, T.; Guo, K. Synthesis of soy-polyols using a continuous microflow system and preparation of soy-based polyurethane rigid foams. *ACS Sustain. Chem. Eng.* **2015**, *3*, 1197–1204.
13. Pan, Y.; Zhan, J.; Pan, H.; Wang, W.; Tang, G.; Song, L.; Hu, Y. Effect of fully biobased coatings constructed via layer-by-layer assembly of chitosan and lignosulfonate on the thermal, flame retardant, and mechanical properties of flexible polyurethane foam. *ACS Sustain. Chem. Eng.* **2016**, *4*, 1431–1438.
14. Bakhshi, H.; Yeganeh, H.; Yari, A.; Nezhad, S.K. Castor oil-based polyurethane coatings containing benzyl triethanol ammonium chloride: Synthesis, characterization, and biological properties. *J. Mater. Sci.* **2014**, *49*, 5365–5377.
15. Ali, A.; Yusoh, K.; Hasany, S. Synthesis and physicochemical behaviour of polyurethane-multiwalled carbon nanotubes nanocomposites based on renewable castor oil polyols. *J. Nanomater.* **2014**, *2014*, 564384.
16. Abdalla, S.; Al-Aama, N.; Al-Ghamdi, M.A. A bio polymeric adhesive produced by photo cross-linkable technique. *Polymers* **2016**, *8*, 292.
17. Daniel da Silva, A.L.; Martín-Martínez, J.M.; Bordado, J.C.M. Influence of the free isocyanate content in the adhesive properties of reactive trifunctional polyether urethane quasi-prepolymers. *Int. J. Adhes. Adhes.* **2006**, *26*, 355–362.
18. Manjula, K.; Kumar, S.; Soare, B.G.; Picciani, P. Biobased chain extended polyurethane and its composites with silk fiber. *Polym. Eng. Sci.* **2010**, *50*, 851–856.
19. Chattopadhyay, D.; Raju, K. Structural engineering of polyurethane coatings for high performance applications. *Prog. Polym. Sci.* **2007**, *32*, 352–418.
20. Silva, B.B.; Santana, R.M.; Forte, M.M. A solventless castor oil-based PU adhesive for wood and foam substrates. *Int. J. Adhes. Adhes.* **2010**, *30*, 559–565.
21. Sharma, V.; Kundu, P. Condensation polymers from natural oils. *Prog. Polym. Sci.* **2008**, *33*, 1199–1215.
22. Xu, Y.; Petrovic, Z.; Das, S.; Wilkes, G.L. Morphology and properties of thermoplastic polyurethanes with dangling chains in ricinoleate-based soft segments. *Polymer* **2008**, *49*, 4248–4258.
23. Calvo-Correas, T.; Martin, M.D.; Retegi, A.; Gabilondo, N.; Corcuera, M.A.; Eceiza, A. Synthesis and characterization of polyurethanes with high renewable carbon content and tailored properties. *ACS Sustain. Chem. Eng.* **2016**, *4*, 5684–5692.
24. Ronda, J.C.; Lligadas, G.; Galià, M.; Cádiz, V. Vegetable oils as platform chemicals for polymer synthesis. *Eur. J. Lipid Sci. Technol.* **2011**, *113*, 46–58.

25. Gallego, R.; González, M.; Arteaga, J.F.; Valencia, C.; Franco, J.M. Influence of functionalization degree on the rheological properties of isocyanate-functionalized chitin-and chitosan-based chemical oleogels for lubricant applications. *Polymers* **2014**, *6*, 1929–1947.
26. Gallego, R.; Arteaga, J.; Valencia, C.; Díaz, M.; Franco, J. Gel-like dispersions of HMDI-cross-linked lignocellulosic materials in castor oil: Toward completely renewable lubricating grease formulations. *ACS Sustain. Chem. Eng.* **2015**, *3*, 2130–2141.
27. Allauddin, S.; Narayan, R.; Raju, K. Synthesis and properties of alkoxysilane castor oil and their polyurethane/urea–silica hybrid coating films. *ACS Sustain. Chem. Eng.* **2013**, *1*, 910–918.
28. Gallego, R.; Arteaga, J.; Valencia, C.; Franco, J. Thickening properties of several NCO-functionalized cellulose derivatives in castor oil. *Chem. Eng. Sci.* **2015**, *134*, 260–268.
29. Głowińska, E.; Datta, J. Bio polyetherurethane composites with high content of natural ingredients: Hydroxylated soybean oil based polyol, bio glycol and microcrystalline cellulose. *Cellulose* **2016**, *23*, 581–592.
30. Deka, H.; Karak, N. Vegetable oil-based hyperbranched thermosetting polyurethane/clay nanocomposites. *Nanoscale Res. Lett.* **2009**, *4*, 758–765.
31. Gurunathan, T.; Chung, J.S. Physicochemical oroperties of amino–silane-terminated vegetable oil-based waterborne polyurethane nanocomposites. *ACS Sustain. Chem. Eng.* **2016**, *4*, 4645–4653.
32. Campanella, A.; Bonnaillie, L.; Wool, R. Polyurethane foams from soyoil-based polyols. *J. Appl. Polym. Sci.* **2009**, *112*, 2567–2578.
33. Ferrer, M.C.C.; Babb, D.; Ryan, A.J. Characterisation of polyurethane networks based on vegetable derived polyol. *Polymer* **2008**, *49*, 3279–3287.
34. Rojek, P.; Prociak, A. Effect of different rapeseed-oil-based polyols on mechanical properties of flexible polyurethane foams. *J. Appl. Polym. Sci.* **2012**, *125*, 2936–2945.
35. Das, B.; Konwar, U.; Mandal, M.; Karak, N. Sunflower oil based biodegradable hyperbranched polyurethane as a thin film material. *Ind. Crops Prod.* **2013**, *44*, 396–404.
36. Kong, X.; Liu, G.; Curtis, J.M. Novel polyurethane produced from canola oil based poly (ether ester) polyols: Synthesis, characterization and properties. *Eur. Polym. J.* **2012**, *48*, 2097–2106.
37. Ogunniyi, D. Castor oil: A vital industrial raw material. *Bioresour. Technol.* **2006**, *97*, 1086–1091.
38. Somani, K.P.; Kansara, S.S.; Patel, N.K.; Rakshit, A.K. Castor oil based polyurethane adhesives for wood-to-wood bonding. *Int. J. Adhes. Adhes.* **2003**, *23*, 269–275.
39. Gallego, R.; Arteaga, J.; Valencia, C.; Franco, J. Chemical modification of methyl cellulose with HMDI to modulate the thickening properties in castor oil. *Cellulose* **2013**, *20*, 495–507.
40. Stuart, B.H. Organic molecules. In *Infrared Spectroscopy: Fundamentals and Applications*; Ando, D.J., Ed.; University of Technology: Sidney, Australia, 2004; pp. 71–93.
41. Corcuera, M.; Rueda, L.; d'Arlas, B.F.; Arbelaiz, A.; Marieta, C.; Mondragon, I.; Eceiza, A. Microstructure and properties of polyurethanes derived from castor oil. *Polym. Degrad. Stab.* **2010**, *95*, 2175–2184.
42. Wang, Z.; Zhang, X.; Zhang, L.; Tan, T.; Fong, H. Nonisocyanate biobased poly (ester urethanes) with tunable properties synthesized via an environment-friendly route. *ACS Sustain. Chem. Eng.* **2016**, *4*, 2762–2770.
43. Ugarte, L.; Gómez-Fernández, S.; Peña-Rodríuez, C.; Prociak, A.; Corcuera, M.A.; Eceiza, A. Tailoring mechanical properties of rigid polyurethane foams by sorbitol and corn derived biopolyol mixtures. *ACS Sustain. Chem. Eng.* **2015**, *3*, 3382–3387.
44. Gallego, R.; Arteaga, J.; Valencia, C.; Franco, J. Rheology and thermal degradation of isocyanate-functionalized methyl cellulose-based oleogels. *Carbohydr. Polym.* **2013**, *98*, 152–160.
45. Gurunathan, T.; Mohanty, S.; Nayak, S.K. Isocyanate terminated castor oil-based polyurethane prepolymer: Synthesis and characterization. *Prog. Org. Coat.* **2015**, *80*, 39–48.
46. Bagdi, K.; Molnár, K.; Sajó, I.; Pukánszky, B. Specific interactions, structure and properties in segmented polyurethane elastomers. *Express Polym. Lett.* **2011**, *5*, 417–427.

Assessing the rheological properties and adhesion performance on different substrates of a novel freen polyurethane based on castor oil and cellulose acetate: A comparison with commercial adhesives

A. Tenorio-Alfonso[a], M.L. Pizarro[a], M.C. Sánchez[a,b], J.M. Franco[a,b]

[a] *Department of Chemical Engineering, Physical Chemistry and Materials Science, University of Huelva, Campus El Carmen, Campus ceiA3, 21071 Huelva, Spain*

[b] *Pro²TecS-Chemical Product and Process Technology Research Centre, University of Huelva, 21071 Huelva, Spain*

Published in: ***International Journal of Adhesion and Adhesives***

Publisher: Elsevier

Editors-in-Chief: Robert Adams and Steve Shaw

Volume 82, pp: 21-26

Year: 2018

DOI: 10.1016/j.ijadhadh.2017.12.012

ISSN: 0143-7496

JCR Impact Factor (2017): 2.065

JCR Category	Rank	Quartile
CHEMICAL ENGINEERING	61/137	Q2
MULTIDISCIPLINARY MATERIALS SCIENCE	141/285	Q2

Annexe I. Published articles

El artículo “Assessing the rheological properties and adhesion performance on differentsubstrates of a novel green polyurethane based on castor oil and celluloseacetate : a comparison with commercial adhesives” que forma parte del annexo I, ha sido retirado de la tesis debido a restricciones relativas a derechos de autor. En sustitución de los artículos ofrecemos la siguiente información: referencia bibliográfica, enlace a la revista y resumen.

- Tenorio Alfonso, A., Pizarro, M.L., Sánchez Carrillo, M.C., Franco Gómez, J.M.: “Assessing the rheological properties and adhesion performance on differentsubstrates of a novel green polyurethane based on castor oil and celluloseacetate : a comparison with commercial adhesives“. International Journal of Adhesion and Adhesives. Vol. 82, págs. 21-26, (2018). DOI: 10.1016/j.ijadhadh.2017.12.012

Enlace al texto complete del artículo: https://doi.org/10.1016/j.ijadhadh.2017.12.012

RESUMEN:
Interest in replacing petroleum-based adhesives with more environmentally friendly materials has grown enormously in recent decades. In this work, a novel bio-sourced polyurethane was synthesized by functionalizing cellulose acetate with 1,6-hexametylene di-isocyanate (HMDI) and then blending the resulting biopolymer with castor oil in a 1:1 weight ratio to obtain a chemical oleogel which was left for curing. The rheological properties and adhesion performance of this new bio-based formulation were compared with those of commercially available adhesives by using small-amplitude oscillatory torsional tests and standardized mechanical tests to evaluate peeling (ASTM D903) and shear strengths, in both single-lap (ASTM D906, D1002, D3163) and lap-joint assemblies (ASTM D3164), on various substrates including wood, polyethylene and stainless steel, as well as flexural strength (ASTM D1184) on wood. As shown here, the new adhesive is suitable for most of the adherends examined, thus exhibiting mechanical strengths comparable to or even better than that of the benchmarks in wood–wood and steel–steel contacts, similarly good rheological response and significantly higher relative elasticity. On the other hand, the adhesion performance of the new adhesive on polyethylene was worse than that of the commercial adhesives.

List of Tables

Chapter 1 Introduction

Chapter 2 State of the art

Chapter 3 Materials and Methods

Chapter 4 Results and Discussion

List of Figures

Chapter 1 Introduction

Chapter 2 State of the art

Chapter 3 Materials and Methods

Chapter 4 Results and Discussion